



universität  
wien

# DISSERTATION

Titel der Dissertation

Stratigraphy, lithofacies and geochemistry of the St. Veit  
Klippenzone and the Flysch units from the Lainz Tunnel,  
Vienna

Verfasser

Mag. Clemens Pfersmann

angestrebter akademischer Grad

Doktor der Naturwissenschaften (Dr. rer. nat.)

Wien, 2013

Studienkennzahl lt. Studienblatt: A 091 426

Dissertationsgebiet lt.  
Studienblatt: Dr.-Studium der Naturwissenschaften Erdwissenschaften  
UniStG

Betreuerin / Betreuer: Ao. Univ. Prof. Dr. M. Wagreich

## Contents

Abstract .....	3
Zusammenfassung.....	5
A. INTRODUCTION.....	7
A.1. Scope of work.....	7
A.2. Geographic and geological setting .....	8
A.3. Applied Methods .....	13
A.4. Tunnel sampling strategy.....	13
B. LITERATURE REVIEW AND PUBLISHED DATA .....	16
B.1. Lithostratigraphic nomenclature of the St. Veit Klippenzone.....	22
B.1.1. Hohenauer Wiese Formation.....	22
B.1.2. Rote Crinoidenkalke (red crinoidal limestone) .....	22
B.1.3. Rotenberg-Formation (Rotenberg Formation) .....	23
B.1.4. Fasselgraben-Formation (Fasselgraben Formation).....	24
C. STRUCTURAL, STRATIGRAPHY AND LITHOLOGY RESULTS .....	26
C.1. Structural Data.....	26
C.2. The Lainz Tunnel section - stratigraphy & lithofacies .....	30
C.2.1. The stratigraphic profile of the Flyschzone (Kahlenberg Nappe) and the St.Veit Klippenzone in the Lainz Tunnel (from youngest to oldest) .....	30
C.2.2. St. Veit Klippenzone in the Lainz Tunnel .....	30
C.3. Flysch Units Description .....	33
C.3.1. Kahlenberg Formation.....	34
C.3.1.1. Biostratigraphic Data.....	34
C.3.2. Hütteldorf Formation in the Lainz Tunnel .....	36
C.3.2.1. Biostratigraphic Data.....	36
C.3.2.2. Mineralogy of additional rock types within the Hütteldorf Formation in the Lainz Tunnel .....	38
C.4. The St.Veit Klippenzone .....	43
C.4.1. Lithologies.....	43
C.4.2. Heavy mineral data.....	67
C.4.3. Carbonate-Analysis .....	74
C.4.4. Mineralogy of sandstones based on XRD Analysis .....	75
C.4.5. Geochemistry and Isotope Geochemistry.....	78
D. DISCUSSION .....	132

D.1. Stratigraphy .....	132
D.2. Relation Flysch to St. Veit Klippenzone .....	134
D.3. Geotectonic Position of the St. Veit Klippenzone .....	135
D.4. Correlation to the Western Carpathians.....	138
D.4.1. Correlation to the Drietoma unit .....	138
E. CONCLUSIONS.....	140
Acknowledgement.....	142
References .....	143
APPENDIX 1 Geochemical results.....	159
APPENDIX 2 XRD results .....	169
APPENDIX 3 Carbonate Analysis results .....	177
APPENDIX 4 Geochemistry Results.....	179
APPENDIX 5 Sample list .....	197

## ABSTRACT

This work aims at a synopsis of data from the Lainz Tunnel section to get more information on the St. Veit Klippenzone and the surrounding flysch unit(s), and to clarify the structures and stratigraphy of units marginal to the Northern Calcareous Alps and the Rhenodanubian Flysch Zone. New data are especially derived from the Lainz Tunnel section which temporary exposed these rocks during tunneling in the years 2007 to 2009.

Stratigraphy and facies of the St. Veit Klippenzone are reviewed. New data are derived from methods like geochemistry and isotope geochemistry, thin section analysis, micropaleontology and microfacies analysis to integrate lithofacies, biofacies and biostratigraphy from the Lainz Tunnel section. These data form the base for a new structural model and for correlations of the St. Veit Klippenzone to other units of the Eastern Alps and the Western Carpathians, and to decipher the geotectonic position of that unit.

A total of 2253m of the tunnel section yielded flysch sediments. The St. Veit Klippenzone was found from 2165m at LT33 to 898m at LT31 (1097m section of Klippenzone rocks) within the middle part of the Lainz Tunnel section. It comprises largely a „block-in-matrix” structure, partly tectonically mixed with flysch units. Tectonic blocks of hard „klippencore” rocks show sizes from cm to several tens of meters. The matrix consists of strongly deformed fine-grained rocks such as shales and marls of Cretaceous and Jurassic age. No primary sedimentary contact of the flysch formations on the St. Veit Klippenzone rocks could be detected.

The composite St. Veit Klippenzone succession detected within the tunnel and combined with literature data includes the following lithologies and stratigraphy:

1. Keuper quartzites (Upper Triassic): light grey to pink quartz with white kaolinitic matrix and red or green clay.
2. Dolomites of probably Upper Triassic age.
3. Kössen Formation (Rhaetian): fossiliferous, dark, bedded marly limestones, limestones and marls with bivalves and brachiopods.
4. Lower/Middle Jurassic sandstones („Gresten Formation“): coal-bearing sandstones, dark sandy limestones, grey crinoidal limestones, brownish-black marly shales and marly limestones. Ammonites (e.g. *Arietites*) indicate lower/middle Liassic; bivalves are common.
5. Lower/Middle Jurassic siltstones and marls („Posidonia marls“): marly/sandy facies.

6. Hohenauer Wiese Formation (Middle Jurassic): grey marly sandstones, sandy limestones, crinoidal limestones, cherty shales and limestones with ammonites of Bajocian, Bathonian and Callovian.
7. Red crinoidal limestones (Kimmeridgian).
8. Rotenberg Formation (Upper Jurassic): red, green and grey radiolarites.
9. Fasselgraben Formation/Aptychus limestone (Tithonian-Neocomian): white limestone with black chert nodules.

Geochemistry, isotope geochemistry, heavy mineral data and microfacies studies are used to describe and interpret the strata and an inventory of rocks is given. New biostratigraphic results from the Klippenzone include data by macrofossils (rare ammonites) radiolaria, calpionellids and nannofossils.

Geochemical data and it's statistical evaluation indicates strong similarities of the St.Veit Klippenzone rocks to the Pieniny Klippen Belt of the Western Carpathians, especially the Drietoma Unit, using geochemical indices and lithology-dependant factor analysis. Significant differences are proven by comparing units from the both the Gresten and Ybbsitz Klippenzones of Austria, thus indicating a different geotectonic environment and a different provenance for the St. Veit Klippenzone.

The geotectonic position of the St. Veit Klippenzone can be discussed based on these results. Neither the Gresten Klippenzone (Helvetic) nor the Ybbsitz Klippenzone (Penninic) provide similar successions. A more reasonable facies correlation can be done with Austroalpine units, i.e. northern („Lower“) Austroalpine successions and the northernmost marginal units of the Northern Calcareous Alps. Compared to the Western Carpathians strong similarities with the Drietoma Unit can be seen, a unit which has affinities to Lower Austroalpine/Fatic/Tatric elements such as the Carpathian Krížna Nappe, but was later on affected by Klippen-style tectonism and included into the Pieniny Klippen Zone. Thus, a correlation to the Pieniny Klippen Zone of the Western Carpathians is most likely and the St. Veit Klippenzone represents therefore not a continuation of klippenzones of the Eastern Alps, but the westernmost extension of the Pieniny Klippen Belt of the Western Carpathians near Vienna.

## ZUSAMMENFASSUNG

Ziel der Arbeit war es einen Überblick über den aktuellen Kenntnisstand zur St.Veiter Klippenzone mit umgebenden Flyscheinheiten zu geben und neue Informationen aus dem Lainzer Tunnel einzubinden. Dies soll zur Klärung des Aufbaus der Strukturen sowie der Stratigraphie der an die Nördlichen Kalkalpen und der Rhenodanubischen Flyschzone angrenzenden Einheiten beitragen. Während des Baus des Lainzer Tunnels (2007-2009) konnten neue Daten aus den temporär freiliegenden Gesteinen des Tunnels gewonnen werden. Bisher erschienene Publikationen über die Stratigraphie und Fazies der St.Veiter Klippenzone (SVK) werden zusammengefaßt und durch neu gewonnene Daten aus geochemischen-, isotopengeochemischen-, und Dünnschliffanalysen, sowie mikropaläontologischen und mikrofazielle Untersuchungen ergänzt. Daraus ergibt sich eine umfassende Darstellung von Lithofazies, Biofazies und Biostratigraphie der St.Veiter Klippenzone im Lainzer Tunnel. Diese Daten bilden die Basis für ein neues Strukturmodell und für Vergleiche der St.Veiter Klippenzone mit anderen Einheiten der Ostalpen sowie Westkarpathen, um die geotektonische Stellung der St.Veiter Klippenzone endgültig zu klären. Der Lainzer Tunnel, mit einer erschlossenen Länge von 2253m, beinhaltet Flyschsedimente und Klippengesteine. Die SVK konnte von Station 2165m Baulos LT33, bis Station 898m Baulos LT31 angetroffen werden, insgesamt ergibt das eine Strecke von 1097m an Aufschlüssen der Klippenzone im Lainzer Tunnel. Die Gesteine zeigten großteils eine sogenannte „Block in Matrix“ – Struktur, teilweise mit Flyscheinheiten tektonisch vermenigt. Tektonische Blöcke der harten „Klippenkerngesteine“ traten von cm bis zu mehrere Meter Mächtigkeit auf. Die Matrix bestand aus stark deformierten, feinkörnigen Sedimenten wie jurassischen und cretazischen Tonen und Mergeln. Es konnte kein primärer Sedimentkontakt der Flysch Formationen auf die SVK nachgewiesen werden. Das zusammengesetzte Profil der Klippenzone aus dem Lainzer Tunnel umfasst die folgenden Lithologien und Stratigraphie:

1. Keuperquarzite (Obere Trias): hellgrauer und rosa Quarz mit weißer kaolinitischer Matrix mit rotem bis grünem Ton.
2. Dolomit, wahrscheinlich Obere Trias.
3. Kössen-Formation (Rhaetium): fossilführende, dunkle, geschichtete, mergelige Kalke mit Bivalven und Brachiopoden.
4. Unter-/Mittel-Jura Sandsteine („Gresten Formation“): Kohleführende, dunkle sandige Grestenkalke, graue crinoidenführende Kalke, braune bis schwarze mergelige Schiefer und

mergelige Kalke. Ammoniten (z.B. *Arietites*) deuten auf ein unter- bis mittelliasisches Alter hin, häufiges Vorkommen von Bivalven.

5. Unter-/Mittel-Jura Siltsteine und Mergel („Posidonienmergel“): mergelig-sandige Fazies.
6. Hohenauer-Wiese-Formation (Mitteljura): graue, mergelige Sandsteine, sandige Kalke, crinoidenführende Kalke, kieselige Schiefer und ammonitenführende Kalke mit Gattungen aus dem Bajocium, Bathonium und Callovium.
7. Rote crinoidenführende Kalke (Kimmeridgium).
8. Rotenberg-Formation (Oberjura): rote, grüne und graue Radiolarite.
9. Fasselgraben-Formation/Aptychenkalke (Tithonium-Neocomium): weiße Kalke mit schwarzen Hornsteinknollen.

Ergebnisse aus der Geochemie, Schwermineralanalyse, Isotopengeochemie und Mikrofaziesanalyse wurden zur Beschreibung und Interpretation der Schichten herangezogen. Weiters wurde eine Auflistung der im Tunnel angetroffenen Gesteine erstellt. Neue biostratigraphische Einzeitungen der Gesteine der Klippenzone beruhen auf Makrofossilien (seltene Ammoniten), Radiolarien, Calpionellen sowie Nannofossilien. Geochemische Daten und ihre statistische Auswertung deuten auf starke Ähnlichkeiten der St. Veiter Klippen Gesteine mit der Pienidischen Klippenzone der Westkarpaten hin, insbesonders der Drietoma Einheit. Signifikante Unterschiede ergeben sich beim Vergleich der SVK mit Einheiten der Grestener und der Ybbsitzer Klippenzone in Österreich. Zusätzlich finden sich zahlreiche Hinweise auf ein anderes geotektonisches Environment und Liefergebiet der St. Veiter Klippengesteine. Die geotektonische Position der St. Veiter Klippenzone muss auf Grund der neuen Ergebnisse überdacht werden. Weder die Grestener Klippenzone (Helvetikum) noch die Ybbsitzer Zone (Penninikum) zeigen gleichartige Abfolgen und Zusammensetzungen. Wahrscheinlicher erscheint die Korrelation der St. Veiter Klippenzonen Fazies mit Austroalpinen Einheiten, z.B. des nördlichen Ostalpins (Unterostalpin) und der nördlichsten randlichen Einheiten der Kalkalpen. Verglichen mit den Westkarpaten zeigen sich große Ähnlichkeiten mit der Drietoma Einheit. Diese Einheit zeigt wiederum Merkmale des Unterostalpins bzw. des Fatrikums/Tatrikums (z.B. der karpatischen Krížna Decke). Die Drietoma Einheit wurde später in die „Klippentekonik“ involviert und in die Pienidische Klippenzone der Westkarpathen eingefügt. Darum ist eine Korrelation der SVK zu der Pieninischen Klippenzone der Westkarpaten sehr wahrscheinlich und die SVK stellt nicht eine Fortsetzung der ostalpinen Klippenzonen dar, sondern die westlichste Fortsetzung der Pieninischen Klippenzone der Westkarpathen nahe Wiens.

## A. INTRODUCTION

### A.1. Scope of work

The Klippenzones in Austria comprise a significant part of the Alpine mountain chain, but are not well understood due to the spotty occurrence and very poor outcrop conditions along strike, especially near Vienna. The St. Veit Klippenzone (e.g. Janoschek et al., 1956) in western Vienna and the Wienerwald area constitutes one of these Eastern Alpine zones. Due to moderate topographic elevations, this part of the Alpine belt usually features strong vegetation, extensive agricultural use, or only offers increasingly restricted access in suburban areas such as in the case of Vienna. Even the continuity of some of the klippenzones from western Lower Austria into the St. Veit Klippenzone is strongly debated and remains unclear. The St. Veit Klippenzone (SVK) and its surrounding flysch units comprise a major tectonic unit within the nappe pile of the Eastern Alps and continue into the 2<sup>nd</sup> floor of the Vienna Basin. The tectonic position, the stratigraphy and lithofacies development of this zone is poorly known (Trauth, 1930, Janoschek, 1956, Prey, 1975 and 1979) and a modern study is completely missing. Inferred stratigraphy and geotectonic position of the SVK are based on outcrops that are largely no longer available, and thus depend on studies mainly from the 1910's to the 1970's that used mainly macrofossils for biostratigraphy. These studies are thus largely outdated and the geotectonic position and affinities of the St. Veit Klippenzone in relation to the Rhenodanubian Flysch are strongly discussed (Trauth, 1930, Janoschek, 1956, Prey, 1975, 1979, Schnabel, 1997, 2002, Wessely, 2006).

The present work aims at a new understanding of the stratigraphy and the geological evolution of the St. Veit Klippenzone and the surrounding flysch units based on unique exposures during tunneling in the last few years. These new data are combined with literature data and compared to adjacent geological units.

The present work was sponsored by an University-OMV E&P cooperation project( FA536006 „Stratigraphy and lithofacies inventory of the St. Veit Klippenzone and the flysch units from the Lainzer Tunnel, Vienna“) and by the Hochschuljubiläumsstiftung der Stadt Wien („Geochemie und Stratigraphie der St. Veiter Klippenzone: Untersuchung einmaliger Gesteinsproben aus dem Lainzer Tunnel“). Cooperation on Klippenzone geology in Slovakia was possible by a grant within the framework of Austrian-Slovak cooperation (Wissenschaftlich-Technische Zusammenarbeit WTZ, SK16/2011, „Paläogeographische und tektonische Beziehungen zwischen den alpinen und karpatischen Klippenzonen“).

## A.2. Geographic and geological setting

The northeastern margin of the Eastern Alps comprises several geological units that were originally positioned north of the Austroalpine-Adriatic margin (e.g. Faupl & Wagreich, 2000): The Gresten Klippenzone, a Helvetic/Ultrahelvetic unit, originally situated at the European shelf to continental slope in the north; the Rhenodanubian Flysch units and its inferred basement, the ophiolithic Ybbsitz (Klippen)Zone, which derived from the Penninic Ocean (both North- and South-Penninic units according to Faupl & Wagreich, 2000); and some questionable intervening small klippenzones like the „Sulzer Klippenzone”, to the north of the Austroalpine Northern Calcareous Alps (e.g. Wessely, 2006). The St. Veit Klippenzone, the main topic of this work, is currently regarded as a continuation of the Ybbsitz Klippenzone (e.g. Schnabel, 2002; Wessely, 2006).

The WSW-ENE striking Rhenodanubian Flyschzone spreads from Vorarlberg to Vienna and consists of marine deepwater sediments, such as turbiditic sandstones, pelites and argillaceous limestones. From the Early Cretaceous until the Eocene, the sediments of the Rhenodanubian Flyschzone were deposited in the North Penninic realm. The Rhenodanubian Flyschzone is divided into the Western and the Eastern Flyschzone. The Western Flyschzone consists of the Northern Zone and the Main Flyschzone. The Eastern Flyschzone in the Wienerwald area consists of four tectonic units: the Northern Zone, the Greifenstein Nappe, the Laab Nappe and the Kahlenberg Nappe (Wessely 2006).

The Gresten, St. Veit and „Sulzer Klippenzone” consist of Mesozoic and Paleogene sediments. The Gresten Klippenzone (e.g. Wessely, 2006), equivalent to the Main Klippenzone in the Wienerwald, starts in the Lower Jurassic with continental coal-bearing arkosic sandstones („Gresten arkose”), followed by marine sandy limestones, marls („Posidonienschichten”) and shales (Lower to Middle Jurassic). From Upper Doggerian to Lower Malmian sedimentation becomes more siliceous with radiolarites (Lampelsberg Formation). Followed by turbidites with increasing carbonate content (Scheibsbach Formation). Middle to Upper Malmian sediments are represented by pelagic limestones („Arzbergkalk”, „Untere Blassensteinschichten”). The „Konradsheimer Schichten” are characterized by fine to coarse-clastic conglomeratic limestones (Oxfordian-Tithonian). The aptychus limestones of the „Obere Blassensteinschichten” can reach up to Barremian/Aptian age.

In contrast, the Ybbsitz Zone starts with an ophiolithic succession followed by Middle to Upper Jurassic deepwater radiolarites (Rotenberg Formation). The highest element is represented by the Fasselgraben Formation (Malmian - Berriasian), consisting of deepwater limestones (Wessely, 2006).

Wessely (2006) also gives a stratigraphic succession of the St.Veit Klippenzone which consists of Upper Triassic Keuper quartzites and fossiliferous Kössen Formation, overlain by sandstones of the Gresten Formation, Posidonia marls, the Hohenauer Wiese Formation (Middle Jurassic) grey marly sandstones, sandy limestones, crinoidal limestones with ammonites, the Rotenberg Formation with radiolarites, red crinoidal limestones, and aptychus limestone of Tithonian to Early Cretaceous age. Most authors correlate the St. Veit Klippenzone and the Ybbsitz Zone (e.g. Schnabel, 2002).

The Lainz Tunnel represents a part of the ÖBB's connection between Südbahn (southern) and Westbahn (western main route). The route of the Lainz Tunnel, built by ÖBB Infrastruktur GmbH, passes through the western outskirts of Vienna to link the southern and western rail route (Fig. 1). The Lainz Tunnel's contract section LT33 (ÖBB Bau AG) was built beginning 2007 from Auhof, in the western part of Vienna heading SE. Contract section LT33 was built from the other side, from the Lainz area, westwards, starting in 2009. The total length of sampled tunnel section is 3350m. Flysch units comprise 2253m (LT33: 2165m + LT31: 88m), Klippenzone units comprise 1097m (LT33: 610m + LT31: 487m). The cut-through to contract section LT31 (coming from SE, Lainz area) was on May 8<sup>th</sup> 2009 at 2775.5m from NW in rocks of the Klippenzone.

In the southwestern part of Vienna and the adjacent Wienerwald area, rocks of the Rhenodanubian Flyschzone, the klippenzones and the Northern Calcareous Alps are found (Plöchinger & Prey, 1993; Schnabel, 1997). In the area of the Lainz Tunnel, at Ober St.Veit-Lainzer Tiergarten- Roter Berg -Lainz, Mesozoic parts of the St.Veit Klippenzone crop out (e.g. Janoschek et al., 1956), surrounded by Rhenodanubian Flyschzone rocks. The St. Veit Klippenzone comprises a poorly exposed, composite succession from Upper Triassic to Lower Cretaceous, mainly limestones, siliceous rocks and minor sandstones (e.g. Janoschek 1956). The surrounding flysch units belong to the Kahlenberg Nappe, consisting mainly of the Hütteldorf Formation (Cenomanian-Santonian, e.g. Wagreich, 2007, 2008) and the Kahlenberg Formation (mainly Campanian, e.g. Tollmann, 1985; Müller, 1987).

According to Prey (e.g. 1973, 1975) the St. Veit Klippenzone is directly sedimentary superimposed by Flysch, including some remnants of mid-Cretaceous strata, and mainly the Hütteldorf Formation (Schnabel, 2002; Wagreich, 2008).

The position of the Lainz Tunnel largely at right angle to the strike of the strata was an unique opportunity for a closer look on the rocks of the SVK and this part of the Rhenodanubian Flysch.

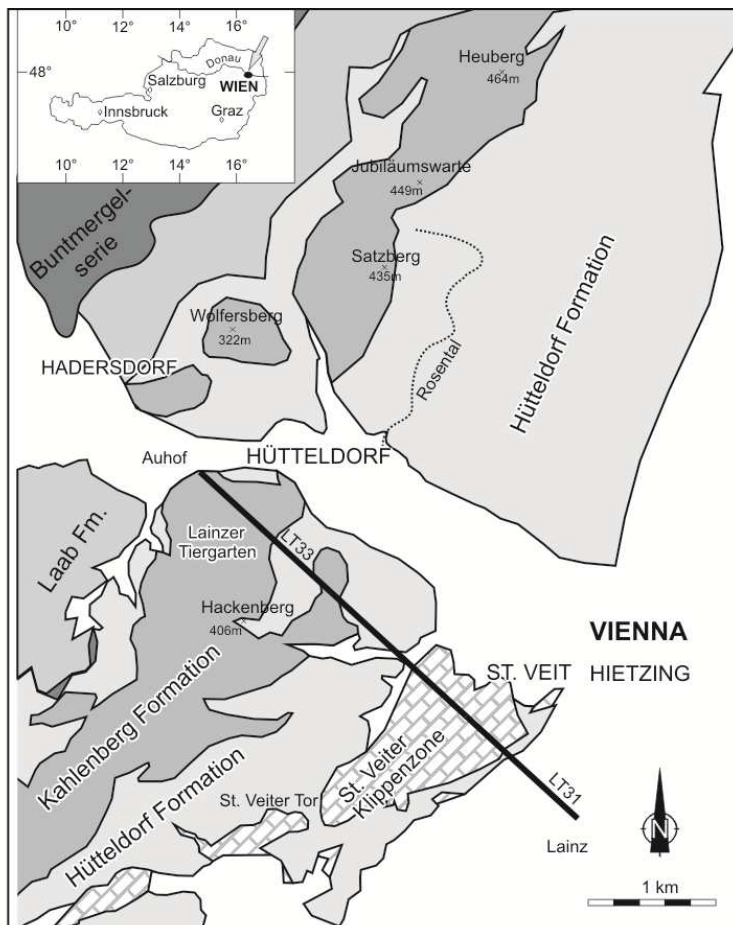


**Fig. 1 Geological site map of the Lainz Tunnel (section LT33+LT31) (sketch based on geological map sheet 58 Baden, Schnabel, 1997).**

The tunnel direction is directed NW-SE, 136°. Coming from the Vienna valley/Auhof, going SE, rocks of the Flyschzone were hit first, up to 2165.5m, followed by St.Veit Klippenzone. In the context of a diploma thesis by Clemens Pfersmann, samples were taken since the start of the construction work at LT33 up to 1000m. Later on, sampling was performed from both sides. Martin Maslo helped to take samples from the LT31 section. At 2165m (LT33) first scattered cherts, associated with the St.Veit Klippenzone, occurred. From 2320m (ammonite), 2592m (calpionellids) and 2552m (nannoplankton) (all LT33) on Lower Cretaceous could

been determined. At 2666m (LT33) (nannoplankton) Jurassic age was proven. Coming from SE first cherts, associated with the St.Veit Klippenzone, emerged at 898m (LT31).

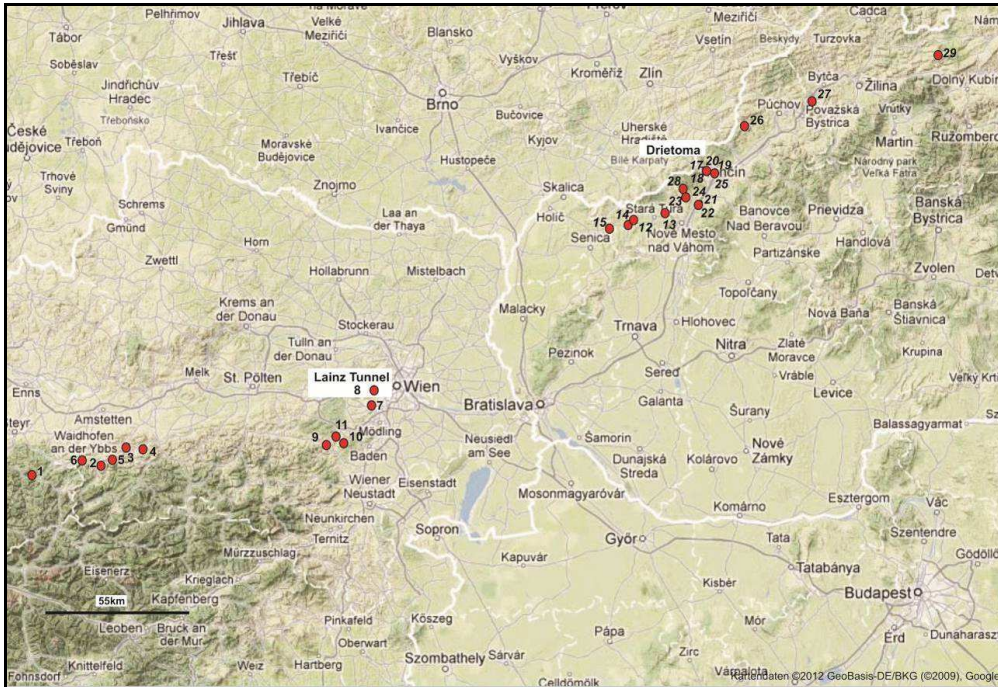


**Fig. 2 Topographic map showing the different sample sites in Austria and Slovakia. The location numbers are explained in the table below (adapted from Google maps).**

No.	Sample site	Coordinates	Correlation
1	Pechgraben	N47°54'38.46.4" E14°33'13.7"	Gresten Klippenzone
2	Steinbruch Reidl	R0491286 U5310354 (UTM33)	Ybbsitz Klippenzone
3	Lampelsberg	R0500757 U5316257 (UTM33)	Gresten Klippenzone
4	Klauskogel	R0507463 U5316017 (UTM33)	Gresten Klippenzone
5	Haselgraben	R0495926 U5312396 (UTM33)	Ybbsitz Klippenzone
6	Arzbergergraben	14°48'23.31"E 47°57'3.60"N	Gresten Klippenzone
7	Antonhöhe	48° 8'56.59"N 16°14'40.75"E	St.Veit Klippenzone
8	Lainz Tunnel entry LT33	48°12'0.30"N 16°14'32.17"E	St.Veit Klippenzone
9	Lainz Tunnel entry LT31	48°10'26.15"N 16°17'03.39"E	St.Veit Klippenzone
10	Groisbach	48° 2'38.54"N 16° 3'13.93"E	Dislodged slice-unknown
11	Gutental	48° 1'15.04"N 16° 5'35.85"E	Dislodged slice-unknown
12	Hafnerberg	48° 1'9.10"N 16° 0'34.84"E	Reisalpen Nappe
13	Myjava1	R0689036 U5402885 (UTM33)	PKB - Kysuca Unit Klippe
14	Bzince pod Javorinou	R07004308 U5406815 (UTM33)	Nedzov Nappe
15	Turá Lúka	(R0689036 U5402885 (UTM33) next to Myjava	PKB - Kysuca Unit
16	Podbranč,	R680085 U5400455 (UTM33)	PKB - Kysuca Unit Klippe
17	Dolný Mlyn	Near Stará Turá	Klippe of the Czorsztyn Unit -PKB
18	Drietoma	N 48°54'2,1" E 17°57'18,2"	Typloc. Drietoma Unit
19	Drietoma	N 48°54'17" E 17°57'22"	Typloc. Drietoma Unit
20	Drietoma	N 48°54'25" E 17°57'18"	Typloc. Drietoma Unit
21	Drietoma	N 48°55'17,4" E 17°56'49,3"	Typloc. Drietoma Unit
22	P10	N 48°48'43,4" E 17°55'19,6"	Kopieniz Fm-Kržna Nappe
23	P11	N 48°48'35,2" E 17°54'49,1"	Kržna Nappe
24	P12	N 48°49'38,6" E 17°49'55,6"	Drietoma "Peri Klippenbelt"
25	P14	N 48°49'47,2" E 17°51'15,9"	Drietoma Unit
26	P16	N 48°54'38,5" E 17°59'59,2"	Drietoma Unit
27	P17	N 49°3'45,3" E 18°9'12,2"	Drietoma Unit
28	P18	N 49°08'25,4" E 18°30'03,9"	Manín Unit
29	P19	N 48°51'43" E 17°49'36,5"	Drietoma Unit
30	Zázrivá	N 49°16'33" E 19° 9'15"	Kržna Nappe

**Fig. 3 Table with the sample sites and GPS data.**

## **Additional informations regarding other sample sites besides the Lainz Tunnel:**

### **1. Grestener Klippenzone:**

The Gresten Klippenzone is regarded as a Helvetic/Ultrahelvetic unit (e.g. Faupl & Wageich, 2000). Sampling was done at the localities Pechgraben/Großraming, Lampelsberg, Klauskogel, Arzberggraben(see Fig. 3 for geographic coordinates). For descriptions see Widder (1988), Decker (1987), Ožvoldová & Faupl (1993).

### **2. Ybbsitz Klippenzone:**

The Ybbsitz Klippenzone is considered as a Penninic (South - Penninic) tectonic element, including ophiolitic remnants, and probably formed parts of the basement of the Rhenodanubian Flysch (e.g. Decker, 1990, Ožvoldová & Faupl, 1993). Sampling was done near Ybbsitz (abandoned quarry Reidl) and Gresten (Haselgraben).

### **3. St. Veit Klippenzone, including the Antonshöhe Klippe:**

The St Veit Klippenzone position is still debated, some authors consider a South-Penninic position(e.g.: Schnabel, 2002), others argue for a correlation with the Gresten Klippenzone and thus a position north of the Penninic Ocean (Prey,1979, Wessely, 2006). The Antonshöhe Klippe (Mauer, SE Vienna) is regarded as belonging to the St. Veit Klippenzone by Prey (1979).

### **4. Dislodged slices at the base of the Göller Nappe, Northern Calcareous Alps:**

Upper Triassic and Jurassic rocks between Lunz Nappe and Tirolicum, informally called „Groisbach Schürflinge”, described as an extra-alpine facies by Wessely (1967). Sampling was done at the Groisbach locality near Alland, SW of Vienna (Wessely, 1967, 2006) and at the „Guten(bach)tal” (Plöchinger,1970, Wessely, 1981, 2006).

### **5. Reisalpen Nappe, NCA:**

Keuper sediments intercalated in Hauptdolomite of the Kaumberg/Altenmarkt an der Triesting region, as described in Plöchinger & Salaj (1991).

### **6. Pieniny Klippen Belt, Kysuca Unit (Western Carpathians):**

The Kysuca Unit consists mainly of deep marine Jurassic sediments (radiolarites). According to Birkenmajer (1977), the Kysuca Unit was placed south of the Czorsztyn Swell.

### **7. Pieniny Klippen Belt, Czorsztyn Czorsztyn Unit (Western Carpathians):**

The Czorsztyn Unit is a shallow marine facies, it consists of Jurassic and Cretaceous shallow marine sediments (Birkenmajer, 1977, Aubrecht, 2004).

### **8. Pieniny Klippen Belt, Drietoma Unit (Western Carpathians):**

The Drietoma Unit belongs to the Faticum and is a „non-Oravic” Periklippenzone. It comprises the Upper Triassic to Cenomanian, basinal succession (Hók et al., 2009).

## **9. Krížna Nappe (Western Carpathians):**

The Krížna Nappe is a „non-Oravic” unit, ranged to the Fatic Superunit (Andrusov et al., 1973), with Lower Triassic to Cenomanian strata.

## **10. Pieniny Klippen Belt, Manín Unit (Western Carpathians):**

The Manín Unit (Lower Jurassic to Cenomanian) consists mainly of platform limestones, and is usually assigned to the Faticum (Mahel', 1978) but some authors prefer a Tatic affiliation of the Manín Unit (Hók, 2005).

### **A.3. Applied Methods**

Applied methods of study use lithofacies logging, microfacies evaluation based on thin section analysis (see chapter C.3.1, C.3.2 and C.4.1), heavy mineral analysis (see chapter C.4.2), geochemistry and geochemistry statistics and isotope geochemistry (see chapter C.4.5). A total of 361 samples were used for this study and are stored at the Department of Geodynamics and Sedimentology, thesis archive (for the whole sample list see Appendix 5).

### **A.4. Tunnel sampling strategy**

In the Lainz Tunnel it was possible to start sampling contract section LT33 in February 2007, sampling at the tunnelface ended with the breakthrough on May 8<sup>th</sup> 2009. The contract section LT31, heading NW towards LT33, was also sampled from June 29<sup>th</sup> 2008 until April 17<sup>th</sup> 2009.

Additional sampling was carried out in two vertical rescue pits (Veitingergasse, Angermayergasse). Work in rescue pit Veitingergasse lasted from September 2<sup>nd</sup> 2008 until December 19<sup>th</sup> 2008, in rescue pit Angermayergasse samples were achieved from July 1<sup>st</sup> 2009 until August 19<sup>th</sup> 2009. Altogether (LT33+LT31) 3360m of tunnel distance was studied. Tunneling was carried out traditionally with digger, mortiser and, if required, blasts, with the heading face being opened in three sections (calotte, stope and floor). Sampling was carried out in preferably short, constant distance as far as possible directly from the heading face in the tunnel. In December 2007 sampling reached 1006.2m. Due to the large amount and volume of the samples, the diploma thesis was limited to the first 1000m (Flysch units). Later on, less frequent sampling was performed for the flysch units, and a denser sampling pattern resumed when the tunnel section approached the SVK, the main interest of this PhD thesis.

Due to the dangerous working conditions in the tunnel, the aim was to gain regular samples but detailed sedimentological section logging was not possible. Several circumstances had to be regarded. According to the lithologies occurring in the tunnel, the time intervals varied for the individual blasts and securing arrangements. Obtaining fresh samples from the tunnel face was possible only in a very short time period, ranging from seconds to a few minutes. Depending on the stability of the rocks, the tunnel face was opened with a mortiser/power shovel or by blasts in several steps and immediately closed and covered with concrete. Additionally to the danger of rockfall from the fresh tunnel face it was also important to sidestep and avoid hindering the machines. The sample amount depended on the lithologies found, never exceeded a backpack load, had to be carried out of the tunnel on foot. Another challenge was that, for some time, two tunnel faces were active (LT33/LT31). Due to circumstances in the tunnel and bad traffic conditions on the way to the site often a whole day was spent getting to the tunnel, waiting for the „right“ moment, collecting the samples, bringing them out of the tunnel and into storage. Noteworthy is also that work in the tunnel never stopped and construction progress varied greatly over time. Regarding all the problems mentioned above, the aim was to obtain samples every 20-30m. If different lithologies were met at tunnel faces attempts were made to sample all of them as far as possible due to construction progress.

During geotechnical documentation, a tunnel documentation („Tunnelband“) was generated by the local engineering geologists. It displays a horizontal and vertical sectional view of the examined area. Along general lines, with the assigned lithologies and biostratigraphic data, the distribution of the formations is visible.



**Fig. 4 LT33:2522.1m** The author (on the left side) investigating rocks of the St.Veit Klippenzone.



**Fig. 5 LT33/2505.20m** The author taking samples of the St.Veit Klippenzone.



**Fig. 6 LT33/2558.50m** Tunnel face (SVK) beeing secured and covered with concrete



**Fig. 7 Picture of workmen and engineers at LT31/1385.00 (last station of LT31)**

## B. LITERATURE REVIEW AND PUBLISHED DATA

Cžjžek (1847, 1849) was the first who made a map of the SVK („Geognostische Karte der Umgebung Wiens“). He described grey crinoidal limestones assigning them a Doggerian age, grey argillaceous cephalopod limestones and red aptychi bearing limestones with chert nodules. Later (1852) Cžjžek mentioned red to green cherts (Malmian), white aptychi and chert nodules bearing crinoidal limestones.

Griesbach (1868, 1869) contributed an accurate map of the SVK, reporting fossiliferous Kössen Formation, light quartz sandstones (suggesting a Liassic age), Gresten limestones (also Liassic age ), Middle Jurassic argillaceous limestones, red to grey siliceous limestones (Bathonian), red crinoidal limestones, red chert and aptychi bearing limestones (Upper Jurassic) and white Neocomian aptychi marlstones/limestones. Neumayer (1886) and Uhlig (1890) were the first who made attempts to compare the SVK with the inner (= „pieniny“) Carpathian Klippenzone.

Stur (1894) published an improved map („Geologische Karte der Umgebungen Wiens“) and listed additional lithologies: „Werfener Schichten“ (= quartzsandstones), Middle Jurassic marlstones, red (Upper Jurassic) with white (Neocomian) cherts / aptychi bearing limestones and „Klausschichten“ (= red crinoidal limestones). He was the first to describe the aptychi bearing limestone klippe at Mauer („Schießstätte“).

In his detailed study „Die Klippe von St. Veit bei Wien“ Hochstetter (1897) compiled the knowledge of his time about the SVK together with his own, mainly palaeontological work. Additional geological descriptions of the SVK were made by Schaffer (1904, 1927), his work primarily reflects the results and opinions of previous authors.

Trauth (1907, 1921, 1923, 1930, 1950) was the first who gave a detailed survey of the rocks that belong to the SVK. His work is mainly based on macrofossil stratigraphy data (brachiopods, ammonites, bivalves). He compares the SVK with the Gresten Klippen Zone of Lower Austria and Upper Austria (e.g. Waidhofen/Ybbs area), and he named most of the units with (litho-)stratigraphic names such as „Blassensteinschichten“, „Rotenbergsschichten“, etc. He also compared units with the Pieniny Klippen Belt in Slovakia („pieninisch“, Trauth, 1921, 1930) without detailed correlations, interpreting the SVK as the westernmost continuation of the classical klippen of the Pieniny Klippen Belt. Trauth (1930) gave the following succession of strata of his „Klippen-Serie“ (from oldest to youngest):

1. Typical Kössen Formation (Upper Triassic, Rhaethian): medium to dark grey, bedded marly limestones and dark grey marly shales, rarely cherty. Bivalves are common as lumachelle layers (Lainzer Tiergarten: NNE Villa Hermes, W Kleefrische Wiese).
2. Gresten beds: light grey arkosic sandstones (probably Lower Jurassic, Hettangian; „Quarzitkonglomerat“ and „Quarzsandstein“ of Griesbach, 1869 and Hochstetter, 1897): coarse quartz sandstones with grey and reddish quartz in a whitish kaolinitic matrix; sometimes including quartz pebbles up to 2cm. Centimeter-thin coaly layers and reddish and grey claystones/shales may be present.
3. Gresten limestone, limy sandstones and spotted marly limestones (Lower Jurassic, Sinemurian-Pliensbachian-Toarcian?): dark grey, sandy limestones and crinoidal limestones, rarely spotted marly limestones and marls („Fleckenkalk“; „Lias-Fleckenmergel“); macrofossils like bivalves (e.g. *Gryphaea*) and brachiopods, ammonites (*Arietites*, *Schlotheimia*).
4. Dark grey crinoidal limestones, shales, spotted marls (Middle Jurassic, Bajocian-Bathonian): includes mainly dark grey limestones and marls („Neuhäuser Schichten“ according to Trauth, 1930), but also some cherty limestones and grey and red crinoidal limestones („Vilser Kalk“ according to Trauth, 1930). At Hohenauer Wiese dark grey sandy limestones with crinoids are dated by ammonites (*Stephanoceras*, *Perisphinctes*, *Parkinsonia*). Marls, shales and marly limestones („Posidonienschiefer“) are probably intercalated (abandoned Glasauer quarry, Gemeindeberg at St. Veit). Medium grey sandy marls and marly limestones without macrofossils are also present.
5. Light reddish to grey siliceous limestones (Middle Jurassic, Bathonian-Callovian?): hard siliceous and cherty limestones („Kieselkalke“, „Hornsteinkalke“, Trauth, 1930, at Gemeindebergkamm). Brachiopods (e.g. *Waldheimia*) and ammonites (*Stephanoceras*, *Perisphinctes*, *Phylloceras*) are present.
6. Red crinoidal limestones (Middle Jurassic, Callovian): only two outcrops of red crinoidal limestones with brachiopods („Vilser Kalk“ of Trauth, 1930) are reported by Trauth (1930) and were already covered in the 1930s.
7. Cherty limestones (Upper Jurassic, Kimmeridgian-Lower Tithonian?): red and greenish-grey limestones with chert nodules (dark red, grey) and layers („Hornsteinkalke“ and radiolarites), sometimes thin marly or shaly layers are present in between. Aptychi and radiolaria are present.

8. White to light grey limestones (Upper Jurassic-Neocomian): limestones with aptychi and grey to black chert layers and nodules, more marly and spotty in the upper (Neocomian) part and marly intercalations. *Calpionella* is present in thin sections.

These klippencore rocks are surrounded by flysch sediments („Klippenhüllflysch“: calcareous sandstones, micaceous sandstones, grey and red marls and shales). Trauth (1930) correlates the SVK both with the Gresten Klippenzone (his „westniederösterreichische Voralpenklippen“) and the Pieniny Klippen Belt. However, summing up his ideas on the geotectonic position, Trauth (1954) already noted also general similarities of the Jurassic facies of the Pieniny Klippenzone (especially in the Waag valley) and the Northern Calcareous Alps. He argued against a direct correlation to the Gresten Klippenzone because of missing Triassic rocks.

The most detailed younger work following Trauth (1930) was a survey by Janoschek et al. (1956). Based on outcrops at Vienna's district St. Veit and older work, especially Trauth (1930) from the Lainzer Tiergarten, Janoschek et al. (1956) described the composite stratigraphic klippencore succession from the SVK (from oldest to youngest, see Fig. 8):

1. Dolomites of probably Triassic age
2. Rhaetian limestones and sandstones with fossils (brachiopods, bivalves, etc.) (Upper Triassic)
3. Grey-greenish shales (Lower Jurassic)
4. Gresten-type arkosic sandstones (Lower Jurassic)
5. Sandy dark limestones, black marls, Gresten-type marly limestones (Lower Jurassic)
6. Shales, marls and marly and sandy limestones (Middle Jurassic)
7. Grey-greenish shales and cherty shales (Upper Jurassic)
8. Red crinoidal limestones (Upper Jurassic, Kimmeridgian-Tithonian)
9. Red cherty limestones (Upper Jurassic)
10. White apytychus limestones and marls (Tithonian-Neocomian)

overlain by a flysch succession of Albian-Cenomanian age and some volcanites.

Janoschek et al. (1956) concluded, based on Trauth (1930, 1954) that the St. Veit Klippenzone belongs to the Pieniny Klippen Zone of the Carpathians („piennidische Klippenzone“) based on facies relations.

Following Janoschek et al. (1956) Prey began to map the area for the Geological Survey of Austria and made several important revisions of the composite succession (Prey, 1975:

Lainzer Tiergarten; Prey, 1979: Baunzen-Klippe), especially in ascribing the quartzitic sandstones to the Upper Triassic Keuper, thus questioning a correlation to Gresten sandstones:

1. Keuper quartzitic arkose and variegated claystones/shales (Upper Triassic)
2. Kössen beds - fossiliferous limestones (Upper Triassic, Rhätian)
3. Black shales, dark limestones and crinoidal limestones (Lower Jurassic)
4. Marls, marly limestones, sandy marls (Middle Jurassic)
5. Grey-greenish shales and cherty shales (upper Middle Jurassic - lower Upper Jurassic)
6. Red cherty limestones and radiolarites (Upper Jurassic)
7. Aptychus limestones and marls (Tithonian-Neocomian)

These klippencore successions are, according to Prey (1975), directly overlain with a sedimentary contact by a flysch cover („Klippenhüllflysch“) of greenish and red shales with calcareous sandstones and muscovite-bearing sandstones and picrites of Albian-Cenomanian age, belonging to the base of the Kahlenberg Nappe. Rarely, an Albian flysch with green and black shales and quartzose sandstones („Bartbergschichten“) may also be present in this interval (Prey, 1979). Prey (1979) was the first to explicitly include the SVK as the base of the Kahlenberg Flysch Nappe. Based on this argument and differences in the Jurassic facies, Prey (1979) interpreted the SVK as a paleogeographic element north of the Pieniny Klippen Zone („Pieninische Klippenzone“), but south of the Gresten Klippenzone depositional area, and as a part of the primary basement of the Rhenodanubian Flysch.

Later on, Schnabel (1997, 2002) largely accepted the concepts of Prey but renamed some of the lithounits as formations (Hohenauer Wiese Formation comprising Middle Jurassic limestones, Hütteldorf Formation comprising the mid-Cretaceous flysch cover). His succession of the SVK as reproduced on the map sheet Baden and shortly described in Schnabel (2002) includes:

1. Arkosic sandstones, quartz sandstones („Keuper“) (Upper Triassic)
2. Kössen Formation - dark limestones, marls, rich in fossils (Upper Triassic, Rhätian)
3. Gresten Formation - including Posidonia shales, sandy limestones, marls, marly limestones (Lower-Middle Jurassic)
4. Hohenauer Wiese Formation - sandy limestones, crinoidal limestones, (Middle Jurassic, Bajocian-Bathonian)
5. Red crinoidal limestones (Middle Jurassic, Callovian)
6. Rotenberg Formation - cherty limestones and radiolarites (Upper Jurassic)
7. Aptychus limestone - light-colored marly limestone (Tithonian-Neocomian)

This klippencore succession is overlain by flysch (Gaultflysch and Hütteldorf Formation) and picrites. Schnabel, by correlating parts of these rocks with Gresten Formation, therefore implies a correlation to the Gresten Klippenzone; however, he also indicates a paleogeographic position at the facies transition between Keuper facies and calcalpine facies, i.e. at the northern margin of Northern Calcareous Alps or Austroalpine unit (Kössen Formation, Schnabel, 2002), and, last but not least, he lumps the SVK together with the Kahlenberg Nappe and the Ybbsitz Zone into the Penninic realm („Penninikum und Äquivalente“, Schnabel, 2002), which, consequently, indicates a (south) Penninic derivation, based on the overlying flysch successions and the occurrence of basic volcanism („Picrite“) as questionable analogies to Ybbsitz Zone ophiolites. Within these few pages of the publication of Schnabel (2002) the fundamental problem in reconstructing the geotectonic position of the St. Veit Klippenzone is highlighted, i.e. either Helvetic (=Gresten Klippenzone), or Penninic (=Ybbsitz Klippenzone), or Australpine affinities (=calcalpine facies).

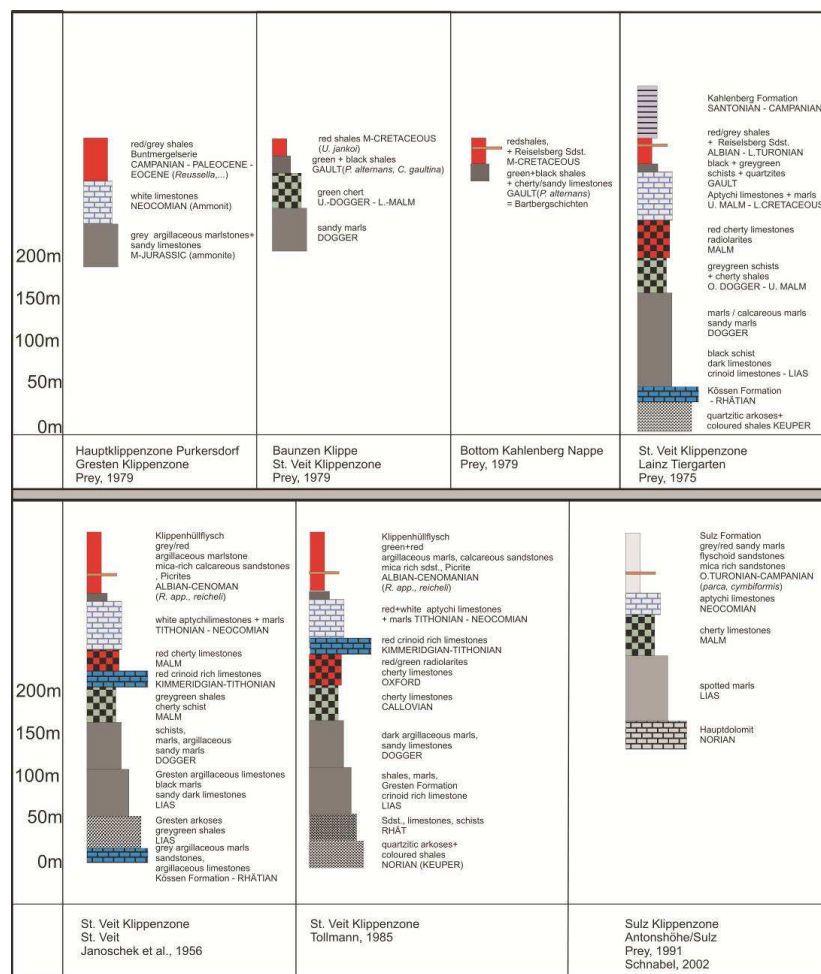


**Fig. 8 Composite stratigraphic succession of St. Veit Klippenzone and related klippen successions in the Wienerwald area according to Janoschek et al. (1956), Prey (1975, 1979, 1991), Tollmann (1985) and Schnabel (2002).**

The most recent overview on the St. Veit Klippenzone was given by Wessely (2006). His stratigraphic succession (based on Prey, 1975 and Schnabel, 1997) named:

1. Keuper quartzites (Upper Triassic): light grey and pink quartz and withish kaolinitic matrix of violet-red to greenish clay.
2. Kössen Formation (Rhaetian): fossiliferous, dark, bedded marly limestones, limestones and marls with bivalves and brachiopods (e.g. *Rhaetina gregaria*).
3. Gresten Formation (Lower Jurassic): coal-bearing sandstones, dark sandy Gresten limestones, grey crinoidal limestones, brownish-black marly shales and marly limestones. Ammonites (e.g. *Arietites*) indicate lower/middle Liassic; bivalves are common.
4. Posidonia marls (Middle Jurassic): marly/sandy facies
5. Hohenauer Wiese Formation (Middle Jurassic): grey marly sandstones, sandy limestones, crinoidal limestones, cherty shales and limestones with ammonites of Bajocian, Bathonian and Callovian.
6. Rotenberg Formation (Upper Jurassic): red, green and grey radiolarites.
7. Red crinoidal limestones (Kimmeridgian)
8. Aptychus limestone: white limestone with black chert nodules (Tithonian-Neocomian)

Wessely (2006) argues for strong similarities with the Gresten Klippenzone, and thus a geotectonic position at the European shelf north of the Penninic Ocean (with the Ybbsitz Zone).

## **B.1. Lithostratigraphic nomenclature of the St. Veit Klippenzone**

According to the stratigraphic chart of Austria (Piller et al., 2004) and the explanatory notes (Wagreich et al., in preparation) the following lithostratigraphic units are known and/or defined from the St. Veit Klippenzone, and can be found also on the most recent geological map (Schnabel, 1997: 1:50.000 map sheet ÖK58 Baden):

### ***B.1.1. Hohenauer Wiese Formation***

Type area: UTM map sheet 5325 Baden, ÖK 50 map sheet 58 Baden, St. Veit Klippenzone of the Lainzer Tiergarten

Type section: outcrop at Hohenauer Wiese in Lainzer Tiergarten, but no type section given so far

Reference section(s): not given

Derivation of name: After the Hohenauer Wiese, a meadow in the Lainzer Tiergarten, currently used as pasture for so-called „Heckrinder”, first named by Schnabel (1997, 2002)

Synonyms: „dunkelgraue feinsandige Kalke und graue Crinoidenkalke” (TRAUTH, 1930)

Lithology: dark grey, sandy limestones with crinoid debris

Fossils: brachiopods, bivalves (e.g. *Gryphaea*), ammonites (e.g. *Lytoceras*), belemnites

Chronostratigraphic age: Bajocian-Bathonian

Overlying units: not defined, but probably crinoid limestones

Geographic distribution: Lainzer Tiergarten

Remarks: Schnabel (1997, 2002) introduced the term Hohenauer Wiese-Formation without giving any description or type section. It is not clear if this formation includes all types of grey crinoid-bearing and/or sandy limestones of the Lower to Middle Jurassic of the St. Veit Klippenzone or only the dark grey limestones with ammonites of the Hohenauer Wiese.

### ***B.1.2. Rote Crinoidenkalke (red crinoidal limestone)***

Type area: UTM map sheet 5325 Baden, ÖK 50 map sheet 58 Baden, St. Veit Klippenzone of the Lainzer Tiergarten

Derivation of name: after the abundance of crinoids

Lithology: grey and red coarse to fine-grained crinoid limestones, partly sandy to detrital grey limestones including transitions into grey mottled pelagic marly limestones and siliceous limestones

Fossils: crinoids, rare ammonites

Chronostratigraphic age: Liassic to Doggerian

Biostratigraphy: ammonites

Thickness: several tens of meters

Underlying units: Hohenauer Wiese Formation

Overlying units: probably radiolarites (Rotenberg Formation) and siliceous limestones

Geographic distribution: Lainzer Tiergarten

Remarks: in the St. Veit Klippenzone grey limestones are more common than red ones

#### ***B.1.3. Rotenberg-Formation (Rotenberg Formation)***

Type area: UTM map sheet 5325 Baden, ÖK 50 map sheet 58 Baden, Roter Berg at Ober St. Veit, Vienna; reference sections at UTM map sheet 4203 Waidhofen an der Ybbs (ÖK 50, map sheet 71 Ybbsitz)

Type section: the quarry Reidl 2.5km WSW Ybbsitz serves as a modern type section, described by Schnabel (1979) and logged in detail by Decker (1987, 1990) (E 014°51'50", N 47°56'20"); Trauth (1930) named an old abandoned and by now largely covered quarry at Rotenberg in Vienna. During works for tunneling the Rotenberg was surveyed and some minor outcrops were sampled.

Reference section(s): Reference sections named by Decker (1990) and Ožvoldová & Faupl (1993) in the Ybbsitz Klippenzone at Ybbsitz and Scheibbs; also includes the klippe of Mauer (Antonshöhe) in Vienna (Prey, 1991)

Derivation of name: After the Rotenberg (Roter Berg/former Rosenberg) at Ober St. Veit in Vienna, first description by Trauth (1950: Rotenberg-Schichten: „...roter oder bunter ... kieselreicher ...Radiolarit-zeigender Kalk“).

Synonyms: Hornsteinkalke (Trauth, 1930)

Lithology: predominantly red radiolarites; at the base Fe/Mn mineralized, predominantly green shales and cherts; at the top transition into red siliceous limestones

Fossils: radiolaria

Origin, facies: deep-water pelagic sediments below CCD, partly radiolarian turbidites, hydrothermal mineralizations at ocean floor/mid-oceanic ridge environment

Chronostratigraphic age: middle Callovian - Oxfordian, partly probably also Kimmeridgian (Ožvoldová & Faupl, 1993)

Biostratigraphy: radiolarians (UA 5-6 to UA 7-8; Ožvoldová & Faupl, 1993)

Thickness: 20m

Lithostratigraphic subdivision: the lower part contains cherts, the higher part contains mainly radiolarites

Underlying units: serpentinites (Ybbsitz area) or crinoid limestones (St. Veit Klippenzone); lower boundary by faults

Overlying units: Fasselgraben Formation (*Calpionella*-limestones), upper boundary defined by the transition from radiolarites to cherty grey limestones

Geographic distribution: from the Ybbsitz Klippenzone at Ybbsitz to the St. Veit Klippenzone in Vienna

Remarks: The klippe of Mauer in Vienna (Prey, 1991) includes a prehistoric mine for cherts

#### ***B.1.4. Fasselgraben-Formation (Fasselgraben Formation)***

Type area: UTM map sheet 4203 Waidhofen an der Ybbs, ÖK 50 map sheet 71 Ybbsitz; area of Haselgraben, Lower Austria

Type section: originally Trauth named the „Fasselgrabenklippe N. des hinteren Eichbergs im Lainzer Tiergarten“ of the St. Veit Klippenzone; creek S Haselgraben, 5.3 km ENE Ybbsitz (Decker, 1990)

Reference section(s): Brettal tectonic window, 3.8 km SE Gresten (Decker, 1987, 1990).

Derivation of name: Fasselgraben is a creek in Lainzer Tiergarten, St. Veit Klippenzone, Vienna; named by Trauth (1950), later on re-defined by Decker (1987, 1990)

Synonyms: Aptychenkalk, Flysch-Neokom (Ruttner & Schnabel, 1988, ÖK 50 map sheet 71).

Lithology: light grey and red calpionellid micritic limestones and limestone-marl rhythmites with chert nodules; rarely lamination visible; minor and thin sandstone turbidites and matrix-supported breccias; red shales at the base; heavy minerals garnet, apatite and zircon-dominated.

Fossils: radiolaria, calpionellids, aptychi, sponge spicules

Origin, facies: pelagic fine-grained carbonates, below aragonite compensation depth, but above calcite compensation depth; redeposition of radiolarians by bottom currents

Chronostratigraphic age: Tithonian-Berriasian

Biostratigraphy: *Crassicollaria* – *Calpionella* – *Calpionellopsis* Zones

Thickness: 20m

Lithostratigraphic subdivision: „Untere -“ and „Obere Fasselgraben-Schichten“ (Trauth, 1950).

Underlying units: Rotenberg Formation

Overlying units: Glosbach Formation

Geographic distribution: Lower Austria to Vienna (Ybbsitz Klippen Zone and St. Veit Klippenzone)

Remarks: Fasselgraben Formation was introduced by Trauth (1950,1954: Fasselgraben-Schichten,), regarded as a synonym of Blassenstein Formation by Kühn (1962), nowadays used for former Aptychenkalke of the Ybbsitz Klippen Zone

Complementary references: Janoschek et al. (1956); Decker & Rögl (1988)

## C. STRUCTURAL, STRATIGRAPHY AND LITHOLOGY RESULTS

### C.1. Structural Data

Structural data from the first 1000m are discussed in Pfersmann (2009).

The Kahlenberg Nappe and the St.Veit Klippen Zone showed similar values of dip/direction, mainly to the NW, along the tunnel course, but changed from station 1340 (LT31) to station 869 (LT31) to dips to the SE, indicating an anticlinal structure. This observation is also supported by age data. In the center of this anticlinal structure Keuper sediments can be found (LT31/1340m to LT31/1150m), whereas biostratigraphic informations e.g. from nannofossils (LT33 2666m lower-middle Jurassic), radiolaria (Veitingergasse lower-middle Bajocian) show a younging in both directions. In Fig. 11 a simplified version of the „Tunnelband” is given. The change of dip can easily be observed comparing the vertical profile next to the center of the anticlinal structure from section LT33, to the vertical profile from section LT31. Right in the center of the structure and in the mixing zones (e.g. LT31/1150m to LT31/869m) the direction of dip changed several times, due to strong tectonic deformation. All in all the Lainz Tunnel section indicates the presence of a large, but internally strong deformed anticline with Klippenzone rocks in the core and surrounding Flysch units. Dips are generally to the NW in the northwestern part of the tunnel, and change to SE (but strongly mixed) in the southeasternmost part of the tunnel.

Particular in the mixing zones a tectonic „Block in Matrix” structure was encountered. One good example of this structure is given in Fig. 12. This figure shows a sketch of the tunnel face at LT31/1197.50m (made by the geologist on duty from the office Bechthold). Several blocks of hard argillaceous limestones are embedded into a soft dissected marlstone/shale matrix. In this case the blocks can be expected to be of Jurassic age and the matrix is most probably of Flysch material („Hüllflysch”). It is not possible to give a representative picture of this tunnel face, because this structure causes construction problems and therefore it was needed to open the tunnel face in several small sections.

Averaged dip/direction values (ss) are:

Kahlenberg Formation from 1000m (LT33) to 1200m (LT33): 272/43

Kahlenberg Formation together with Hütteldorf Formation 1200m (LT33) to 2165m (LT33): 279/43

St. Veit Klippenzone 2165m (LT33) to 1340m (LT31): 270/47

St. Veit Klippenzone 1340m (LT31) to 1150m (LT31) center anticlinal structure: 129/10

St. Veit Klippenzone mixed with Hütteldorf Formation 1150m (LT31) to 869m (LT31): 161/11

Hütteldorf Formation 799m (LT31) to 869m (LT31): 159/24

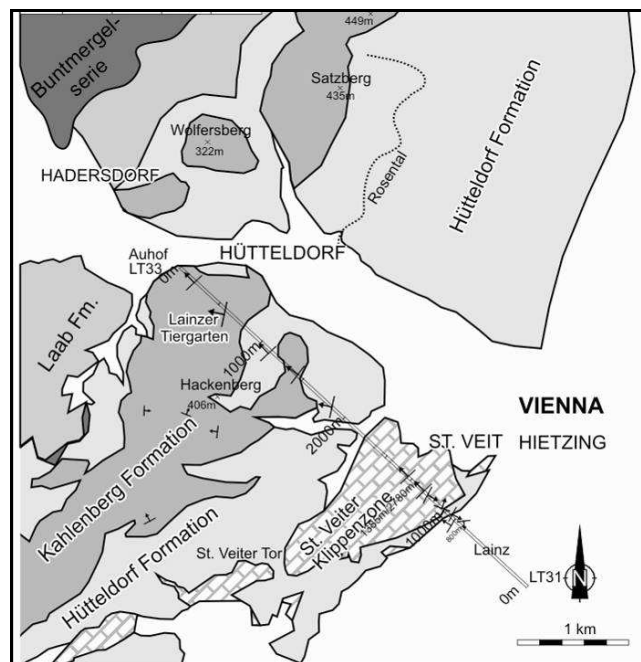
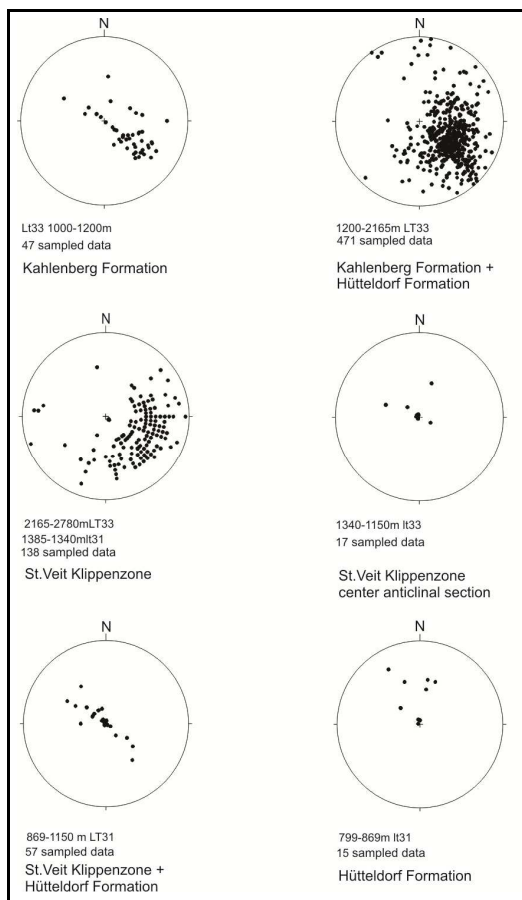


**Fig. 10 Tunnel section with indications of mean dip of strata observed.**

**Fig.9 Bedding planes in Schmidt' net segmented for tunnel section intervals (LT33/station 1000 to 2780m and LT31/station 799 to 1385m ).**

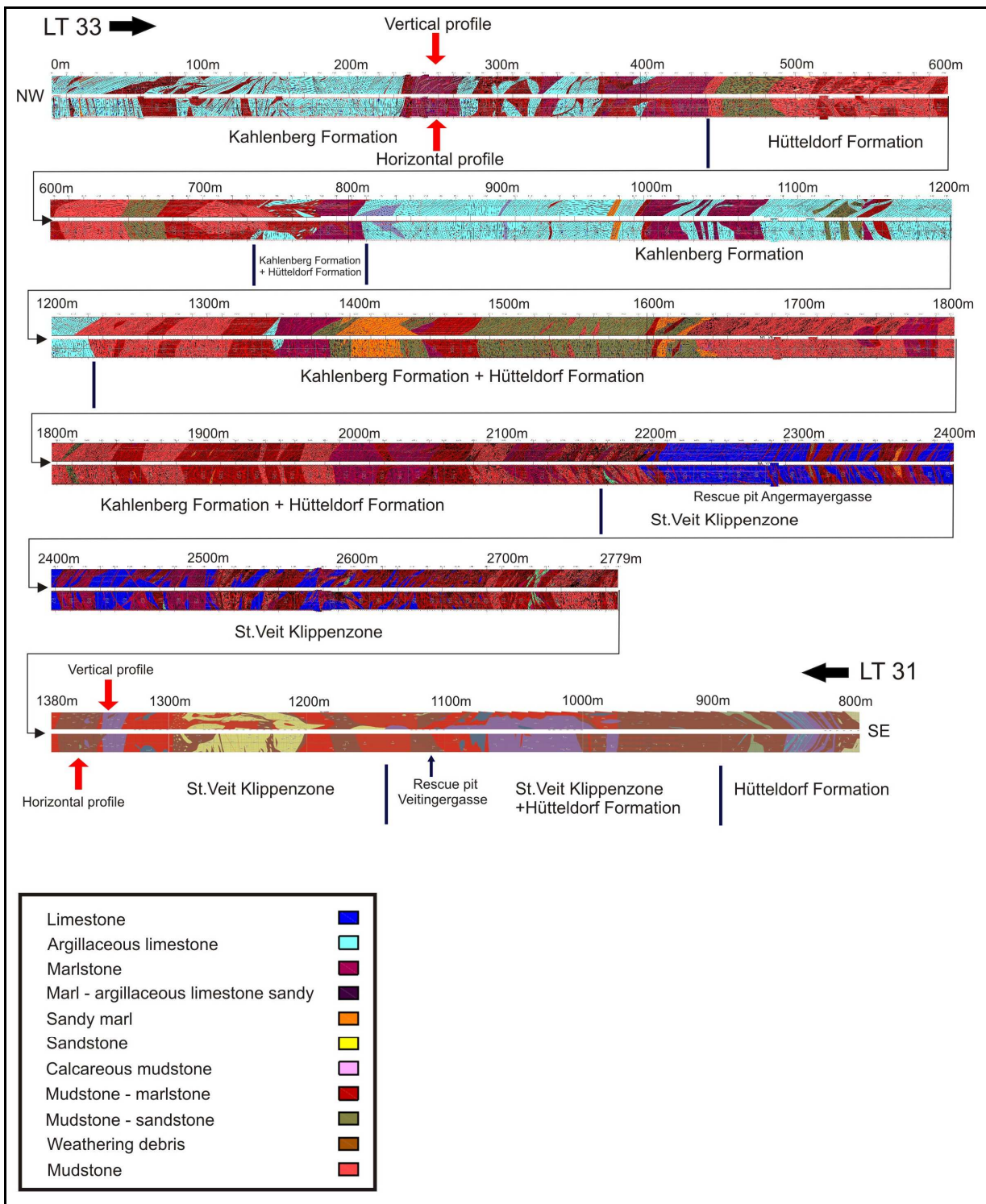


**Fig. 11 Simplified and adapted „Tunnelband“ from the Lainz Tunnel (LT33 + LT31), showing a vertical and a horizontal profile with formations assigned. Between station 1300 to 1200m (LT31) (Keuper sandstone) the center of the anticlinal structure can be found. The original „Tunnelband“ was generated and provided by office Bechthold. Different colour impressions comparing LT33 and LT31 are caused by different mapping styles of the geologists.**

Bauwerk: LT 31	Vortrieb: W NEU	Ausbuch: Kalotte	Querschnitt: RQ 51D	Bearbeiter: Schierl	Datum: 11.02.2009 Ifd. Nr.: 108
Station [m]: 1197,50	Abschlagslänge [m]: 1.00	Projekt km: 4+813.3	Überlagerung [m]: 49.9	Richtung [°]: 316	Uhrzeit: 13:35 Maßstab: 1:100

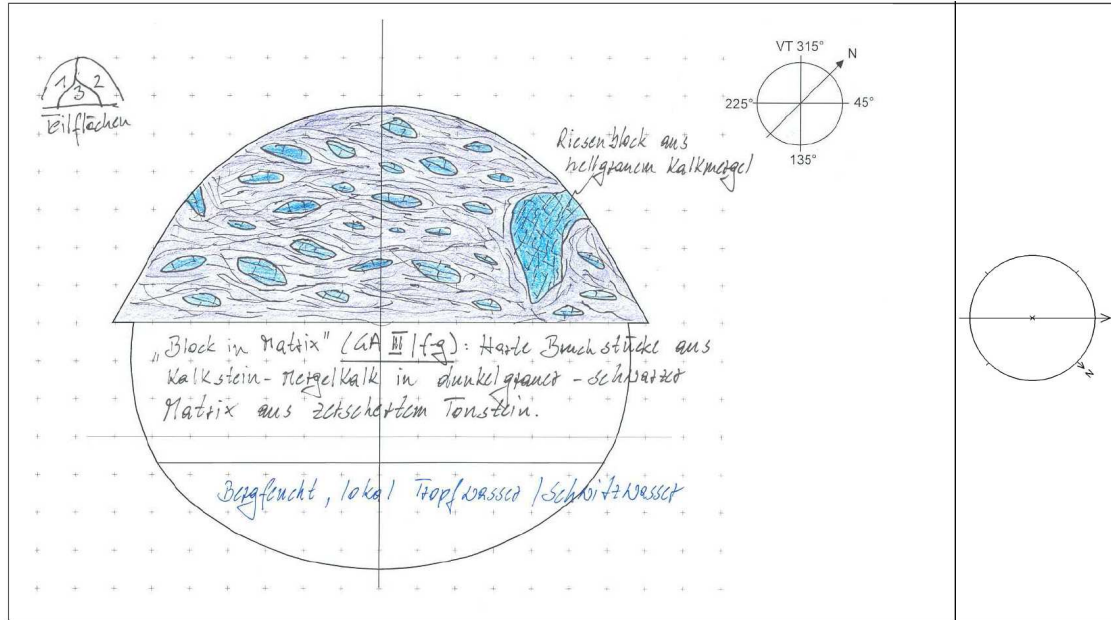


**Fig. 12** Sketch of the tunnel face at LT31/1197.5m showing an example of „block in matrix“ structure. In this case the blocks can be expected to be of Jurassic age and the matrix is most probably of Flysch material ( sketch provided by office Bechthold).

## **C.2. The Lainz Tunnel section - stratigraphy & lithofacies**

Based on the sampled intervals of the Lainz Tunnel, the tunnel section can be subdivided into two major geological units:

- (1) the flysch units (Kahlenberg Nappe)
- (2) the St. Veit Klippenzone

However, due to strong deformation these units can not be separated easily, but transitional zones with strong tectonic mixing of rocks of these two units occur. In general, the Lainz Tunnel and the geological mapping suggest a broad SW-NE trending anticline with a core of SVK rocks surrounded both in the NW and the SE by younger flysch rocks. Anyhow, in detail, a much more complex picture of a „block in matrix” type of tectonic melange describes the structure of the SVK far better.

### **C.2.1. The stratigraphic profile of the Flyschzone (Kahlenberg Nappe) and the St. Veit Klippenzone in the Lainz Tunnel (from youngest to oldest)**

Kahlenberg Formation and Hüttdorf Formation are described in Pfersmann (2009).

At the base of the Hüttdorf Formation occurs a „Picrite”/strongly altered basalt.

### **C.2.2. St. Veit Klippenzone in the Lainz Tunnel**

#### **Green chert (Valanginian):**

The cherts occur as hard, brittle, isolated blocks, embedded in a shale/marl matrix.

#### **White silicified limestone (Uppermost part of Middle and Late Berriasian):**

The limestone is conchate breaking, fine-grained, white to light grey colour and often embedded into a black shale matrix. Carbonate contents range from 53% to 65%.

#### **Grey marl to argillaceous limestone (Tithonian-Valanginian):**

hard, brittle, breaking, with thinner layers up to layers in decimeter range, grey colour, often bioturbated, with carbonate contents of 48% up to 85%.

### **Red chert and red shale (Lower/Middle Bajocian):**

The dark red to red-brown, hard, brittle, conchate breaking chert occurs thin bedded up to several dm. Together with a calcareous mudstone, dark red to red-brown coloured, rather soft, splintered breaking, thin-bedded up to several centimeters, sometimes aptychi bearing, with carbonate contents up to 21%.

### **Sandy marl (Liassic/Doggerian):**

grey to dark grey, fine grained, massive, sometimes laminated, hard calcareous sandstones, often bioturbated, thickness up to several decimeters, carbonate contents are around 18 %.

### **Coarse Sandstone (Norian/Keuper?):**

coarse, sometimes light-pink sandstone, consisting mainly of quartz, little feldspar and calcite. The sandstone occurs with some red to green shales embedding the sandstone blocks.

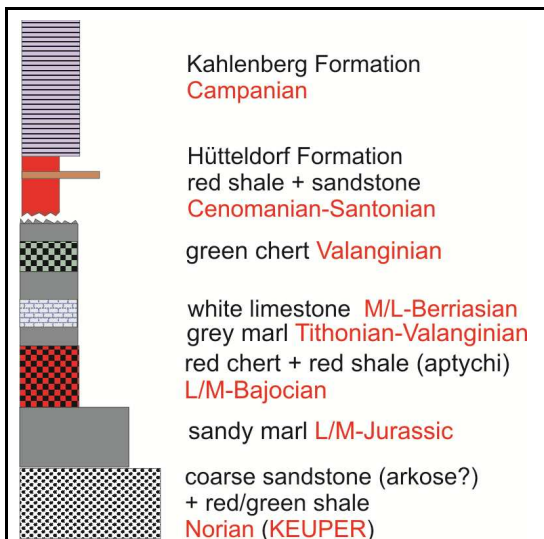


**Fig. 13 Composite stratigraphic log from the Lainz tunnel (no scale).**



**Fig. 14 Legend of lithologies for Fig. 13, Fig. 15.**

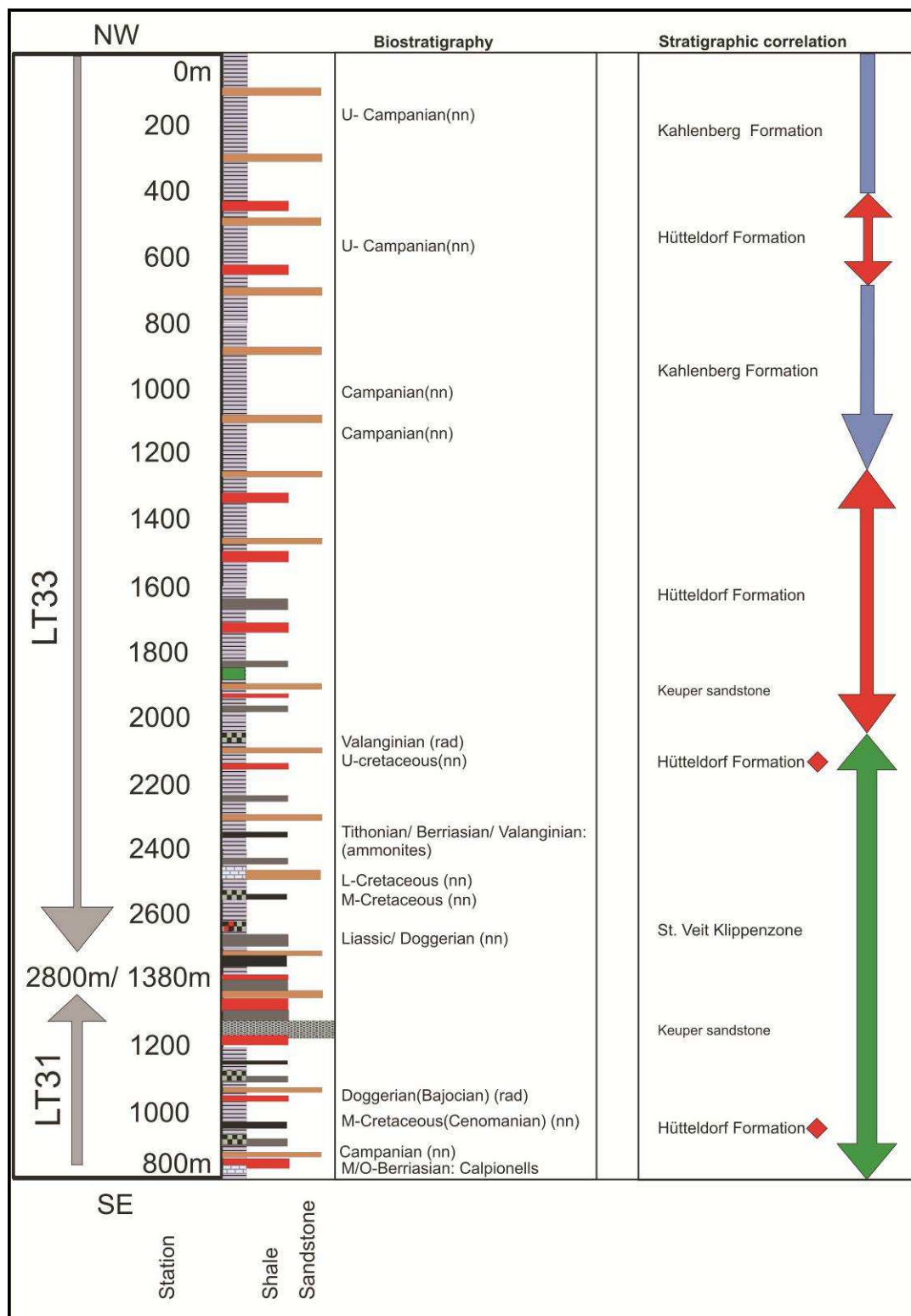


**Fig. 15** Strongly simplified section from the Lainz tunnel (lithologies see Fig. 14).

**In the following, new information for the flysch units from the Lainz Tunnel is given and the SVK sections are described in detail.**

### **C.3. Flysch Units Description**

The diploma thesis of Clemens Pfersmann (Pfersmann, 2009) and a following publication of the main scientific results (Pfersmann & Wagreich, 2009) deal with the first 1000m of the Lainz Tunnel in the Rhenodanubian Flysch Zone, comprising Hüttdorf-Formation and Kahlenberg-Formation.

The main results of this work were:

In the first 1000m of the tunnel (section LT33), heading towards SE, only rocks of the Flysch units, mainly Kahlenberg Formation, were found. The rocks consisted of pelites, without makrofossils, but bearing tracefossils. In some sequences graded turbiditic sandstones, showing cross-stratification, were found.

Parts associated with the Kahlenberg Formation consisted of lightgrey to greyblue fine-grained, banked, hard calcareous sandstone, lightgrey hard marls and grey, greygreen or greybrown marlstones. Typical carbonate contents lie between 50 to 70% (argillaceous limestones), carbonate-free shales occur very seldom.

Nannofossils found show Campanium ages, starting with nannozones CC20-22ab (Upper-Campanium) in the beginning of the tunnel, changing from 541.9m on to nannozones CC18b-19 (Lower-Campanium).

Older parts were not found, but that could be caused by the low carbonate contents in the shale-rich sections of the tunnel.

Rocks associated with the Hüttdorf Formation consisted mainly of darkred to redbrown, green or grey coloured shales/shale marl sequences. The shales bore mainly no carbonate, seldom some layers showed contents up to 20%. Additionally thin, stratified sandstone-layers and calcareous sandstones occurred. The pelitic parts were mostly tectonically dissociated.

Within the Hüttdorf Formation some whitegrey volcanic ash layers were found.

In general, the rocks of the Kahlenberg Formation and the Hüttdorf Formation were strongly deformed, folded and partly mixed up. Additional information and new results from the flysch units are given below. Biostratigraphic information from the tunnel section include nannofossil samples (evaluated by Michael Wagreich), washed samples and thin sections, dealing mainly with foraminifera and radiolaria (determined by Marta Bak, Krakow). A few pollen samples of different Jurassic strata were tested by Polina Pavlishina (Sofia), but no palynological remnants have been found.

### C.3.1. Kahlenberg Formation

#### C.3.1.1. Biostratigraphic Data

LT33		1075,9	1103,6	1172,8	2113,4	2229,5		2552,0	2552,2
Preservation		p	vp	m	m	vp		vp	vp
Abundance		5	2	15	1	2		1	1
Ahmuellerella octoradiata				x					
Arkhangelskiella cymbiformis				x					
Broinsonia enormis		x							
Broinsonia parca constricta		x	x						
Broinsonia parca parca		x							
Biscutum cf. magnum				x					
Calculites obscurus		x	x	x		x			
Calculites ovalis		x	x						
Chiastozygus litterarius		x	x	x					
Corlithion exiguum					x				
Cribrosphaerella ehrenbergii		x	x	x					
Cyclagelosphaera sp.						x			
Eiffellithus eximus		x		x	x				
Eiffellithus turiseiffelii		x		x	x				
Gartnerago obliquum		x							
Lithastrinus grillii				x					
Lithraphidites cf. acutus						x			
Lithraphidites carniolensis		x		x	x				
Lucianorhabdus cayeuxii		x	x	x		x			
Lucianorhabdus cayeuxii B		x		x					
Lucianorhabdus maleformis		x				x			
Kamptnerius magnificus				x					
Manivitella pommatoidea		x	x						
Micula decussata		x	x	x	x	x			
Prediscosphaera cretacea		x	x	x	x				
Quadrum cf. gartneri		x							
Reinhardtites anthophorus		x		x					
Rhagodiscus angustus		x							
Rhagodiscus reniformis						x			
Stradneria crenulata		x		x	x		x	x	
Tranolithus minimus		x	x						
Tranolithus orionatus		x	x						
Watznaueria barnesae		x	x	x	x	x	x	x	
Zeugrhabdotus embergeri							x	x	
Zygodiscus diplogrammus		x		x					
Zygodiscus sp.							x		
CC-Nanno Zones	18b-19	18-19	17-19	14-22	17-19		Cretac.	CC10	
AGE	L.ower CAMPANIAN					CENOM			

**Fig. 16 Results of nannofossil analysis LT33, from 1000 - 2593m, (only samples with nannofossil markers included), zonal marker species indicated grey (Preservation: vp - very poor; p - poor; m - medium; abundance in nannofossils per field(s) of view). Nannofossil standard zonation by Perch-Nielsen (1985: CC zones).**

LT31		841,5	857,0#2		898,0	962,5	993,5#2	1039,5
<i>Preservation</i>		p	m		p	p	p	m
<i>Abundance</i>		2	4		2	5	1	8
<i>Arkhangelskiella cymbiformis</i>								
<i>Braarudosphaera bigelowi</i>					x	x		
<i>Broinsonia parca constricta</i>	x							
<i>Broinsonia parca parca</i>	x							
<i>Biscutum constans</i>				x				
<i>Biscutum cf. magnum</i>	x							
<i>Calculites obscurus</i>		x						
<i>Calculites ovalis</i>	x							
<i>Chiastozygus litterarius</i>	x							
<i>Corllithion kennedyi</i>				x		x		
<i>Cribrosphaerella ehrenbergii</i>	x							
<i>Eiffellithus eximius</i>	x	x						
<i>Eiffellithus turriseiffelii</i>	x			x				
<i>Eprolithus floralis</i>			x	x	x	x		
<i>Gartnerago obliquum</i>	x							
<i>Lithastrinus cf. septenarius</i>				x		x		
<i>Lithraphidites carniolensis</i>				x				
<i>Lucianorhabdus cayeuxii</i>		x						
<i>Lucianorhabdus cf. maleformis</i>	x			x		x		
<i>Manivitella pemmatoides</i>			x	x				
<i>Micula decussata</i>	x	x						
<i>Nannoconus sp.</i>					x			
<i>Nannoconus truitti</i>					x			
<i>Prediscosphaera cretacea</i>	x	x		x		x		
<i>Radiolithus planus</i>				x				
<i>Reinhardtites anthophorus</i>	x							
<i>Rhagodiscus splendens</i>				x				
<i>Stradneria crenulata</i>	x	x		x	x			
<i>Tranolithus orionatus</i>	x	x		x				
<i>Watznaueria barnesae</i>	x	x	x	x	x	x	x	
<i>Zygodiscus diplogrammus</i>	x		x	x				
<i>Zygodiscus erectus</i>	x	x		x				
<b>CC-Nanno Zones</b>	<b>18b-19</b>	<b>17b-19</b>		<b>8-10</b>	<b>10</b>	<b>8-10</b>	<b>10</b>	
<b>AGE</b>	<b>L. CAMP.</b>		<b>ALB/CEN</b>					

**Fig. 17 Results of nannofossil analysis LT31, from 841.5 - 1039m (only samples with nannofossil markers included). For legend and abbreviations see Fig. 16.**

### C.3.2. *Hütteldorf Formation in the Lainz Tunnel*

#### C.3.2.1. *Biostratigraphic Data*

At LT31/ 962.5m and 1039.5m the marker species *Corollithion kennedyi* occurs together with *Eprolithus floralis*, *Eprolithus* cf. *octopetalus* and *Lithastrinus* cf. *septenarius* indicating a Cenomanian to earliest Turonian age (nannofossil zone CC10) for that part of the Hütteldorf Formation. At LT31 993.5m *Nannoconus truitti* and *Eprolithus floralis* again indicate a middle Cretaceous age. At LT33, 2592.2m *Lithraphidites* cf. *acutus* confirms again a Cenomanian age (CC10).

Along the tunnel course, the Hütteldorf Formation was sometimes encountered in sections attributed in general to the St.Veit Klippenzone. This was caused by tectonic mixing of the Formations (see also Fig. 11). In one case (LT33/2576m) it was possible to differentiate the units, not only by their lithologies, but also with a thin-section showing foraminifera species (*Marginotruncana* spp.) which is most probably Upper Cretaceous.

The picture from the tunnel face at LT33/2576m (Fig. 18) and the corresponding sketch (Fig. 19) give a good impression of the tectonic situation. The lithologies from the St.Veit Klippenzone (e.g. radiolarites) are placed next to lithologies from the Hütteldorf Formation (e.g. red marls) due to tectonical processes.



**Fig. 18** Tunnel face at LT33/2576m, lithologies from the Hütteldorf Formation (red shales) are tectonically mixed with rocks from the St.Veit Klippenzone (brownish radiolarite and grey limestones).

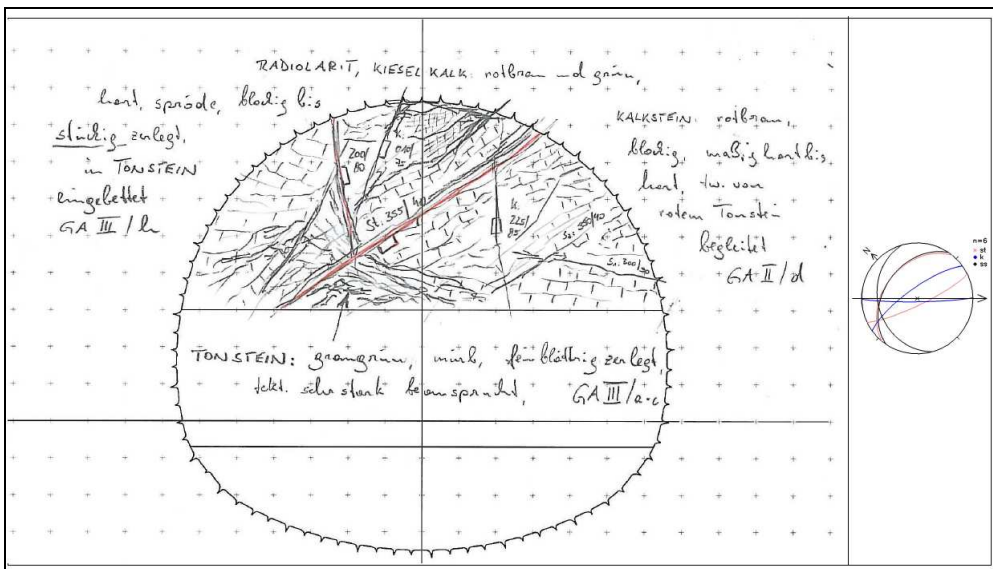


**Fig. 19** Sketch from the tunnel face at LT33/2576m showing fault zones. The different lithologies are classified according to their rheology (provided by office Bechthold).

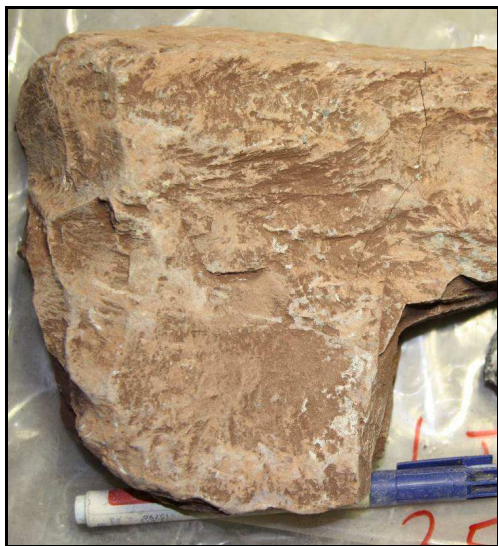


**Fig. 20** Red marlstone from LT33/2576m.

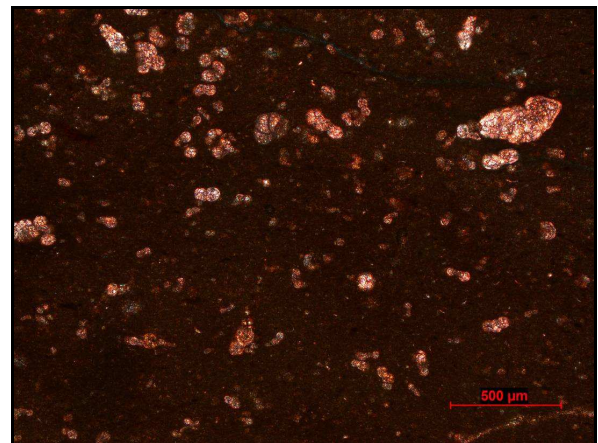


**Fig. 21** Thin-section from LT33/2576m, red marlstone with foraminifera *Marginotruncana* spp. Lower/ Upper Cretaceous.

### **C.3.2.2. Mineralogy of additional rock types within the Hütteldorf Formation in the Lainz Tunnel**

Additional lithologies, that have not been found in the first 1000m of the Lainz Tunnel are a dolomite breccia at 1874m (LT33), a strongly altered volcanite at LT33/1850m and at 1862m (LT33) a strongly altered basalt. These lithologies were sampled and are described in the following.

#### **Dolomite breccia:**

At 1874m (LT33) a grey beige coloured block, embedded in a red brown shale matrix, was sampled. The strongly fragmented surrounding matrix also contained blocks of sandy marls and strongly altered basalt („Picrite“). The components of the block averaged up to 5mm. In thin sections the dolomite breccia shows a non-planar texture with crystals in a xenotopic sieve mosaic.



**Fig. 22 Tunnel face at LT33/1873.40m, the block of dolomite breccia is visible at the right bottom.**



**Fig. 23** Partial view of the right bottom tunnel face at LT33/1873.40m showing a block of dolomite breccia. Bottomline of the picture measures approx. 60cm.

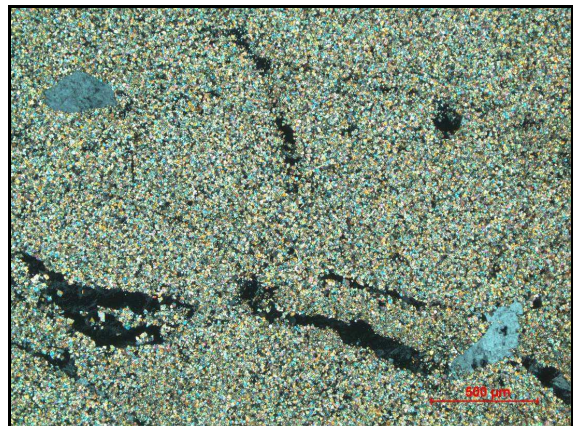


**Fig. 24** Thin-section of the dolomite breccia at LT33/1874m texture: non-planar crystals in a xenotopic mosaic (XPL).

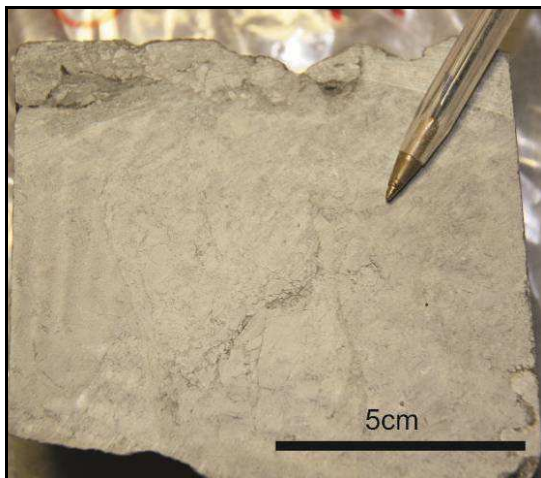


**Fig. 25** Dolomite breccia at LT33/1874m.

### **Strongly altered basalt**

At 1862m (LT33) a greenish block of strongly altered basalt was found in a red brown shale matrix. The block measured approximately 2 cubic meter, with no visible layering. The strongly altered basalt consisted of a green coloured matrix with some calcite filled voids of maximally 3mm size and was dense, massy and hard. The block was surrounded by a few centimeters of calcite margin.

In thin-sections pseudomorphosis can be observed. Voids filled partly with calcite represent strongly altered feldspar-, pyroxene-, amphibole- and olivine phenocrysts in a chloritisized matrix.



**Fig. 26** Tunnel face at LT33/1861.4m, general view with the embedded block of strongly altered basalt in red shales of the Hüttdorf Formation.



**Fig. 27** Partial view of the left tunnel face at LT33/1861.4m showing a block of strongly altered basalt. The picture depicts approximately 3m of tunnel face.



**Fig. 28** Strongly altered basalt: LT33/1861.4m.

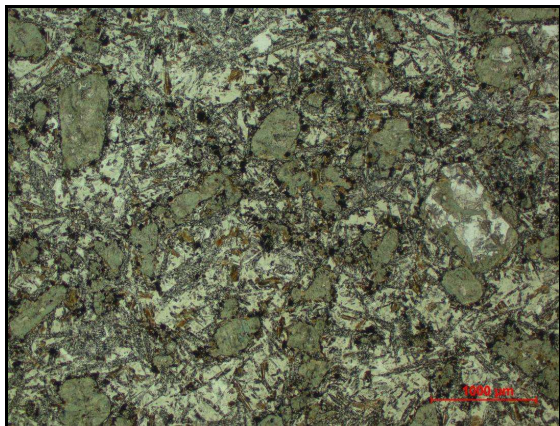


**Fig. 29** Strongly altered basalt: LT33/1861.4m (LPL), pseudomorphosis of strongly altered feldspar-, pyroxene-, amphibole- and olivine phenocrysts in a chloritized matrix. Voids are filled partly with calcite.

### **Strongly altered volcanite**

At LT33/1850m several small (max.40cm diameter) dark red blocks of strongly altered volcanite were found in a red brown shale matrix. The blocks were found together with grey sandy marls in a „block-in-matrix“-structure, embedded in red shales.

The strongly altered volcanite consisted of a dark red coloured matrix, with a lot of max. 4mm calcite filled voids, and was dense, massive, hard. The blocks were dissected by a lot of calcite veins. In thin sections a lot of calcite filled voids can be observed, some of them could be relicts of strongly altered feldspar. In a heavy mineral analysis carried by the OMV lab, the sample yielded some brookite/anatas grains. Anatas can be a weathering product of different TiO<sub>2</sub>-minerals, this would fit the picture of a strongly altered volcanite.



**Fig. 30** Tunnel face at LT33/1850.4m, several small (max.40cm diameter) dark red blocks of strongly altered volcanite were found in a red brown shale matrix at the left bottom.



**Fig. 31** Strongly altered volcanicic rock:  
LT33/1850m.

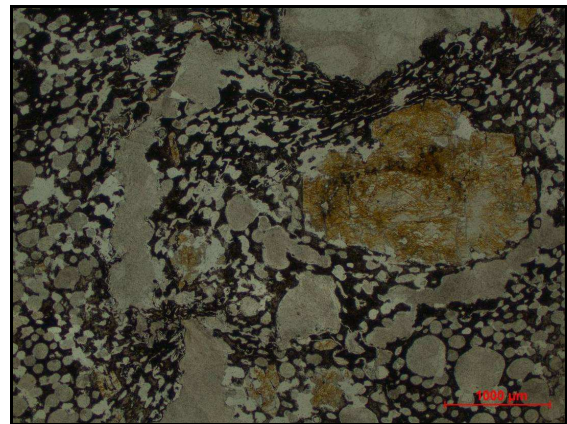


**Fig. 32** Thin section strongly altered volcanicic rock: LT33/1850m (LPL), calcite filled voids together with some relicts of strongly altered feldspar.

### ***Discussion of volcanites, formerly described as „Picrites“***

Former authors like Götzinger (1954) and Janoschek et al. (1956) indicated the presence of more than 30 scattered occurrences of picrites (an olivine rich alkali basalt) and more seldom tuff in the Rhenodanubian Flysch Zone. Because of the findings at the „Hörndlwald“ area (Janoschek et al., 1956) they argued for a primary contact of such flows or dykes to Flysch sediments. Janoschek describes three different types of picrites with variable content of olivine, biotite and augite, and assumes an Upper Cretaceous age.

The data from the „Hörndlwald“ represents mainly surface information from shallow pipe trench constructions.

Judging from the tunnel section no arguments for a primary contact of volcanic rocks to coeval Flysch sediments can be given. The presence of strongly altered basalts as tectonic blocks within the Hütteldorf Formation indicates a tectonic mixing and not a primary Cretaceous ocean floor volcanism connected with the Hütteldorf Formation. Also, the petrology and geochemistry (Univ.-Prof. Dr. F. Koller pers. comm.) argues against a picritic volcanism, and indicates basalts of probably within-plate character.

## **C.4. The St.Veit Klippenzone**

The St. Veit Klippenzone covers a tunnel length of 1097m, the interval from 2165m (LT33) to 898m (LT31). At 2165m (LT33) first scattered cherts, associated with the St. Veit Klippenzone, occurred. From 2320m (ammonite), 2592m (calpionells) and 2552m (nannoplankton) (all LT33) on Lower Cretaceous could be determined. At 2666m (LT33) (nannoplankton) Jurassic age was proven. Coming from SE, first cherts associated with the St.Veit Klippenzone, emerged at 898m (LT31).

### **C.4.1. Lithologies**

Lithologies are described in stratigraphic order, from old to young.

#### ***Keuper (Upper Triassic) sandstone/arkose:***

Sandstone with light grey, pink to green grey colour, coarse to medium grained, massive, hard and sized up to several decimeters (maximally 60cm), was found for example at LT31/1215.5m (coarse sandstone) or LT31/1277.2m (coarse sandstone).

The moderately to poorly sorted sandstone showed sometimes varying strength/hardness. In thin-sections the following minerals were identified: quartz, lithic rock fragments, feldspar, kaolinite, mica, and seldom dolomite. The main content is quartz (50 - 80%) and lithic rock fragments (consisting of quartzite) (20 - 40%) followed by feldspar (10 – 30%) and its alteration product kaolinite. Mica is not frequent (single grains) and sometimes part of the lithic rock fragments. In general the quartz grains are subangular to rounded, and show very often undulatory extinction. In the lithic rock fragments the quartz grains are frequently sutured and elongated. The feldspars are often altered to brown clay minerals and often only relicts of feldspars are present. It is very likely that the clay minerals consist beside others of the kaolinite determined in chapter C.4.4 (mineralogy). In most cases the matrix is clayey developed, but can also have some calcite content.

Following samples were investigated:

LT31/1164.5m, LT31/1188.5(b)m, LT31/1200m, LT31/1215.5m, LT31/1219.5m,

LT31/1257.7m, LT31/1277.2m, LT33/1893.4m and LT33/1900m.

Two sandstones from the SVK (LT33/1893.4m and LT33/1900m), were not found in context with the anticlinal structure (see C.1). These two samples showed a different colour (pale green) and mineralogy (C.4.4) than the surrounding Hütteldorf Formation sandstones. The heavy mineral assemblage is also different from the flysch units (C.4.2). For this reasons these two samples are regarded also as Keuper sandstones.

Age:

No direct evidence for the age of these sandstones could be found. Comparing with literature data, these sandstones were either attributed to the Upper Triassic Keuper (e.g. Prey, 1975) or to the Lower Jurassic Gresten beds (e.g. Trauth, 1930). In accordance with Prey (1975) a Late Triassic age is probable, based on the sandstone petrology and geochemical data (see chapter C.4.5), which compare well with other Keuper sediments from the Eastern Alps and the Carpathians.



**Fig. 33 LT31/1215.50m, light grey, hard sandstone (Keuper) together with red shale (Keuper).**



Fig. 34 31/1277.20m, sandstone (Keuper).

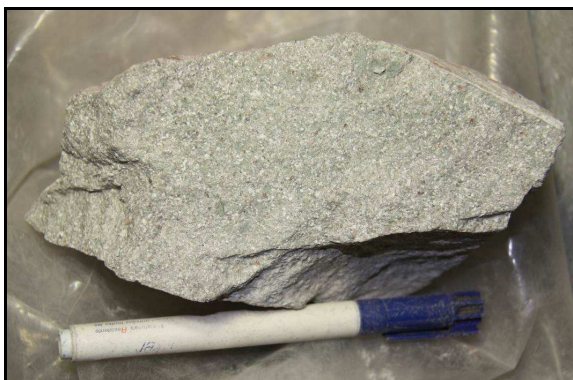


Fig. 35 Sandstone/arkose (Keuper) LT31/1277.2 m.



Fig. 37 Sandstone from the SVK (LT33/1893.4m) although a different colour (pale green), mineralogy and heavy mineral assemblage indicate Keuper sandstone.

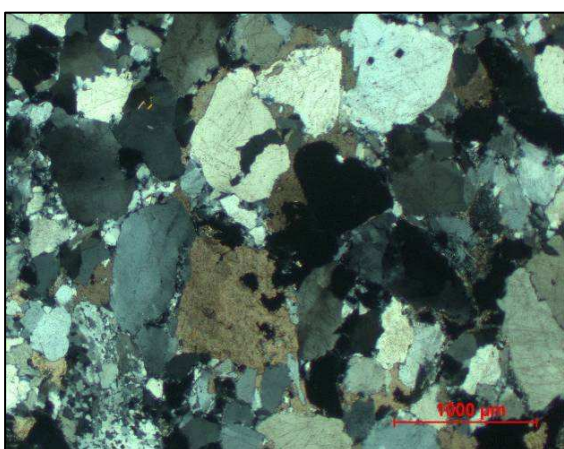


Fig. 36 Thin section of arkose sandstone (Keuper), LT31/1277m, containing quartz, feldspar, kaolinite, lithic rock fragments (consisting of quartzite) (XPL).



Fig. 38 Sandstone from the SVK (LT33/1900m) the colour (pale green), mineralogy and heavy mineral assemblage indicate also Keuper sandstone.

**- Shale/mudstone (Keuper):**

Keuper shale/mudstones from the St.Veit Klippenzone are in most cases red, but also dark grey, green or black. The mudstones are soft, often highly fragmented and tectonized. All collected samples were found in direct contact with assumed Keuper sandstones. The samples show no primary bedding or lamination, they also have no or a very low silt content. Carbonate analysis showed no carbonate content. The geochemical results of the Keuper shales (C.4.5) confirm that they can be separated from the Jurassic shales.

**Age:**

No direct evidence for the age of the shales exists, however, as those shales occur in direct contact together with the Keuper sandstones a Late Triassic age is inferred.

According to literature (e.g. Prey, 1975; Wessely, 2006) varicoloured shales are typical interlayers of Keuper-type sediments.



**Fig. 39** Green/red shale/mud from LT31/1277.2m found in direct contact with the Keuper sandstones.



**Fig. 40** Grey /red shale/ mud from LT31/1381.2m found next to the Keuper sandstones.



**Fig. 41** Red shale/ mud from LT31/1200m found in direct contact with the Keuper sandstones.

### **Dolomite (Keuper):**

Dolomite occurred at LT31/1277.2m. It was red coloured, fractured and embedded in red shale. Flaser-like inclusions of shale within the dolomite are present (Fig. 42).

In thin-sections several generations of calcite veins were identified. The dolomite fabric can be described as a nonplanar, equigranular sutured mosaic crystallisation texture. Crystals have sizes around 20 µm. No fossil remains or other primary structures could be found, the dolomite seems to be totally recrystallized.

### **Age:**

No direct evidence for the age of the dolomite could be found, however, as the dolomite was embedded into shales attributed to the Late Triassic Keuper facies, a Late Triassic age is also inferred for the dolomites. Altogether, an assemblage of (arkosic) sandstones, varicoloured shales and dolomite layers is typical for Keuper facies (see, e.g., Faupl, 2003, etc.).



**Fig. 42 Dolomite (Keuper)LT31/1277.2m.**

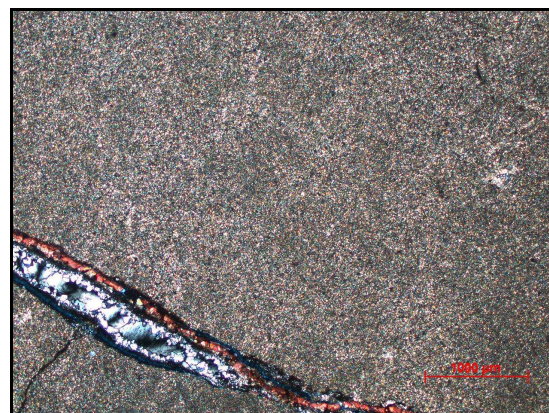


**Fig. 43 Thin section of dolomite (Keuper): LT31/1277.2m (XPL) totally recrystallized, with a nonplanar, equigranular sutured mosaic crystallisation texture. The calcite vein in the left bottom shows several generations (colored with Alicarin S; calcite = red, calcite + Fe = magenta, dolomite = colourless, Fe-rich ankerite =light blue, pores = intense blue).**

**-Sandstone/siltstone (Lower/Middle Jurassic):**

At 2666m/LT33 a grey to dark grey, fine grained, massive, sometimes laminated, hard calcareous sandstone to siltstone was found. Thickness reached several decimeters. The material showed bioturbation and carbonate contents around 18 % were measured. To produce a thin section of this material, it was necessary to grind it with alcohol instead of water, because it was water soluble. In the thin-section the bioturbated sandstone/siltstone consists of quartz, mica, biotite, feldspar, dolomite, and lesser amounts of organic matter (coal) in a fine-grained grey matrix. Some agglutinating foraminifera are also present.

**Age:**

Based on a comparison with biostratigraphically dated outcrop strata (e.g. Trauth, 1930; Janoschek et al., 1956) these fine-grained calcareous sandstones are generally attributed to the Lower (to Middle) Jurassic („Gresten“ beds of some former authors, e.g. Trauth, 1930). Such an early to middle Jurassic age is also confirmed by nannofossils from sample 2666m/LT33:

LT33 2666m (bad preservation, 1 nannofossil/2 fields of view)

*Lotharingius cf. sigillatus* (L. Toarcian? - U. Pliensbachian - M. Oxfordian)

*Discorhabdus* sp. aff *D. striatus* (Toarcian - U. Oxfordian)

*Watznaueria* sp. (starts in U. Toarcian)

This nannofossil assemblage indicates probably a Middle Jurassic age (range U. Toarcian - M. Oxfordian). Only this single sample from the Klippenzone yielded an interpretable nannofossil assemblage of clearly Jurassic age.

Other probably Jurassic samples are from LT33 2731m, with *Discorhabdus* sp. and from LT31 1366.9m with *Schizosphaerella* sp. and *Watznaueria* sp. beside unidentifiable other forms.

Additionally to age data from nannofossils, age informations were achieved from fragments of ammonites that were also found e.g.: LT31/1160m and LT31/1200m (= endocast): ammonites out of the group of *Arnioceras* (Sinemurian).

Also the nautiloid (sens. lat.) from 1188/LT31 gives some age indication. It shows a round profile, therefore it is rather more probably Sinemurian than Hettangian in age (verbal information from Martin Maslo and Leopold Krystyn).

A thin section from sample LT33/2401m showed a foraminifera (maybe *Gypsina moussavian*). Even though not found in the needed section for better identification, it gives a rough age and facies information. *Gypsina moussavian* is a shallow water-species.

The tunnel face at LT33/2401m consisted only of lithologies attributed to the St.Veit Klippenzone and no „Hüllflysch” was detected.

LT33	2666	2731	LT31	1367
Preservation	p	vp		vp
Abundance	1/2	2		2
Biscutum? sp.		x		
Cyclagelosphaera? sp.				x
Discorhabdus sp.		x		
Discorhabdus cf. striatus	x			
Lotharingus cf. sigillatus	x			
Schizospaerella sp.				x
Tranolithus? sp.				x
Watznaueria sp.		x		x
	Pli-Oxf	Jurassic		Jurassic?
AGE				

**Fig. 44 Results of nannofossil analysis of presumably Jurassic samples of LT31 and LT33. For legend and abbreviations see Fig. 16.**



**Fig. 45 Sandstone/siltstones (Lower/Middle Jurassic) at LT33/2666m.**



**Fig. 46** Sandstone/siltstone of Lower/Middle Jurassic age LT33/2666m which yielded a probably Early/Middle Jurassic age, according to nannofossils.

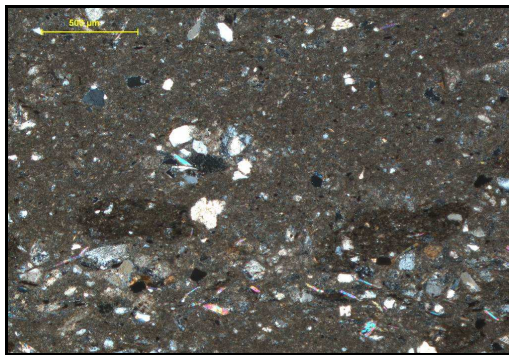


**Fig. 47** Thin-section of sandstone/siltstone, Lower/Middle Jurassic LT33/2666m which yielded a probably Early/Middle Jurassic age, according to nannofossils, consisting of quartz, mica, biotite, feldspar and some coal in a bioturbated grey shale/silt matrix.(XPL).



**Fig. 48** Marlstones of probably Early/Middle Jurassic age at LT31/1366.9m according to nannofossils.

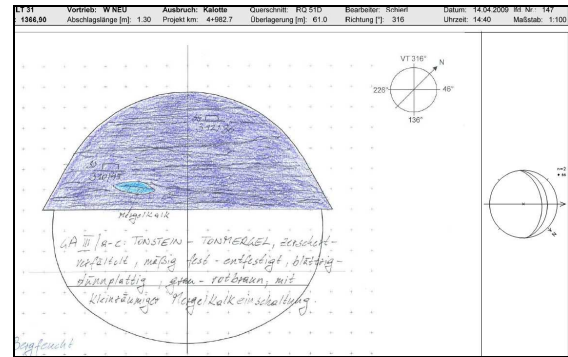


**Fig. 49** Sketch from LT31/1366.9m showing a typical „Block-in-matrix“ structure, according to nannofossils probably Early/Middle Jurassic age (provided by office Bechthold).



**Fig. 50** Sample from LT31/1366.9m which yielded a probably Early/Middle Jurassic age, according to nannofossils.



**Fig. 51** (calcareous) marlstones of probably Early/Middle Jurassic age at LT33/2730m according to nannofossils.

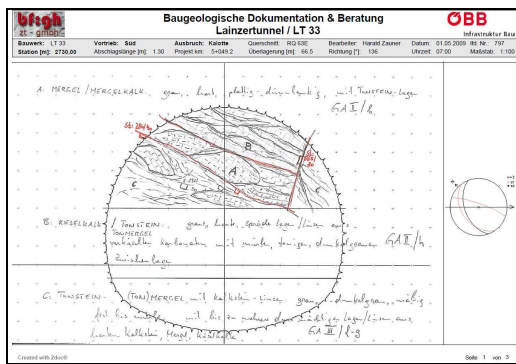


**Fig. 52** Sketch from LT33/2730m showing the tectonic mixing of different Jurassic rocks (provided by office Bechthold).



**Fig. 55** Fragments of ammonites (Arnioceras: Sinemurian) were found at LT31/1160m in a „Block-in-matrix“ situation, together with calcareous mudstones.



**Fig. 53** Sample from LT33/2730m which yielded of probably Early/Middle Jurassic age, according to nannofossils.

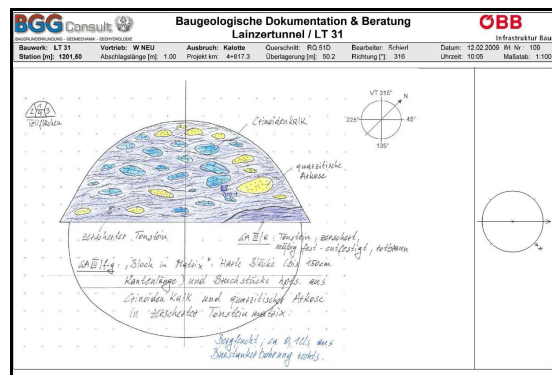


**Fig. 56** Sketch from LT31/1201.5m typical „Block-in-matrix“ situation, fragments of ammonites indicate probably Sinemurian age (provided by office Bechthold).



**Fig. 54** Fragments of ammonites were found at LT31/1200m in a „Block-in-matrix“ situation. Because of stability problems the tunnel face was only opened in small sections.

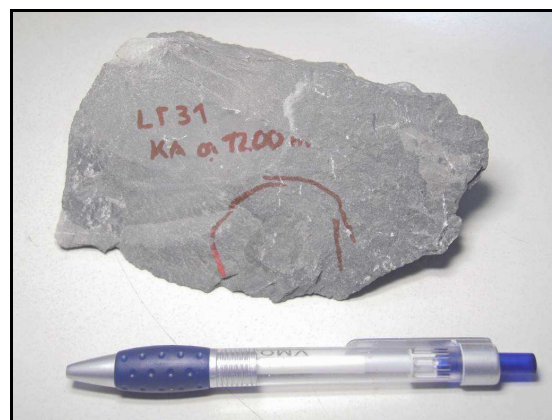


**Fig. 57** Sample LT31/1200m: sandy calcareous marlstone with endocast of an ammonite.

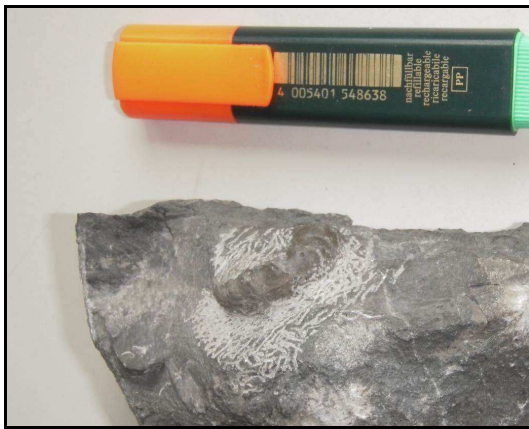


**Fig. 58** Sample LT31/1160m: sandy calcareous marlstone with ammonite (*Arnioceras*: Sinemurian).

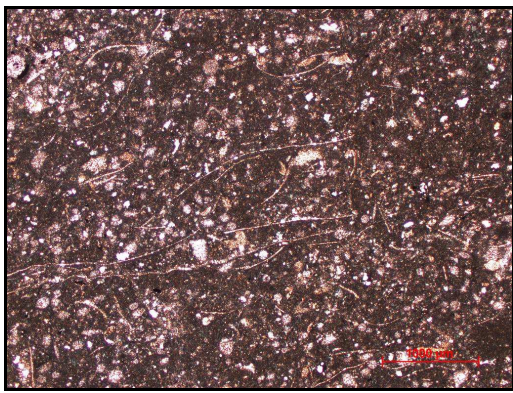


**Fig. 59** Thin-section of sample LT31/1200m (Sinemurian) biomicritic packstone / calcareous marlstone (66% CaCO<sub>3</sub>) containing radiolaria, spiculae, filaments (planktonic bivalvae), crinoids and some coal particles in a micritic matrix (LPL).



**Fig. 60** Tunnel face at 1188/LT31m where a nautiloid (probably Sinemurian) was found.

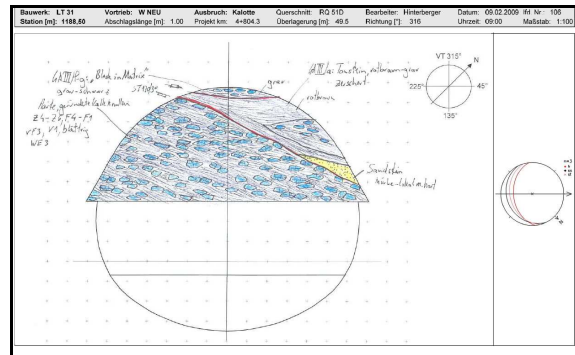


**Fig. 61** Sketch from LT31/1188.5m with typical „Block-in-matrix“ situation, were the nautiloid (probably Sinemurian) was found (sketch provided by office Bechthold).



**Fig. 62** Nautiloid from LT31/1188.5m (probably Sinemurian age), cut and polished. Partly pyritized in the center.



**Fig. 63** Tunnel face at LT33/2401m klippen rocks of probably Early/Middle Jurassic age.



**Fig. 64** Samples from LT33/2401m klippen rocks of probably Lower/Middle Jurassic age.

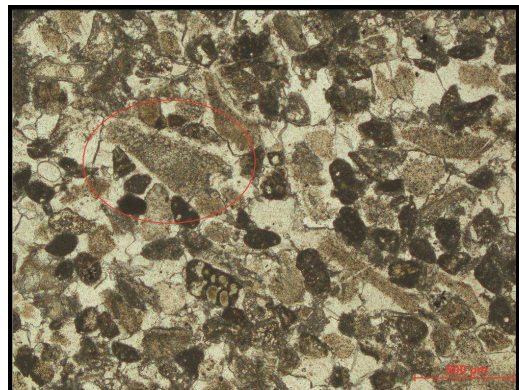


**Fig. 65** Thin-section 33/2401m: pelletal grainstone / argillaceous limestone ( $\text{CaCO}_3=85\%$ ), the foraminifera in the red circle is a shallow water species (maybe *Gypsina moussavian*) (LPL).

#### ***Calcareous mudstone (Middle Jurassic, lower - middle Bajocian):***

At the top of the rescue shaft Veitengergasse, thin layers of red calcareous mudstone were intercalated between the chert beds. The mudstones were dark red to redbrown coloured, rather soft, splintery breaking, thin bedded up to several cm, sometimes aptychi bearing, with carbonate contents up to 21%.

In thin-sections a lot of filaments are bedded in the red matrix, sometimes crinoids can be found.

#### **Age:**

The only fossil found in shales was an aptychus (Fig. 67) confirming a Jurassic to Cretaceous age. No other age indication was found for these shales. As they are intercalated with red cherts/radiolarite of Bajocian age, a Middle Jurassic age is inferred for these shales.

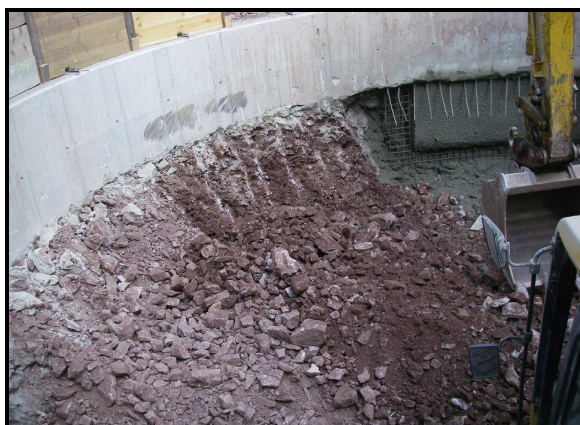


**Fig. 66** Calcareous mudstone (lower - middle Bajocian) Rescue pit Veitengergasse 0-2m.

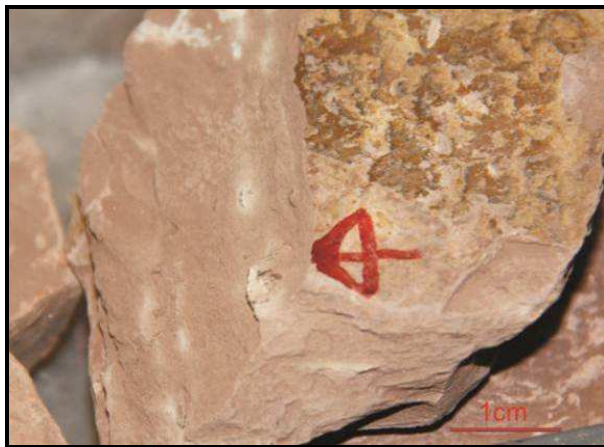


**Fig. 67** Rescue pit Veitingergasse calcareous mudstone with an aptychus (lower - middle Bajocian) sample no. RSVG1m.

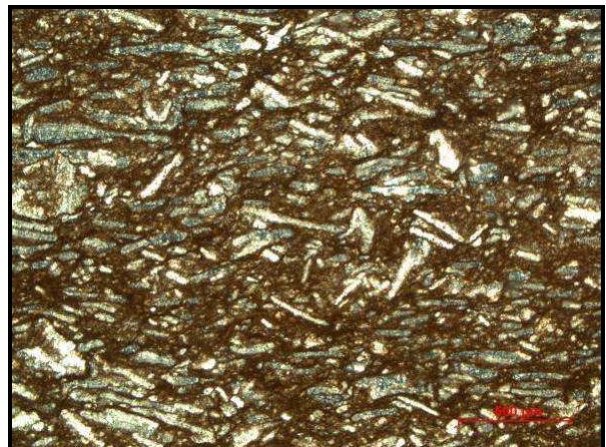


**Fig. 68** Thin-section from rescue pit Veitingergasse: calcareous/bioclastic packstone (lower - middle Bajocian) with filaments and crinoidal debris. Sample RSVG 0/1m containing aptychi (XPL).

#### *Chert/radiolarite (Lower - Middle Bajocian)*

At the top of the rescue shaft Veitingergasse a hard, brittle, conchate breaking, dark red to redbrown coloured, thinly bedded (up to 15cm) chert was found.

Between the chert beds thin layers of red calcareous mudstone were intercalated.

In thin sections the chert appears spotty , rich in calcite veins, bioturbated, most radiolaria are filled with calcite, the matrix is grey to redbrown.

#### **Age:**

A rather precise biostratigraphic age was indicated by radiolaria from a sample at 1m of the rescue shaft Veitingergasse: *Paronaella skowkonaensis*; *Parvingula dhimenaensis*; *Parvingula schoolhonsensis* ssp. A *Quinquecapsularia megasphaerica*; *Sethocapsa funatoensis*; *Yamatoum spinosum* indicate an early to middle Bajocian age according to Marta Bak (Krakow, pers. comm.).



**Fig. 69** Rescue shaft Veitingergasse: outcrop of red cherts and shales station 1-2m (picture bottom approx. 2m).



**Fig. 70** Chert (early - middle Bajocian) Rescue pit Veitingergasse 1m.

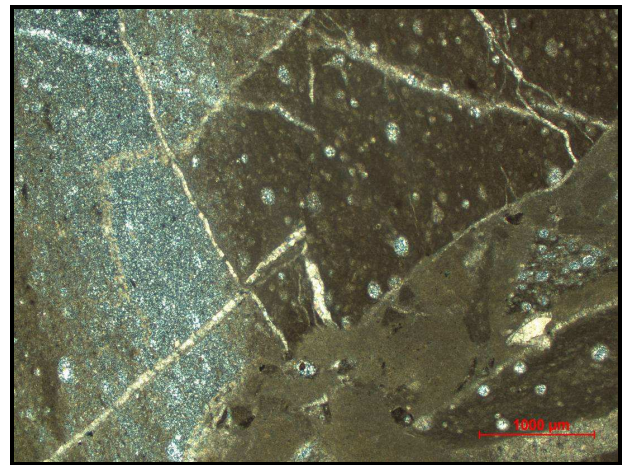


**Fig. 71** Rescue pit Veitingergasse:thin-section of a chert (early - middle Bajocian) sample RSVG 1m with some radiolaria. The calcite veins show different generations (XPL) .

### ***Chert/radiolarite (Valanginian)***

At 2165.5m/LT33 a tectonically deformed, hard, brittle, conchate breaking, light grey to green coloured, chert/radiolarite block was found. The chert body was bedded, dissected and up to 100cm thick, embedded in brown and grey shales.

#### ***Age:***

Radiolaria confirm a Valanginian age for these rocks (M. Bak, pers. comm.): *Crucella lipmanae*, *Sethocapsa tricornis*. Such a siliceous rock type with an Early Cretaceous (Valanginian) age is so far not known from the outcrops of the SVK (e.g. Janoschek et al., 1956) and confirms that the deepwater shaly-siliceous sedimentation continued from the Late Jurassic into the Early Cretaceous.



**Fig. 72 Tunnel face at 2165.5m/LT33 with a chert/radiolarite block in the uppermost right part of the picture.**

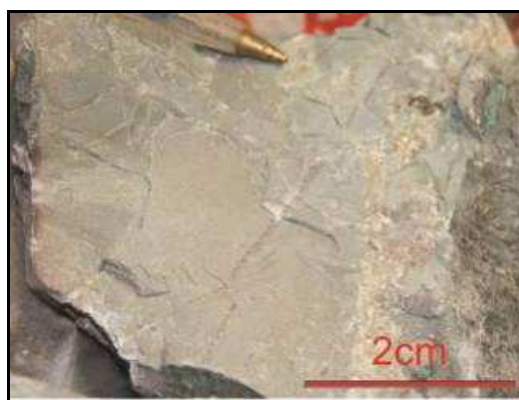


**Fig. 73 Chert (Valanginian) found at LT33/2165m.**

### ***Chert (age unknown, probably Jurassic)***

Of some blocks of chert, found in the Lainz Tunnel, the age could not be determined. These rocks were hard, brittle, conchate breaking, red brown or blue grey, isolated blocks or layers embedded in a shale/marlstone matrix.

#### **Age:**

In comparison with previous works from the SVK, these cherts are attributed to the Jurassic, probably Middle to Late Jurassic in age (e.g. Trauth, 1930; Janoschek et al., 1956; Prey, 1975, Tollmann, 1985). However, no proof for an age could be found, but lithological similarities to the Bajocian cherts/radiolarites also suggest such a Jurassic age. From the Lainz Tiergarten outcrop samples of the SVK (MM08/28 = "Maurerwald", MM 08/65 = „Steinbruch Saulackenmais", 08/70 „Steinbruch Wildpretwiese") there is evidence that this siliceous, radiolaria-bearing facies ranges up into the late Valanginian to early Aptian (sample MM08/28: late Valanginian to early Aptian, *Sethocapsa dorysphaeroides*; MM08/65: late Valanginian to early Aptian, *Zhamoidellum testatum*; MM08/70: late Valanginian - early Hauterivian, *Crucella* sp. aff. *C. espartoensis*, *Paronaella annemarie*, *Spongocapsula* sp. aff. *S coronata*, *Zhamoidellum testatum*, *Obesacapsula bullata*, *Xitus channelli*, *Crolanium pythiae* (M. Bak, pers. comm.).



**Fig. 74 Chert from LT31/898m.**



**Fig. 75 LT31/1364.3m: Chert nodule in siliceous limestone (Lower Cretaceous, Middle and Upper Berriasian).**

### ***Marlstone to argillaceous limestone (Tithonian-Berriasian/Valanginian)***

Marlstone to argillaceous limestone was found either thin-bedded or with beds up to decimeter thickness. The grey coloured material is hard, brittle breaking, and often bioturbated. Carbonate contents range from 48% up to 85%.

In thin sections different bioclasts can be found: echinoids (crinoids), filaments, spiculae, radiolaria and sometimes foraminifera.



**Fig. 76** Tunnel face with marlstone to argillaceous limestone (Tithonian-Berriasian/Valanginian) LT33/2333m.



**Fig. 77** Tunnel face with marlstone to argillaceous limestone (Tithonian-Berriasian /Valanginian) LT33/2552m.



**Fig. 78** Argillaceous limestone with Tithonian-Berriasian/Valanginian ammonite (*Protancyloceras* sp) LT33/2333m.



**Fig. 79** Marlstone to argillaceous limestone showing bioturbation (Tithonian-Berriasian/Valanginian) LT33/2552m.

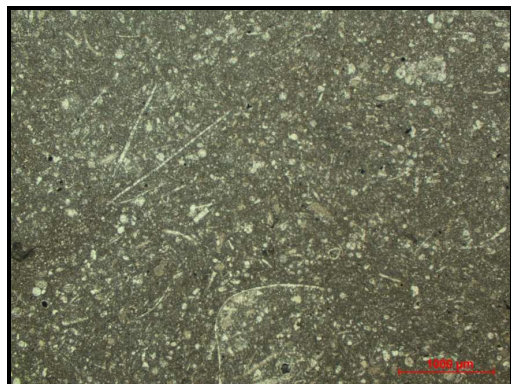


**Fig. 80** Thin-section LT33/2333: marlstone to argillaceous limestone/bioclastic packstone showing filaments (Tithonian-Berriasian/Valanginian) (LPL).

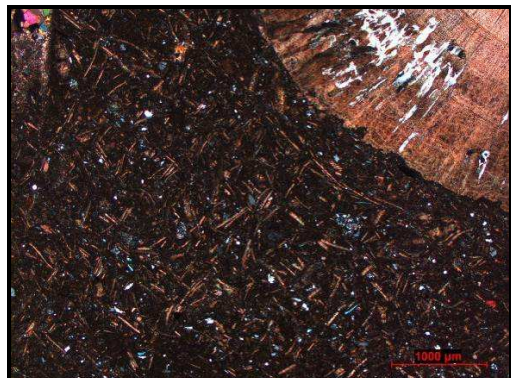


**Fig. 81** Thin-section LT33/2552m: marlstone to argillaceous limestone (Tithonian-Berriasian/Valanginian): bioclastic packstone showing bioclasts (filaments) and a big crinoid stem (XPL).

### **Age:**

Several ammonites were found in the tunnel. One specimen (LT33/2333m) found by Michaela Sapp (office Bechthold) was prepared and determined by Alexander Lukeneder (NHM Vienna). It is a *Protancyloceras* sp., an elongated form ranging from Tithonian to Berriasian (sometimes Valanginian).

One ammonite fragment from LT33/2320.m (argillaceous limestone) was not determinable.

Two samples from the Rescue pit Angermayergasse (=LT33/2280m) yielded macrofossils: station RsAg/241m a marlstone with a belemnite and one marlstone with a pectinid.

In two thin sections of this lithology foraminifera were observed: LT33/2165m: *Trocholina* spp. (~Upper Triassic - Upper Cretaceous), *Textularia* spp. (*Spirotexularia*?) and LT31/975m: Upper Jurassic - Lower Cretaceous forms of small sized planktonic species.

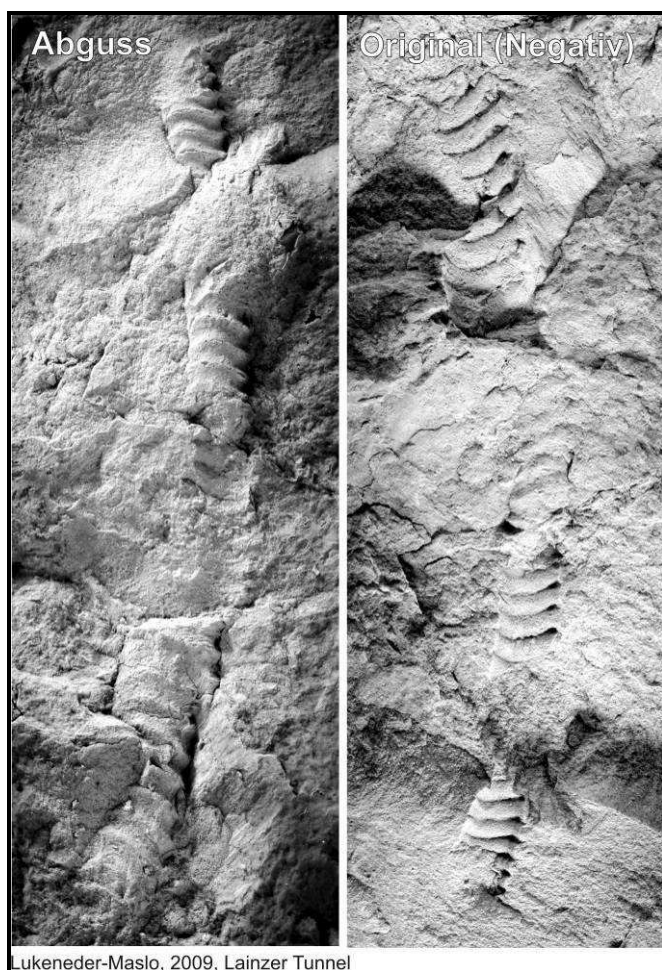


**Fig. 82 Original/mould close up of the Tithonian-Berriasian/Valanginian ammonite (*Protancyloceras* sp.) LT33/2333m.**



**Fig. 83 Argillaceous limestone with unidentified ammonite fragment LT33/2320.6m.**



**Fig. 84 Rescue pit Angermayergasse 241m=LT33/2280m; marlstone with belemnite.**



**Fig. 85 Rescue pit Angermayergasse 241m=LT33/2280m, marlstone with pectinid.**



**Fig. 86 Tunnel face at LT33 2165.5m: the sample discussed in this chapter below derived from the marlbody in the upper right area.**



**Fig. 87: Different samples archived from LT33/2165.5m, at the bottom of the picture lies a argillaceous limestone. The sample is still partly covered with some sheared mudstones.**



Fig. 88 Thin section LT33/2165m: argillaceous limestone with *Trocholina* spp. (~Upper Triassic - Upper Cretaceous) right in the middle of the picture (LPL) (colored with Alicarin S).



Fig. 91 marlstone from LT31/975.5m - reflections are caused by calcite crystals on the surface.

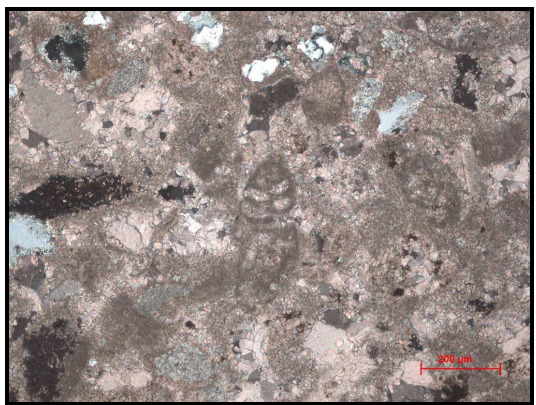


Fig. 89 Thin section LT33/2165m: argillaceous limestone with *Textularia* spp right in the middle of the picture (LPL) (colored with Alicarin S).

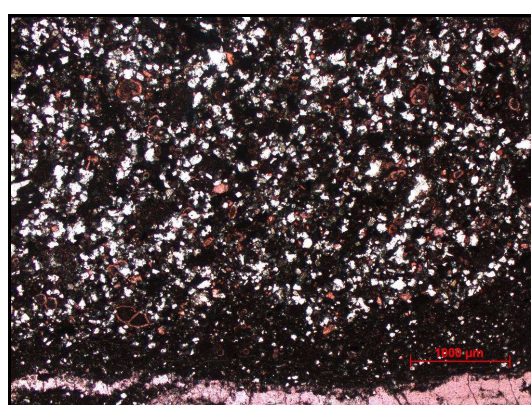


Fig. 92 Thin section LT31/975m: sandy marlstone with Upper Jurassic- Lower Cretaceous - small sized planktonic foraminifera species (LPL)(colored with Alicarin S).



Fig. 90 Tunnel face at LT31/975.5m below red and grey mudstone a bigger block of marlstone was encountered.

- **Siliceous limestone (Lower Cretaceous, Middle and Upper Berriasian):**

Several isolated blocks (max. 40cm diameter) of hard, brittle, conchate breaking fine-grained limestone, with white to light grey colour, often bioturbated, were found. The blocks were embedded in a grey shale/marl matrix. The carbonate contents of these limestones range from 53% to 65%. The single blocks were often found to be coated by black shale. In thin-sections the siliceous biomictic limestone (mudstone) has a fine grey matrix and prominent calcite veins. Additional to calpionellids, bioclasts of bivalves, echinoids (crinoids), foraminifera, radiolaria, filaments and some small particles of coal were found. In general, these rocks have the appearance of fine-grained pelagic limestones with varying siliceous content, sometimes up to chert nodules.



**Fig. 93** Tunnel face at LT33/2552.0m, blocks of siliceous limestone were embedded in the grey shale/marl matrix on the right side.



**Fig. 94** Light grey blocks of siliceous limestone (Middle and Upper Berriasian) at LT31/869m.

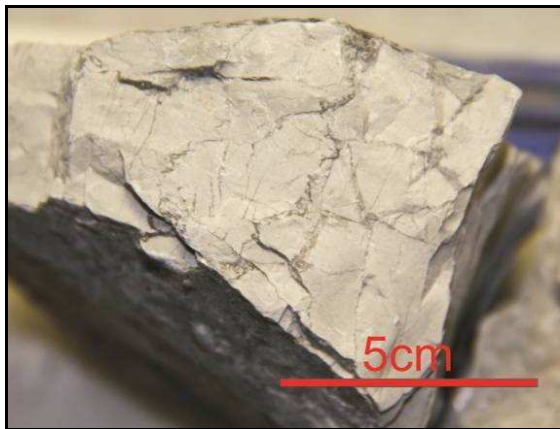


**Fig. 95** Siliceous limestone (Middle and Upper Berriasian) LT33/2552m.

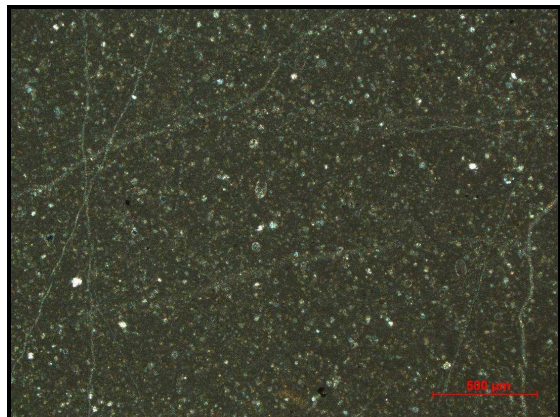


**Fig. 96** Thin-section: Siliceous biomicritic limestone (Middle and Upper Berriasian) LT31/860m containing calpionellids (XPL).

#### **Age:**

In several thin-sections of siliceous limestone calpionellids were found (e.g.: LT31/869.5m, LT31/993.5, LT31/1054.5m, LT33/2244.5m, LT33/2592.2m), one (LT31/869.5m) was rich enough for biostratigraphic age determination. The classification was carried out by Alexander Lukeneder (NHM Wien) and Daniela Rehakova (Bratislava).

Thin section 869.5, biomicritic limestone (mudstone):

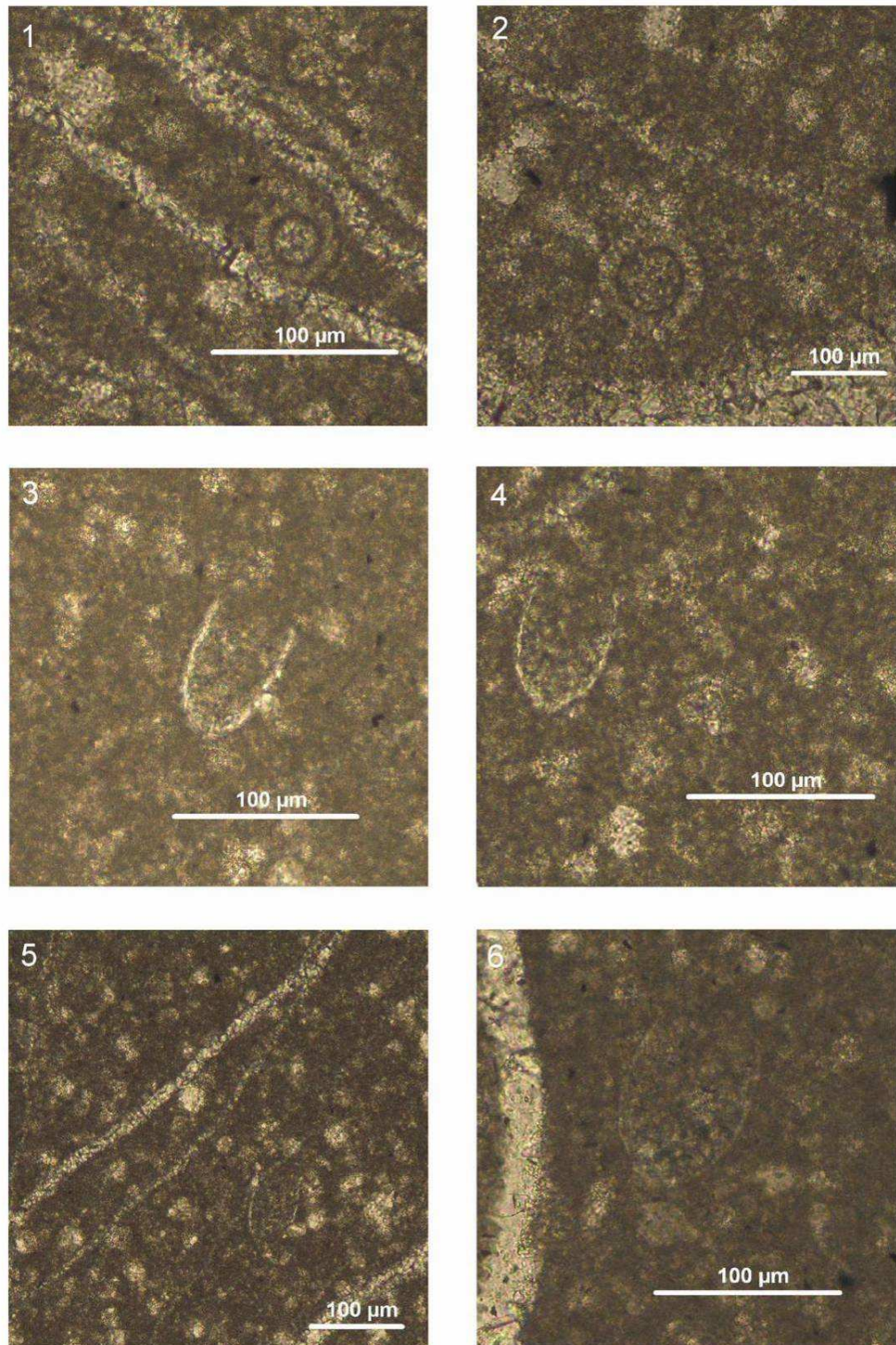
Bioclasts are not very frequent. Matrix is silicified and penetrated by thin calcite veins of different orientation. It contains calcareous dinoflagellates: *Schizosphaerella minutissima* (Colom), *Colomisphaera carpathica* (Borza), *Cadosina semiradiata fusca* (Wanner).

Among the calpionellid association *Calpionella alpina* Lorenz, *Tintinnopsella carpathica* (Murgeanu et Filipescu), *Calpionella elliptica* Cadisch, *Calpionellopsis oblonga* (Cadisch), *Calpionella minuta* Houša, *Remaniella borzai* Pop, *Remaniella cadischiana* (Colom), *Lorenziella hungarica* Knauer are present.

Some of calpionellid loricas are covered by black rings, consisting of microgranular pelitic matter. One aptrych fragment, one fragment of an oyster shell, *Lenticulina* sp., and several fragments of crinoids are also visible.

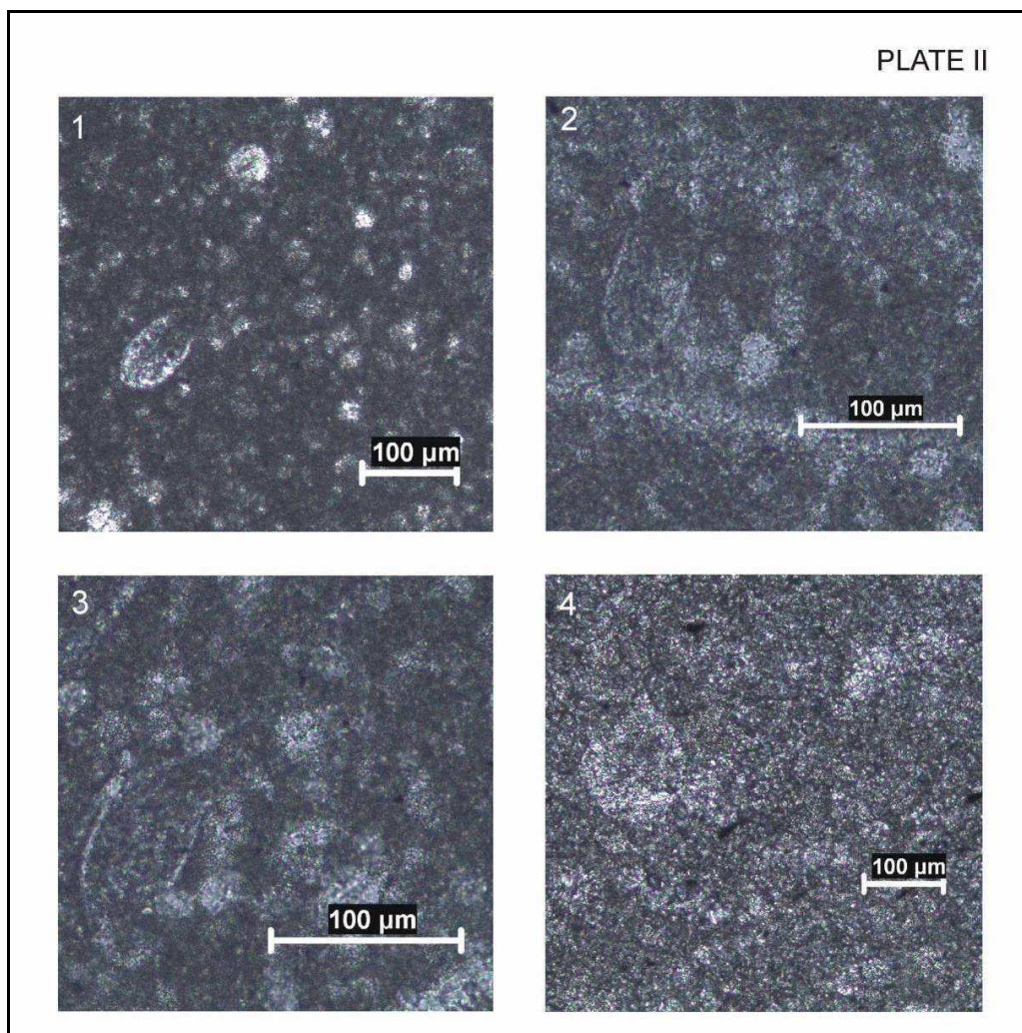
The association is typical for the *Oblonga* Subzone of the standard *Calpionellopsis* Zone of the uppermost part of the Middle and the Late Berriasian (see Fig. 97 - Fig. 99).

PLATE I



**Fig. 97** Thin section photographs of calpionellids (see text above for identification). 1-2. *Colomisphaera carpathica* (Borza) 3. *Calpionellopsis oblonga* (Cadisch) 4-5. *Tintinnopsella carpathica* (Murgeanu et Filipescu) 6. *Remaniella filipescui* Pop All pictures thin section of sample LT31/869.5 (plate 1 was made by A. Lukeneder and D. Rehakova).

PLATE II



**Fig. 98 Thin section photographs of calpionellids:** *Calpionella elliptica* Cadisch, *Remaniella cadischiana* (Colom) *Tintinnopsella carpathica* (Murgeanu et Filipescu) 1 - 3 thin section sample LT31/869.5 (plate 2 was made by A. Lukeneder and D. Rehakova).

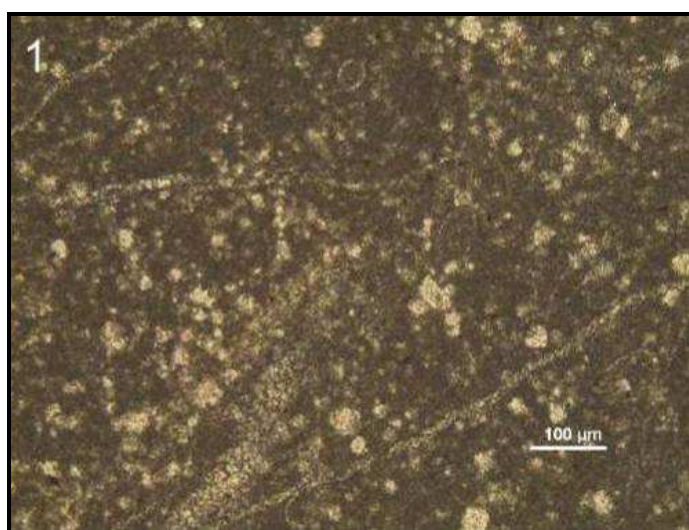


**Fig. 99 Thin section photograph of calpionellids:** Slightly bioturbated and silicified biomicrite limestone (mudstone to wackestone). It contains predominantly sponges, less radiolarians and rarely calpionellid loricas. Thin section LT31/869.5m. (picture was made by A. Lukeneder and D. Rehakova).

#### C.4.2. Heavy mineral data

Heavy mineral analysis of the samples of the Lainz Tunnel were provided by the OMV laboratory. Fig. 100 shows the heavy minerals found in the samples from the Lainz Tunnel. Heavy mineral analyses by OMV lab were done on most of the suitable lithologies of the tunnel section. According to R. Sauer (OMV) the high contents of baryte and pyrite handicapped the analyses. Additionally, because all samples were treated with HCl-acid, apatites were largely or completely dissolved.

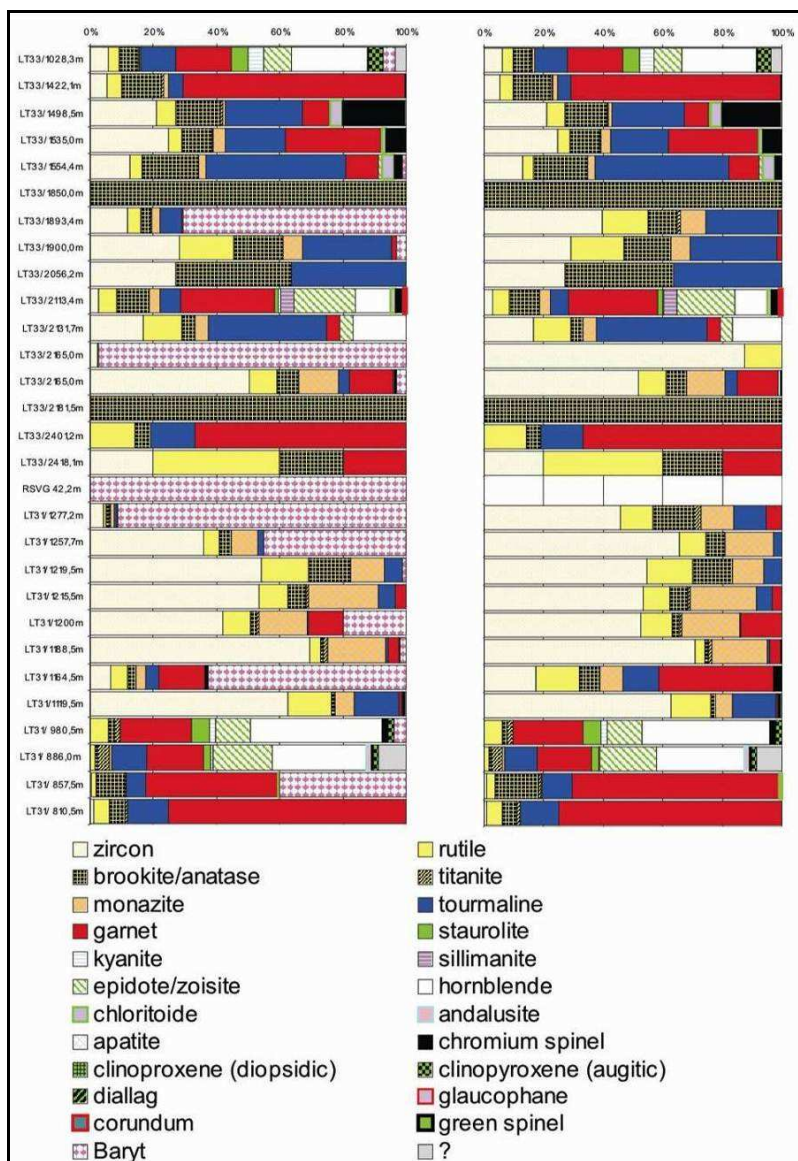


Fig. 100 Heavy mineral analysis of the samples of the Lainz Tunnel, table on the right side shows calculated heavy mineral contents without baryte. Samples arranged according to tunnel section meter (LT33/LT31).

## *Heavy mineral characteristics of the Lainz Tunnel sandstones*

### **Kahlenberg Formation**

Sandstones of the Kahlenberg Formation (e.g.: LT33/1028.3m) show high amounts of garnet (44%), hornblende (12%) and tourmaline (9%). Additional minerals are anatas/brookite, zircon, rutile, epidote/zoisite, staurolite, kyanite, and clinopyroxene.

	LT33/1028.3m	LT33/1422.1m	LT33/2131.7m	Σ
zircon	12	12	4	28
rutile	7	10	3	20
brookite/anatas	12	29	1	42
titanite	1	1		2
monazite	1	4	1	6
tourmaline	22	10	9	41
garnet	36	158	1	195
staurolite	11			11
kyanite	10			10
epidote/zoisite	18		1	19
hornblende	49		4	53
chromium spinel	1	1		2
clinopyroxene (augitic)	9			9
baryte	8			8
Σ	204	225	24	453

**Fig. 101 Kahlenberg Formation sandstones: counts of heavy minerals found in the samples and total numbers of heavy minerals counted per sample.**

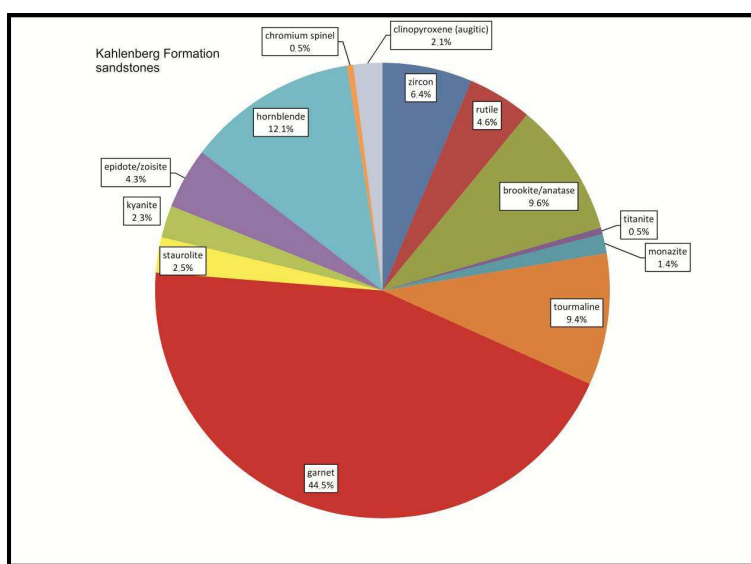


**Fig. 102 Kahlenberg Formation sandstones: mean percentage of heavy minerals, without baryte.**

## Hütteldorf Formation

Samples of sandstones of the Hütteldorf Formation (e.g.: LT33/1498.5m, LT33/1535.0m, LT33/1554.4m) contain some chromium spinel (a few percent up to ca. 20%) as an indicator mineral for some ophiolithic detritus. Garnet (40%), tourmaline (15%), brookite/anatas (10%) and zircon (8%) are common in greater amounts, in addition rutile, hornblende and chloritoide can be found.

	LT33/810.5 m	LT33/857.5 m	LT33/886.0 m	LT33/980.5 m	LT33/1498.5	LT33/1535.0 m	LT33/1554.4 m	LT33/2113.4 m	$\Sigma$
zircon	2	2			44	56	10	4	118
rutile	11	9	2	3	12	9	3	8	57
brookite/anatas	10	47	1	1	30	22	14	15	140
titanite	2	2	5	1	1	1			12
monazite		1	1		2	8	2	5	19
tourmaline	27	32	14		51	43	35	9	211
garnet	156	221	23	12	17	68	8	43	548
staurolite			3	3	1		2	9	
kyanite		1	1				1	3	
sillimanite							6	6	
epidote/zoisite			24	6			1	28	59
hornblende			38	22		1		16	77
chloritoide	2				8	2	3	2	17
andalusite		2						2	
chromium									
spinel									
clinopyroxene					1	1	15	2	64
(augitic)			2	1				3	
corundum							1	1	
baryte	210		2				1		213
$\Sigma$	208	526	117	53	207	225	79	144	1559

**Fig. 103 Hütteldorf Formation sandstones: counts of heavy minerals found in the samples and total numbers of heavy minerals counted per sample.**

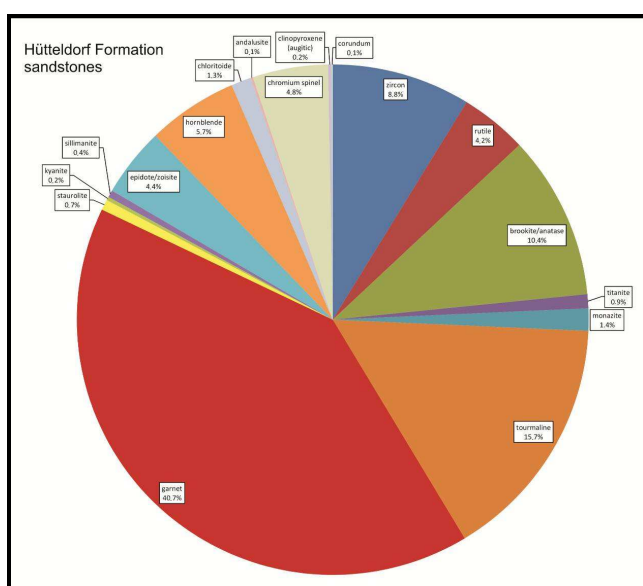


**Fig. 104 Hütteldorf Formation sandstones: mean percentage of heavy minerals, without baryte.**

## Jurassic sandstones

Beside the high amount of baryt of some of the Jurassic sandstones (e.g.LT33/2165m), typical Jurassic sandstones from the SVK show high amounts of zircon (56%), rutile (11%), tourmaline (10%), additionally garnet (8%), monazite (8%), brookite/anatas (5%).

	LT33/2056.2m	LT33/2165.0m B	LT33/2181.5m	RSVG 42.2m	LT31/1119.5m	LT33/2401.2m	LT33/2418.1m	LT33/2165.0mA
zircon	3	7			148		1	96
rutile		1			32	3	2	17
brookite/anatas e	4		2		3	1	1	13
monazite					14			24
tourmaline	4				34	3		7
garnet					1	14	1	26
hornblende					1			1
chromium spinel					2			1
baryte		275		241				6
?					1			
$\Sigma$	11	283	2	241	236	21	5	191

**Fig. 105 Jurassic sandstones: counts of heavy minerals found in the samples and total numbers of heavy minerals counted per sample.**

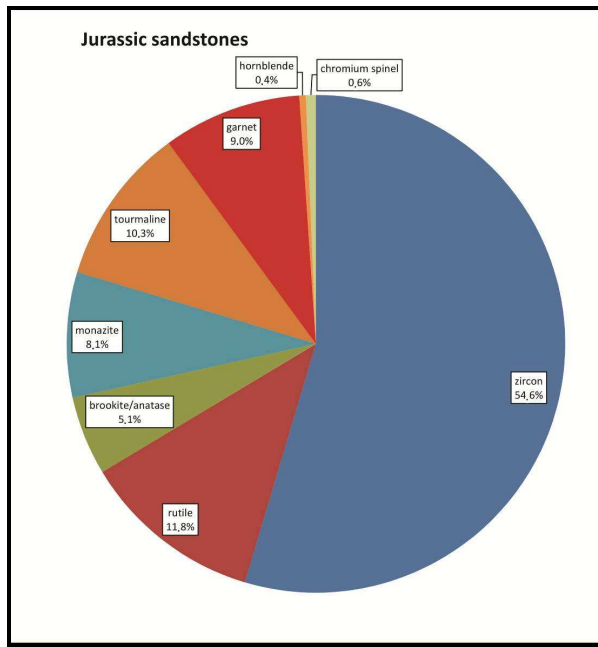


**Fig. 106 Jurassic sandstones: mean percentage of heavy minerals, without baryte.**

## Keuper quartzite

Typical samples of Keuper quartzite (LT31/1188.5m, LT31/1200.5m -coarse, LT31/1215m - coarse, LT31/1219.5m, LT31/1257.7m, LT31/1277.2m-coarse) show high amounts of zircon (average 56%) and significantly higher amounts of monazite (16%) than the other lithologies. Lesser amounts of rutile (9%), brookite/anatas (6%), garnet (6%) and tourmaline (3%) occur additionally. Zircon-monazite dominance therefore characterizes the samples from the SVK.

	LT31/1164.5m	LT31/1188.5m	LT31/1200m	LT31/1215.5 m	LT31/1219.5 m	LT31/1257.7m	LT31/1277.2m	$\Sigma$
zircon	13	146	110	111	111	157	17	665
rutile	11	7	22	19	31	21	4	115
brookite/anatas e	5	2	5	12	27	16	5	72
titanite		3	2	2			1	8
monazite	6	38	40	46	22	38	4	194
tourmaline	9	2	1	11	12	7	4	46
garnet	29	7	29	7			2	74
chromium spinel	2	1						3
baryte	126	4	52		2	197	377	758
$\Sigma$	201	210	261	208	205	436	414	1935

**Fig. 107 Keuper sandstones: counts of heavy minerals found in the samples and total numbers of heavy minerals counted per sample.**

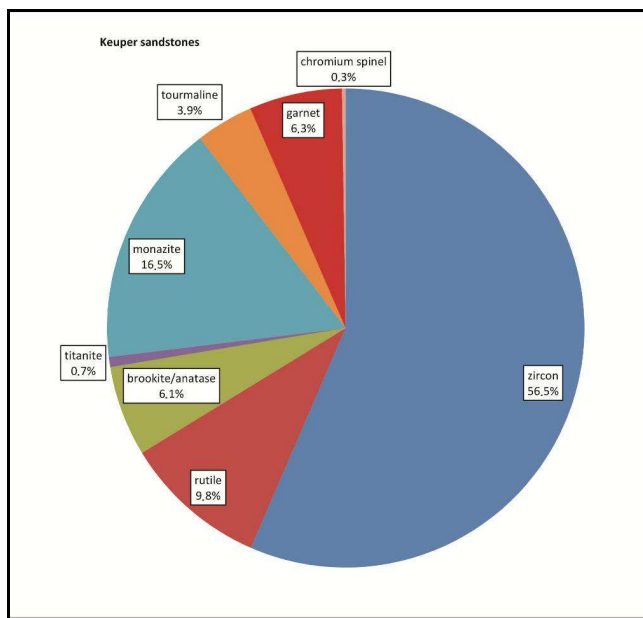


**Fig. 108 Keuper sandstones: mean percentage of heavy minerals, without baryte.**

### **Keuper sandstones at LT33/1893m and LT33/1900m**

Two samples from the SVK (LT33/1893.4m and LT33/1900m) showed a different colour (pale green) and mineralogy than the surrounding Hütteldorf Formation sandstones. The heavy mineral assemblage with high amounts of zircon (36%), tourmaline (25%), rutile (15%) and monazite (7%) is also different. This assemblage is more characteristic for the Keuper sandstones and thus these greenish sandstones represent probably blocks of Keuper sandstones.

	LT33/1893.4m	LT33/1900m	$\Sigma$
zircon	61	18	79
rutile	23	11	34
brookite/anatase	15	10	25
titanite	2		2
monazite	13	4	17
tourmaline	37	18	55
garnet	2	1	3
baryte	365	2	367
$\Sigma$	518	64	582

**Fig. 109 Keuper sandstones: counts of heavy minerals found in the samples and total numbers of heavy minerals counted per sample.**

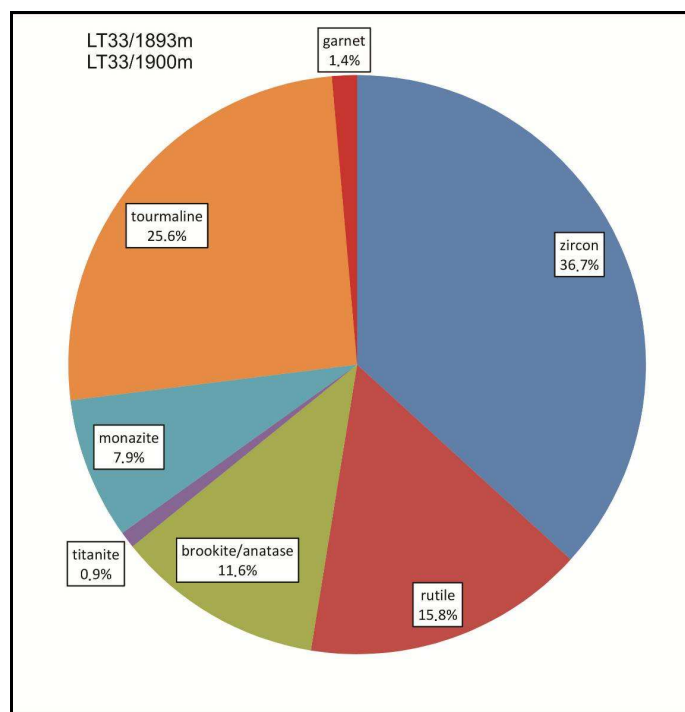


**Fig. 110 Keuper sandstones: mean percentage and total numbers of heavy minerals, without baryte.**

## ***Discussion of heavy minerals***

Heavy mineral data from the Flysch units are in accordance with previously published data (e.g. Woletz, 1967a,b). The Kahlenberg Formation in general shows a predominance of garnet (e.g. Müller, 1987; Schnabel, 1992). Other metamorphic minerals like staurolite, epidote/zoisite and kyanite point to a metamorphic source area, which may be the rising Austroalpine crystalline to the south during the Late Cretaceous (see Müller, 1987, Trautwein, 2001). A few grains of clinopyroxenes and traces of chrome spinel indicate a very minor additional ophiolithic source.

The same hinterland situation is inferred principally for the Hüttdorf Formation where the addition of chrome spinels is more conspicuous as already noted by Prey (1973; see also Faupl, 1996, Schnabel, 1992). Typical heavy mineral assemblages show the dominance of garnet and varying amounts of zircon, tourmaline, rutile and apatite (Prey, 1973, Faupl, 1996).

In contrast, zircon- and other stable mineral (ZTR-zircon-tourmaline-rutile)-dominated assemblages with some monazite are typical for the Keuper sandstones (e.g.: Al-Juboury et al., 1994). Similar heavy minerals are known from the Lunz sandstones of the Upper Triassic of the Northern Calcareous Alps (Behrens, 1972). Such heavy mineral assemblages, that are strongly dominated by stable minerals, are in accordance with long fluvial transport of Keuper sediments from the north into the alpine depositional area.

Häusler (1988) studied the composition of Jurassic clastic sediments of the Lower Austroalpine and reported also zircon-tourmaline-rutile dominated assemblages together with some traces of chrome-spinel in some regions. Jurassic sandstones of the SVK dominated by stable minerals, i.e. zircon, are largely similar to those reported by Häusler (1988). Whereas the heavy mineral contents of the Gresten Formation of the Gresten Klippenzone show dominance of garnet and apatite, e.g. Faupl (1975) reports a general garnet-apatite dominance with additional zircon, tourmaline and rutile in marine Gresten sandstones. However, Faupl (1975) and Schnabel (1970) also show a possible eastward trend with higher contents of zircon in the East. Woletz (1967a,b) described „Gresten sandstones” of the St.Veit Klippen with high contents of zircon, together with garnet and apatite. Aubrecht (1994) reported similar heavy mineral assemblages as in the SVK with a lack of garnet from Jurassic units of the Tatic (Lower Austroalpine?) of the Male Karpaty Mountains.

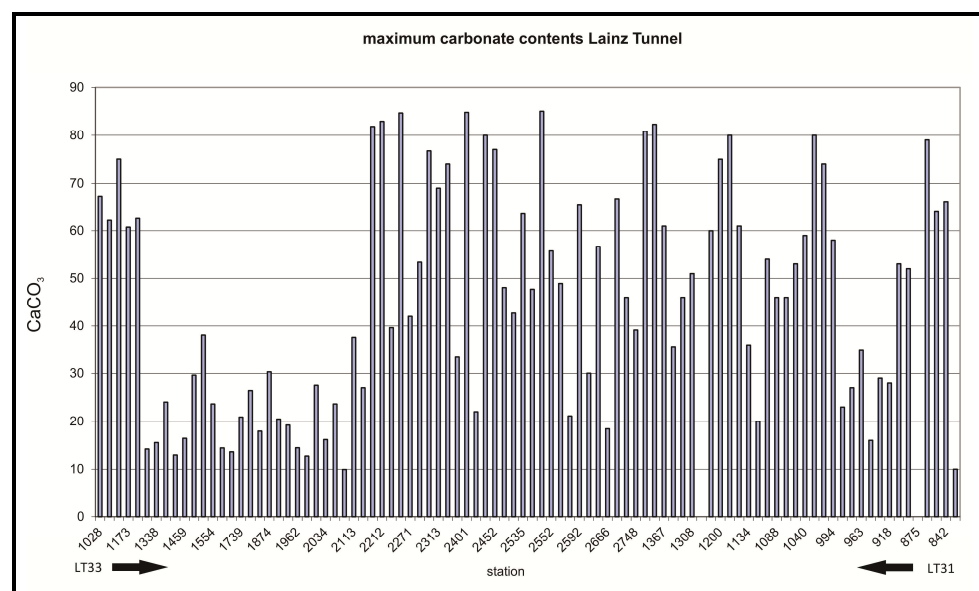
### C.4.3. Carbonate-Analysis

Fig. 112 shows the maximum carbonate contents of the Lainz Tunnel station LT33/1028m to LT31/842m, information from the first 1000m (Kahlenberg Formation and Hütteldorf Formation) can be found in Pfersmann (2009).

Consistently with the other results of this work distinct higher carbonate contents can be observed along the distance attributed to the St.Veit Klippenzone (station 2165m/LT33 to 869m/LT31), for average values from specific lithologies see also Fig. 111. The higher contents from LT33/1028m to approximately. LT33/1173m are assigned to the Kahlenberg Formation, while the lower contents from LT33/1338m to approximately. LT33/2113m are assigned to the Hütteldorf Formation. A table with detailed results of the carbonate analyses carried out can be found in the Appendix 3.

Lithology	CaCO <sub>3</sub>
Keuper sandstone (U Triassic)	0%
Keuper shale/mudstone (U Triassic)	0%
Sandstone/siltstone (L/M Jurassic)	9% to 18%
Calcareous mudstone (M Jurassic, Bajocian)	12% to 34%
Marlstone - argillac. limestone (Tithonian-Berriasian/Valanginian)	48% to 85%
Siliceous limestone (L Cretaceous, M/U Berriasian)	53% to 65%

**Fig. 111 Carbonate contents of different lithologies found in the St.Veit Klippenzone.**



**Fig. 112 Maximum carbonate contents in the Lainz Tunnel plotted along section.**

#### **C.4.4. Mineralogy of sandstones based on XRD Analysis**

In Pfersmann (2009) the mineralogy of sandstones from the first 1000m (Kahlenberg Nappe) of the Lainz Tunnel were described. This work deals with samples from station LT33/1028 to station 917/LT31.

Of altogether 35 sandstones analysed nine were suspected, due to their lithology and position in the tunnel section, to be Keuper sandstones and were additionally treated with ethylenglycol. The  $2\mu$  fraction was extracted from seven of the nine sandstones. Then the samples were treated by heating (+550°C), ethylenglycol,  $K^+$ ,  $Mg^{+2}$ ,  $K^+$  in combination with ethylenglycol and  $Mg^{+2}$  in combination with glycerine.

All seven sandstones contain quartz, feldspar, chlorite, kaolinite, mica and a regular interstratified (illit/smectite) mixed layer mineral in considerable amounts.

Fig. 115 shows a typical Keuper sandstone containing a regular interstratified (illit/smectite) mixed layer mineral. This seems to be a distinctive feature of Keuper sandstones from the St.Veit Klippenzone. Krumm (1964) describes considerable amounts of an illite-montmorillonite mixed layer mineral in Middle Keuper clays.

Faupl (1975) also reports an illite-montmorillonite mixed layer clay mineral from the Gresten sandstones of Liassic to Mid-Jurassic age. Faupl (1975) explains the differences between his investigated samples and the clay mineral composition by climatic and transport factors. This conclusion could also fit for the Keuper sandstones from the St.Veit Klippenzone.

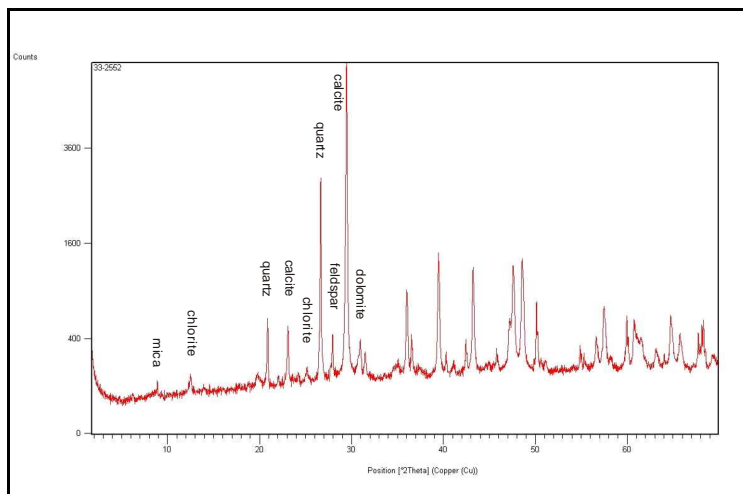
In all the other sandstones significant amounts of calcite, quartz, dolomite, feldspar, chlorite and mica could be determined.

Fig. 114 shows the result (XRD) of one sample considered to be a typical Jurassic sandstone from the St.Veit Klippenzone. All those determined minerals are a typical/normal association for marine sandstones, the illite-montmorillonite mixed layer mineral is missing.

The table below lists the samples used for XRD analysis and shows which samples were selected for additional treatments (ethylenglycol,  $2\mu$  +ethylenglycol/ glycerine/ temperature). The result of all XRD analysis carried out can be found in the Appendix 2.

lithology	sample no.	add. treatment	results
Cretaceous sandstone	LT33/1028m		quartz, calcite, feldspar, chlorite, mica and dolomite
Cretaceous sandstone	LT33/1380m		quartz, calcite, feldspar, chlorite, mica and dolomite
Cretaceous sandstone	LT33/1422m		quartz, calcite, feldspar, chlorite, mica and dolomite
Cretaceous sandstone	LT33/1498 m		quartz, calcite, feldspar, chlorite, mica and dolomite
Cretaceous sandstone	LT33/1554m		quartz, calcite, feldspar, chlorite, mica and dolomite
Cretaceous sandstone	LT33/1600m		quartz, calcite, feldspar, chlorite, mica and dolomite
Cretaceous sandstone	LT33/1739m		quartz, calcite, feldspar, chlorite, mica and dolomite
Cretaceous sandstone	LT33/1874m		quartz, calcite, feldspar, chlorite, mica and dolomite
Cretaceous sandstone	LT33/1893m	+EG	quartz, feldspar, chlorite, kaolinite, mica, calcite and mixed layer mineral
Cretaceous sandstone	LT33/1900m	+EG	quartz, feldspar, chlorite, kaolinite, mica and mixed layer mineral
Cretaceous sandstone	LT33/2005m		quartz, calcite, feldspar, chlorite, mica and dolomite
Cretaceous sandstone	LT33/2056m		quartz, calcite, feldspar, chlorite, mica and dolomite
Cretaceous sandstone	LT33/2113m		quartz, calcite, feldspar, chlorite, mica and dolomite
Cretaceous sandstone	LT33/2131m		quartz, feldspar, chlorite, mica and dolomite
Jurassic sandstone	LT33/2181m		quartz, calcite, feldspar, chlorite, mica and dolomite
Jurassic sandstone	LT33/2270m		quartz, calcite, feldspar, chlorite, mica and dolomite
Jurassic sandstone	LT33/2285m		quartz, calcite, feldspar, chlorite, mica and dolomite
Jurassic sandstone	LT33/2401m		quartz, calcite, feldspar, chlorite, mica and dolomite
Jurassic sandstone	LT33/2552m		quartz, calcite, feldspar, chlorite, mica and dolomite
Jurassic sandstone	LT33/2775m		quartz, calcite, feldspar, chlorite, mica and dolomite
Jurassic sandstone	LT33/2666m		quartz, calcite, feldspar, chlorite, mica and dolomite
Jurassic sandstone	LT31/1385m		quartz, calcite, feldspar, chlorite, mica and dolomite
Keuper sandstone	LT31/1277m	+EG	quartz, feldspar, chlorite, kaolinite, mica and mixed layer mineral
Keuper sandstone	LT31/1257m	+EG	quartz, feldspar, chlorite, kaolinite, mica and mixed layer mineral
Keuper sandstone	LT31/1219m	+EG	quartz, feldspar, chlorite, kaolinite, mica and mixed layer mineral
Keuper sandstone	LT31/1215m	+EG	quartz, feldspar, chlorite, kaolinite, mica and mixed layer mineral
Keuper sandstone	LT31/1200m	+EG	quartz, feldspar, chlorite, kaolinite, mica and mixed layer mineral
Keuper sandstone	LT31/1188m		quartz, feldspar, chlorite, kaolinite, mica and mixed layer mineral
Keuper sandstone	LT31/1164m	+EG	quartz, feldspar, chlorite, kaolinite, mica and mixed layer mineral
Jurassic sandstone	LT31/1133m	+EG	quartz, calcite, feldspar, chlorite, mica and dolomite
Jurassic sandstone	LT31/1119m	+EG	quartz, calcite, feldspar, chlorite, mica and dolomite
Cretaceous sandstone	LT31/944m		quartz, calcite, feldspar, chlorite, mica and dolomite
Cretaceous sandstone	LT31/917m		quartz, calcite, feldspar, chlorite, mica and dolomite
Cretaceous sandstone	LT31/857m		quartz, calcite, feldspar, chlorite, mica and dolomite
Cretaceous sandstone	LT31/810m		quartz, calcite, feldspar, chlorite, mica and dolomite

**Fig. 113 Lists of samples used for XRD analysis and results.**



**Fig. 114 LT33/2552** The figure shows the result (XRD) of one sample considered to be a typical Jurassic sandstone from the St.Veit Klippenzone with significant amounts of calcite, quartz, dolomite, feldspar, chlorite and mica.

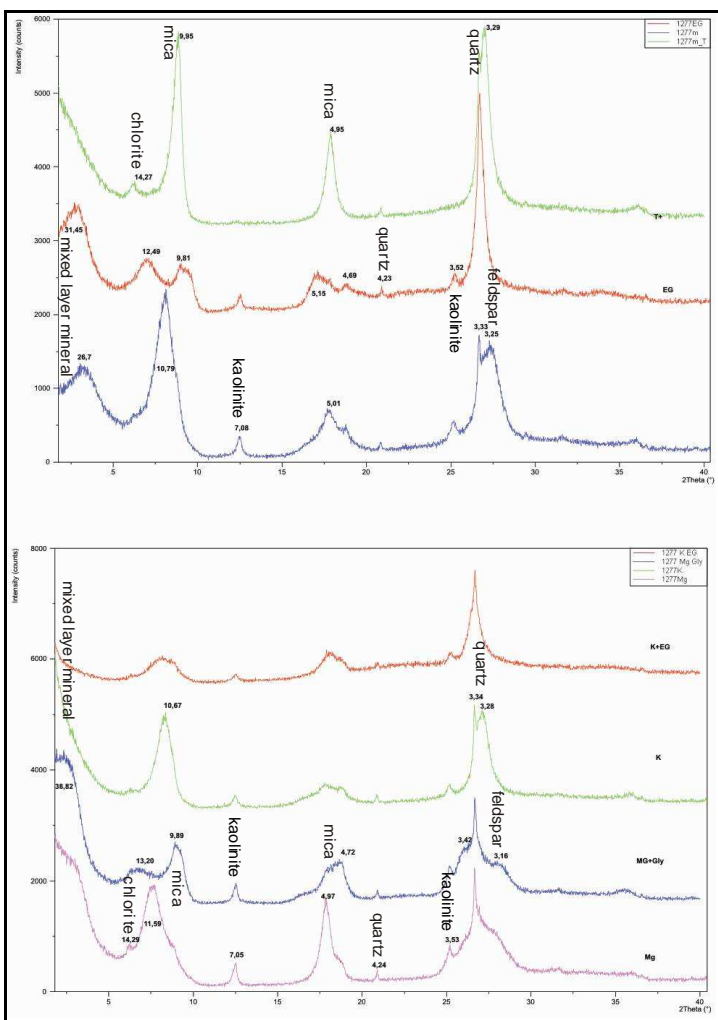


**Fig. 115 LT31/1277m XRD analysis (+ 2 $\mu$  fraction) of one sample considered to be a typical Keuper sandstone containing quartz, feldspar, chlorite, kaolinite mica and a regular interstratified (illit/smectite) mixed layer mineral (top diagram: green graph = tempered at +550°C, red graph = treated with ethylenglycol, blue graph = no treatment; bottom diagram: red graph = treated with K + ethylenglycol, green graph = treated with K, blue graph = treated with Mg + glycerine, purple graph = treated with Mg).**

#### **C.4.5. Geochemistry and Isotope Geochemistry**

##### **Methods whole-rock geochemistry**

For the geochemical bulk rock analysis 142 different sediment samples such as shales, siltstones, sandstones, marls, limestones and some cherts were used. The different samples derive from the Lainz Tunnel and different units and locations in Austria and Slovakia for comparision and correlation. The geochemical samples from the Lainz Tunnel were grouped according to lithology and age:

**Arkose/sandstone:** Keuper

**Shale mud:** Keuper

**Carbonates, calcareous shales and calc. sandstones:** Lower/Middle Jurassic

**Chert:** Bajocian, Valanginian ,various age

**Siliceous limestone with calpionellids:** Berriasian

The chemical analysis was done by AcmeLabs (Acme Analytical Laboratories Ltd., [www.acmelab.com](http://www.acmelab.com)) in Vancouver (Canada).

ICP-emission spectroscopy was used to detect oxides ( $\text{SiO}_2$ ,  $\text{Al}_2\text{O}_3$ ,  $\text{Fe}_2\text{O}_3$ ,  $\text{MgO}$ ,  $\text{CaO}$ ,  $\text{Na}_2\text{O}$ ,  $\text{K}_2\text{O}$ ,  $\text{TiO}_2$ ,  $\text{P}_2\text{O}_5$ ,  $\text{MnO}$  and  $\text{Cr}_2\text{O}_3$ ), some minor elements (Ni, Ba, Be, Co, Cs, Ga, Hf, Nb, Rb, Sn, Sr, Ta, Th, U, V, W and Zr) and the loss on ignition (LOI).

For the analysis of trace elements ICP-mass spectroscopy was used (REE: Sc, Y, La, Ce, Pr, Nd, Sm, Eu, Gd, Tb, Dy, Ho, Er, Tm, Yb and Lu; Noble and Base metals: Mo, Cu, Pb, Zn, Ni, As, Cd, Sb, Bi, Ag, Au, Hg, Tl and Se). Accuracy, precision and detection limits information of these analyses can be found at [www.acmelab.com](http://www.acmelab.com).

The main aims of the geochemical analysis was to characterize the sediments and to distinguish between units for a conclusive interpretation and correlation of the geotectonic position of the SVK versus related units of the Eastern Alps and the Western Carpathians, i.e. Klippenzone rocks. Factor function analysis was applied to the data set to determine provenance signatures (Roser and Korsch, 1988) in order to distinguish different source areas and different basins.

Concentrations of major and trace elements were used to draw conclusions about geological conditions, such as syndepositional weathering, and also to infer sediment provenance.

Depending on the lithology of the sample, investigated higher element values can be linked to

different minerals. In clastic sediments, such as sandstones, silica is mainly sourced by quartz, cherts, feldspars and clay minerals.  $\text{Al}_2\text{O}_3$  and  $\text{K}_2\text{O}$  are associated with potassium feldspars (orthoclase and microcline), illite and mica.  $\text{Na}_2\text{O}$  is commonly related to plagioclase feldspar.  $\text{CaO}$ , abundant in marine sediments, can be e.g. derived from calcite cement or rock fragments. High  $\text{MgO}$  contents are often caused by dolomitic materials such as rock fragments or cement. Iron contents could be related to iron oxide minerals and some Fe-containing clay minerals. Rutile and some tiopaque minerals deliver  $\text{TiO}_2$ . Higher  $\text{Zr}$  values can be explained with abundant zircon ( $\text{ZrSiO}_4$ ). Commonly Cr values are high with abundant Cr-spinel  $[(\text{Mg}, \text{Fe}^{2+})\text{O}(\text{Cr}, \text{Al}, \text{Fe}^{3+})_2\text{O}_3]$ . Because Ni can also replace Cr in Cr-spinel, it is used together with Cr to identify mafic to ultramafic sediment provenance. High Ni values can be caused by chlorite, a product of pyroxene alteration, also indicating mafic influence. For pure claystones this conclusion can't be used, because Cr and Ni are chemical constituents of some clay minerals. The Chemical Index of Alteration (CIA), using the formula:  $\text{CIA} = [\text{Al}_2\text{O}_3 / (\text{Al}_2\text{O}_3 + \text{CaO}^* + \text{Na}_2\text{O} + \text{K}_2\text{O})] \times 100$  ( $\text{CaO}^*$  represents the  $\text{CaO}$  only from the silicate fraction), given by Nesbet and Young (1982), was used to gather paleoweathering information (Fedo et al., 1997; Yan et al., 2010). Some samples contained marine carbonate, therefore as an approximation, the  $\text{CaO}^*$  was assumed to be equivalent to  $\text{NaO}$  (McLennan, 1993). The Chemical Proxy of Alteration (CPA) (Buggle et al., 2011) is additionally used to avoid the use of  $\text{CaO}^*$ . The formula is:  $[\text{CPA} = 100 \times \text{Al}_2\text{O}_3 / (\text{Al}_2\text{O}_3 + \text{Na}_2\text{O})]$

A summary of different approaches and indices used to classify clastic provenance and tectonic setting by geochemical means is given in the table below.

Reference	Plot	What it separates
Bhatia, 1983	100x $\text{Fe}_2\text{O}_3/\text{SiO}_2$ &100x $\text{Al}_2\text{O}_3/\text{SiO}_2$ $\text{Fe}_2\text{O}_3/(100-\text{SiO}_2)\&\text{Al}_2\text{O}_3/(100-\text{SiO}_2)$ $\text{Al}_2\text{O}_3/\text{SiO}_2\&(\text{Fe}_2\text{O}_3+\text{MgO})$ $\text{Fe}_2\text{O}_3/\text{TiO}_2\&\text{Al}_2\text{O}_3/(\text{Al}_2\text{O}_3+\text{Fe}_2\text{O}_3)$ $\text{SiO}_2\&(\text{Al}_2\text{O}_3+\text{K}_2\text{O}+\text{Na}_2\text{O})$ $\text{K}_2\text{O}/\text{Na}_2\text{O}\&\text{SiO}_2$ $\text{TiO}_2/\text{Fe}_2\text{O}_3+\text{MgO})$ CRV&YNi Th/Sc&Zr/Sc	near ridge/cont. margin near ridge/cont. margin passive margin/active cont. margin/cont. arc/oceanic arc near ridge/pelagic/cont. margin chemical maturity islandic arc/ act cont margin/ passive margin passive margin/active cont. margin/cont. arc/oceanic arc ophiolitic influence compositional variation& recycling upper crust/depleted mantle source& weathering
McLennan et al., 1993	Th/U&Th Th&Sc&Zr/10 La&Th&Sc Th&Co&Zr/10	sorting& o.c.isl.arc/ cont.isl.arc/ act.cont.margin/ passive margin sorting& o.c.isl.arc/ cont.isl.arc/ act.cont.margin/ passive margin sorting& o.c.isl.arc/ cont.isl.arc/ act.cont.margin/ passive margin
Taylor and McLennan, 1985	V/Zr & Zr/ $\text{Al}_2\text{O}_3$ V/Zr & Zr/Al2O3 Zr/Cr & Ti/Cr V/Zr & Ti/Zr	mafic/intermed/acid influence mafic/intermed/acid influence mafic/intermed/acid influence
Schnabel and Adamova, 1999	Sc/<math>\text{SiO}_2+\text{Al}_2\text{O}_3+\text{Fe}_2\text{O}_3+\text{MgO}+\text{Na}_2\text{O}+\text{TiO}_2</math> Ce/<math>\text{SiO}_2+\text{Al}_2\text{O}_3+\text{Fe}_2\text{O}_3+\text{MgO}+\text{Na}_2\text{O}+\text{TiO}_2</math> Th/<math>\text{SiO}_2+\text{Al}_2\text{O}_3+\text{Fe}_2\text{O}_3+\text{MgO}+\text{Na}_2\text{O}+\text{TiO}_2</math>	trace elements assoc.with clastic mat. trace elements assoc.with clastic mat. trace elements assoc.with clastic mat.
Madhavaraju, 2010	La/<math>\text{SiO}_2+\text{Al}_2\text{O}_3+\text{Fe}_2\text{O}_3+\text{MgO}+\text{Na}_2\text{O}+\text{TiO}_2</math>	trace elements assoc.with clastic mat.
Bhatia, 1985; . McLennan et al., 1993	REE	provenance

**Fig. 116 Different geochemical approaches to classify clastic provenance and tectonic setting.**

In the following chapters the geochemistry of individual sedimentary units or groups is discussed together with similar rock types from correlatable or discriminable units.

## 1. Sandstones

### ***Geochemistry of Keuper sandstones and Gresten quartzites***

#### ***General data info statistics***

The different samples of Keuper sandstones from the Lainz Tunnel consist of coarse quartzites and arkoses of coarse to fine grain size. The comparison samples from other locations are medium to coarse grained. This is important, because the geochemical approach to investigate the geological relations is handicapped by different grain sizes, i.e. coarser and finer material. It can be expected that fine grained variations of the same material show some variation and shift in chemistry. In many cases this leads to a higher amount of clay minerals and therefore e.g.  $\text{Al}_2\text{O}_3$ .

As long as there are no additional geochemical investigations, this should be regarded as a first step to differentiate geological units based on geochemistry.

The Gresten arkosic sandstones were included into this comparison as a reference because in older literature (e.g.: Trauth, 1930, Janoschek et al., 1956) the Keuper sandstones were interpreted as Gresten sandstones.

The table below gives an overview of the different units and samples compared.

Correlation	Sample site	Sample label	Add. lab label
Keuper sandstones			
St.Veit KZ	Lainz Tunnel	1900 m LT33 Sandst gr	
St.Veit KZ	Lainz Tunnel	LT31 1277 SST	
St.Veit KZ	Lainz Tunnel	LT31 1219,5 SST	
St.Veit KZ	Lainz Tunnel	1188,5 m LT31 Sandst	
St.Veit KZ	Lainz Tunnel	1164,5 m LT31 AKST	
dislodged slice-unknown	Groisbach	Keuper	32
Drietoma Unit	Typeloc.Driet	Quartzite/Sst	no.4/2011
Drietoma Unit	Typeloc.Driet	grad. Breccie	no.6/2011
Krížna Nappe	Zazriva	Keuper,sst	36

Kopieniz Fm-Krížna Nappe	Kopieniz Fm	SstN	no.13/2011
Krížna Nappe	Krížna Nappe	Keuper	
Correlation	Sample site	Sample label	
Gresten			
quartzites			
Gresten Klippenzone	Gresten	GRE1	
Gresten Klippenzone	Gresten	GRE2	
Gresten Klippenzone	Gresten	GRE3	
Gresten Klippenzone	Gresten	GRE4	
Gresten Klippenzone	Gresten	GRE5	

**Fig. 117 Samples of Keuper sandstones and Gresten quartzites.**

## Factor analysis

Comparing the samples with the help of factor analysis is handicapped by the low number of samples. The influence of the first three main factors can be seen in the Screeplot below. In the componentmatrix plot (see Appendix 4) the impact of different elements on the factors is listed. In factor 1 elements like Yb, Lu, U, Tm, Nb, Th, TiO<sub>2</sub>, Zr, Al<sub>2</sub>O<sub>3</sub>, K<sub>2</sub>O... can be found. Factor 2 includes elements like SiO<sub>2</sub>, MnO, As, Cu, Na<sub>2</sub>O. This suggests that the main discrimination between the different groups can be found within minerals including rare elements such as Lu, Yb,... Commonly REEs are enriched in fine grain sizes, therefore it is problematic to compare different grain sizes and heritated information. In the plot below (Fig. 119) this problem can be observed. Sample 47 and 43 are fine grained varieties of Keuper sandstones from the Lainz Tunnel, they plot quite far away from the other samples.

Beside the fact that there are by far not enough samples for statistical significance, a rough separation of the Gresten sandstones from the other samples can be seen in this plot, but this of course is only interpretation. At least, the trends of SVK versus Gresten sandstones are distinctly different in the plot of factor 1 vs. factor 2.

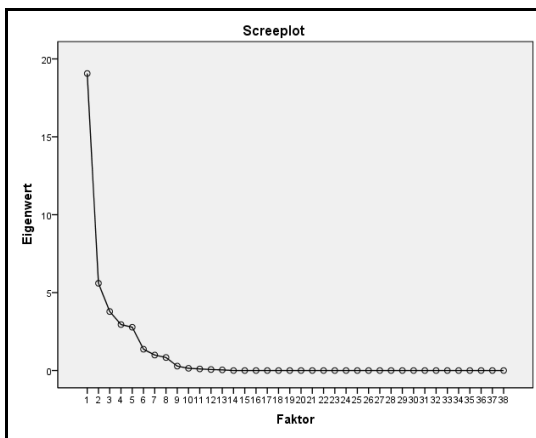


**Fig. 118 Screeplot Keuper sandstones and Gresten quartzites: Importance of the factors.**

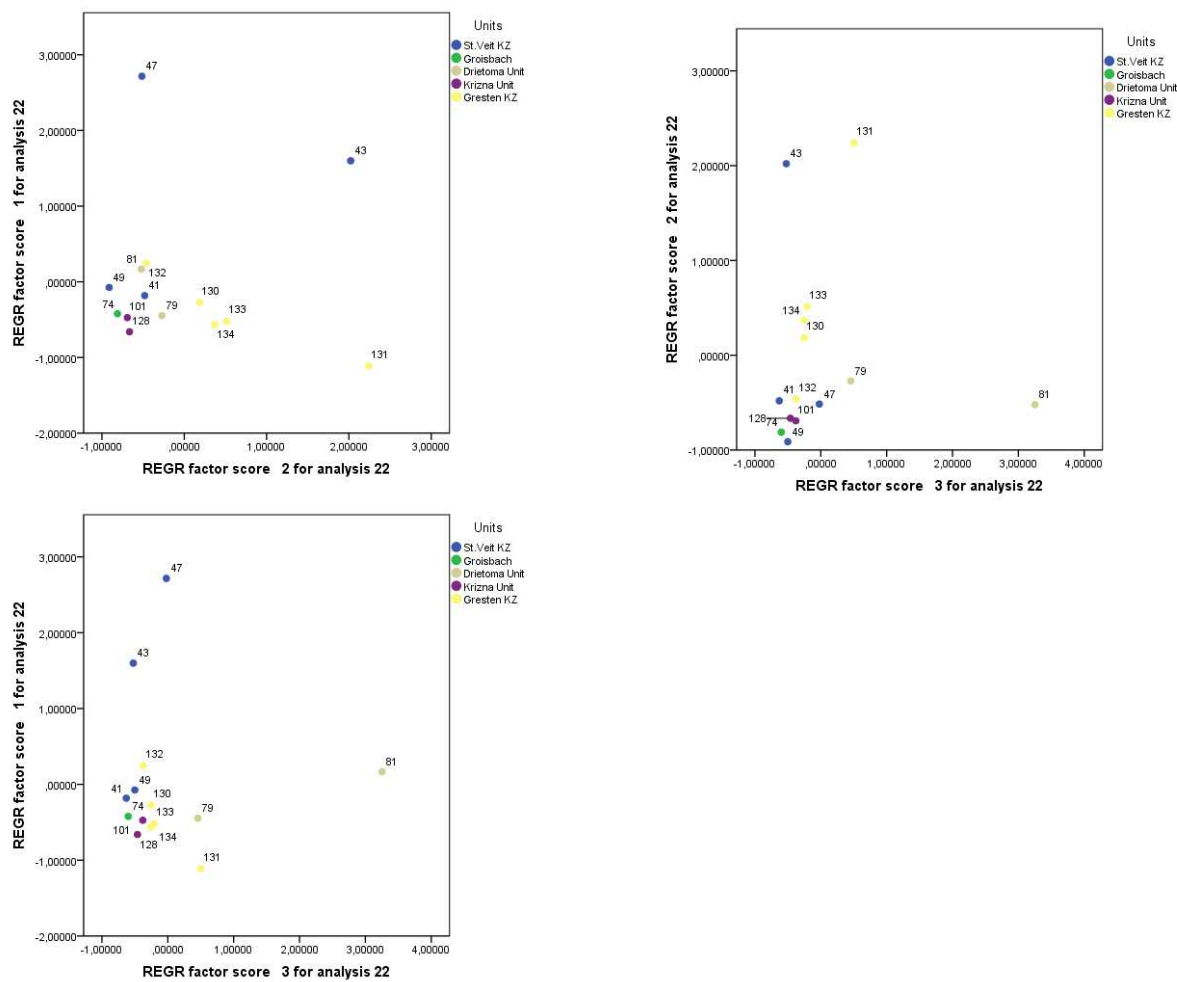


**Fig. 119 Factor vs. factor plots of the Keuper and Gresten sandstones.**

## **Major and trace elements**

The low number of samples makes it difficult to give statistical representative information about the sample groups and therefore this is only a first attempt to differentiate the groups. This is also the reason why no r values for correlations are given. In the Cr vs TiO<sub>2</sub> plot (Fig. 120) the Gresten samples have significant Cr values, while all the other groups have Cr values below the detection limit, the TiO<sub>2</sub> values of the Gresten samples are also higher than all others. This plot is normally used to differentiate between different sources with or without mafic material input. Here, because both Cr and TiO<sub>2</sub> of the Gresten samples show higher values, it could be interpreted that the Gresten samples consist of more different minerals and, hence, source areas, and therefore are not as well sorted and compositionally mature as the others.

A similar interpretation can be made in the TiO<sub>2</sub> vs V plot (Fig. 121). The TiO<sub>2</sub> value normally is used as an acidic material representative whereas V represents more mafic material.

Most samples plot below the detection limit of V values, but three Gresten samples have higher V values and all Gresten samples have higher TiO<sub>2</sub> values compared to the other groups. This could be also interpreted that the Gresten material consists of different minerals in higher contents. The Th/U vs Th plot (Fig. 122) is usually a tool for differentiating weathering conditions and sources (Mc Lennan et al., 1993). Higher values of Th and Th/U together with a positive correlation would indicate higher degrees of weathering. Th/U values higher than approximately 4 indicate an upper crustal material source. The Gresten samples have no Th/U value higher than 4.

The 100xFe<sub>2</sub>O<sub>3</sub>/SiO<sub>2</sub> vs 100xAl<sub>2</sub>O<sub>3</sub>/SiO<sub>2</sub> plot (Fig. 123) (Bhatia 1983) shows a slight differentiation between the Gresten sandstones and the other groups. The differences are mainly higher Al<sub>2</sub>O<sub>3</sub> values and one higher Fe<sub>2</sub>O<sub>3</sub> value of the Gresten samples.

This higher Al<sub>2</sub>O<sub>3</sub> contents can also be observed in the Al<sub>2</sub>O<sub>3</sub>/SiO<sub>2</sub> vs Fe<sub>2</sub>O<sub>3</sub>+MgO plot.

In the K<sub>2</sub>O/Na<sub>2</sub>O vs SiO<sub>2</sub> plot (Fig. 125) the Keuper sandstones have higher SiO<sub>2</sub> values and the Gresten samples the highest K<sub>2</sub>O/Na<sub>2</sub>O value.

The SiO<sub>2</sub> vs (Al<sub>2</sub>O<sub>3</sub>+K<sub>2</sub>O+Na<sub>2</sub>O) plot (Fig. 126) compares SiO<sub>2</sub> content to elements found in shale minerals or feldspar, the Gresten sandstones have higher values of these elements.

Beside this fact this plot shows a negative correlation of SiO<sub>2</sub> and (Al<sub>2</sub>O<sub>3</sub>+K<sub>2</sub>O+Na<sub>2</sub>O).

The TiO<sub>2</sub> vs (Fe<sub>2</sub>O<sub>3</sub>+MgO) plot (Fig. 127) was used to differentiate between acidic (TiO<sub>2</sub>) and more mafic (Fe<sub>2</sub>O<sub>3</sub>+MgO) influence. Here the Gresten sandstones show higher contents of TiO<sub>2</sub>, but there is no significant difference in Fe<sub>2</sub>O<sub>3</sub> or MgO content.

Th, Ce, La and Sc vs  $(\text{SiO}_2 + \text{Al}_2\text{O}_3 + \text{Fe}_2\text{O}_3 + \text{MgO} + \text{Na}_2\text{O} + \text{TiO}_2)$  plots (Fig. 128) are used for characterizing different geological groups. These trace elements are known for their relative immobility (Madhavavaju, 2010). In all four plots the Gresten samples group in a different way than the other groups. The V/Zr vs Zr/Ni, Zr/ $\text{Al}_2\text{O}_3$ , Ti/Zr plots (Fig. 129) (Schnabel and Adamova, 1999) show clear separation of the Gresten group from the others in context with a higher V/Zr and the Ti/Zr ratio.

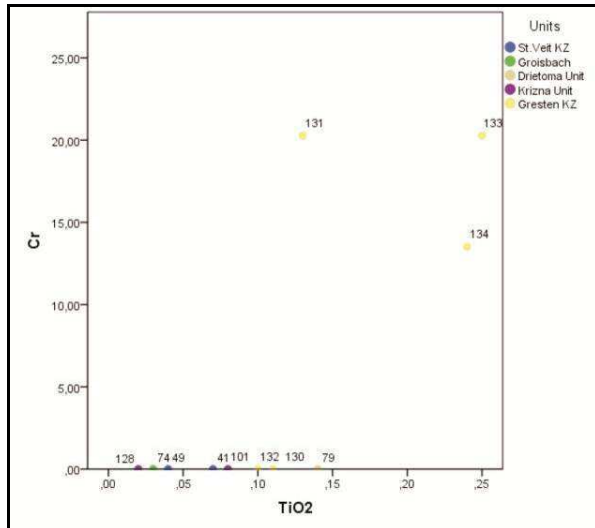


**Fig. 120** Cr vs  $\text{TiO}_2$  plot of the Keuper and Gresten sandstones.

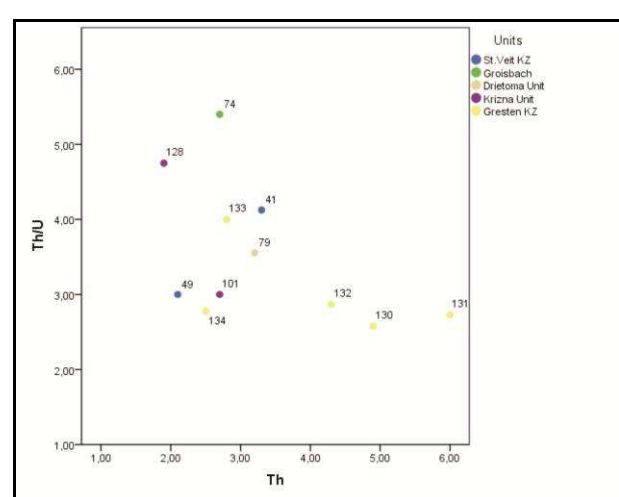


**Fig. 122** Th/U vs Th plot of the Keuper and Gresten sandstones (adapted after Mc Lennan et al., 1993).

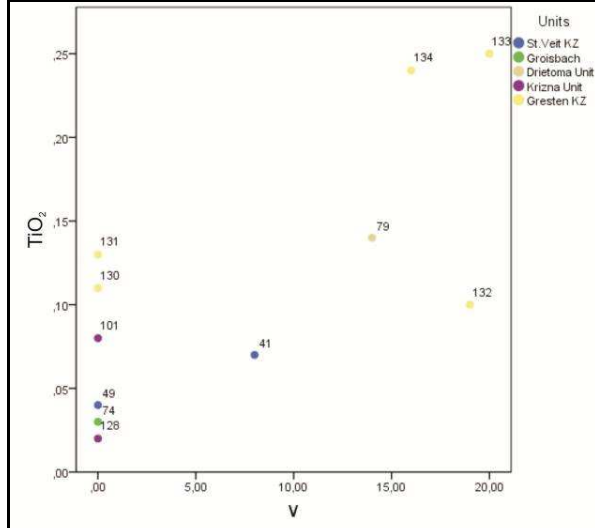


**Fig. 121**  $\text{TiO}_2$  vs V plot of the Keuper and Gresten sandstones.

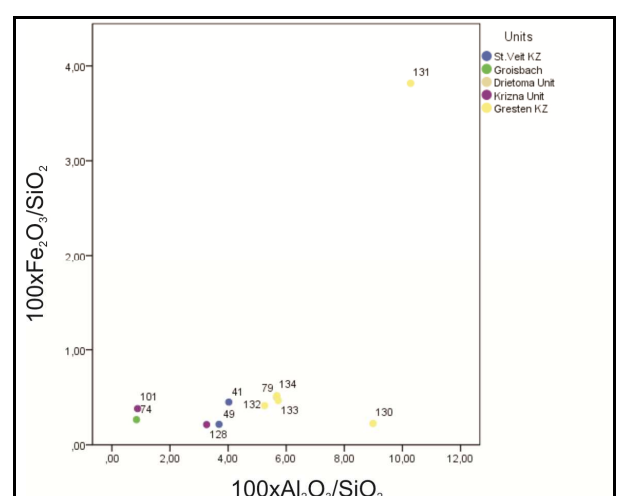


**Fig. 123**  $100x\text{Fe}_2\text{O}_3/\text{SiO}_2$  vs  $100x\text{Al}_2\text{O}_3/\text{SiO}_2$  plot of the Keuper and Gresten sandstones (adapted after Bhatia, 1983).

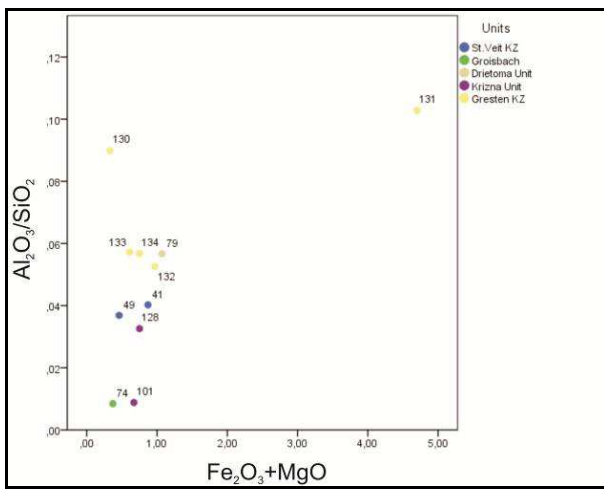


**Fig. 124**  $\text{Al}_2\text{O}_3/\text{SiO}_2$  vs  $\text{Fe}_2\text{O}_3 + \text{MgO}$  plot of the Keuper and Gresten sandstones (adapted after Bhatia, 1983).

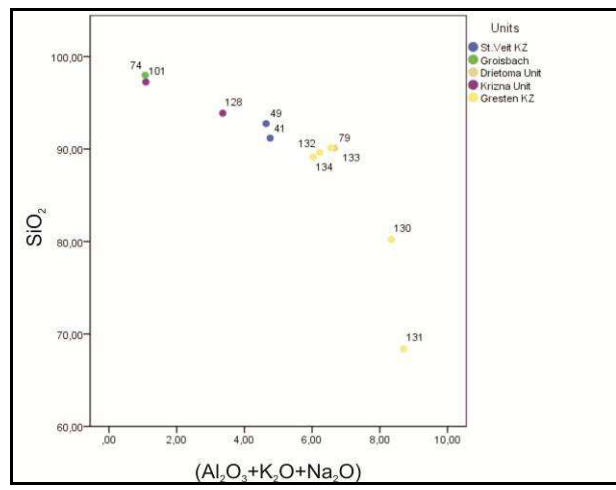


**Fig. 126**  $\text{SiO}_2$  vs  $(\text{Al}_2\text{O}_3 + \text{K}_2\text{O} + \text{Na}_2\text{O})$  plot of the Keuper and Gresten sandstones (adapted after Bhatia, 1983).

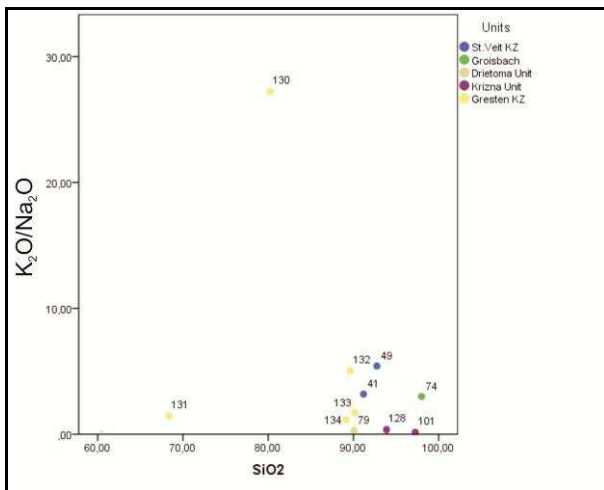


**Fig. 125**  $\text{K}_2\text{O}/\text{Na}_2\text{O}$  vs  $\text{SiO}_2$  plot of the Keuper and Gresten sandstones (adapted after Bhatia, 1983).

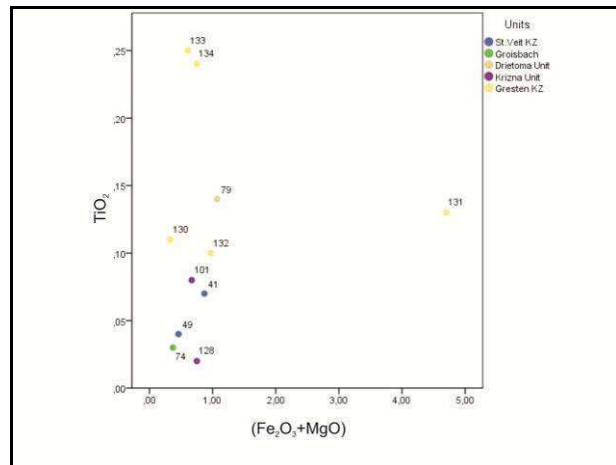


**Fig. 127**  $\text{TiO}_2$  vs  $(\text{Fe}_2\text{O}_3 + \text{MgO})$  plot of the Keuper and Gresten sandstones (adapted after Bhatia, 1983).

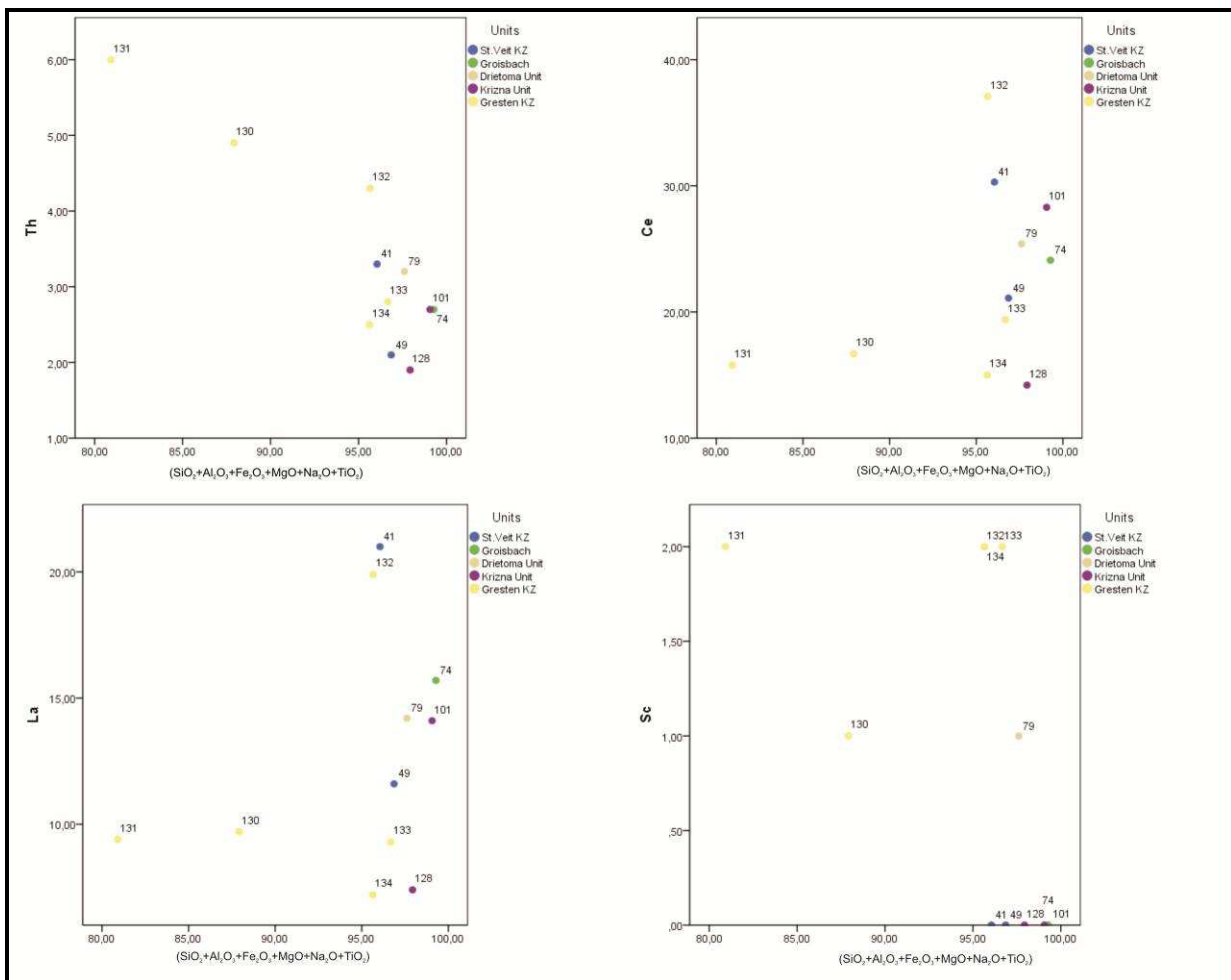


**Fig. 128 Th, Ce, La and Sc vs  $(\text{SiO}_2 + \text{Al}_2\text{O}_3 + \text{Fe}_2\text{O}_3 + \text{MgO} + \text{Na}_2\text{O} + \text{TiO}_2)$  plots of the Keuper and Gresten sandstones (adapted after Madhavavaju, 2010).**

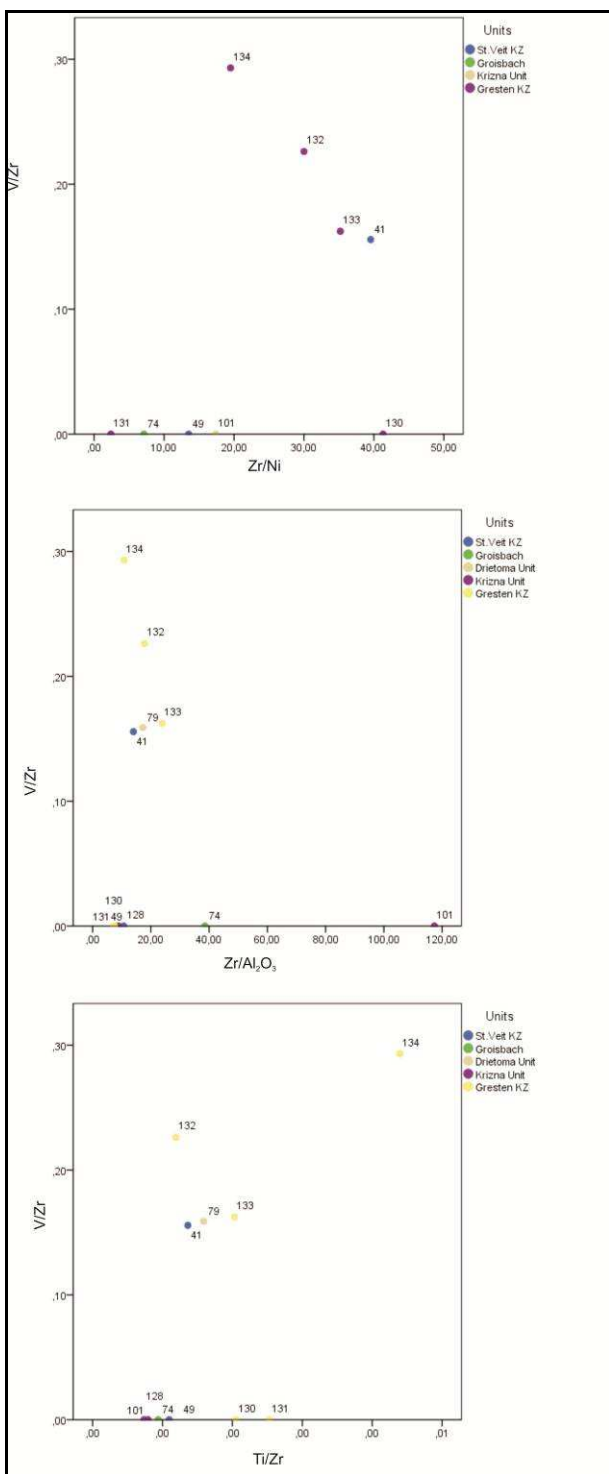


**Fig. 129** V/Zr vs Zr/Ni, Zr/Al<sub>2</sub>O<sub>3</sub>, Ti/Zr plots of the Keuper and Gresten sandstones (adapted after Schnabel and Adamova, 1999).

## **REE from Keuper and Gresten sandstones**

Most of the samples show no or only a slight Ce anomaly when normalized against chondrite. The Eu anomaly found in St.Veit Klippenzone and Drietoma Unit samples are stronger than the anomaly found in Gresten sandstones. One effect regarding the grain size can be observed in the diagrams: the coarser samples seem to have a higher content of REE's. The coarser St.Veit Klippenzone samples (1219/31; 1188/31) seem not to change the overall pattern, whereas this is not the case with the other group.

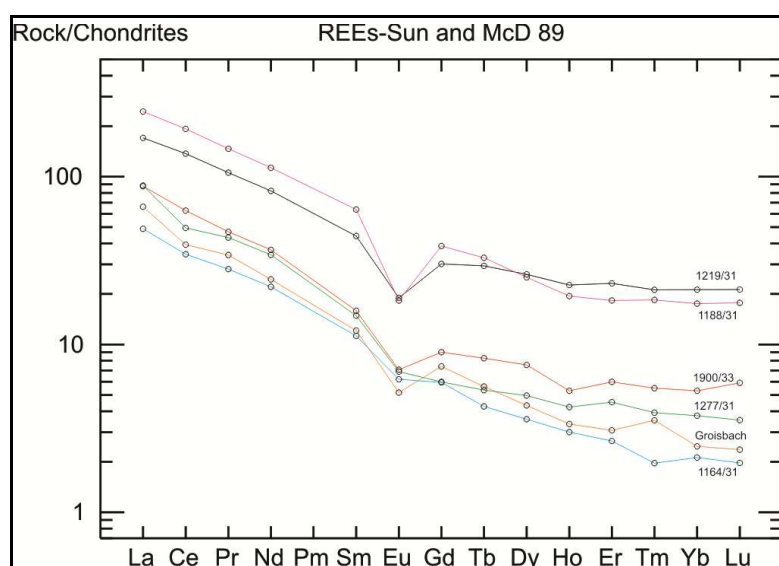


**Fig. 130 REE plot from St.Veit Klippenzone and Groisbach Keuper sandstones.**

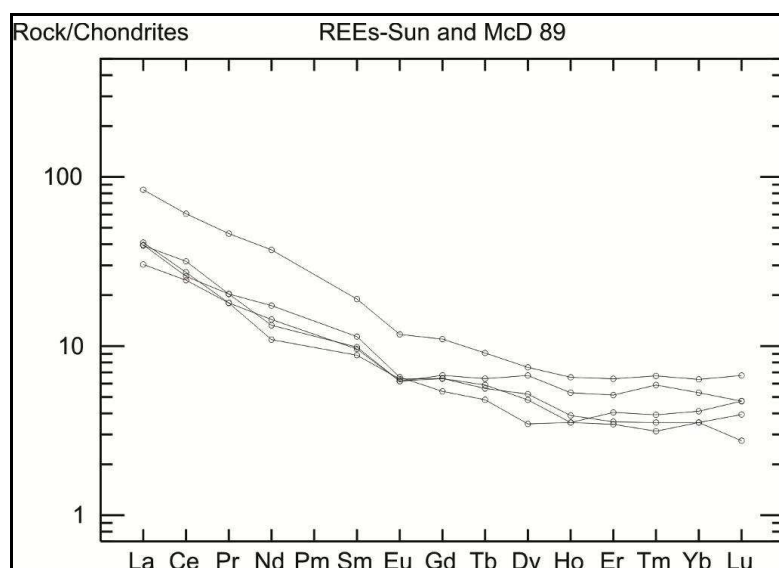


**Fig. 131 REE plot from Gresten Klippenzone sandstones.**

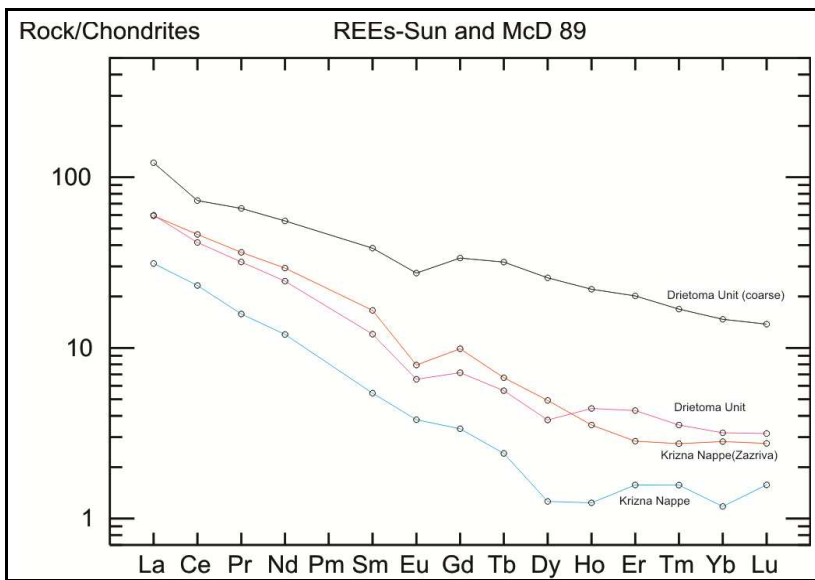


**Fig. 132 REE plot from Drietoma Unit Keuper sandstones.**

### **CIA of the Keuper and Gresten sandstones**

The Chemical Index of Alteration (CIA) and the Chemical Proxy of Alteration (CPA) were plotted against each other to see if both correlate. Fig. 133 shows the correlation of these related indices. In the A-CN-K diagram (Fig. 134) the samples from the Gresten Klippenzone and the St.Veit Klippenzone show higher CIA values, but the variation in CIA values may be caused by changes in grain size, the proportion of feldspars and various clay minerals in the samples analyzed.

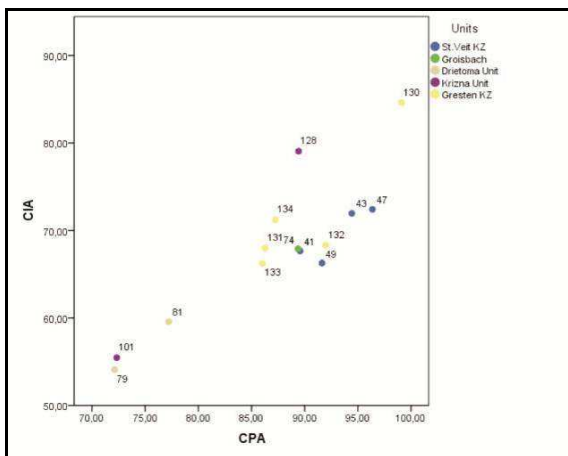


**Fig. 133 CIA vs CPA plot from Keuper and Gresten sandstones.**

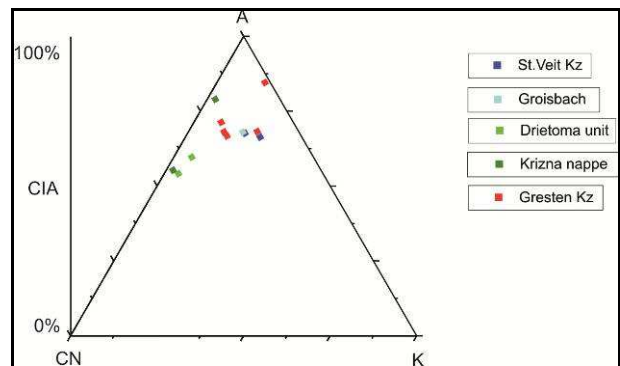


**Fig. 134 CIA plot from Keuper and Gresten sandstones.**

## **Geochemistry of Jurassic sandstones**

One question that had to be considered in the Lainz Tunnel dealing with the Jurassic sandstones, was how to distinguish between some fine grained Keuper sandstones and Jurassic sandstones. Beside obvious properties like (grey) colour, texture and direct undisturbed contact to other lithologies with known age, Jurassic sandstones show in most cases some calcite/carbonate content (for more information see also chapter C.4.3 (Carbonate analysis) and chapter C.4.4 dealing with mineralogy). This higher values can also be observed in the geochemistry data. In general, elements associated with marine environment like CaO, MgO, P<sub>2</sub>O<sub>5</sub> and Sr are enriched, compared to Keuper sandstones of similar grain size. The table below lists the samples used for geochemistry comparisons.

	Correlation	Sample site	Sample label	Add. lab label
Sandstones				
	St.Veit KZ	Lainz Tunnel	LT31 1385 SST	
	St.Veit KZ	Lainz Tunnel	810,5 m LT31 Sandst.	
	dislodged slice-unknown	Gutenbachtal	Lias,Sandst	35
	Drietoma Unit	Typeloc.Driet	Liassic Sst	no.7/2011
	Drietoma Unit	Typeloc.Driet	Liassic Sst	no.8/2011
	Drietoma Unit	Drietoma	SstN	no.5/2011
	Kržna Nappe	Zazriva	Lias Sandst,P3	40
	Manín Unit	P18	Gresten Sst	no.22/2011

**Fig. 135 Jurassic sandstones from different sample sites.**

## **Factor analysis**

The influence of the first three main factors can be seen in the Screeplot below. In the componentmatrix plot (see Appendix 4) the impact of different elements on the factors is listed. In factor 1, elements like  $\text{TiO}_2$  (0.938),  $\text{Al}_2\text{O}_3$  (0.907), Lu (0.907) or  $\text{P}_2\text{O}_3$  (0.751) with high input factor can be found. In factor 2, elements like  $\text{CaO}$  (0.785) or TOC (0.793) with also high input are found. This suggests that the difference between the two groups is based on marine associated elements and elements that are found in shale minerals. In the factor vs factor plots the two groups separate quite well. The scattered data points of the Keuper sandstones are to some extend explained by grain size effects, as mentioned in the chapter about Keuper sandstones (samples no. 43 and 47 are fine grained) and the low number of samples.

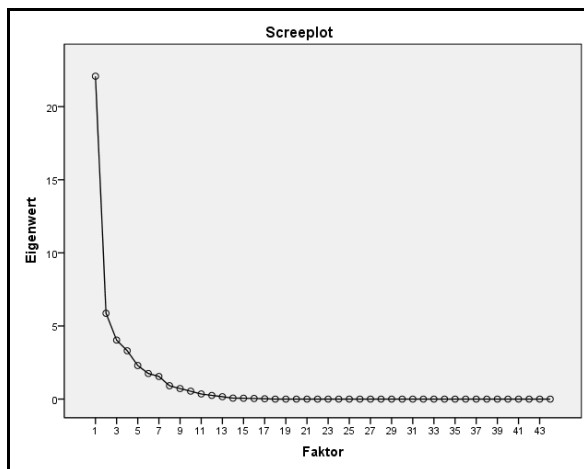


**Fig. 136 Screeplot of Jurassic sandstones and Keuper sandstones: Importance of the factors.**

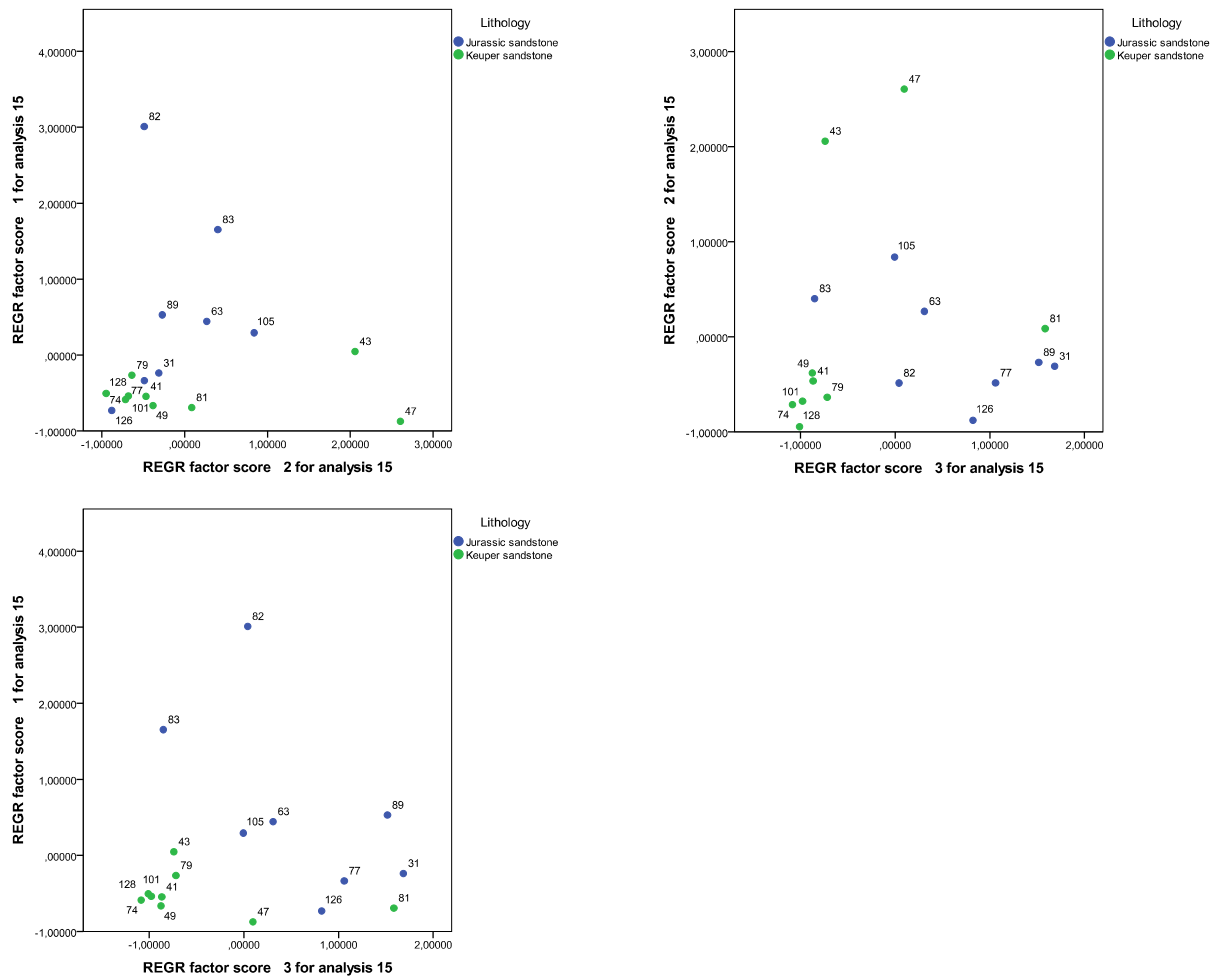


**Fig. 137 Factor vs factor plots of the Keuper and Jurassic sandstones.**

### Major elements

As it can be seen in the plots Fig. 137 to Fig. 140, the Jurassic sandstones consist of more  $\text{Al}_2\text{O}_3$ ,  $\text{Fe}_2\text{O}_3$ ,  $\text{MgO}$  and  $\text{TiO}_2$ . In the  $100x\text{Fe}_2\text{O}_3/\text{SiO}_2$  vs  $100x\text{Al}_2\text{O}_3/\text{SiO}_2$  plot the Jurassic sandstones have a  $r$  value of 0.973 ( $R^2=0.946$ ) compared to  $r=0.426$  ( $R^2=0.181$ ). Similar results can be given with the  $\text{Al}_2\text{O}_3/\text{SiO}_2$  vs  $\text{Fe}_2\text{O}_3/\text{MgO}$  plot, Jurassic sandstones have a  $r$  value of 0.637 ( $R^2=0.405$ ) and Keuper sandstones have a  $r$  value of 0.730 ( $R^2=0.532$ ). The  $\text{TiO}_2$  vs  $(\text{Fe}_2\text{O}_3+\text{MgO})$  plot can be described with Jurassic sandstones  $r= 0.509$  ( $R^2= 0.259$ ) compared to Keuper sandstones with  $r= 0.760$  ( $R^2= 0.577$ ). The Th vs La plot (Fig. 141) show similar  $r$  values for the Jurassic sandstones ( $r=0.891$ ) and Keuper sandstones ( $r=0.867$ ), but higher amounts of La, Th in the Jurassic sandstones. This could be caused by the coarser grain size effect or by a better sorting of the Keuper sandstones. The lower content of trace elements in the Keuper sandstones can also be observed in the Th vs Sc plot (Fig. 142)

(Jurassic sandstones  $r=0.851$ ,  $R^2=0.724$ ; Keuper sandstones  $r=0.477$ ,  $R^2=0.227$ ) Most of the Keuper sandstones Sc values are close to detection limit or below.

The Th/U vs Th plot (Fig. 143) (Mc Lennan et al., 1993) shows different behaviour of these two groups, but it remains unclear if weathering conditions and/or material sources are the reason, because a strong positive correlation is missing in both groups.

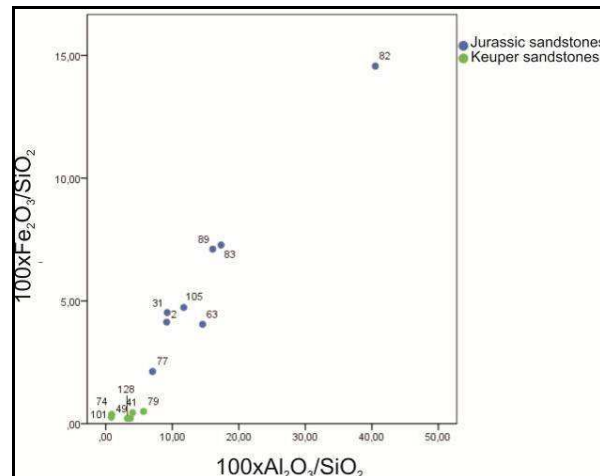


**Fig. 138**  $100x\text{Fe}_2\text{O}_3/\text{SiO}_2$  vs  $100x\text{Al}_2\text{O}_3/\text{SiO}_2$  plot of Jurassic and Keuper sandstones (adapted after Bhatia, 1983).

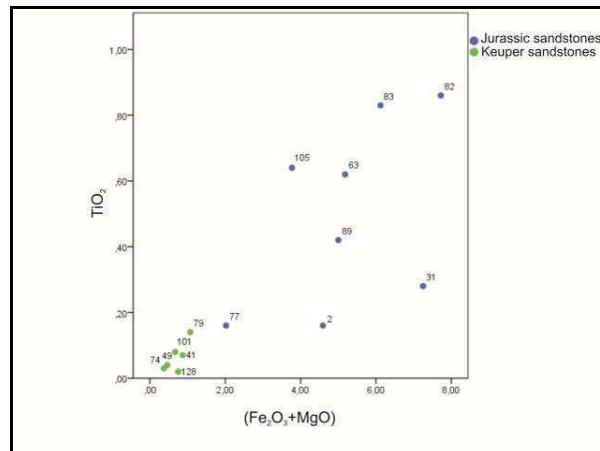


**Fig. 140**  $\text{TiO}_2$  vs  $(\text{Fe}_2\text{O}_3+\text{MgO})$  plot of Jurassic and Keuper sandstones (adapted after Bhatia, 1983).

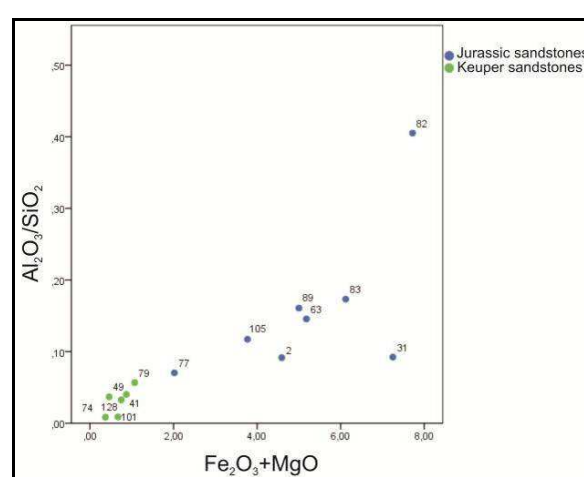


**Fig. 139**  $\text{Al}_2\text{O}_3/\text{SiO}_2$  vs  $\text{Fe}_2\text{O}_3/\text{MgO}$  plot of Jurassic and Keuper sandstones (adapted after Bhatia, 1983).

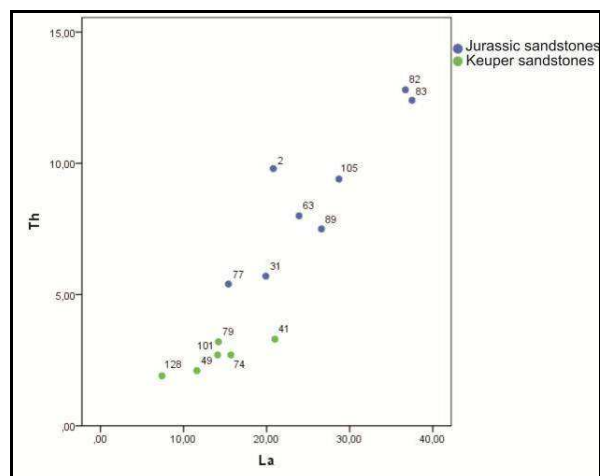


**Fig. 141** Th vs La plot of Jurassic and Keuper sandstones.

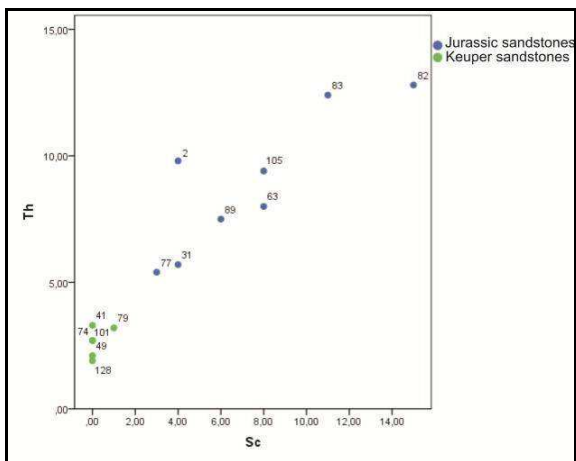


**Fig. 142** Th vs Sc plot of Jurassic and Keuper sandstones.

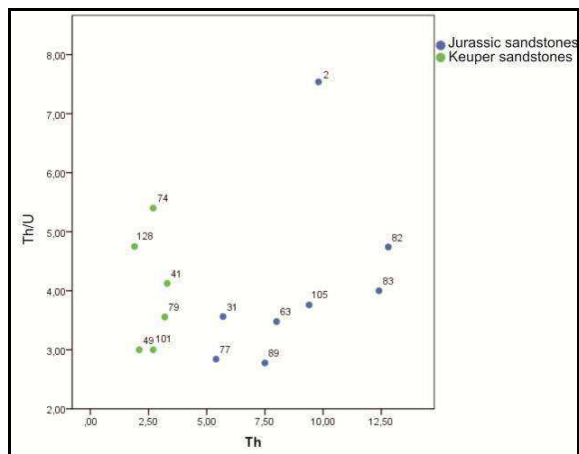


**Fig. 143** Th/U vs Th plot of Jurassic and Keuper sandstones (adapted after Mc Lennan et al., 1993).

### **REE from Jurassic sandstones**

The different samples of Jurassic sandstones showed quite homogeneous patterns of REE's, with no Ce anomaly but an Eu anomaly. The Manín Unit, in contrast to that, has both anomalies and is also depleted in Tm and Yb.

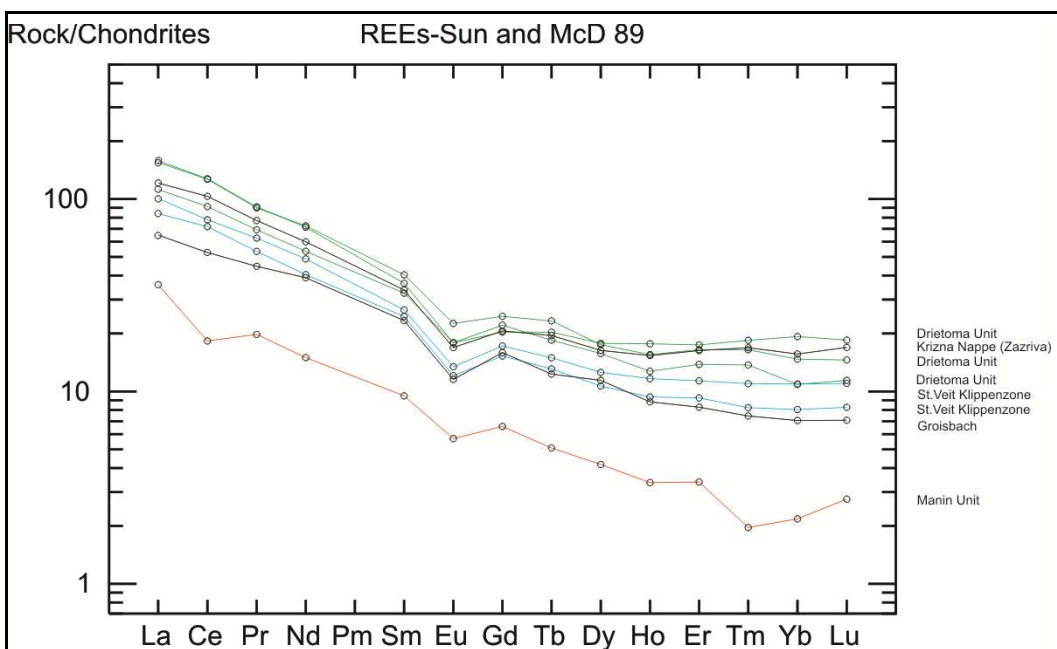


**Fig. 144** REE plot of Jurassic sandstones from the St.Veit Klippenzone, Groisbach, Drietoma Unit and Manin Unit.

## CIA of Keuper and Jurassic sandstones

The Chemical Index of Alteration (CIA) and the Chemical Proxy of Alteration (CPA) correlate well (Fig. 145). In the A-CN-K diagram, Fig. 146, there is no separation of Keuper from Jurassic samples. The variation may be caused by changes in grain size, in most cases the Jurassic sandstones are finer grained with changing amounts of feldspars and various clay minerals.

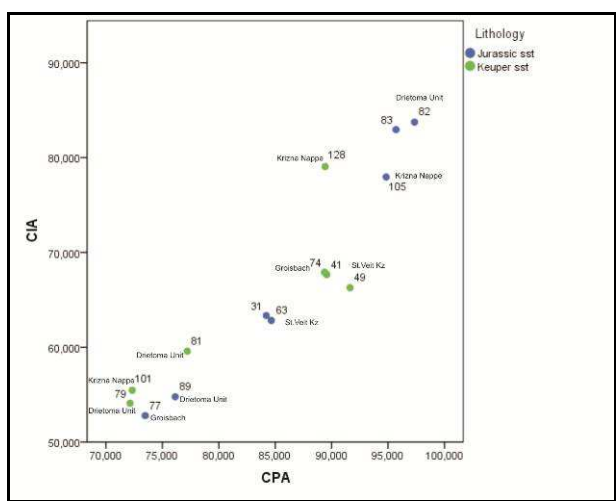


Fig. 145 CIA vs CPA plot from Keuper and Jurassic sandstones.

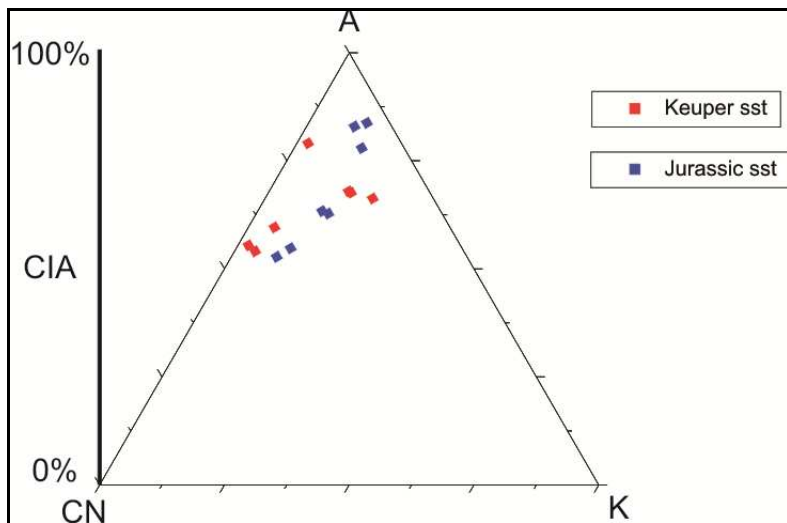


Fig. 146 CIA plot from Keuper and Jurassic sandstones.

## **Summary of results for Keuper, Jurassic sandstones and Gresten sandstones**

Comparing the Keuper sandstones from the St.Veit Klippenzone with definite Gresten sandstones showed some distinct differences. The Gresten samples display a higher diversity in element content. Compared to the Keuper sandstones, the Gresten arkoses are enriched in  $\text{Al}_2\text{O}_3$ ,  $\text{TiO}_2$ , Cr, V, also the  $\text{K}_2\text{O}/\text{Na}_2\text{O}$ ,  $\text{V}/\text{Zr}$  and  $\text{Ti}/\text{Zr}$  ratios are higher.

In the Th, Ce, La and Sc vs ( $\text{SiO}_2+\text{Al}_2\text{O}_3+\text{Fe}_2\text{O}_3+\text{MgO}+\text{Na}_2\text{O}+\text{TiO}_2$ ) plots (Fig. 128) (Madhavavaju, 2010) plots the Gresten samples group away from the other groups. These trends can also be found in the factor analysis and it could be interpreted that the Gresten samples consist of a greater variety of different minerals and, hence, source areas, and therefore are not as well sorted and compositionally mature as the Keuper sandstones from the St.Veit Klippenzone. Regarding the REE's, the St.Veit Klippenzone and Drietoma Unit samples show a slightly stronger Eu anomaly than found in the Gresten sandstones.

In the A-CN-K diagram (Fig. 134), the samples from the Gresten Klippenzone and the St.Veit Klippenzone show higher CIA values. The variation in CIA values may be caused by some minor changes in grain size or the proportion of feldspars and various clay minerals in the samples analyzed.

Comparing the Keuper sandstones with the Jurassic sandstones from the St.Veit Klippenzone showed also significant differences. In general, in the Jurassic sandstones elements associated with marine environments like  $\text{CaO}$ ,  $\text{MgO}$ ,  $\text{P}_2\text{O}_5$  and  $\text{Sr}$  are enriched, compared to Keuper sandstones of similar grain size.

Jurassic sandstones consist also of more  $\text{Al}_2\text{O}_3$ ,  $\text{Fe}_2\text{O}_3$ ,  $\text{MgO}$ ,  $\text{TiO}_2$ , La, Th, and Sc. This could be caused by the grain size effect or by a better sorting of the Keuper sandstones.

The factor analysis also reveals that the difference between the two groups is based on marine associated elements and elements that are found in shale minerals.

The different samples of Jurassic sandstones showed quite homogeneous patterns of REE's, with no Ce anomaly but a Eu anomaly. The Manín Unit, in contrast to that, has both anomalies and is also depleted in Tm and Yb.

In the A-CN-K diagram (Fig. 146), there is no separation of Keuper from Jurassic samples. The variation may be caused by changes in grain size, in most cases the Jurassic sandstones are finer grained with changing amounts of feldspars and various clay minerals.

## 2. Shales

### ***Geochemistry of Keuper shales***

In the Lainz Tunnel it was sometimes problematic to assign which of the shales encountered belong to the St.Veit Klippen and which are Hütteldorf Formation. This was caused by the tectonic deformation found in the Klippen, and the fact that Keuper shales can show a variety of colours including red, the same colour of the shales of the „Klippenhüllflysch”. Therefore only samples in direct contact to Keuper sandstones were used for geochemical analyses.

To verify the assumption that the samples taken are Keuper shales, they are compared to Jurassic shales from the St.Veit Tunnel. Fig. 147 gives an overview of the different units and samples compared.

### ***Geochemistry of Jurassic shales***

Comparisons of fresh shales from the Lainz Tunnel with outcropping units are handicapped by the typical properties of these soft rocks that lead to bad and weathered exposures. Soft shales of other Klippen units are seldom exposed, due to the fact that they are vulnerable to erosion and weathering. In addition, these incompetent shales are often strongly deformed by tectonic processes, therefore surrounding sediments could be mistaken due to tectonic juxtaposition. In this work only shale samples with clear correlation and attribution were used, and compared with shales of (assumed) Keuper age. A list of the used samples is given in Fig. 148 below.

	Correlation	Sample site	Sample label	Add. lab label
Keuper shales				
	St.Veit KZ	Lainz Tunnel	31/1257 shale red	12
	St.Veit KZ	Lainz Tunnel	LT31 1277 shale	
	St.Veit KZ	Lainz Tunnel	31/1219 shale red	9
	Drietoma Unit	Typeloc.Drietoma	shale red	no.3/2011
	Křížna Nappe	Zazriva	Keuper, shale red	37
	Křížna Nappe	Křížna Nappe	Keuper shale red	no.14/2011

**Fig. 147 Samples of Keuper shales.**

	Correlation	Sample site	Sample label	Add. lab label
Shales				
	St.Veit KZ	Lainz Tunnel	33/2211,5 shale	18
	St.Veit KZ	Lainz Tunnel	LT33 2576 shale	
	St.Veit KZ	Lainz Tunnel	LT33 2592 shale	
	St.Veit KZ	Lainz Tunnel	LT33 2592 shale	
	St.Veit KZ	Lainz Tunnel	LT33 2713 shale	
	St.Veit KZ	Lainz Tunnel	33/2775,3 shale gr	28
	St.Veit KZ	Lainz Tunnel	LT31 1366 shale	
	St.Veit KZ	Lainz Tunnel	LT31 1326 shale	
	St.Veit KZ	Lainz Tunnel	31/1188,5 shale	6
	St.Veit KZ	Lainz Tunnel	31/1133,5 shale	11
	St.Veit KZ	Lainz Tunnel	31/1133,5 shale	5
	St.Veit KZ	Lainz Tunnel	31/869,5gr shale	1
	Drietoma Unit	Typeloc.Driet	Liassic shale	no.9/2011

**Fig. 148 Jurassic shales from the Lainz Tunnel and Drietoma Unit.**

### Factor analysis

The samples of the Jurassic shales were compared with Keuper shales. The influence of the first three main factors can be seen in the Screeplot below. In the component matrix plot (see Appendix 4) the impact of different elements on the factors is listed. In factor 1 elements like TiO<sub>2</sub>, Ga, Sc, Ce, La, Yb,... can be found with high values (e.g.:Sc: 0.954). In the factor versus factor plots the Keuper shales separate quite well from the Jurassic shales. This would verify the previous assumption of different units and provenance.

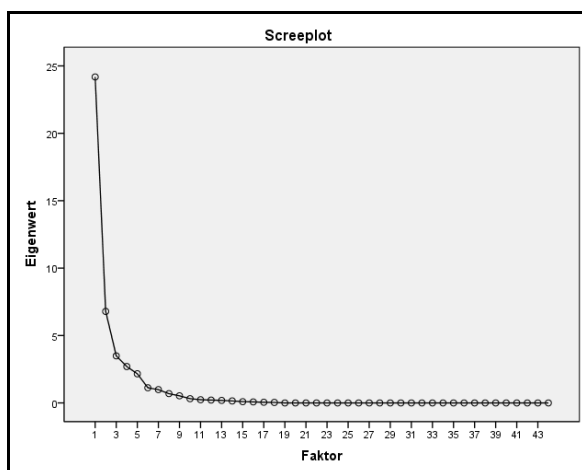


**Fig. 149 Screeplot Keuper shales and Jurassic shales: Importance of the factors.**

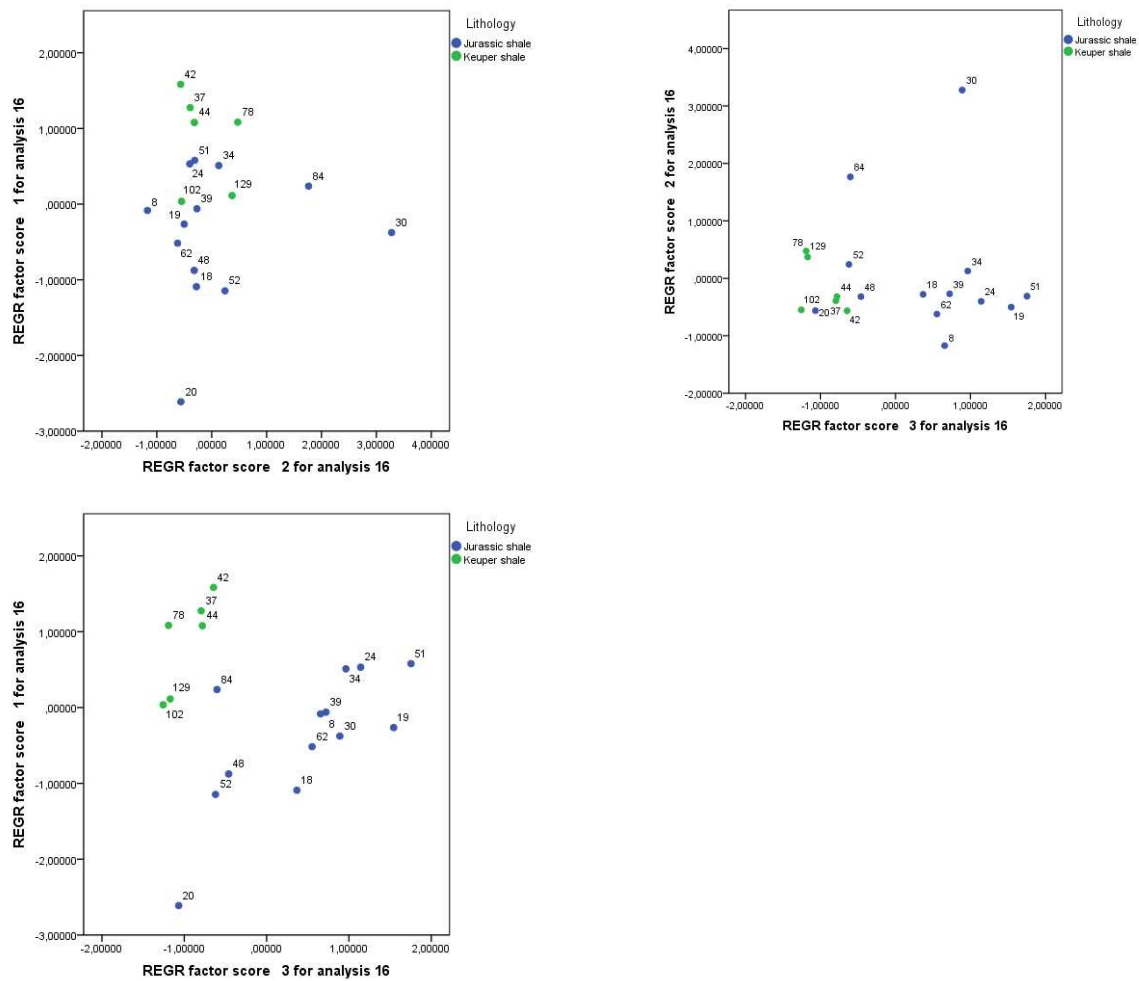


**Fig. 150 Factor vs factor plots of the Keuper and Jurassic shales.**

### **Major and trace elements**

Like the factor analysis, the bivariate plots show good separation between Jurassic and Keuper shales. In the  $K_2O/Na_2O$  vs  $SiO_2$  plot (Fig. 151) the r values can be given for the Jurassic shales with  $r = -0.382$ ;  $R^2 = 0.145$ , whereas the Keuper shales can be described with  $r = -0.594$  and  $R^2 = 0.3528$ .

The different  $K_2O/Na_2O$  ratio is also represented in the  $SiO_2/Al_2O_3$  vs  $K_2O/Na_2O$  plot (Fig. 152), with the Jurassic shales having a r value of -0.257 and  $R^2 = 0.066$ . The Keuper shales have a r value of -0.302 and  $R^2$  of 0.091. The  $Th/U$  vs  $Th$  plot (

Fig. 153), a tool for differentiating weathering conditions and sources (Mc Lennan et al., 1993), shows higher values of  $Th/U$  together with a positive correlation for the Keuper shales. This would indicate a higher degree of weathering. This trend goes along with the results from the CIA calculation (see Fig. 156; Fig. 157).  $Th/U$  values higher than approximately 4 would indicate an upper crust material source, all Keuper shale samples have higher values.

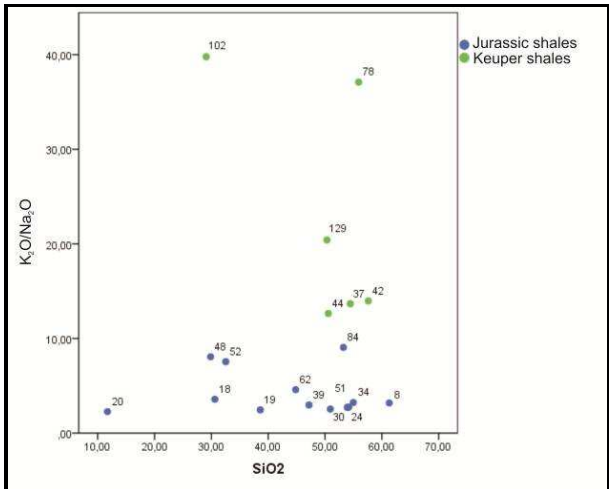


**Fig. 151**  $K_2O/Na_2O$  vs  $SiO_2$  plot of Keuper and Jurassic shales (adapted after Bhatia, 1983).

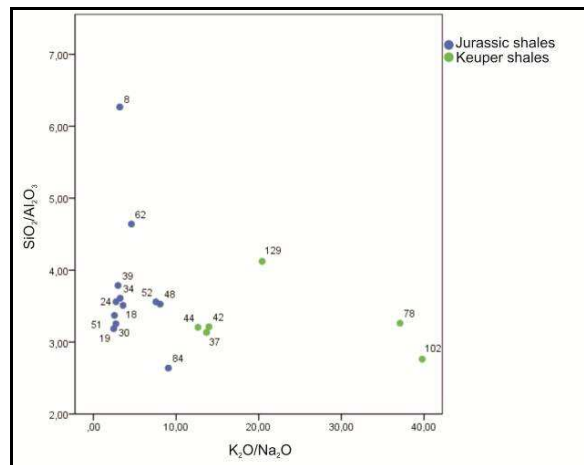


**Fig. 152**  $SiO_2/Al_2O_3$  vs  $K_2O/Na_2O$  plot of Keuper and Jurassic shales (adapted after Bhatia, 1983).

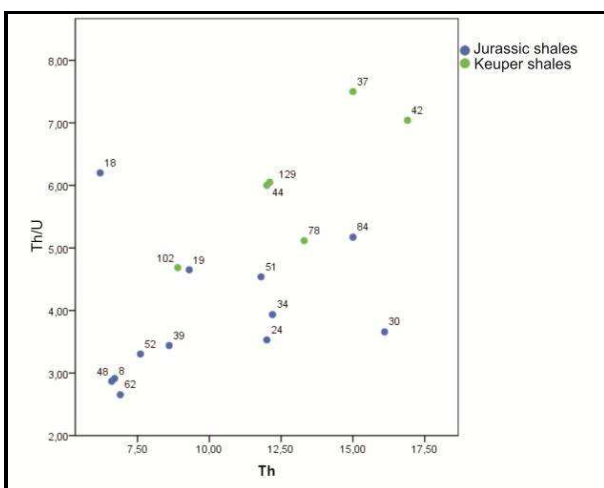


**Fig. 153**  $Th/U$  vs  $Th$  plot of Keuper and Jurassic shales (adapted after Mc Lennan et al., 1993).

## **REE from Keuper and Jurassic shales**

The REE patterns from Jurassic and Keuper shales are very similar, both show no or only a light Ce anomaly and a clear Eu anomaly. Based on this patterns it is not possible to differentiate between these two groups.

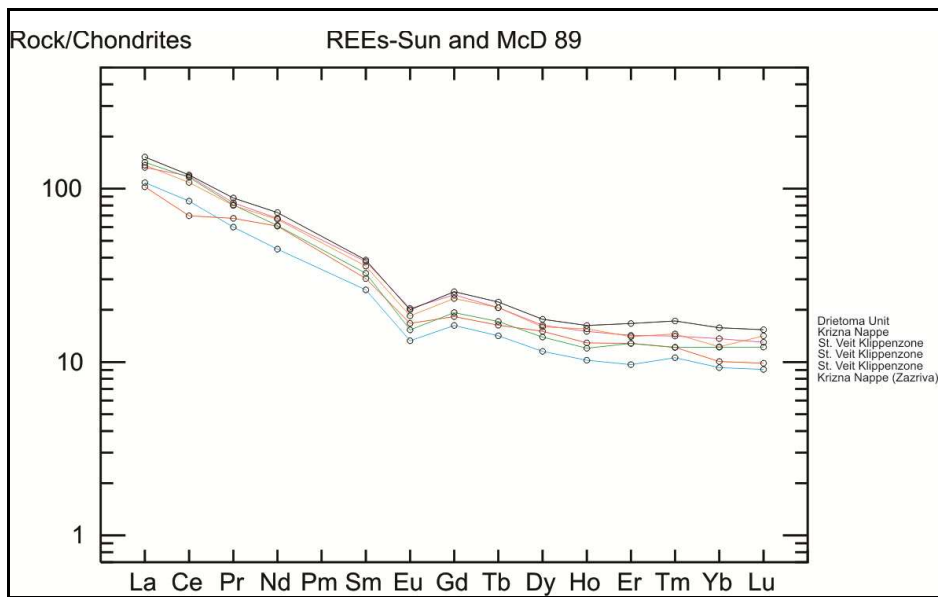


**Fig. 154 REE plot of Keuper shales from the St.Veit Klippenzone and Drietoma Unit.**

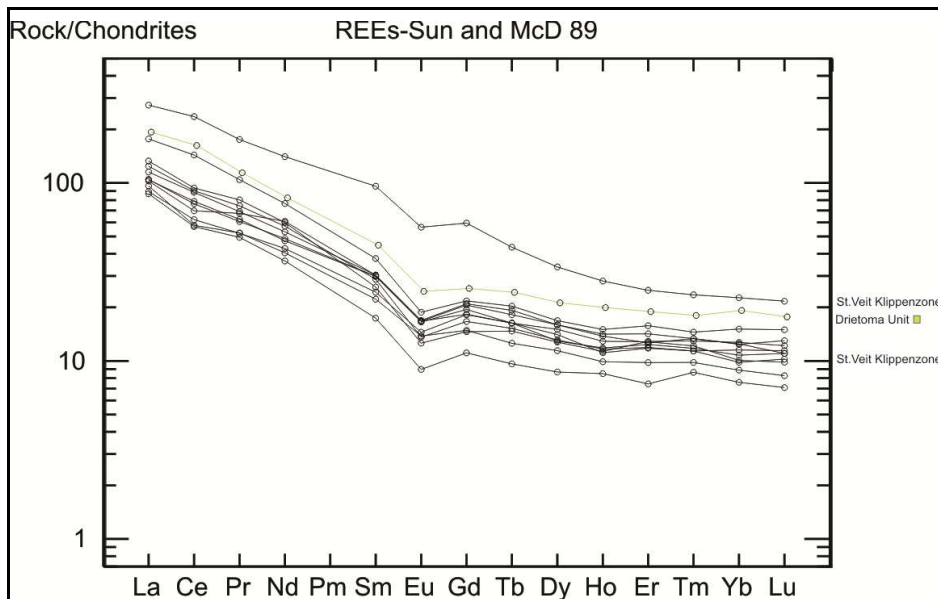


**Fig. 155 REE plot of Jurassic shales from the St.Veit Klippenzone and Drietoma Unit.**

## **CIA of Keuper shales and Jurassic shales**

The Chemical Index of Alteration (CIA) and the Chemical Proxy of Alteration (CPA) show a good correlation (Fig. 156). In the A-CN-K diagram Fig. 157 the samples from the Jurassic shale samples separate quite well from the Keuper shales, which show higher CIA values. This is consistent with the results from the Th/U vs Th plot (Fig. 153).

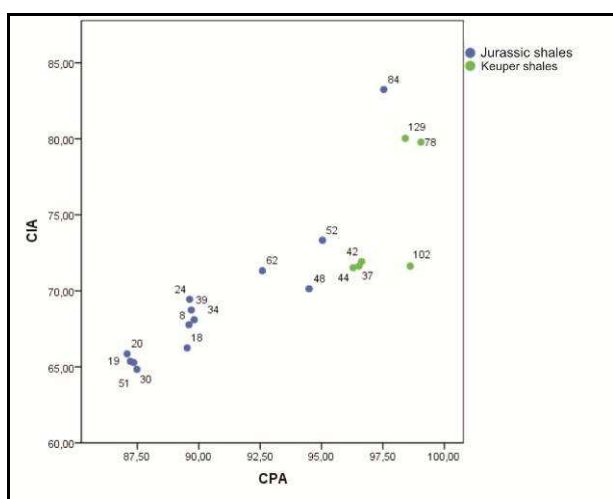


**Fig. 156 CIA vs CPA plot from Keuper shales and Jurassic shales.**

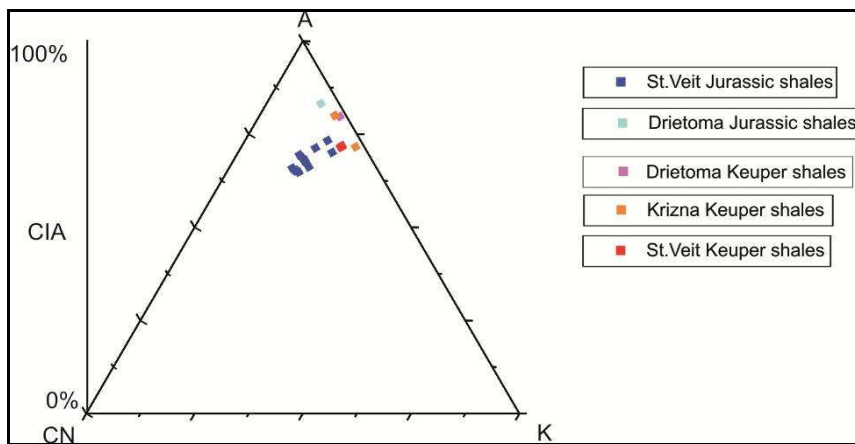


**Fig. 157 CIA plot from Keuper shales and Jurassic shales.**

## ***Discussion of results for Keuper shales and Jurassic shales***

Regarding the factor analysis the Keuper shales separate quite good from the Jurassic shales. This would verify the previous assumption of different units and provenance.

Like the factor analysis, the bivariate plots show good separation between Jurassic and Keuper shales.

As an example in the  $K_2O/Na_2O$  vs  $SiO_2$  plot (Fig. 151) the  $r$  values from the Jurassic shales ( $r = -0.382$ ,  $R^2 = 0.145$ ) and the Keuper shales ( $r = -0.594$ ,  $R^2 = 0.3528$ ) are quite different.

The Th/U vs Th plot (

Fig. 153) (Mc Lennan et al., 1993), indicates a higher degree of weathering for the Keuper shales. This trend goes along with the results from the CIA calculation. The Chemical Index of Alteration (CIA) and the Chemical Proxy of Alteration (CPA) show a good correlation ( Fig. 156). In the A-CN-K diagram Fig. 157 the samples from the Jurassic shale samples separate quite well from the Keuper shales, which show higher CIA values. The REE patterns from Jurassic and Keuper shales are very similar, both show no or only a light Ce anomaly and a clear Eu anomaly. Based on this patterns it is not possible to differentiate between these two groups. The results from the Keuper shales indicating a strong weathering in Late Triassic times and long transport of Keuper sediments resulting in higher maturity, are the same as observed with the Keuper sandstones and are consistent with literature (e.g.: Faupl, 2003).

### 3. Carbonates

#### ***Geochemistry of Jurassic carbonates***

The Jurassic carbonates analysed are characterized by their diversity in age, different carbonate contents, and varying terrigenous content. All carbonatic rocks of assumed Jurassic age were put together into one group, because of missing more specific statigraphic data. A list of the used samples is given in the table below.

Carbonates	Correlation	Sample site	Sample label	Add. lab label
St.Veit KZ		Lainz Tunnel	2074,4 m LT33 M	
St.Veit KZ		Lainz Tunnel	33/2165m	15
St.Veit KZ		Lainz Tunnel	33/2181kM	16
St.Veit KZ		Lainz Tunnel	33/2211,5 kM l	17
St.Veit KZ		Lainz Tunnel	33/2270 kM	20
St.Veit KZ		Lainz Tunnel	33/2299,5 kM	19
St.Veit KZ		Lainz Tunnel	2313 m/LT33 AmmnFm	
St.Veit KZ		Lainz Tunnel	33/2331 kM	21
St.Veit KZ		Lainz Tunnel	2401,2 m LT33 Crinsp k	
St.Veit KZ		Lainz Tunnel	LT33 2451 KM	
St.Veit KZ		Lainz Tunnel	33/2525 kM	22
St.Veit KZ		Lainz Tunnel	LT33 2552 Ksst	
St.Veit KZ		Lainz Tunnel	33/2592gr m	23
St.Veit KZ		Lainz Tunnel	33/2666,3 kM	24
St.Veit KZ		Lainz Tunnel	33/2694,9 kM	25
St.Veit KZ		Lainz Tunnel	LT33 2748 M	
St.Veit KZ		Lainz Tunnel	LT33 2775 KM	27
St.Veit KZ		Lainz Tunnel	33/2775,5Km	
St.Veit KZ		Lainz Tunnel	31/1381,2 kM	14
St.Veit KZ		Lainz Tunnel	LT31 1366 M	
St.Veit KZ		Lainz Tunnel	31/1364,3 kM	13
St.Veit KZ		Lainz Tunnel	LT31 1326 KM	
St.Veit KZ		Lainz Tunnel	LT31 1308 KM	
St.Veit KZ		Lainz Tunnel	31/1201,5M	8
St.Veit KZ		Lainz Tunnel	1188,5 m LT31 kM	
St.Veit KZ		Lainz Tunnel	31/1133,5 kM	10
St.Veit KZ		Lainz Tunnel	31/1101,5gr m	7
St.Veit KZ		Lainz Tunnel	31/1073,5 kM	3
St.Veit KZ		Lainz Tunnel	980,5 m LT31m2	
St.Veit KZ		Lainz Tunnel	0m RS VG Aptych	
St.Veit KZ		Lainz Tunnel	45,2 m RS VG CrinK	

St.Veit KZ	Lainz Tunnel	31/1087,5 TM	4
St.Veit KZ	Lainz Tunnel	33/2713 M	26
dislodged slice-unknown	Groisbach	Lias M,sandy	29
dislodged slice-unknown	Groisbach	Lias M	30
dislodged slice-unknown	Groisbach	kl Waldwiese,gryph,	31
dislodged slice-unknown	Groisbach	Blaschke,K	33
Drietoma Unit	Typeloc.Driet	Fm	no.10/2011
Drietoma Unit	Typeloc.Driet	Crinoidenk	no.11/2011
Drietoma Unit	Typeloc.Driet	Fk	no.12/2011
Drietoma Unit	Drietoma	Fm	no.23/2011
Drietoma Unit	Drietoma	rM	no.25/2011
Drietoma Unit	Drietoma	r K	no.27/2011
Drietoma Unit	Drietoma	r K	no.29/2011
Kržna Nappe	Zazriva	Allgäuschichten,Fleckenmergel	41
Gresten Klippenzone	Gresten	Pechgraben/Scheibsbachfm,dkl	
Gresten Klippenzone	Pechgraben	Pechgraben/Blassensteinsch,gr	
Gresten Klippenzone	Gresten	Lampelsbergsch,2 TM	
Gresten Klippenzone	Gresten	Lampelsbergsch,3 TM	
Gresten Klippenzone	Klauskogel	Posidonienmergel Klauskogel	
Ybbsitz Klippenzone	Gresten	Haselbachgrabendunkler M	
Klippe of the Czorsztyn Unit -PKB	Dolný Mlyn	Dolny Mlyn 2	KP 28
Klippe of the Czorsztyn Unit -PKB	Dolný Mlyn	Dolny Mlyn 3	KP 29
PKB - Kysuca Unit klippe	Podbranč	Podbranc 1	KP 24
PKB - Kysuca Unit klippe	Podbranč	Podbranc 2	KP 25
PKB - Kysuca Unit klippe	Podbranč	Podbranc 3	KP 26
Nedzov Nappe	Bzince pod Javorinou	Brinze pod Javorinou 1	KP 16
Nedzov Nappe	Bzince pod Javorinou	Brinze pod Javorinou 2	KP 17
Nedzov Nappe	Bzince pod Javorinou	Brinze pod Javorinou 3	KP 18
Nedzov Nappe	Bzince pod Javorinou	Brinze pod Javorinou 4	KP 19
Nedzov Nappe	Bzince pod Javorinou	Brinze pod Javorinou 5	KP 20
Gresten Klippenzone	Lampelsberg	Lampelsbergsch.1	KP 8
Gresten Klippenzone	Lampelsberg	Lampelsbergsch.2	KP 9
Gresten Klippenzone	Lampelsberg	Lampelsbergsch.3	KP 10
Gresten Klippenzone	Klauskogel	Posidonienmergel Klauskogel	KP 11
Ybbsitz Klippenzone	Haselgraben	Haselbachgraben	KP 12
Gresten Klippenzone	Arzberggraben	Arzberggraben Blassensteinsch.	KP 13
PKB - Kysuca Unit Klippe	Myjava	Myjava1	KP 14
Gresten Klippenzone	Pechgraben	Pechgraben/Konradsheimfm.	KP 1
Gresten Klippenzone	Pechgraben	Pechgraben/Scheibsbachfm.	KP 2
Gresten Klippenzone	Pechgraben	Pechgraben/Blassensteinsch.	KP 3
Klippe of the Czorsztyn Unit -PKB	Dolný Mlyn	Dolny Mlyn 1	KP 27

**Fig. 158 Jurassic carbonates from the Lainz Tunnel and comparison units.**

## **Factor analysis**

The influence of the first three main factors can be seen in the Screeplot below. In the componentmatrix plot (see Appendix 4) the impact of different elements on the factors is listed. In factor 1, elements like  $\text{TiO}_2$  (0.969),  $\text{Al}_2\text{O}_3$  (0.977),  $\text{CaO}$  (0.845) or  $\text{K}_2\text{O}$  (0.943) with high input factor can be found. In factor 2, rare elements like Lu (0.876), Tm (0.963) or Eu (0.944) with also high input are found. This suggests that the difference between the groups is based on marine/terrigenous elements and REEs. In the factor vs factor plots the groups separate in various degrees depending on the factors used. It seems that some groups of samples like the Kysuca Unit, the Nedzov Unit and the Czorztyn Unit separate from the others in plot factor 1vs factor 3 and plot factor 2 vs 3. In addition, it could be interpreted that the Gresten and Ybbsitz Units tend to separate in the factor 2 vs factor 3 and factor 1vs factor 2 plots.

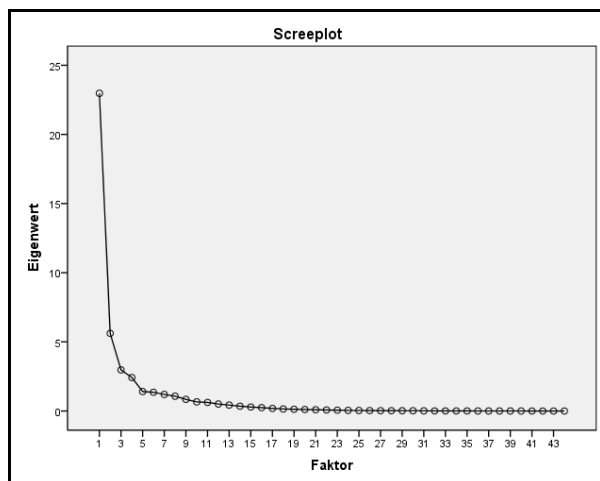


**Fig. 159** Screeplot of Jurassic carbonates: Importance of the factors.

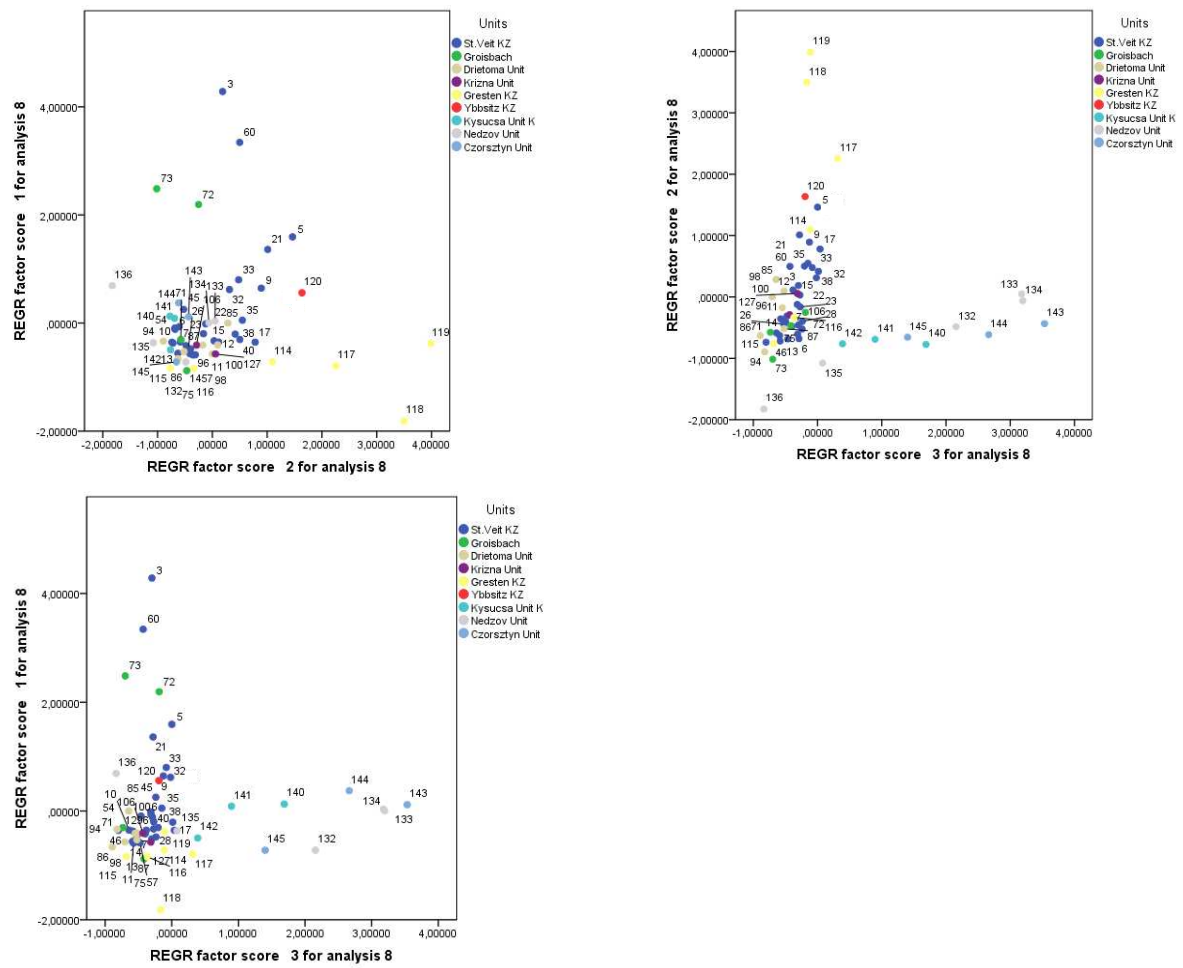


**Fig. 160 Factor vs. factor plots of the Jurassic carbonates.**

## **Major elements**

In the Th-Sc-La plot (Fig. 162) (Taylor and McLennan, 1985) only one sample from the Ybbsitz Klippenzone plots far away from the others. In the Th/U vs Th plot (Fig. 163) (Mc Lennan et al., 1993) the St.Veit Klippenzone shows a positive correlation, e.g.:  $r=0.625$   $R^2=0.390$ , whereas the Gresten Klippenzone shows a correlation of  $r=0.259$   $R^2=0.067$ .

In the Ce, La, Sc and Th vs ( $\text{SiO}_2+\text{Al}_2\text{O}_3+\text{Fe}_2\text{O}_3+\text{MgO}+\text{Na}_2\text{O}+\text{TiO}_2$ ) plots of the Jurassic carbonates (Fig. 164) (Madhavavaju, 2010). the carbonates from the Gresten Klippenzone tend to group separately from the other samples. This behavior of the Gresten samples is also visible by the different angle of the interpolated trendline compared to the St.Veit Klippenzone in the plots.

The V/Zr vs Zr/Ni, Zr/ $\text{Al}_2\text{O}_3$ , Ti/Zr plots (Fig. 165) (Schnabel and Adamova, 1999) show some differentiation of the Gresten group from the other groups in context with a higher Zr/ $\text{Al}_2\text{O}_3$  and Ti/Zr ratio. The correlation values for Fig. 164 and Fig. 165 can be found in the table below, the negative correlation values of the Drietoma samples could also be caused by the low amount of samples.

	St.Veit Klippenzone	Gresten Klippenzone	Drietoma Klippenzone	Pieninny Klippen B.
	( $\text{SiO}_2+\text{Al}_2\text{O}_3+$ $\text{Fe}_2\text{O}_3+\text{MgO}+$ $\text{Na}_2\text{O}+\text{TiO}_2$ )	( $\text{SiO}_2+..+\text{TiO}_2$ )	( $\text{SiO}_2+..+\text{TiO}_2$ )	( $\text{SiO}_2+..+\text{TiO}_2$ )
Ce	0.786	0.772	-0.187	0.574
La	0.781	0.628	-0.18	0.528
Sc	0.927	0.872	0.56	0.784
Th	0.915	0.786	0.726	0.778
	V/Zr	V/Zr	V/Zr	V/Zr
Zr/Ni	-0.419	-0.269		0.04
TiO <sub>2</sub> /Zr	0.66	0.883	0.374	0.019
Zr/ $\text{Al}_2\text{O}_3$	-0.576	-0.952	-0.303	-0.302

**Fig. 161 Pearson Correlation values „r” of selected characteristics.**

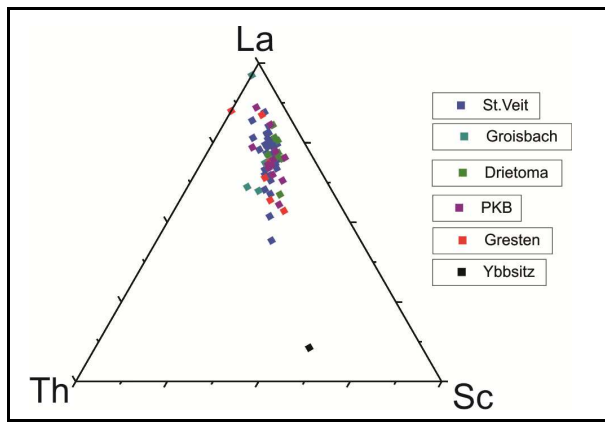


**Fig. 162** Th-Sc-La plot of the Jurassic carbonates (adapted after Taylor and Mc Lennan, 1985).

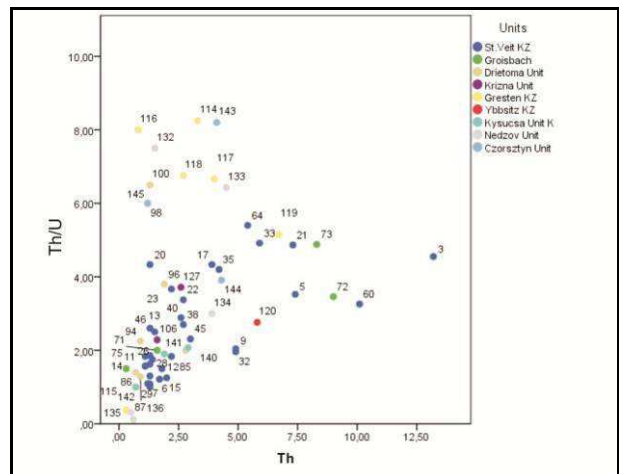


**Fig. 163** Th/U vs Th plot of the Jurassic carbonates (adapted after Mc Lennan et al., 1993).

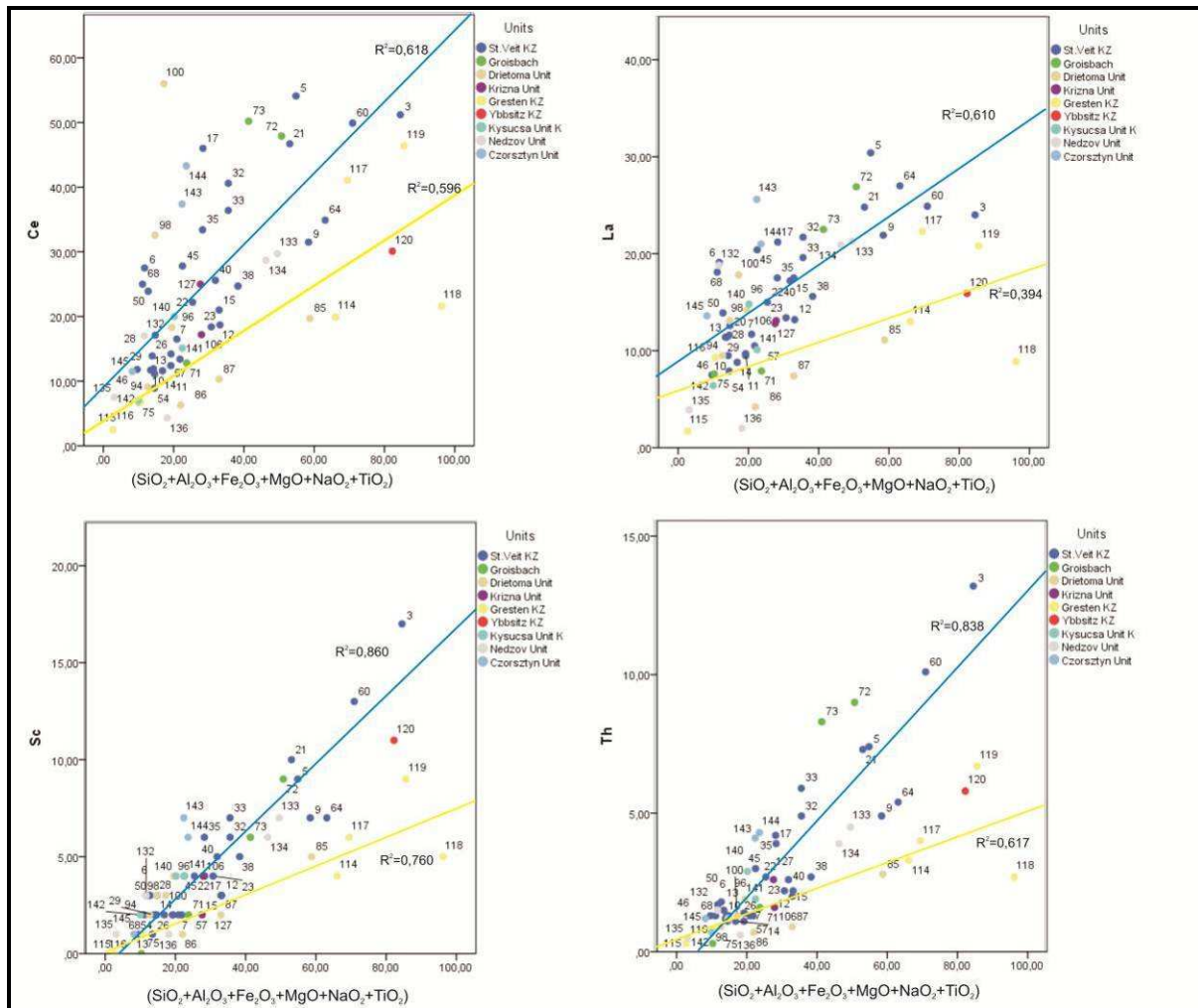


**Fig. 164** Ce, La, Sc and Th vs  $(\text{SiO}_2 + \text{Al}_2\text{O}_3 + \text{Fe}_2\text{O}_3 + \text{MgO} + \text{Na}_2\text{O} + \text{TiO}_2)$  plots of the Jurassic carbonates (adapted after Madhavavaju, 2010).

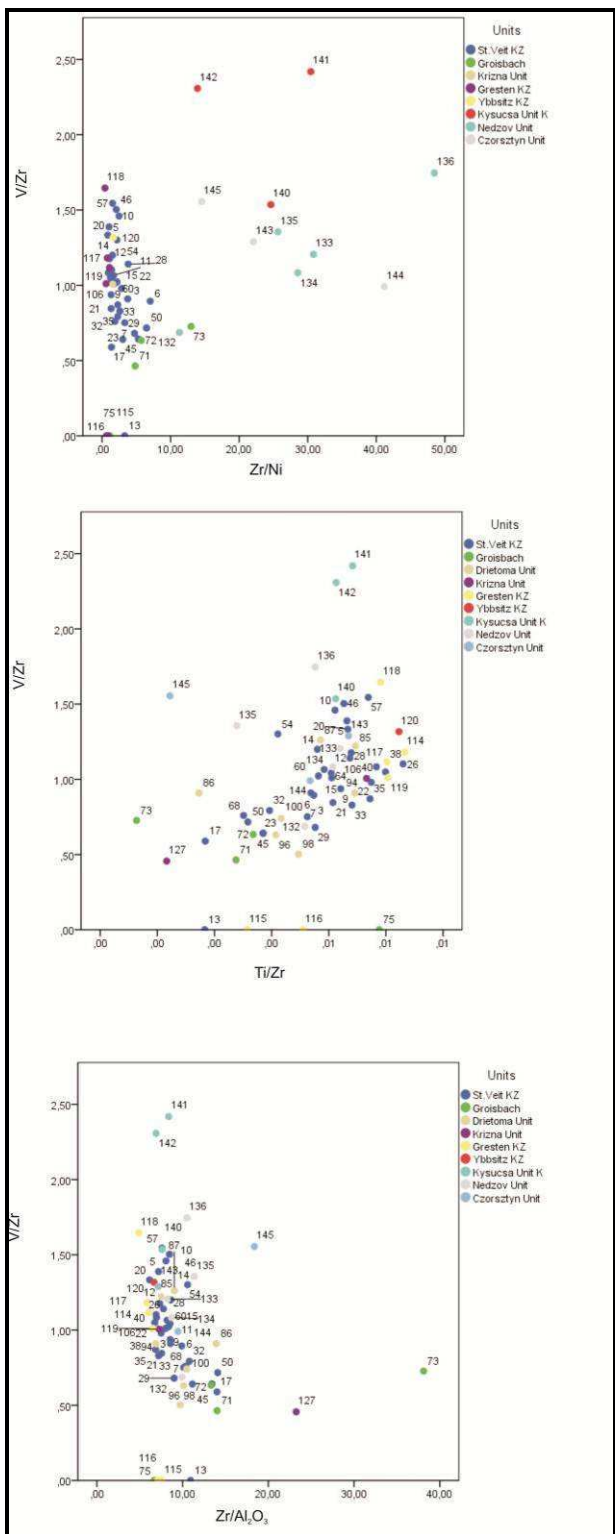


**Fig. 165** V/Zr vs Zr/Ni,Ti/Zr and Zr/Al<sub>2</sub>O<sub>3</sub> plots of the Jurassic carbonates (adapted after Schnabel and Adamova, 1999).

## **REE from Jurassic carbonates**

Most of the analysed samples show a more or less homogeneous pattern of REE's and most of the diagrams below show Ce and/or Eu anomalies. Overall, there are no significant differences in the REE patterns between the various carbonates from the Klippenzones visible.

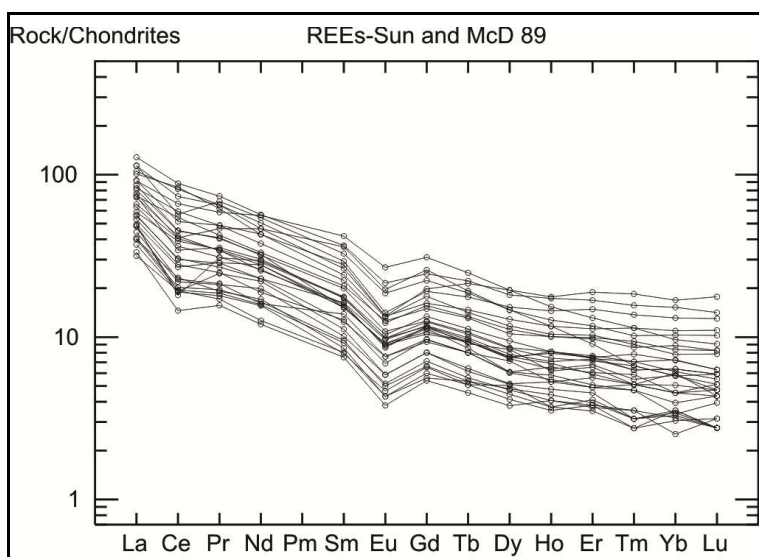


**Fig. 166 REE plot of Jurassic carbonates from the St.Veit Klippenzone.**

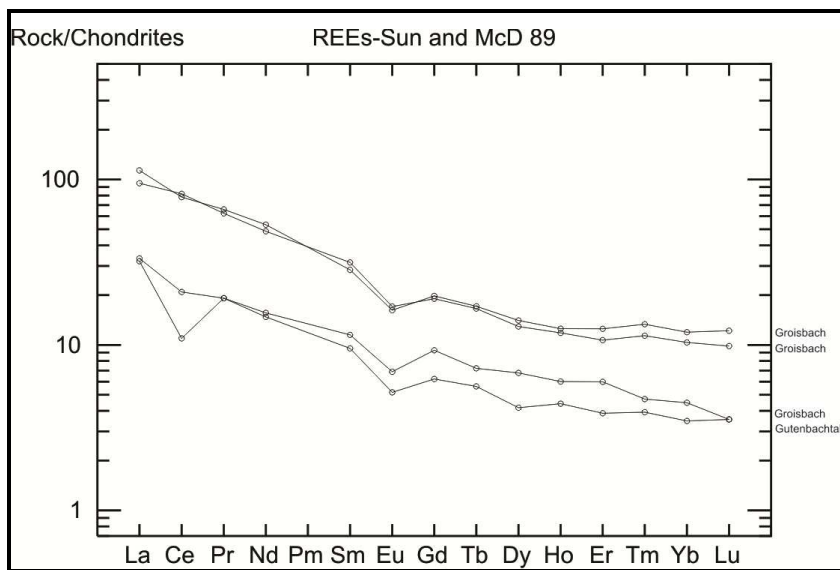


**Fig. 167 REE plot of Jurassic carbonates from Groisbach.**

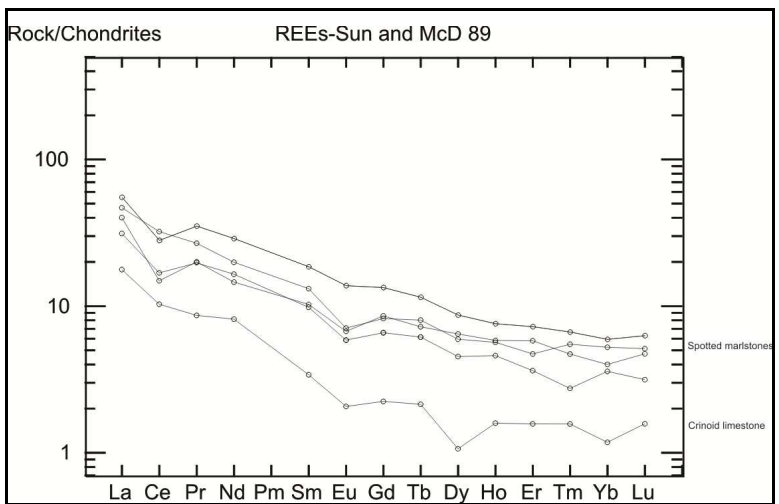


**Fig. 168 REE plot of Jurassic carbonates from the Drietoma Unit.**

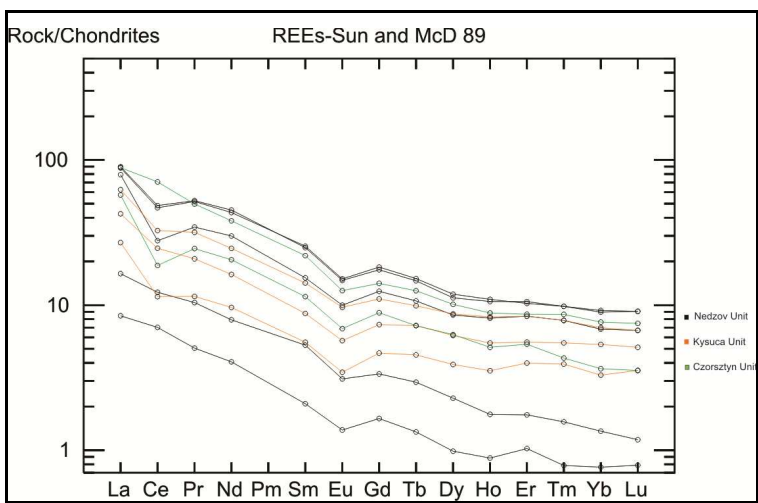


**Fig. 169 REE plot of Jurassic carbonates from the PKB.**

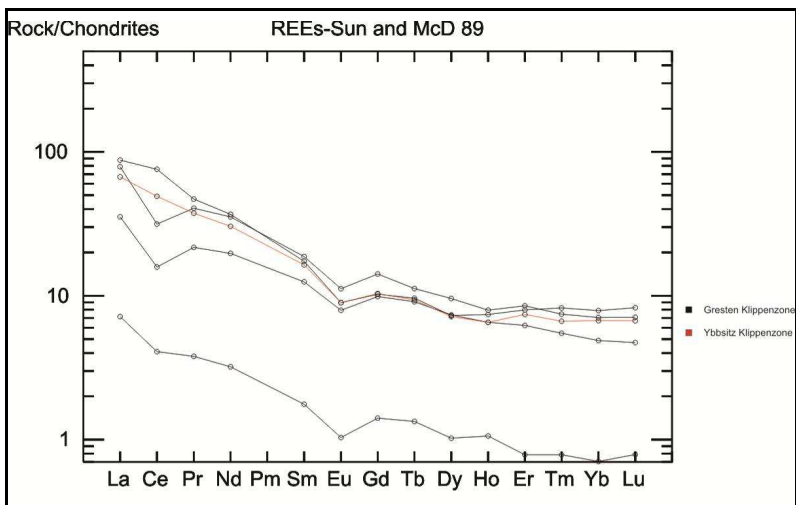


**Fig. 170 REE plot of Jurassic carbonates from the Gresten and Ybbsitz Klippenzone.**

## CIA of the Jurassic carbonates

The Chemical Index of Alteration (CIA) and the Chemical Proxy of Alteration (CPA) correlate well as it can be seen in Fig. 171. In the A-CN-K diagram (Fig. 172) the St.Veit Klippenzone, the Drietoma Unit and Krížna Nappe samples tend to have lower CIA values than the others, like the Gresten Klippenzone samples.

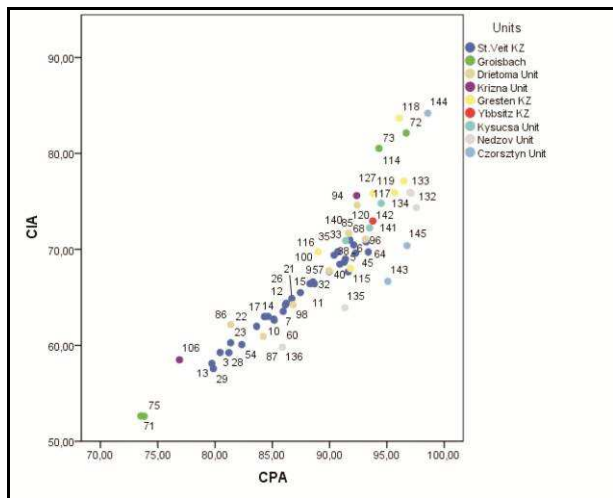


**Fig. 171 CIA vs CPA plot from Jurassic carbonates.**

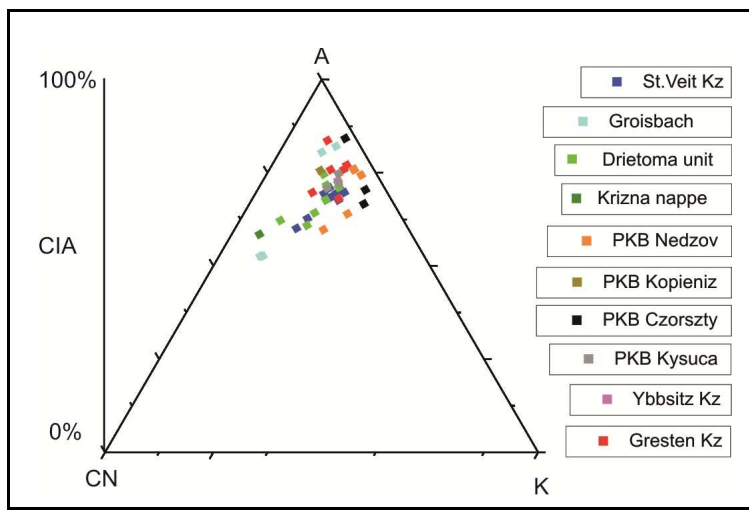


**Fig. 172 CIA plot from Jurassic carbonates.**

## **Summary of results for Jurassic carbonates**

The factor analysis suggests that the difference between the groups is based on marine/terrigenous elements and REEs. Some groups like the Kysuca Unit, the Nedzov Unit, the Czorsztyn Unit, the Gresten and Ybbsitz Units tend to separate in the various factor vs factor plots. The different signature of the Gresten Klippenzone seems to be linked to elements such as Ce, La, Sc and Th, as observed in the Madhavavaju (2010) plot (Fig. 164) or the Mc Lennan et al. (1993) Th/U vs Th plot (Fig. 163), indicating different weathering conditions for the Gresten Unit. The Gresten samples also show higher Zr/Al<sub>2</sub>O<sub>3</sub> and Ti/Zr ratios (Fig. 165). This also indicates a different provenance for the Gresten carbonates compared to the St.Veit Klippenzone samples.

As the samples show a more or less homogeneous pattern of REE's with Ce and/or Eu anomalies, there are no significant differences in the REE patterns between the various klippenzones.

In the A-CN-K diagram (Fig. 172) the St.Veit Klippenzone, the Drietoma Unit and Krížna Nappe samples tend to have lower CIA values than the others, like the Gresten Klippenzone samples; this correlates with the Th/U vs Th plot (Fig. 163). Overall the results show a different composition of the Gresten Klippenzone carbonates regarding Ce, La, Sc, Th, Zr/Al<sub>2</sub>O<sub>3</sub> and Ti/Zr ratios, thus indicating a different hinterland setting and weathering condition. In contrast, no difference between the St.Veit Klippenzone and the Drietoma Unit was detected.

## 4. Siliceous rocks (cherts, radiolarites, siliceous limestones)

### ***Geochemistry of Jurassic cherts***

It was expected that from the analyzed chert units, the samples from the Ybbsitz Klippenzone should indicate a strong mafic signature as depicted by Decker (1989). This would include high Cr, Ni, MnO and Fe<sub>2</sub>O<sub>3</sub> values, all characteristic elements indicating mafic to ultramafic sediment provenance. Unfortunately the samples from the Ybbsitz Klippenzone, which is thought to belong to the Southpenninic realm (Decker, 1989; Faupl & Wagreich, 2000), do not show high amounts of Cr and Ni values. For this reason it is very difficult to compare the samples to the others, and the relevant diagrams should be interpreted with caution. It was tried to compensate this handicap with other suitable plots to gain more information about the relationships of the different units to each other. Wherever possible, additional data of the Ybbsitz Zone from Decker (1989) were included into the plots. It is important to note that the samples from Decker (1989) also show some variation, for example in the Cu vs Ni plot (Fig. 179). A list of the samples used is given in the table below.

	Correlation	Sample site	Sample label	Add. lab label
Cherts				
	St.Veit Klippenzone	Lainz Tunnel	1133,5 m LT33 Radiol,	
	St.Veit Klippenzone	Lainz Tunnel	2165 m LT33 Radiol,	
	St.Veit Klippenzone	Lainz Tunnel	LT33 2552 HAST	
	St.Veit Klippenzone	Lainz Tunnel	LT33 2775 HST	
	St.Veit Klippenzone	Lainz Tunnel	LT31 1364 HST	
	St.Veit Klippenzone	Lainz Tunnel	1119,5 m LT31 Radiol,	
	St.Veit Klippenzone	Lainz Tunnel	31/898chert bunt	2
	St.Veit Klippenzone	Lainz Tunnel	35,6 m RS VG Radiol,	
	St.Veit Klippenzone	Lainz Tunnel	40, 6 m RS VG Radiol,	
	St.Veit Klippenzone	Antonshöhe	weiße Aptychenschichten	KP 31
	St.Veit Klippenzone	Antonshöhe	rote Aptychenschichten	KP 32
	Dislodged slice-unknown	Gutenbachtal	Radiolarit	34
	Drietoma Unit	Drietoma	Radiolarit	no.18/2011
	Drietoma Unit	Drietoma	Radiolarit	no.21/2011
	Drietoma Unit	Drietoma	Radiolarit	no.26/2011
	Drietoma Unit	Drietoma	Radiolarit	no.28/2011
	Drietoma Unit	Drietoma	Radiolarit	no.24/2011
	Krížna Nappe	Zazriva	Kieselkalk,dunkel P5	42
	Krížna Nappe	Zazriva	Kieselkalk P5	43
	Krížna Nappe	Zazriva	Radiolarit,grau P6	44

Krížna Nappe	Zazriva	Radiolarit, rot P6	45
PKB - Kysuca Unit	Turá Lúka	Turá Lúka 1	KP 21
PKB - Kysuca Unit	Turá Lúka	Turá Lúka 2	KP 22
PKB - Kysuca Unit	Turá Lúka	Turá Lúka 3	KP 23
Ybbsitz Klippenzone	Steinbruch Reidl	Steinbruch Reidl 1	KP 4
Ybbsitz Klippenzone	Steinbruch Reidl	Steinbruch Reidl 2	KP 5
Ybbsitz Klippenzone	Steinbruch Reidl	Steinbruch Reidl 3	KP 6
Ybbsitz Klippenzone	Steinbruch Reidl	Steinbruch Reidl 4	KP 7
PKB - Kysuca Unit Klippe	Myjava	Myjava 2	KP 15

**Fig. 173 Jurassic cherts from the Lainz Tunnel and comparison units.**

### **Factor analysis**

The influence of the first three main factors can be seen in the Screeplot below. Notably is that the second and third factor have a quite similar impact. In the componentmatrix plot (see Appendix 4), the impact of different elements on the factors is listed. In factor 1, elements like TiO<sub>2</sub> (0.988), Al<sub>2</sub>O<sub>3</sub> (0.979), Zr (0.987), K<sub>2</sub>O (0.980), Th (0.975) or La (0.913) with high input factors can be found. In factor 2, elements like SiO<sub>2</sub> (0.945), CaO (0.955) or Sr (0.860) with also high input are found. This suggests that the main difference between the samples, beside normal variations of elements like SiO<sub>2</sub>, CaO and Sr, could be found in different amounts of more immobile elements like Th or La. As it can be seen in the factor 1 vs factor 2 and factor 1 vs factor 3 plots it seems that the Ybbsitz Klippenzone and the Kysuca unit tend to spread more and group separately from the others.

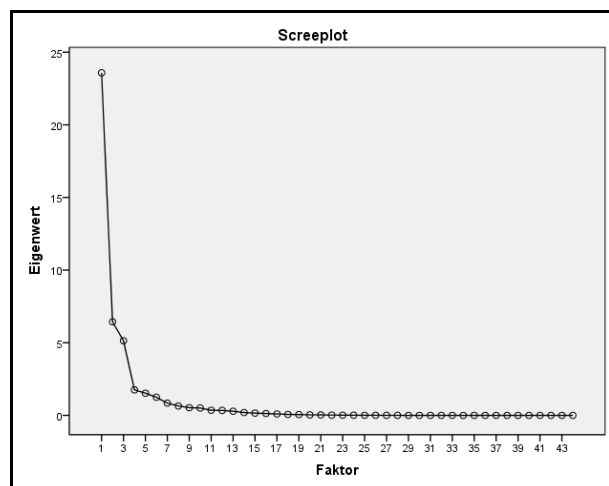


**Fig. 174 Screeplot of Jurassic cherts: Importance of the factors.**

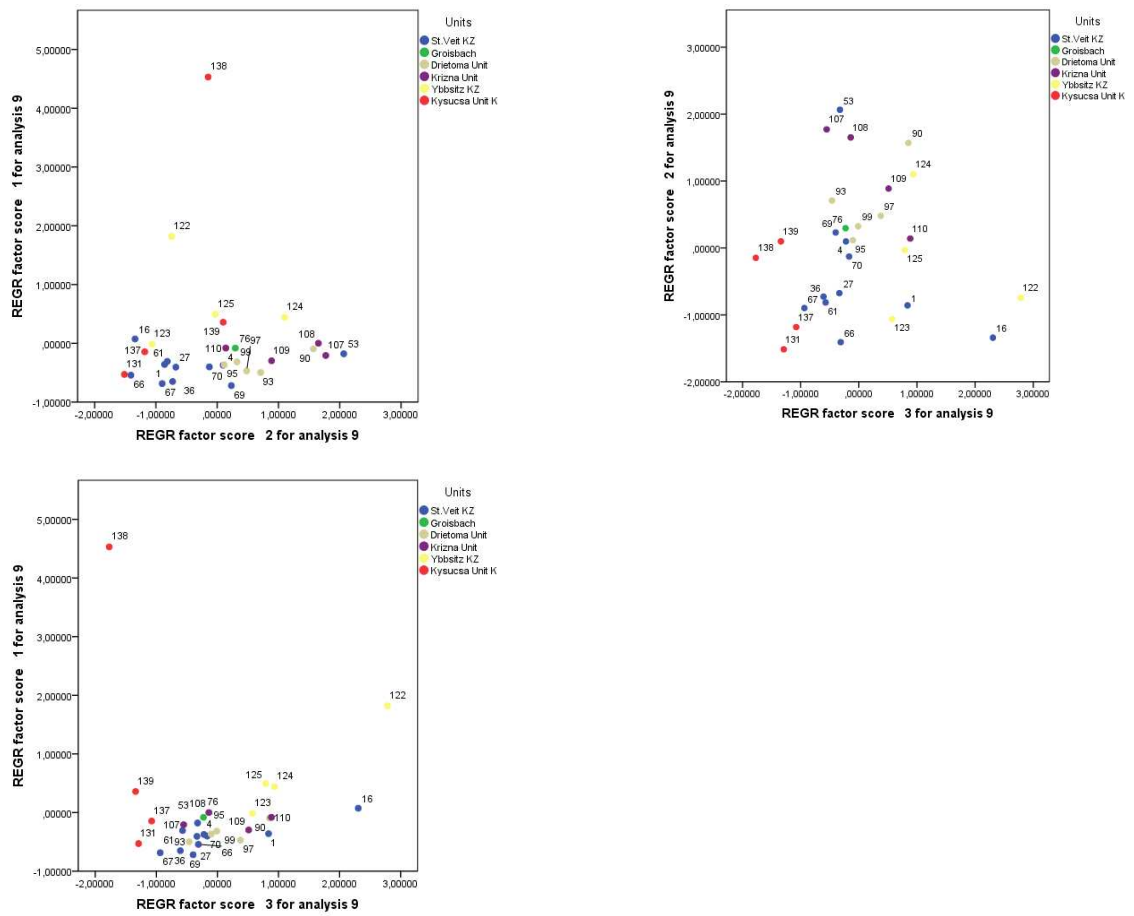


**Fig. 175 Factor vs.factor plots of the Jurassic cherts.**

### Major elements

The Plots Fig. 179 to Fig. 183 show that higher contents of Cu, Ni, Zn, TiO<sub>2</sub>, MnO, Fe<sub>2</sub>O<sub>3</sub> and (Al<sub>2</sub>O<sub>3</sub>+K<sub>2</sub>O+Na<sub>2</sub>O) are found in the Ybbsitz Klippenzone. Elements like Cu, Ni, Zn, MnO and Fe<sub>2</sub>O<sub>3</sub> are often associated with hydrothermal and mafic settings (e.g. Mc Lennan, 1993). This is in accordance with data by Decker (1990). The combination of Al<sub>2</sub>O<sub>3</sub>, K<sub>2</sub>O and Na<sub>2</sub>O was used here to represent shale mineral content. The correlation ratios of the elements used in the plots here, divided for the different groups are given in the tables below.

The La, Sc, Ce and Th vs (Al<sub>2</sub>O<sub>3</sub>+K<sub>2</sub>O+Na<sub>2</sub>O) plots were used to see if important trace elements are associated with elements representing shale minerals and if they correlate positively. In all four plots the Ybbsitz Klippenzone, together with the Kysucsa Unit, has significant higher amounts of trace elements, Al<sub>2</sub>O<sub>3</sub>, K<sub>2</sub>O and Na<sub>2</sub>O.

	Ni	Zn	TiO <sub>2</sub>	MnO	Fe <sub>2</sub> O <sub>3</sub>	SiO <sub>2</sub>	AlKNa	La	Ce	Sc	Th
Cu	0.821	0.772	0.619	0.003	0.680	0.086	0.694	0.224	0.51	0.645	0.563
Ni		0.885	0.825	-0.367	0.351	0.332	0.861	0.152	0.646	0.750	0.752
Zn			0.885	-0.236	0.493	0.155	0.943	0.406	0.809	0.896	0.872
TiO <sub>2</sub>				-0.304	0.187	0.152	0.987	0.536	0.905	0.939	0.971
MnO					0.265	-.890	-0.291	0.528	-0.022	-0.126	-0.33
Fe <sub>2</sub> O <sub>3</sub>						-0.04	0.299	0.126	0.151	0.312	0.241
SiO <sub>2</sub>							0.159	-.670	-0.136	-0.008	0.201
AlKNa								0.499	0.884	0.938	0.966
La									0.774	0.658	0.502
Ce										0.968	0.880
Sc											0.930

**Fig. 176 St Veit Klippenzone: selected correlations of elements used in the plots below.**

	Ni	Zn	TiO2	MnO	Fe2O3	SiO2	AlKNa	La	Ce	Sc	Th
Cu	0.510	0.889	0.728	0.645	0.512	-0.108	0.784	0.960	0.952	0.841	0.866
Ni		0.995	0.693	0.549	0.672	0.166	0.987	0.733	0.964	0.990	0.974
Zn			0.942	0.722	0.999	0.122	0.973	0.792	0.986	0.986	0.978
TiO2				0.356	0.678	-0.059	0.989	0.724	0.892	0.985	0.983
MnO					0.486	-0.465	0.82	0.686	0.673	0.819	0.85
Fe2O3						0.115	0.965	0.808	0.991	0.981	0.974
SiO2							0.075	-0.382	0.072	0.031	-0.061
AlKN a								0.708	0.926	0.995	0.983
La									0.864	0.773	0.822
Ce										0.955	0.956
Sc											0.995

**Fig. 177 Ybbsitz Klippenzone: selected correlations of elements used in the plots below.**

	Zn	TiO2	MnO	Fe2O3	SiO2	AlKNa	La	Ce	Sc	Th
Cu	0.401	0.601	0.514	0.713	-0.362	0.703	0.707	0.582	0.748	0.779
Zn		0.118	0.778	0.705	-0.223	0.362	-0.175	0.874	0.69	0.4
TiO2			0.507	0.632	-0.242	0.967	0.61	0.579	0.775	.943
MnO				0.965	-0.688	0.669	0.328	0.910	0.755	0.684
Fe2O3					-0.693	0.778	0.521	0.898	0.83	0.809
SiO2						-0.293	-0.662	-0.343	-0.19	-0.321
AlKNa							0.559	0.76	0.907	0.993
La								0.151	0.317	0.597
Ce									0.924	0.775
Sc										0.924

**Fig. 178 Drietoma Unit: selected correlations of elements used in the plots below.**

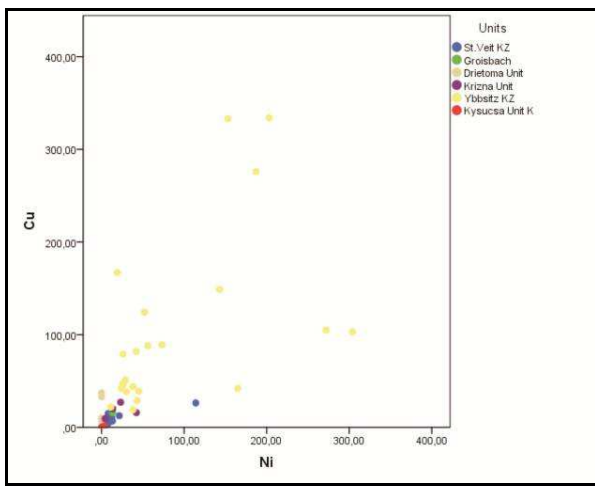


**Fig. 179 Cu vs Ni plot of Jurassic cherts.**

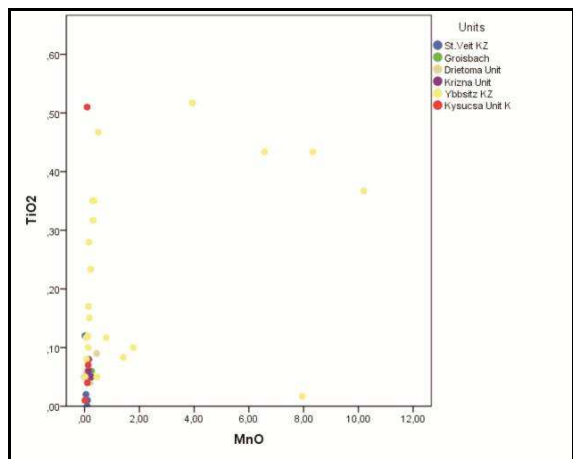


**Fig. 181 TiO<sub>2</sub> vs MnO plot of Jurassic cherts.**

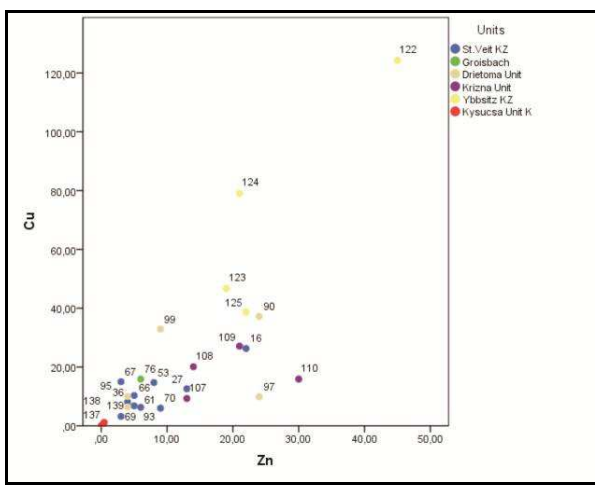


**Fig. 180 Cu vs Zn plot of Jurassic cherts.**

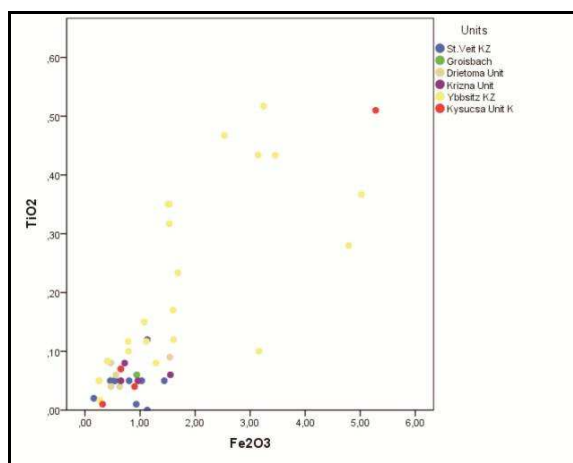


**Fig. 182 TiO<sub>2</sub> vs Fe<sub>2</sub>O<sub>3</sub> plot of Jurassic cherts.**

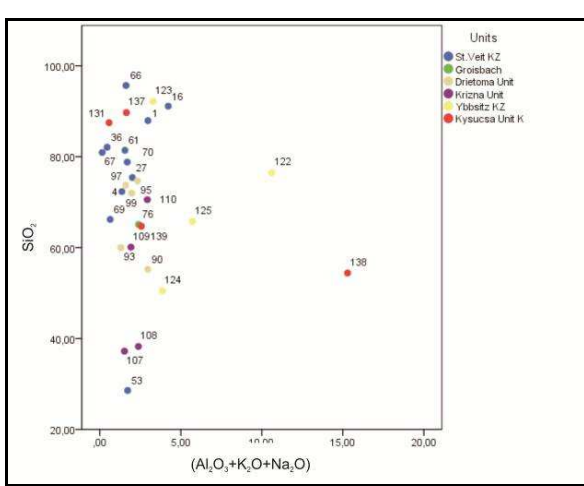


**Fig. 183 SiO<sub>2</sub> vs (Al<sub>2</sub>O<sub>3</sub>+K<sub>2</sub>O+Na<sub>2</sub>O) plot of Jurassic cherts (adapted after Bhatia, 1983).**

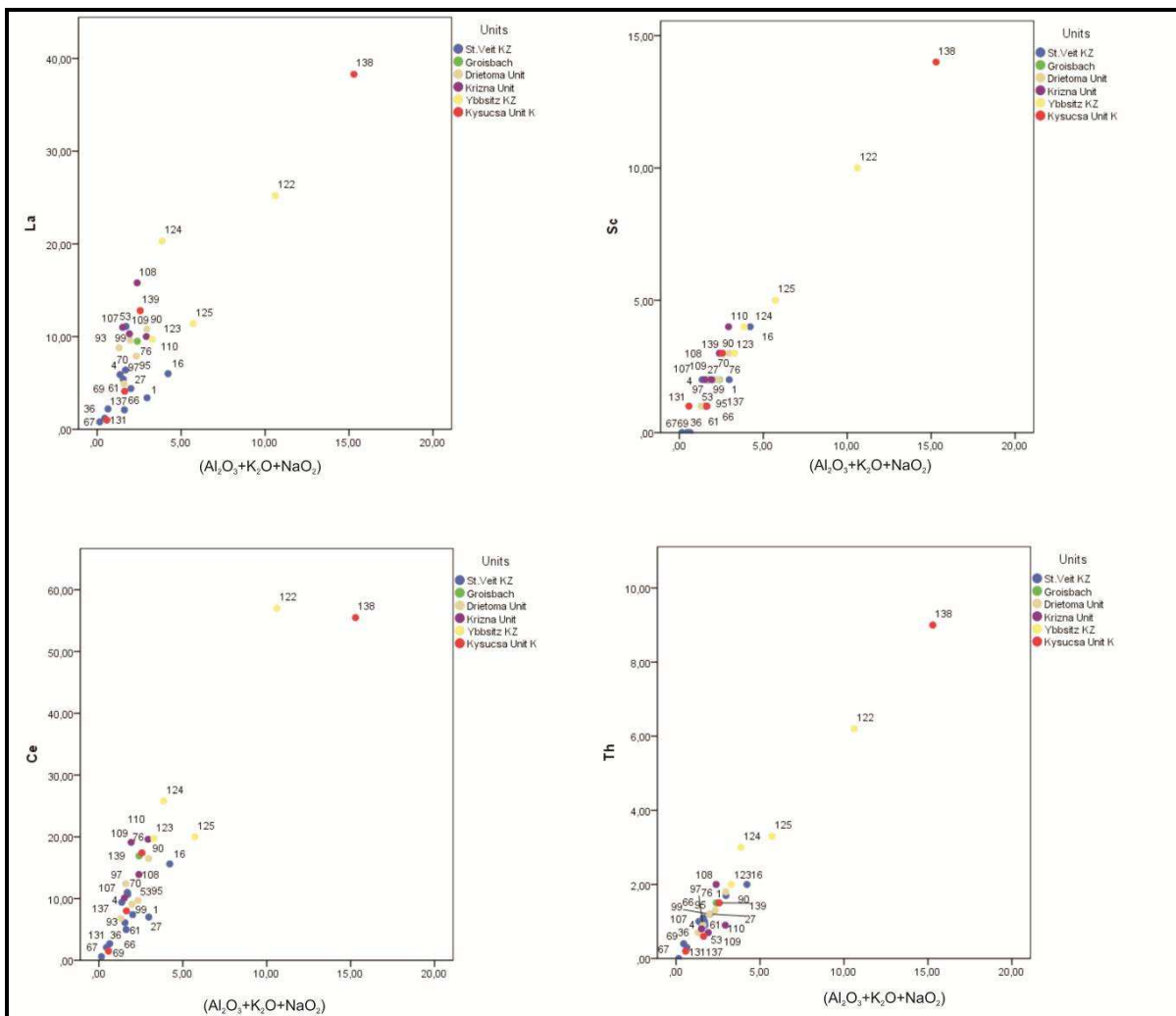


**Fig. 184 La, Sc, Ce and Th vs  $(\text{Al}_2\text{O}_3 + \text{K}_2\text{O} + \text{Na}_2\text{O})$  plots of Jurassic cherts (adapted after Madhavavaju, 2010).**

## REE from Jurassic cherts

Several samples from St.Veit Klippenzone and Kysuca Unit seem to be depleted compared to the REE standard. This can be explained by the siliceous nature of the samples where a lot of chemical reactions can happen during (dia-)genesis. Overall, as the diagrams show (Fig. 185, Fig. 186, Fig. 187), there are no significant differences in the REE patterns between the various cherts from the Klippenzones that were sampled. As long as the groups are more or less inhomogeneous, characteristics as e.g. Ce or Eu anomalies can't be used for differentiation. It would be helpful to have more detailed stratigraphic separation of the samples.

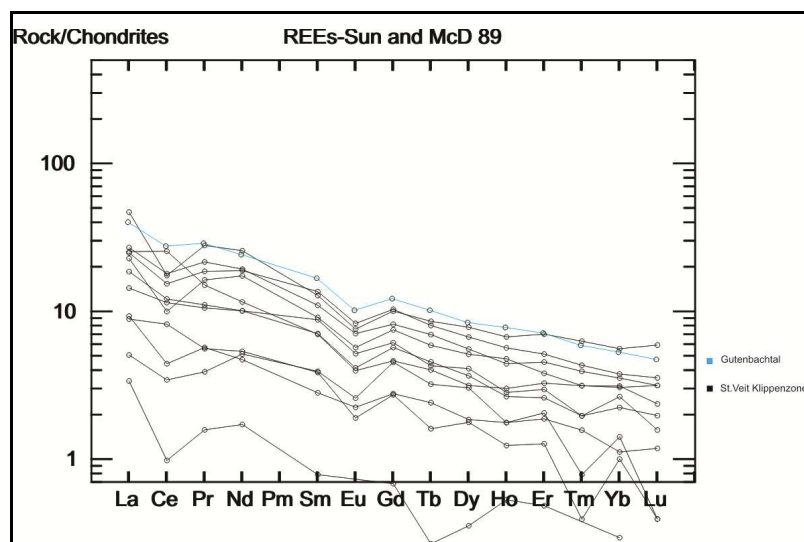


**Fig. 185** REE plot from the St.Veit Klippenzone and Gutenbachtal.

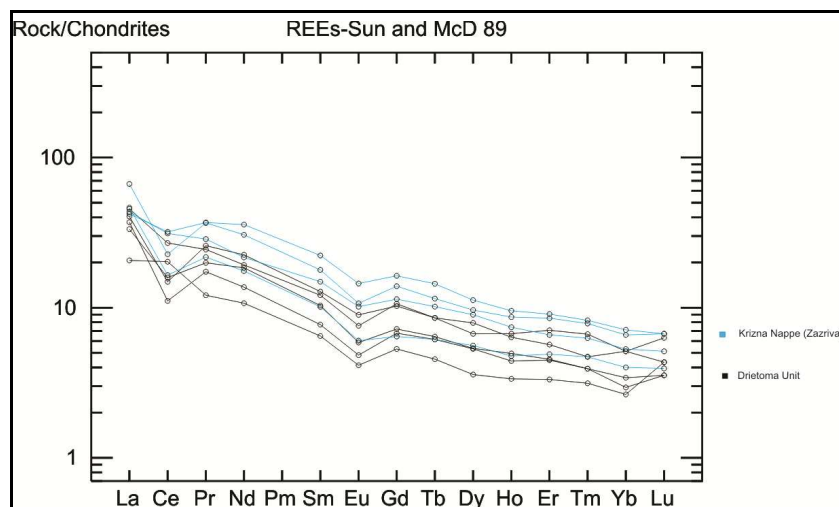


**Fig. 186** REE plot from Drietoma Unit and Krížna Nappe.

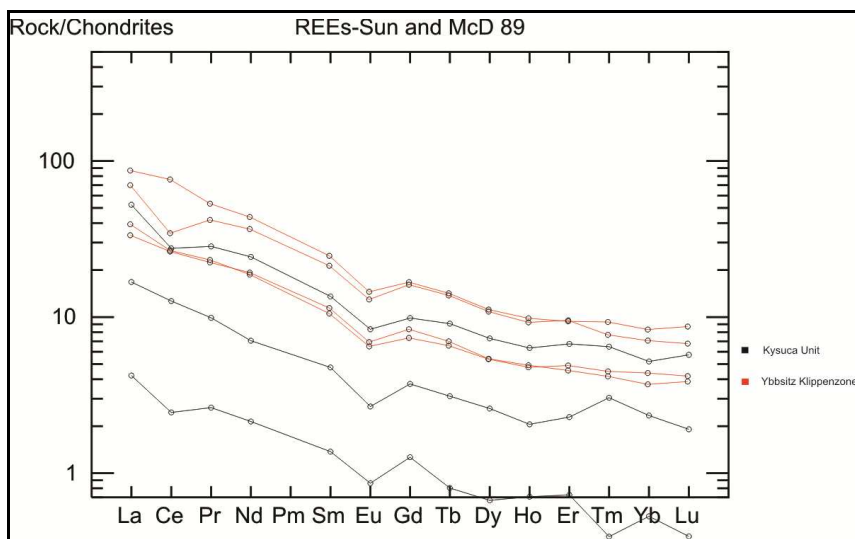


**Fig. 187 REE plot from Ybbsitz Klippenzone and Kysuca Unit (PKB).**

### CIA of the Jurassic cherts

The Chemical Index of Alteration (CIA) and the Chemical Proxy of Alteration (CPA) correlate (Fig. 188). In the A-CN-K diagram (Fig. 189) the samples from the St.Veit Klippenzone, like the Drietoma Unit and Krížna Nappe samples, show a wide range of CIA values, the Ybbsitz Klippenzone samples seem to plot closer to each other. The reason for that could be that the mentioned „wide spread groups” consist of samples with varying age while the samples of the Ybbsitz Klippenzone have a more homogenous age. Another important factor is the lithology itself, cherts are very fine grained (chemical) sediments and some geochemical interactions with the surrounding sediments could be expected.

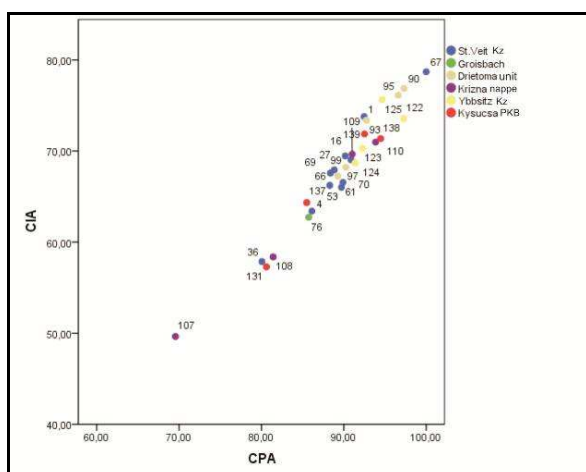


**Fig. 188 CIA vs CPA plot from Jurassic cherts.**

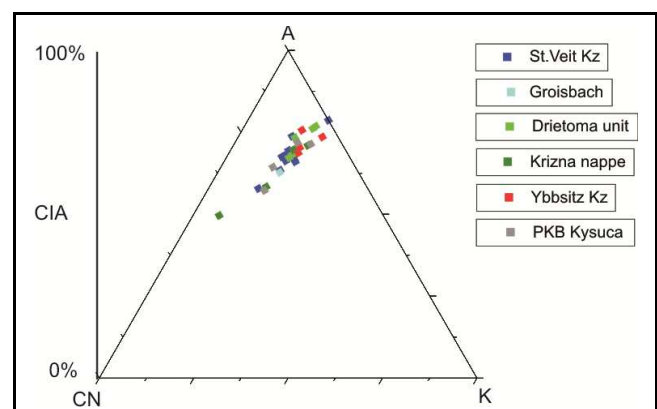


**Fig. 189 CIA plot from Jurassic cherts.**

## Siliceous *Calpionella* limestones

While it was easy to determine the stratigraphic age of the *Calpionella* limestones, a geochemical approach was quite difficult. Strong variations in the silica content and the very low number of samples strongly restricts the informative value of the factor analysis. Because this group is defined very clearly by its age it was treated on its own and not mixed with others. This would have concealed the other results. A list of the used samples is given in the table below.

	Correlation	Sample site	Sample label	Add. lab label
Siliceous limestones				
	St.Veit KZ	Lainz Tunnel	993,5 m LT31 weißer Kalk	
	St.Veit KZ	Lainz Tunnel	14 m RS VG weißer Kalk	
	Drietoma Unit	Drietoma	Neocom.	no.16/2011
	Drietoma Unit	Drietoma	Calpion.Kalk	no.19/2011
	Kržna Nappe	Zazriva	Calpionella K	46
	Kržna Nappe	Zazriva	Neokommergel	47
	Gresten KZ	Gresten	Pechgraben/Konradsheimfm,heller K	
	Gresten KZ	Gresten	Arzberggraben Blassensteinsch,hell	
	PKB - Kysuca Unit	Myjava	Myjava2b	

Fig. 190 Siliceous *Calpionella* limestones from the Lainz Tunnel and comparison units.

## Factor analysis

The influence of the first three main factors can be seen in the Screeplot below. As it can be seen in the factor vs factor plots any conclusion is impossible. The very low number of samples strongly restricts the informative value of the factor analysis. Thus, the factor analysis was only carried out for integrity reasons.

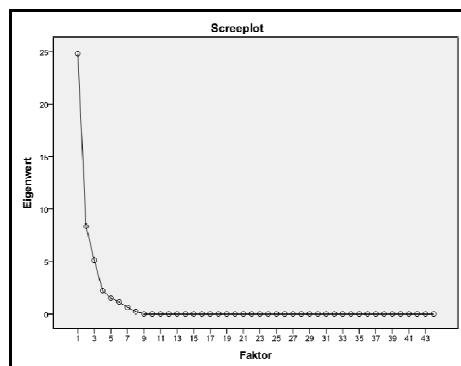
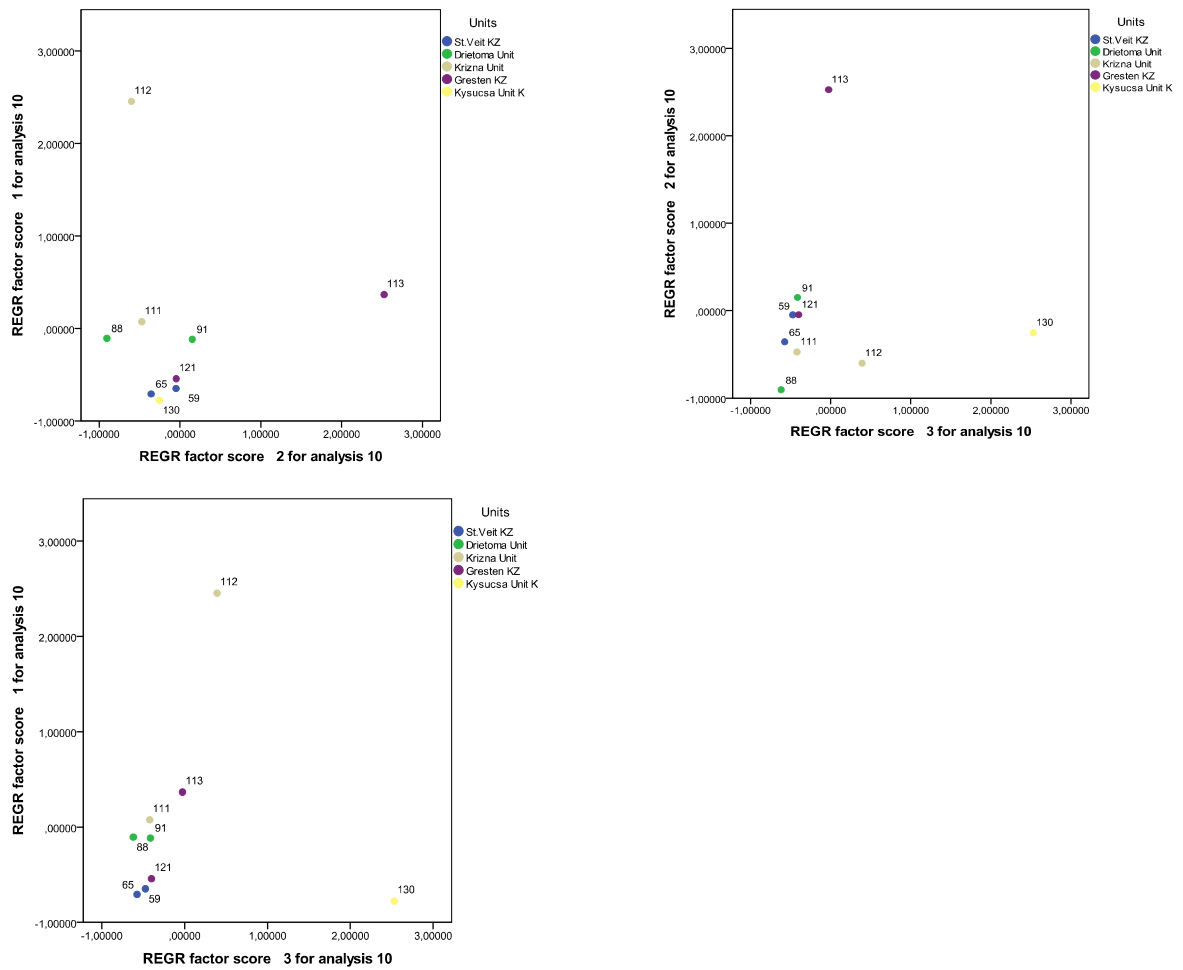


Fig. 191 Screeplot of siliceous *Calpionella* limestones: Importance of the factors.



**Fig. 192 Factor vs.factor plots of the siliceous *Calpionella* limestones.**

## **REE from siliceous *Calpionella* limestones**

As the diagramms below show; there are no significant differences in the REE patterns between the various *Calpionella* limestones from the klippenzones that were analysed.

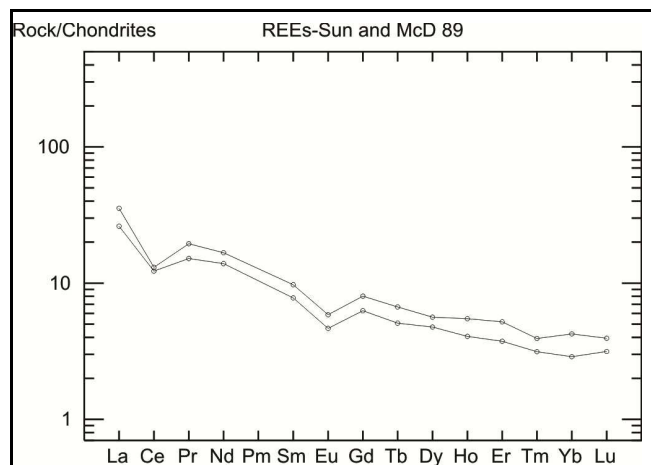


**Fig. 193 REE plot from siliceous *Calpionella* limestones from the St.Veit Klippenzone.**

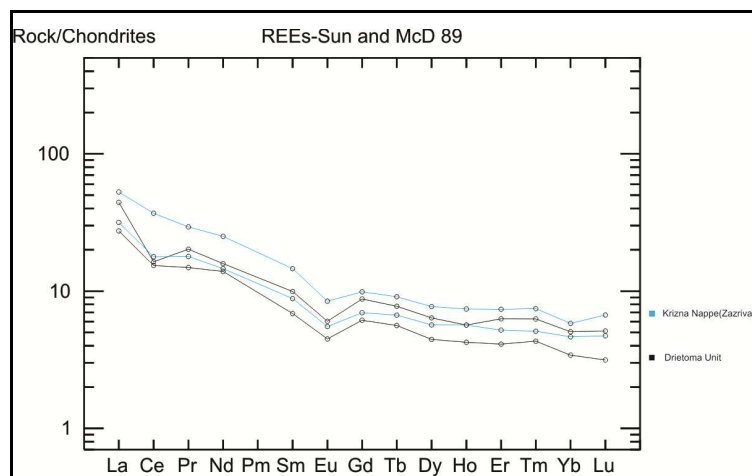


**Fig. 194 REE plot from siliceous *Calpionella* limestones from the Drietoma Unit and Krízna Nappe.**

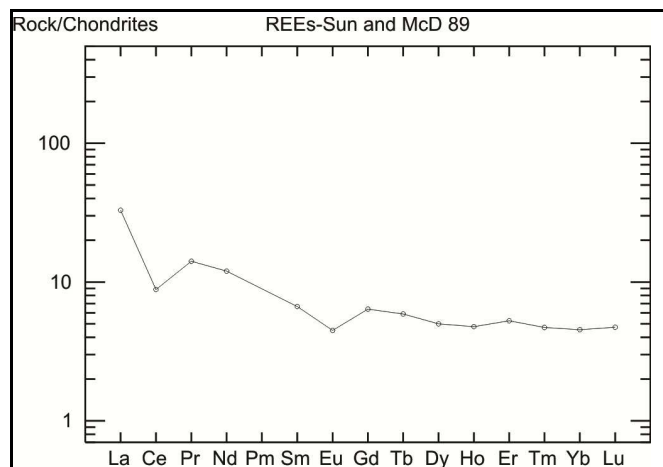


**Fig. 195 REE plot from siliceous limestones from the Kysuca unit (PKB).**

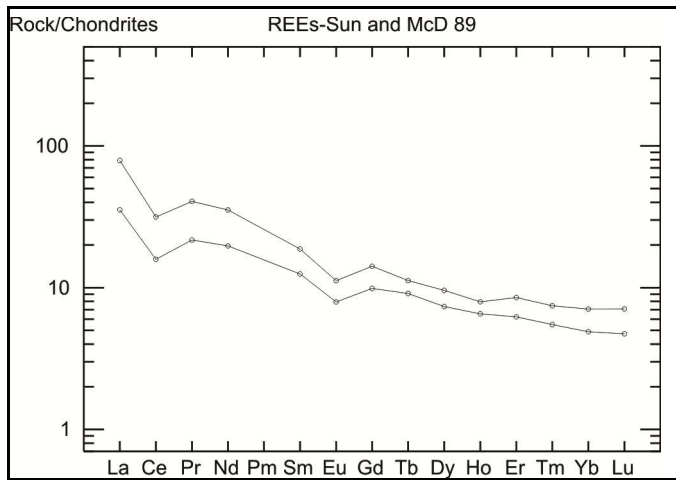


**Fig. 196 REE plot from Siliceous limestones from the Gresten Klippenzone.**

### CIA of the siliceous *Calpionella* limestones

The Chemical Index of Alteration (CIA) and the Chemical Proxy of Alteration (CPA) correlate (Fig. 197). In the A-CN-K diagram (Fig. 198) the St.Veit Klippenzone and Krížna Nappe samples have lower values compared with the Gresten Klippenzone or Drietoma Unit samples. Likewise the cherts discussed previously, fine grained sediments like the *Calpionella* limestones are problematic using CIA investigations. During genesis and diagenesis a lot of different geochemical reactions can mask the „real” CIA.

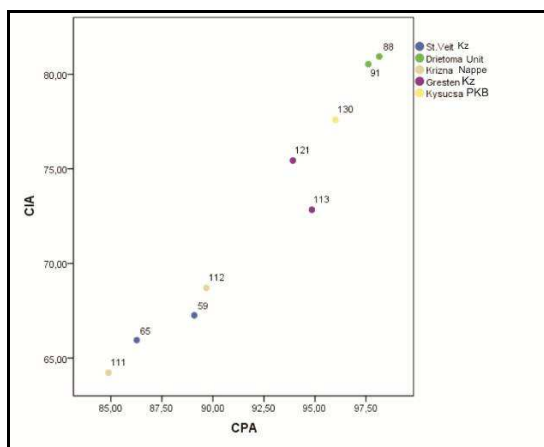


**Fig. 197 CIA vs CPA plot from siliceous *Calpionella* limestones.**

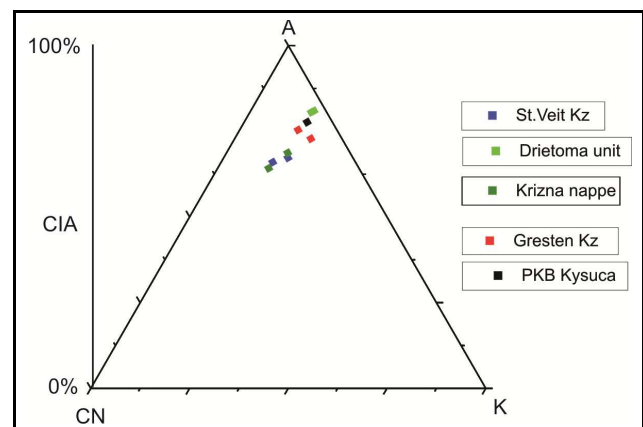


**Fig. 198 CIA plot from siliceous *Calpionella* limestones.**

## **Summary of results for siliceous rocks (cherts, radiolarites, siliceous limestones)**

The factor analysis suggests that the main difference between the samples, beside normal variations of elements like SiO<sub>2</sub>, CaO and Sr, could be found in different amounts of more immobile elements like Th or La. It also seems that the Ybbsitz Klippenzone and the Kysucsa unit tend to spread more and group separately from the others.

In general the Ybbsitz Klippenzone shows higher contents of Cu, Ni, Zn, TiO<sub>2</sub>, MnO, Fe<sub>2</sub>O<sub>3</sub> and (Al<sub>2</sub>O<sub>3</sub>+K<sub>2</sub>O+Na<sub>2</sub>O) than the St.Veit Klippenzone. The Ybbsitz Klippenzone, together with the Kysucsa Unit, has significant higher amounts of trace elements (such as La, Sc, Ce and Th). Because elements like Cu ,Ni, Zn, MnO and Fe<sub>2</sub>O<sub>3</sub> are often associated with hydrothermal and mafic settings (e.g. Mc Lennan, 1993), and elements such as Al<sub>2</sub>O<sub>3</sub>, K<sub>2</sub>O and Na<sub>2</sub>O likely representing a higher shale mineral content, together with higher La, Sc, Ce and Th contents, a different paleogeographic setting, i.e. higher "mafic" trend, for the Ybbsitz Klippenzone cherts compared to the St.Veit Klippenzone cherts can be assumed.

There are no significant differences in the REE patterns between the various cherts from the klippenzones that were sampled. As long as the groups are more or less inhomogeneous, characteristics as e.g. Ce or Eu anomalies can't be used for differentiation.

In the A-CN-K diagram (Fig. 189) the samples from the St.Veit Klippenzone, like the Drietoma Unit and Krížna Nappe samples, show a wide range of CIA values, the Ybbsitz Klippenzone samples seem to plot closer to each other. The reason for that could be varying age or that cherts are very fine grained (chemical) sediments and some geochemical interactions with the surrounding sediments could be expected.

A geochemical approach for the *Calpionella* limestones was quite difficult. Because this group is defined very clearly by its age, it was treated on its own and not mixed with others. There are no significant differences in the REE patterns between the various *Calpionella* limestones from the klippenzones that were analysed.

In the A-CN-K diagram (Fig. 198) the St.Veit Klippenzone and Krížna Nappe samples have lower values compared with the Gresten Klippenzone or Drietoma Unit samples. Likewise cherts, fine grained sediments like the *Calpionella* limestones are problematic using CIA investigations. During genesis and diagenesis a lot of different geochemical reactions can mask the „real” CIA.

## Strontium isotopes

Several samples (bulk rock carbonate) from the tunnel and the Lainzer Tiergarten outcrops were tested for  $^{87}\text{Sr}/^{86}\text{Sr}$ -isotopes (measured at TIMS, Department of Lithospheric Research, University of Vienna). The results indicate that most of the values are too high if compared with the strontium seawater curve (McArthur et al., 2001), compared to the possible stratigraphic age and thus cannot give a clear and improved stratigraphic information. Diagenesis/chemical mobilisation could have caused the higher levels. Only eight samples gave a suitable age indication (Kössen Formation, outcrop in Lainzer Tiergarten, LT-E, 0.707828 - age around the Triassic/Jurassic boundary, and if including the error range, may fall into the Rhaetian; LT31/1160 "Arnioceras spp." 0.707777~Sinemurian; outcrop Doggerian limestone, Inzersdorfer Wald in Lainzer Tiergarten, 0.707735; LT31/1366, 0.707449; Hohenauer Wiese in Lainzer Tiergarten, brachiopod shell 0.707206; Gemeindeberggasse belemnite 0.707225).

Sample No.	description	$^{87}\text{Sr}/^{86}\text{Sr}$	$\pm 2\text{s}_m$
LT-E	Brachiopod limestone, Kössen Formation	0.707828	0.000033
LA08/8	Aptychus limestone	0.70778	0.000005
LA08/1	Aptychus limestone(Tithonian-Neokomian)	0.70759	0.000006
LA08/6	Middle Jurassic spotted limestone	0.70901	0.000032
LA08/7	Brachiopod, red ammonite limestone, Stockwiese	0.707252	0.000006
H.W.	Brachiopod, Hohenauer Wiese, Jura (MM)	0.707206	0.000005
I.W.	Dogger Klippe, crinoidal limestone, Inzersdorfer Wald	0.707735	0.000008
W.T.	Aptychus limestone west of Teichhaus	0.707657	0.000004
CK	Crinoidal limestone	0.707796	0.000004
K.W.	Kössen layers, Kleefrischwiese	0.707931	0.000005
S.W.	Ammonite limestone Stockwiese	0.70753	0.000005
LT33/2333	<i>Protancyloceras</i> (Tithonium/Berriasium)	0.707452	0.000003
Gemeindeberggasse	Belemnite	0.707225	0.000004
LT33/2666	Sample with nannostratigraphy age (Lias/Dogger)	0.708118	0.000003
LT31/1160	„Arnioceras“ Sinemurium	0.707777	0.000003
LT31/1366	Sample with nannostratigraphy age (Lias/Dogger)	0.707449	0.000003
RSVG 1	Sample with radiolaria / aptychus age (Bajocium)	0.707644	0.000004

Fig. 199 Table of samples used for  $^{87}\text{Sr}/^{86}\text{Sr}$ -isotopes from the Lainz Tunnel and Lainzer Tiergarten.

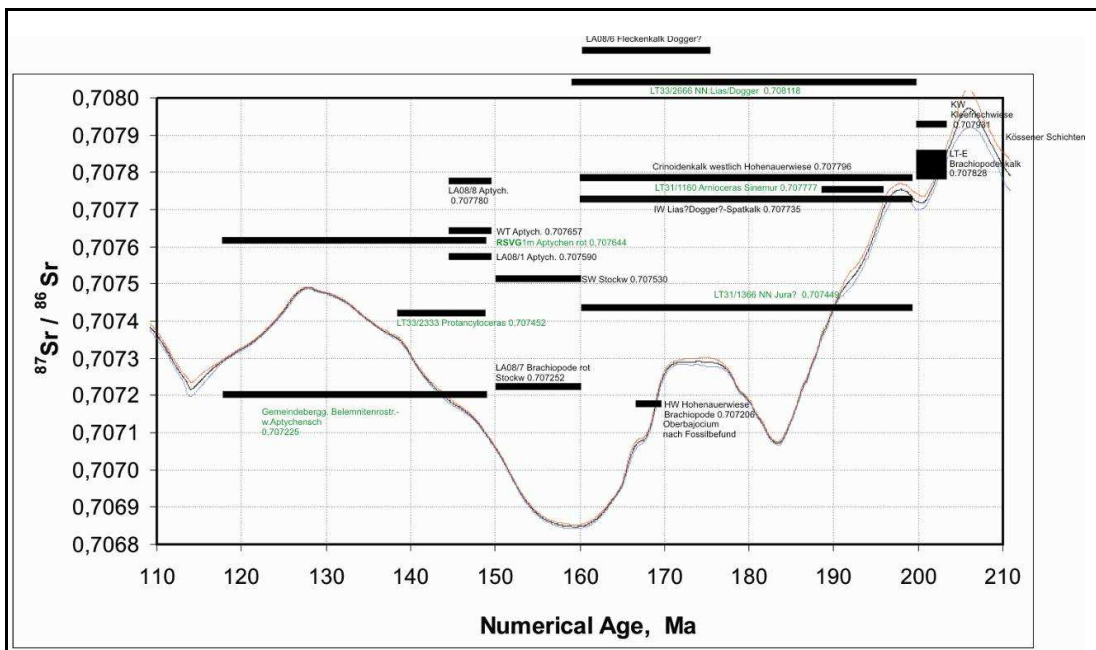


**Fig. 200:**  $^{87}\text{Sr}/^{86}\text{Sr}$  results of the Lainz Tunnel and the Lainzer Tiergarten plotted into the Sr-curve of McArthur et al. (2001).

## Stable isotopes

Stable isotope measurements were done on carbonate-rich samples (bulk rock) from the Lainz tunnel section at the University of Innsbruck (C. Spötl). The diagram of carbon vs. oxygen isotopes shows some positive correlation indicating a diagenetic influence on the samples (see Fig. 202). Plotted against the seawater values for the Jurassic given by Jenkyns (2002), most of the measured values plot within the possible range of Jurassic seawater (Fig. 203), but no detailed chronostratigraphic information can be given, especially as no high-resolution, continuous section could be sampled to identify specific carbon isotope excursions.

Sample	d <sup>13</sup> C	d <sup>18</sup> O
LT33/1028m	2.18	-4.22
LT33/1232m	1.10	-5.16
LT33/1498m	0.08	-3.73
LT33/1739m	1.05	-3.01
LT33/1923m	0.35	-3.83
LT33/2005m	0.18	-3.73
LT33/2113m	-0.10	-3.62
LT33/2229m	1.86	-3.42
LT33/2299m	1.00	-2.63
LT33/2918m	1.69	-3.01
LT33/2505m	0.95	-2.33
LT33/2609m	1.34	-2.84
LT33/2731m	-0.71	-5.67
LT31/1366m	0.24	-2.92
LT31/1200m	-1.13	-4.74
LT31/1133m	-0.13	-3.37
LT31/1073m	1.02	-5.25
LT31/1008m	2.13	-2.56
LT31/962m	0.80	-4.08
LT31/898m	0.34	-4.44

**Fig. 201 Stable isotope measurements of the Lainz Tunnel.**

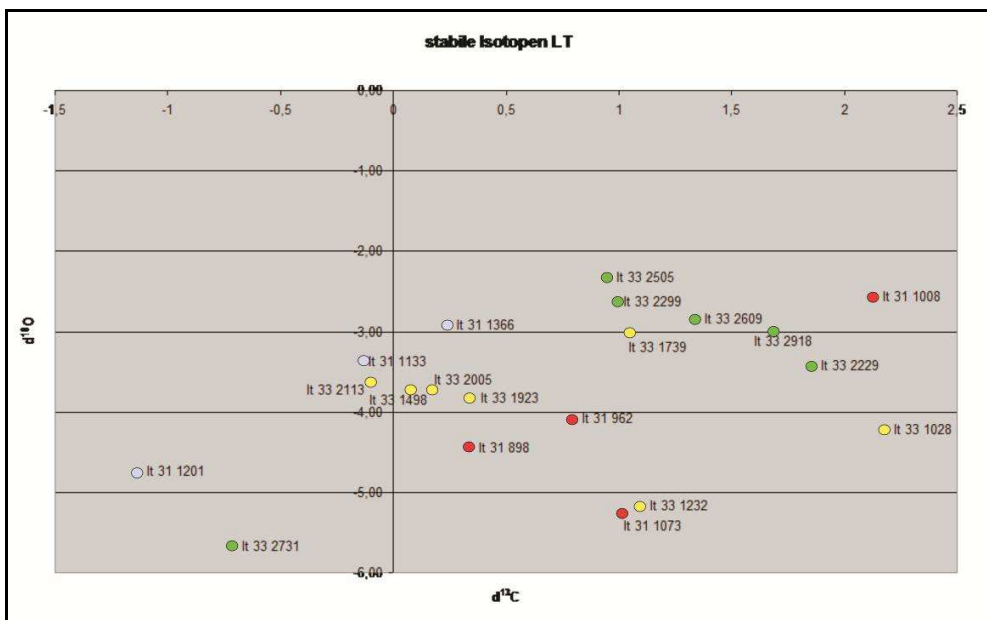


**Fig. 202** Plot of carbon vs. oxygen isotope ratios (red = Hütteldorf Formation, yellow = Kahlenberg Formation/Hütteldorf Formation, green = L/M-Jurassic carbonates LT33, blue = L/M-Jurassic carbonates LT31).

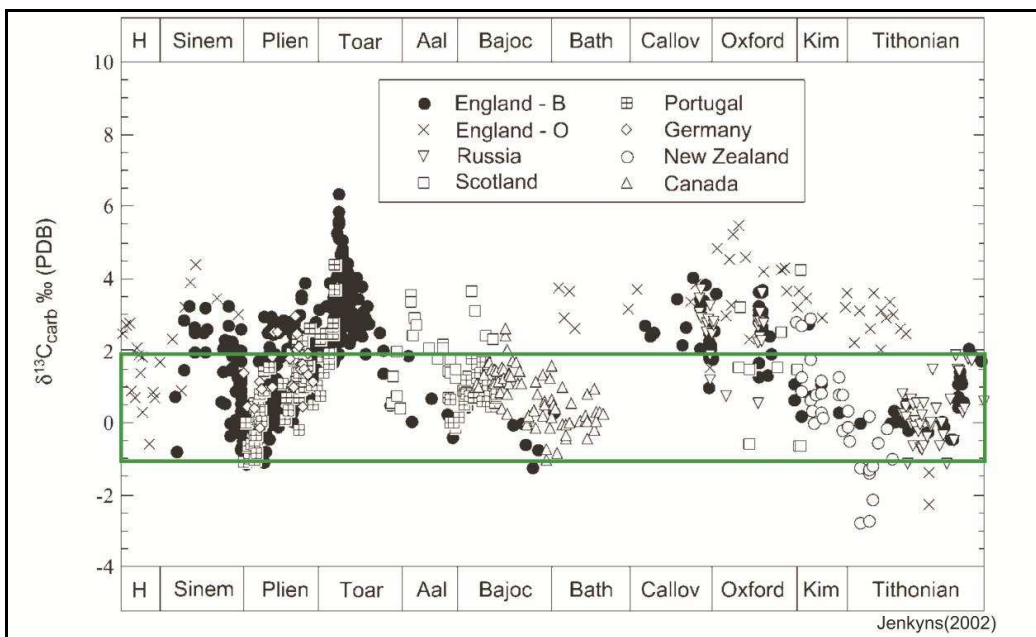


**Fig. 203** Plot of carbon isotope values against Jurassic seawater values of Jenkyns et al. (2002) (green bracket indicates range of values measured).

## D. DISCUSSION

### D.1. Stratigraphy

Based on preliminary results from tunnel sampling, stratigraphy, lithofacies and biostratigraphy, the St. Veit Klippenzone in the Lainz Tunnel displays the following stratigraphic units:

- (1) Upper Triassic sandstones („arkosic“) (Keuper; not biostratigraphically dated, but geochemical data and heavy minerals correlate well with dated Keuper strata)
- (2) Lower/Middle Jurassic sandy marls (badly dated)
- (3) Middle Jurassic red chert and red shale (L/M Bajocian, dated by radiolarians)
- (4) Grey marl to argillaceous limestone (Tithonian-Valanginian, dated by calpionellids)
- (5) White silicified limestone (Middle/Upper Berriasian; dated by calpionellids)
- (6) Green chert (Valanginian; dated by radiolaria)

Combined with literature data and some additional own investigations, the St. Veit Klippenzone comprises the following composite stratigraphy:

1. Keuper quartzites (Upper Triassic): light grey and pink quartz with whitish kaolinitic matrix and violet-red to greenish clay (Prey, 1975, 1979). The presence of dolomites of probably Triassic age is reported by Janoschek et al. (1956). Although some dolomite blocks are present in the Lainz Tunnel, the Triassic age could not be confirmed, although dolomites occur together with Keuper rocks.
2. Kössen Formation (Rhaetian): fossiliferous, dark, bedded marly limestones, limestones and marls with bivalves and brachiopods according to Griesbach (1868, 1869). No such rock types were found in the Lainz Tunnel. Outcrops in the Lainzer Tiergarten (e.g.: Kleefrischwiese) could be additionally dated by Sr isotopes near the Triassic-Jurassic boundary.
4. Lower/Middle Jurassic sandstones „Gresten Formation“: coal-bearing sandstones, dark sandy Gresten limestones, grey crinoidal limestones, brownish-black marly shales and marly limestones. Ammonites (e.g. *Arietites*) indicate lower/middle Liassic; bivalves are common. (e.g. Griesbach, 1868, 1869, Trauth, 1930)
5. Lower/Middle Jurassic siltstones and marls („Posidonia marls“): marly/sandy facies (e.g. Schnabel, 1997, 2002). Some sandy marls encountered in the Lainz Tunnel may be included into this stratigraphic unit.
6. „Hohenauer Wiese Formation“ (Middle Jurassic): grey marly sandstones, sandy limestones, crinoidal limestones, cherty shales and limestones with ammonites of Bajocian, Bathonian

and Callovian (Schnabel, 1997, 2002). Although crinoidal limestones are present in the Lainz Tunnel, the age could not be confirmed. Cherts with a similar Bajocian age may indicate the presence of different facies types of the same age within the SVK.

7. Red crinoidal limestones (Kimmeridgian) (Schnabel, 1997, 2002), only known from outcrops in Lainzer Tiergarten, not found in Lainz Tunnel.

8. „Rotenberg Formation“ (Upper Jurassic): red, green and grey radiolarites, described by Schnabel (1979), Decker (1987, 1990) and Trauth (1930). These siliceous rock types were found within the tunnel, although covering a considerably larger stratigraphic interval, from Middle Jurassic (Bajocian) to Lower Cretaceous (Valanginian).

9. „Fasselgraben Formation“/Aptychus limestone: white and grey, partly siliceous limestones with black chert nodules (Tithonian-Neocomian) (Trauth, 1930) were found also within the Lainz Tunnel, e.g. *Calpionella* limestones.

Data from the Lainz Tunnel help to clarify the problem if (arkosic) sandstones encountered in the SVK are representatives of the Keuper facies, and thus Late Triassic in age, or if they are of Gresten affinity, and thus Early Jurassic in age. Strong geochemical similarities with Keuper sandstones of the Carpathians, and clear geochemical separation from Gresten sandstones suggest a Keuper-related Upper Triassic age of these sandstones in the sense of Prey (1975, 1979) and argues against the occurrence of Gresten sandstones in the SVK as suggested by Trauth (1930). Furthermore, according to literature (e.g. Prey, 1975; Wessely 2006), dolomite and varicoloured shales are typical interlayers of these Keuper-type sediments.

Rhaetian limestones with bivalves are only known from outcrop areas of the Lainzer Tiergarten but not from the Lainz Tunnel itself. Therefore, no new details can be given about this lithology. Although the lithofacies strongly resembles parts of the Kössen Formation of the NCA, the fossil content seems to be different.

Regarding Lower to Middle Jurassic sediments from the SVK the same rock types as described in literature (e.g. Trauth, 1930, Prey, 1975) were encountered in the Lainz Tunnel and the Lainzer Tiergarten. Like other authors mentioned before (e.g. Trauth, 1930), the Lower to Middle Jurassic sediments of the „Gresten type facies“ in the SVK are difficult to be divided. Because the term „Hohenauer Wiese Formation“ after Schnabel (1997, 2002) is not clearly defined, it is difficult to assign rock types from the Lainz Tunnel to this term.

The red cherts and red shales (from the Lainz Tunnel/ Veitingergasse) of determined Lower/Middle Bajocian age could represent a very early stage of the Rotenberg Formation as

they were found at the rescue pit Veitingergasse near the former type locality „Roter Berg“ (Trauth, 1930). This compares well with data from the Ybbsitz and the Gresten Klippenzones, from there were also Middle Jurassic ages reported (e.g. Ožvoldová & Faupl, 1993).

Other additional radiolarites of probably Upper Jurassic age from the Lainz Tunnel can also be assigned to the Rotenberg Formation, whereas red crinoidal limestones are only known from the Lainzer Tiergarten (Prey, 1975).

The grey marl/argillaceous limestone found in the Lainz Tunnel (LT33/2333m) of Tithonian to Valanginian age represents the Fasselgraben Formation (Trauth, 1950).

The white silicified limestone of Middle to Late Berriasian age, found in the Lainz Tunnel, fit very well the descriptions of the aptychus limestones (e.g. Prey, 1975).

An additional siliceous rock type (chert) with an Early Cretaceous (Valanginian) age was found at 2165.5m/LT33 and is so far not known from the outcrops of the SVK (e.g. Janoschek et al., 1956) and confirms that the deepwater shaly-siliceous sedimentation continued from the Late Jurassic into the Early Cretaceous.

## **D.2. Relation Flysch to St. Veit Klippenzone**

The Lainz Tunnel section gives no unambiguous information about the relation of the (Rhenodanubian) Flysch (Kahlenberg Nappe) and the SVK. Due to the extreme deformation, no sedimentary contact between these two units could be found in the tunnel section. However, the sampled intervals do not indicate any unknown intervening units as suggested by Prey (1985). So, the general stratigraphy and tectonic superposition still allows to infer a continuous succession from Lower Cretaceous aptychus limestones to the Albian?-Cenomanian-Turonian flysch units (i.e. Hüttdorf Formation). However, a remarkable stratigraphic gap is then ascertained, from the youngest age of the aptychus limestone of Valanginian/Hauterivian? (upper boundary 130 Ma) to the oldest age of the surrounding flysch (probably Upper Albian, lower boundary 107 Ma) - this would indicate a more than 20 Ma stratigraphic gap from which no rocks are found. Taking this into mind, a continuous succession of the SVK into the Kahlenberg Nappe becomes strongly doubtful and thus an attribution of the SVK as a primary basement of the Rhenodanubian Flysch and the Kahlenberg Nappe (in the sense of Prey, 1979, and Schnabel, 2002) is highly uncertain and speculative - alternatives may still be envisaged.

Taking this into account, it is more probable that the Kahlenberg Nappe of the Rhenodanubian Flysch and the SVK are primarily separated units that were put into a tectonic contact during

the first deformational phase of the Flysch units, i.e. in Paleocene to Eocene times, as the youngest unit of the Kahlenberg Nappe is of Maastrichtian age (Sievering Formation, Faupl et al., 1970; Piller et al., 2004). The anticlinal structure was probably also formed during this time. Later on, during Oligocene to Miocene times, these units were progressively deformed together at the northern margin of the Alpine thrust pile, and hard competent klippen rocks and soft, incompetent flysch shales were mixed to form the present structure.

### D.3. Geotectonic Position of the St. Veit Klippenzone

Different opinions and hypotheses about the original paleogeographic and geotectonic position of the SVK exist, with an attribution either to (Fig. 204):

- (1) the distal European continental margin north of the Penninic Ocean (e.g. Trauth, 1930; Wessely, 2006), similar to the Gresten Klippenzone („ultrahelvetic“ or "subpenninic" position);
- (2) a high within the Penninic Ocean in a Middle Penninic position (similar to Middle Penninic positions suggested for parts of the PKB, Faupl and Wagreich, 1992);
- (3) a South Penninic element similar to the Ybbsitz Zone (e.g. Schnabel, 2002), i.e. an oceanic position with ophiolitic allocation;
- (4) or an Austroalpine element related to the Lower Austroalpine and the Northern Calcareous Alps (e.g. Prey, 1987) which formed the southern margin of the Penninic Ocean, tectonically active since the Cretaceous.

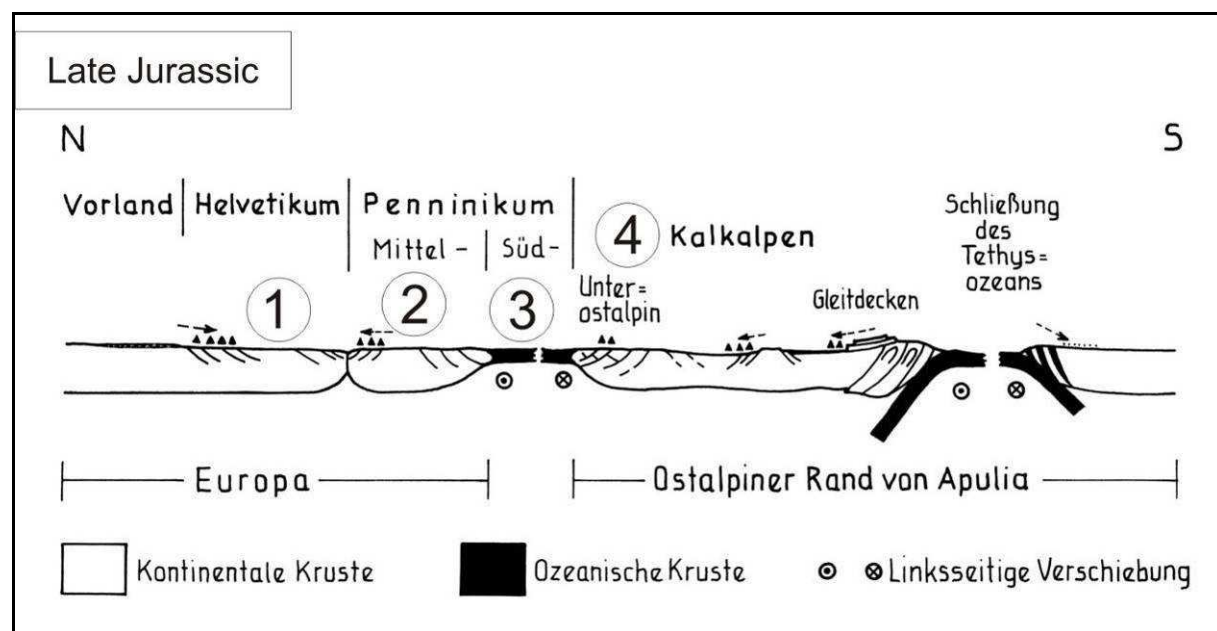


Fig. 204 Schematic N-S section through the Eastern Alps in Late Jurassic time (based on Faupl & Wagreich, 2000) and possible positions of the St. Veit Klippenzone (1-4).

Based on the results on stratigraphy, facies, heavy minerals and geochemistry, a correlation to the Gresten Klippenzone can be ruled out because of the presence of Triassic strata, i.e. Keuper sandstones and shallow-water limestones (Kössen Formation), which are completely absent in the Gresten Klippenzone. The Gresten Klippenzone (and equivalents below the Molasse Zone) show an Early to mid-Jurassic transgression onto equivalents of the Bohemian Massif. Also geochemical data show a clear separation of these two units, the SVK and the Gresten Klippenzone, especially for Keuper sandstones vs Gresten sandstones and SVK vs Gresten Klippenzone carbonates (Fig. 119 and Fig. 160).

A Middle Penninic position (Subpenninic in the sense of, e.g. Schmid et al., 2004) may be possible, however, unequivocal Middle Penninic (Brianconnais) units end in western Austria, in the Unterengadin Window, and do not show siliceous Jurassic sediments, but shallow-water Upper Jurassic carbonate rocks. In addition, successions of interpreted „Middle Penninic“ in the Tauern Window do have a (metamorphic) Triassic succession similar to „Germanic Triassic“ (Faupl, 2003) with Keuper-type sediments, but rock types like Kössen Formation or Jurassic crinoidal limestones, marls and shales are missing. No comparable Middle Penninic could be sampled during the course of this study. However, if parts of the PKB, i.e. the Czorsztyn swell, are regarded as Middle Penninic (Faupl and Wagreich, 1992), some similarities in facies may be found, but no geochemical correlations are possible.

Against a South Penninic derivation of the SVK and thus a direct continuation of the Ybbsitz Klippenzone (as indicated in most recent publications, e.g. Schnabel, 2002) argues the complete lack of ophiolitic rocks, especially serpentinites (as compared to the Ybbsitz zone) and again the presence of Triassic rocks which absolutely cannot be present within the South Penninic Ocean which started to exist only in Jurassic times (Decker, 1990). Geochemical data, (e.g. Fig. 175) emphasize this argument, as rocks from the SVK clearly separate from those of the Ybbsitz Klippenzone in various geochemical plots and indices. No ophiolithic/MORB affinities or signals can be found in the SVK in general, in contrast to the Ybbsitz Klippenzone (see also Decker, 1990). In addition, the heavy mineral data from the SVK indicate missing to very low contents of chrome spinels, which can be seen as an additional indicator for ophiolitic provenance, and which is frequent in the Lower Cretaceous of the Ybbsitz Klippenzone (Decker, 1990).

In this respect, also the data from the Lainz Tunnel concerning „picrites“ becomes important. Although these volcanites occur dispersed within the surrounding flysch units (Janoschek et al., 1956), their presence and primary contact with mid-Cretaceous flysch units was used as an

argument for the similarity between the ophiolithic Ybbsitz Klippenzone and the SVK (as real picrites are oceanic basalts, i.e. high-magnesium, olivine-rich alkali basalts). Data from the Lainz Tunnel indicate that (a) the volcanite blocks encountered are strongly altered basalts but not picrites, and (b) there is no primary contact of volcanites to the flysch sediments but only tectonic blocks in a sheared flysch shale matrix to occur. This may then also indicate that the age of the basaltic volcanism is not constrained, and may be considerably older than mid-Cretaceous, e.g. Triassic or even Paleozoic.

A northern Austroalpine position („Lower“ Austroalpine facies in the sense of Tollmann, 1977) is supported by the presence of both Keuper and Kössen-type Upper Triassic rocks, crinoidal limestones and marls of Lower/Middle Jurassic age, Middle/Upper Jurassic siliceous limestones and radiolarites, and aptychus limestones (see also Häusler, 1988). Given the fact, that Keuper layers are even present in the Upper Triassic Hauptdolomit in the northern tectonic units of the eastern NCA (e.g. Lunz Nappe, Wessely, 2006), a position adjacent to the north of the NCA during the Late Triassic is suggested by the Keuper facies rocks. Lower Austroalpine units such as the Semmering area and the Radstädter Tauern, now metamorphosed, show a mixing of such a northern-Alpine facies (including Kössen Formation) and the Germanic Triassic facies (especially the Keuper beds in the Semmering area, e.g. Tollmann, 1977, 1985; Faupl, 2003; Wessely, 2006). Crinoidal limestones, marls and Jurassic siliceous rocks are all also known as metamorphosed counterparts from the Lower Austroalpine of the Radstädter Tauern (Tollmann, 1977; Häusler, 1988), thus supporting evidence for a northern-Austroalpine primary position of the SVK.

However, breccias which may be typical for Jurassic Lower Austroalpine successions (Häusler, 1988), are so far completely unknown from the SVK. On the other side, further evidence for a derivation from the northern margin of the Austroalpine microplate comes from correlations to the Western Carpathians.

An additional argument are the similarities of the SVK succession with the succession reconstructed from dislodged slices at the base of the Göller Nappe, a Tyrolian unit of the NCA. These slices comprise some Keuper, Jurassic sandstones, and other Jurassic rocks equivalent to the SVK (for overview see Wessely, 2006), and thus indicate incorporation (probably out of sequence thrusting) of rocks very similar to the SVK succession into the NCA.

## **D.4. Correlation to the Western Carpathians**

Several authors, starting with classical publication by Neumayr and Trauth (1930, 1954) regarded the SVK as the continuation of the Pieniny Klippen Belt (PKB) from Slovakia and Poland to Vienna, although these authors regarded also parts of the Gresten Klippenzone to the west as „pienidic”. Although the position of the PKB itself is still strongly debated, a correlation with undisputed PKB core units (e.g. Czorsztyn and Pieniny units) can hardly be established, although similar Jurassic facies types such as crinoidal limestones, radiolarites, marly limestones and spotty marls can be noticed. However, strong similarities can be found to a special unit within the PKB, the Drietoma unit, a „periklippen” unit sensu Plasienka (2006).

### **D.4.1. Correlation to the Drietoma unit**

The following description of the Drietoma unit is taken from Hók et al. (2009):

*„The Drietoma unit is a structural element incorporated into the western segment of the Pieniny Klippen Belt (PKB). In the area between Podbranč and Drietoma (Fig. 1) a sequence of sedimentary rocks in the stratigraphic range of Upper Triassic (Norian) to Lower Turonian, has been originally described as a part of the Manín unit (Begán, 1969). Later Rakús (1977) classified mentioned sediments into the Drietoma unit. However, mainly the Cretaceous lithostratigraphic members of the Drietoma unit were interpreted ambiguously. The tectonic position of the Drietoma unit was interpreted similar ambiguously (e.g. Salaj, 1990). Based on our research of structural position and lithology, we conclude that the Drietoma unit is an allochthonous tectonic unit incorporated into present PKB structures, lying over its external elements (Kysuca and Czorsztyn units), and over the Klape unit. Stratigraphic range of the Drietoma sequence is from Upper Triassic (Norian) to Lower Cretaceous (Berriasian). There are no proofs that the younger lithostratigraphic formations (Albian and younger) are an integral part of the Drietoma sequence, no direct sedimentary contact was found until now. The tectonic transport was generally top to NW oriented. The Fatricum and the Hronicum tectonic units are in tectonic superposition above the Drietoma unit. The Drietoma unit is a particular structural element displaced into the area of recent course of PKB from internal or southern zones after the Turonian.” (Hók et al., 2009).*

The Drietoma unit contains a significant interval of Carpathian Keuper sandstones (Al-Juboury, 2007), followed by limestones with lumachelles of Rhaetian age (similar to Kössen Formation), then Lower Jurassic limestones and spotty marly limestones (Allgäu-type limestones), Middle Jurassic to Oxfordian radiolarites and siliceous limestones, and Upper Jurassic-Berriasian pelagic limestones (Hók et al., 2009). This succession is similar to the reconstructed succession of the SVK, especially regarding Keuper sandstones and shales, Kössen-type limestones of Rhaetian age, and marly limestones and siliceous rocks of Jurassic age.

Geochemical data from this thesis give also evidence for close similarities of SVK rocks with those of the Drietoma units. In several plots (e.g. Fig. 125, Fig. 164, Fig. 179) these units plot closely together and define one geochemical group in regard of provenance and environments, separated from other zones like the Gresten Klippenzone and the Ybbsitz Zone.

Hók et al. (2009) argue for an originally internal position of the Drietoma unit south of the PKB which can be compared to Manín and Fatic Units, the Krížna Nappe, i.e. a northern Austroalpine position in terms of the Eastern Alps (Tollmann, 1977, 1985) which is then similar to the conclusions from the Lainz Tunnel.

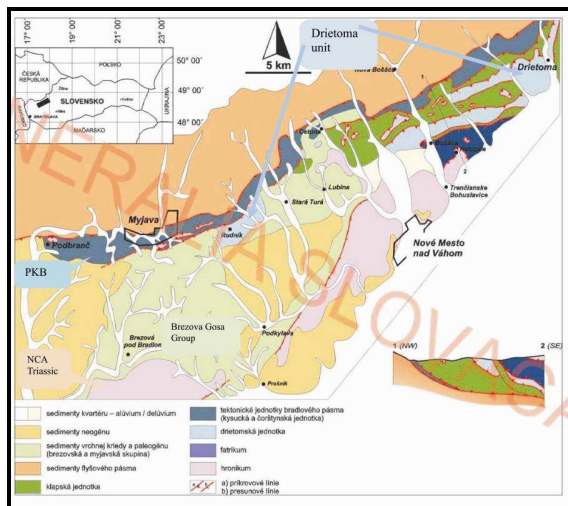
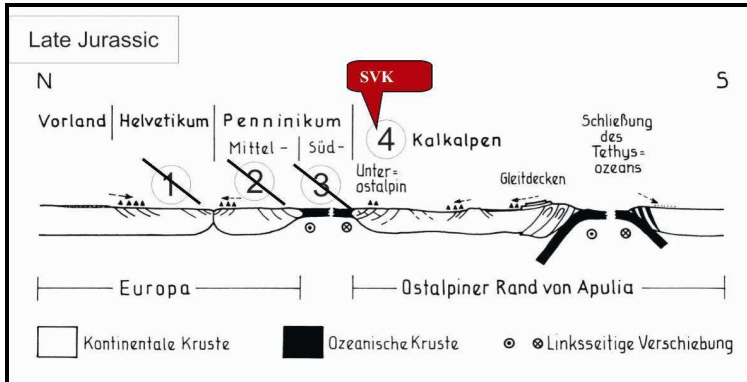
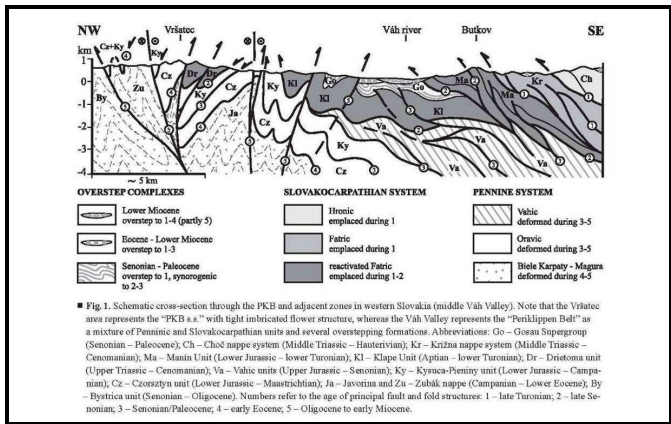


**Fig. 205** Map of the western part of the Western Carpathians indicating the Drietoma unit (light blue) at the southern margin of the Pieniny Klippen Belt (PKB), north of equivalents to the Northern Calcareous Alps (NCA Triassic + Brezova Gosau Group); taken from Hók et al. (2009).



## E. CONCLUSIONS

The St.Veit Klippenzone forms a complex tectonic structure between the NCA and the Rhenodanubian Flysch. Flysch units encountered in the Lainz Tunnel include the Kahlenberg Formation (Campanian) and the Hütteldorf Formation (Cenomanian-Turonian) of the Kahlenberg Nappe, which were strongly deformed, folded and tectonically mixed with the St. Veit Klippenzone along a large, complexly deformed anticlinal structure. The St. Veit Klippenzone comprises a block-in-matrix structure, partly tectonically mixed with the flysch units.

Due to the extreme deformation, no primary sedimentary contact between the SVK and the Kahlenberg Nappe could be found in the tunnel section. The sampled intervals do not indicate any unknown intervening units.

The stratigraphic succession of the St. Veit Klippenzone includes Triassic Keuper sandstones, Jurassic carbonates and siliceous rocks, and Lower Cretaceous pelagic limestones.

Based on the results, a continuous succession of the SVK into the Rhenodanubian Flysch is strongly doubtful and thus an attribution of the SVK as a primary basement of the Rhenodanubian Flysch and the Kahlenberg Nappe (in the sense of Prey, 1979) is highly uncertain and speculative.

The geotectonic position of the St. Veit Klippenzone is interpreted as a northern Austroalpine unit. A northern Austroalpine original position of the SVK is supported by the presence of Keuper and Kössen-type Triassic rocks, crinoidal limestones and marls of Lower/Middle Jurassic age, Middle/Upper Jurassic siliceous limestones and radiolarites, and Lower Cretaceous aptychus limestones.

Direct correlations to units, especially the Drietoma unit of the Pieniny Klippen Belt (PKB) in Slovakia can be given and argue for a direct continuation of the PKB in the basement of the Vienna Basin up to the SVK.

The SVK thus forms the westernmost part of the Pieniny Klippen Belt of the Carpathians.

## **ACKNOWLEDGEMENT**

First and foremost, I would like to thank my advisor Ao. Univ. Prof. Dr. M. Wagreich for his constant support and encouragement on this work.

For his commitment and guidance with the slovakian outcrops I am grateful to Doc.Dr. Roman Aubrecht from the Comenius University (Bratislava).

Ao. Univ.-Prof. Dr. S. Gier helped me with the XRF analysis and petrological questions, I want to thank her for that.

Furthermore, I am grateful to OMV for financially supporting this project. I was very fortunate to have Mag. Gerhard Arzmüller as my supervisor from OMV his geological knowledge was really helpful. I also want to thank his colleague at the OMV Lab Roman Sauer, for helping me with the heavy mineral analysis.

I'm especially indebted to Dipl.-Ing. Thomas Buismann und Dipl.-Ing. Wolfgang Pistauer (ÖBB -Infrastruktur Bau AG) for their support. Without the agreement from the ÖBB, sampling and the project itself would have been infeasible.

Special thanks go to the employees from the office Bechthold: Mag. M. Sapp, Mag. G. Koch and Dr. B. Haunschmid. They helped me with everything that mattered tunnelgeology and assisted me with sampling. I also want to thank Martin Maslo for doing some sampling and providing his knowledge about the Klippen in the Lainz Tiergarten.

I owe my colleague and friend Mag.V. Koukal a lot for her support onsite as well with the numerous work in the laboratory.

Last but not least I want to thank my mother, without her help this would have been impossible.

## REFERENCES

- Adamová M., Schnabel, W., 1999. Comparison of the East Alpine and West Carpathian Flysch Zone -A Geochemical Approach. Abh. d. Geol. Bundesanstalt, 56/2: 567-584.
- Al-Juboury, A., 2007. Petrography and major element geochemistry of Late Triassic Carpathian Keuper sandstones: Implications for provenance. Bulletin de l'Institut Scientifique, Rabat, section Sciences de la Terre, 2007, n 29, 1-14.
- Andrusov, D. & Bystricky, J. & Fusán, O., 1973. Outline of the Structure of the WestCarpathians. - Guide-Book geol. excurs., X. Congr. Carpathian-Balkan Geol. Assoc, 44 S., 5 Abb., Bratislava (Geol. Ustav D. Stura).
- Aubrecht, R., 1994. Heavy Mineral Analyses from „Tatric“ Units of the Malé Karpaty Mountains (Slovakia) and their consequences for Mesozoic Paleogeography and Tectonics. Mitt. Österr. Geol. Ges. 92, 86, 121-132.
- Aubrecht, R., Gaži, P., Bučová, J., Hlavatá, J., Sestrienka, J., Schlögl, J. & Vlačíky, M., 2004. On the age and nature of the so called Zázrivá Beds (Pieniny Klippen Belt, Western Carpathians). Mineralia Slovaca (Košice), 36, 1, 1-6.
- Began, A., 1969. Geologické pomery bradlového pásma na strednom Považí. In: Zbor. geol. Vied, Západ. Karpaty (Bratislava), 11, 55 – 103.
- Behrens, M., 1973. Schwermineralverteilung und Sedimentstrukturen in den Lunzer Schichten. Jb. Geol. B.-A., 116.
- Bhatia, M. R., 1983. Plate tectonics and geochemical compositionof sandstones. J Geol 91 : 611-627.
- Bhatia, M. R., 1985. Rare earth element geochemistry of AustralianPaleozoic graywackes and mudrocks: provenance and tectonic control. Sed Geol 45 : 97-113.
- Birkenmajer K., 1977. Jurassic and Cretaceous lithostratigraphic units of the Pieniny Klippen Belt, Carpathians. Studia Geologica Polonica, 45, 158p.
- Buggle, B., Glaser, B., Hambach, U., Gerasimenko, N. and Marković, S., 2011. An evaluation of geochemical weather indices in loess-paleosol studies. Quaternary International, 240, 12-21.
- Burnett, J.A., 1998. Upper Cretaceous. In: Bown, P.R. (ed.): Calcareous Nannofossil Biostratigraphy: 132-199, (Chapman & Hall) Cambridge.
- Czjzek, J., 1847. Geognostische Karte der nächsten Umgebung von Wien. (Mitteilung darüber.) W. Haidingers Ber. üb. d. Mitt. d. Freunde d. Naturwiss. in Wien. I. Bd., S: 10 (Wien).
- Czjzek, J., 1849. Erläuterungen zur geognostischen Karte der Umgebungen Wiens. (In Commission bei W. Braumüller, Wien.).
- Czjzek, J., 1852. Aptychenschiefer in Niederösterreich. Jahrb. d. k. k. geol. R.-A., III. Bd., 3. Vierteljahr, S. 1.
- Decker, K., 1987. Faziesanalysen der Oberjura- und Neokomenschichtfolgen der Grestener und Ybbsitzer Klippenzone im westlichen Niederösterreich. Unpublished PhD Thesis, Universität Wien, 248 pp.
- Decker, K., 1990. Plate tectonics and pelagic facies: Late Jurassic to Early Cretaceous deep-sea sediments of the Ybbsitz ophiolite unit (Eastern Alps, Austria). Sedimentary Geology 67: 85-99.
- Decker, K. & Rögl, F., 1988. Early Cretaceous agglutinated foraminifera from limestone-marl rhythmites of the Gresten Klippen Belt, eastern Alps (Austria). Abhandlungen der Geologischen Bundesanstalt, 41: 41-59.

- Faupl, P., 1975. Kristallinvorkommen und terr. Sedimentgesteine in der Grestener Klippenzone von Ober- und Niederösterreich. *Jb Geol. B.-A.*, 118, 1-74, Wien.
- Faupl, P., 1996. Exkursion A 2. Tiefwassersedimente und tektonischer Bau der Flyschzone des Wienerwaldes. *Berichte der Geol. B.-A.*, 33 (1996): A2, 1-32 (Exkursionsführer Sediment '96, 11. Sedimentologentreffen), Wien.
- Faupl, P., 2003. Historische Geologie. 2. Aufl. Wien (Fakultas UTB).
- Faupl, P., Grün, W., Lauer, G., Maurer, R., Papp, A., Schnabel, W. & Sturm, M., 1970: Zur Typisierung der Sieveringer Schichten im Flysch des Wienerwaldes. *Jahrbuch der Geologischen Bundesanstalt*, 113: 75.158.
- Faupl, P. & Wagreich, M., 1992. Cretaceous flysch and pelagic sequences of the Eastern Alps: correlation, heavy minerals and palaeogeographical implications. - *Cretaceous Research*, 13, 387-403, Academic Press Ltd., London.
- Faupl, P. & Wagreich, M., 2000. Late Jurassic to Eocene palaeogeography and geodynamic evolution of the Eastern Alps. *Mitt. Österr. Geol. Ges.* 92, 79-94.
- Fedo, C.M., Young, G.M. and Nesbitt, G.M., 1997. Paleoclimatic control on the composition of the Paleoproterozoic Serpent Formation, Huronian Supergroup, Canada: A greenhouse to icehouse transition. *Precambrian Research*, 86, 201-223.
- Götzinger, G., 1954. Die Flyschzone. In Erläuterungen zur geol. Karte der Umgebung von Wien. 43-93, (Geol.B.-A.), Wien.
- Griesbach, K., 1868a. Der Jura von St. Veit bei Wien. *Verh. d. k. k. geol. R.-A.*, 1868, 54 (Wien).
- Griesbach, C., 1868b. Kössener und Juraschichten im k. k. Thiergarten bei Wien. *Verh. d. k. k. geol. R.-A.*, 1868, S. 198 (Wien).
- Griesbach, C.L., 1869. Die Klippen im Wiener Sandsteine. *Jahrb. d. k. k. geol. R.-A.*, XIX. Bd., S. 217.
- Häusler, H., 1988. Unterostalpine Jurabreccien in Österreich. Versuch einer sedimentologischen und paläogeographischen Analyse nachtriadischer Breccienserien im unterostalpinen Rahmen des Tauernfensters (Salzburg-Tirol). *Jahrbuch der Geologischen Bundesanstalt*, 131: 21-125, Wien.
- Hochstetter, E.W.v., 1897. Die Klippe von St. Veit bei Wien. *Jahrb. d. k. k. geol. R.-A.*, XLVII., 95.
- Hók J., Kráí J. and Kotulová J., 2005. Recent structure of lithosphere and neotectonics of the Western Carpathians (in Slovak). Manuscript, Archive ŠGÚDŠ Bratislava.
- Hók, J., Pešková, I. & Potfaj, M., 2009. Lithostratigraphy and tectonic position of the Drietoma Unit (Western part of the Pieniny Klippen Belt, Western Carpathians). *Mineralia Slovaca*, 41 313-320 (2009).
- Janoschek, R., Küpper, H. & Zirkl, E.J., 1956. Beiträge zur Geologie des Klippenbereiches bei Wien. *Mitt. Österr. Geol. Ges.*, 47, 235-308.
- Jenkyns, H.C., Jones, C.E., Gröcke, D.R., Hesselbo, S.P. & Parkinson, D.N., 2002. Chemostratigraphy of the Jurassic system: applications, limitations and implications for palaeoceanography. *J. Geol. Soc. (London)* 159 (2002), 351-378.
- Krumm, H., 1962. Mineralbestand und Genese fränkischer Keuper- und Lias-Tone. *Beiträge zur Mineralogie und Petrographie* 11, 91-137, (1965) München.
- Kühn, O., 1962: Autriche. *Lexique Stratigr. Int., Europe* 8, 1—646.
- Madhavaraju, J., González-León, C.M., Lee, I. Y., Armstrong-Altrin, J.S., Reyes-Campero, L.M., 2010. Geochemistry of the Mural Formation (Aptian-Albian) of the Bisbee Group, Northern Sonora, Mexico. *Cretaceous Research*, 31, 400-414.

Mahel', M., 1951. Islandic character of KlippenBelt: Vahicum Contiuation of southern Penninicum in Westcarpathians. Geol. Sbornik, 32/3, 293-305, Bratislava.

McArthur, J.M., Howarth, R.J. & Bailey, T.R., 2001. Strontium isotope stratigraphy: LOWESS Version 3: best fit to the marine Sr-isotope curve for 0-509 Ma and accompanying look-up table for deriving numerical age. Journal of Geology, 109, 155-170.

McLennan, S.M., 1993. Weathering and global denudation. Journal of Geology, 101, 295-303.

McLennan, S. M., Hemming, S., McDaniel, D. K. & Hanson, G. M., 1993. Geochemical approaches to sedimentation, provenance, and tectonics. In: Johnsson, M. J. & Basu, A. (Ed.), Processes Controlling the Composition of Clastic Sediments. Geological Society of America, Special Papers, 284, pp.21-40.

Müller, A., 1987. Zur Lithofazies und Stratigraphie der Kahlenberger Schichten der Flyschzone des Wienerwaldes. Diss. Formal- u. Naturwiss. Fak. Univ. Wien, 195 p., Wien.

Müller, G. & Gastner, M., 1971. The „Karbonat-Bombe“, a simple device for the determination of the carbonate content in sediments, soils and other materials. N. Jb. Mineral., 10: 466-469, Stuttgart.

Nesbitt, H.W. and Young, G.M., 1982. Early Proterozoic climates and plate motions inferred from major element chemistry of lutites. Nature, 299, 715-717.

Neumayr, M., 1886. Erdgeschichte. 1. Auflg. (Leipzig und Wien), 671 S

Nowy, W. & Leithner, W., 1999. Ingenieurgeologische Erkundungsphasen beim Lainzer Tunnel. Mitt. f. Ingineurgeol u. Geomech., 2: 52-61, Wien.

Ožvoldová, L. & Faupl, P., 1993. Radiolarien aus kieseligen Schichtgliedern des Juras der Grestener und Ybbsitzer Klippenzone (Ostalpen, Niederösterreich). Jahrbuch der Geologischen Bundesanstalt, 136: 479-494.

Perch-Nielsen, K., 1985. Mesozoic calcareous nannofossils. - In: Bolli, H.M., Saunders, J.B. & Perch-Nielsen, K. (Eds.): Plankton Stratigraphy, 329-426, (Cambridge Univ. Press) Cambridge.

Pfersmann, C., 2009. Stratigraphie und Sedimentpetrographie der Gesteine der Flyschzone im Lainzer Tunnel. Diplomarb. Formal- u. Naturwiss. Fak. Univ. Wien, 72 S., Wien.

Pfersmann, C., Wagreich, M. 2009. The geology of the western part of the Lainz Tunnel of the Rhenodanubian Flysch Zone in the Wienerwald (Austria): Kahlenberg Formation and Hütteldorf Formation (Cretaceous). Journal of Alpine Geology 51, 59-71.

Piller, W.E., et al., 2004. Die stratigraphische Tabelle von Österreich 2004. – Wien (Komm. F. d. paläont. u. strat. Erforschung Österreichs d. Österr. Akad. D. Wiss. und Österr. Strat. Komm.).

Plašienka, D. & Jurewicz, E., 2006. Tectonic Evolution of the Pieniny Klippen Belt and its Structural Relationships to the External and Central Western Carpathians. Geolines 20, 106-108 (Abstracts CETEG 2006).

Plöchinger, B., 1970. Erläuterungen zur Geologisch – Geotechnischen Karte 1:10000 des Schwechattal - Lindkogel – Gebietes W Baden (Niederösterreich). -58 S., (Geol. B.-A.).

Plöchinger, B. & Salaj, J., 1991. Der Nordrandbereich der Nördlichen Kalkalpen zwischen Kaumberg und Altenmarkt an der Triesting (Niederösterreich) und der Mikrofossilinhalt seines Kreide-Paläogen-Anteils. Jb. Geol. B.-A., 134, 783-808, Wien.

Plöchinger, B. & Prey, S., 1993. Der Wienerwald. Samml. Geol. Führer 59, 1-168, Berlin (Gebr. Bornträger).

Prey, S., 1973. Der südöstlichste Teil der Flyschzone in Wien, ausgehend von der Bohrung Flötzersteig 1. Ver. Geol. Bundesanst., 1973, 67-94.

Prey, S., 1975. Neue Forschungsergebnisse über Bau und Stellung der Klippenzone des Lainzer Tiergartens in Wien (Österreich). Ver. Geol. Bundesanst., 1975, 1-15.

- Prey, S., 1979. Der Bau der Hauptklippenzone und der Kahlenberger Decke im Raume Purkersdorf - Wienerwaldsee (Wienerwald). Verh. Geol. B.-A., 205-228.
- Prey, S., 1985. Betrachtungen über die Klippenhülle im Gelände des Faniteums (Wien, XIII. Bezirk) in der St. Veiter Klippenzone. Jb. Geol. B.-A., 128, 628-629.
- Prey, S., 1987. Probleme am Flysch-Kalkalpenrand mit besonderer Berücksichtigung der Klippenzone von Sulz im Wienerwald. Jb. Geol. B.-A., 129, 621-629.
- Prey, S., 1991. Zur tektonischen Position der Klippe der Antonshöhe bei Mauer - Eine Richtigstellung. Jahrbuch der Geologischen Bundesanstalt, 134, 845-847.
- Rakús, M., 1977. Doplňky k lithostratigrafii a paleogeografii jury a kriedy manínskej série na strednom Považí. In: Geol. Práce, Spr. (Bratislava), 68, 21 – 38.
- Roser, B.P. and Korsch, R.J., 1988. Provenance signatures of sandstone-mudstone suites determined using discriminant function analysis of major-element data. Chemical Geology, 67, 119-139.
- Ruttner, A., & Schnabel, W., 1988. Geologische Karte der Republik Österreich 1:50.000, Blatt 71 Ybbsitz. Wien (GBA).
- Salaj, J., 1990. Geologická stavba bradlovej a pribradlovej zóny stredného Považia a litologická klasifikácia kriedových sedimentov novovymedzených sekvencií. In: Miner. Slov. (Bratislava), 22, 2, 155 – 174.
- Schaffer, F. X., 1904. Geologie von Wien. I. Teil (1904), S. 32; dazu die „Geolog. Karte der k. k. Reichshaupt- und Residenzstadt Wien“ (1:25.000); II. Teil (1906), S. 36 ff., m. Taf. II; III. Teil (1906), S. 82. (Verlag R. Lechner [W. Müller], Wien).
- Schaffer, F. X., 1927. Geologische Geschichte und Bau der Umgebung Wiens. S. 26, 32, 44 bis 45, 55 bis 56. (Verlag F. Deuticke, Leipzig u. Wien.).
- Schmid, S., Fügenschuh, B., Kissling, E. & Schuster, R., 2004. Tectonic map and overall architecture of the Alpine orogene. Swiss Journal of Geosciences, 07, 1, 93-117.
- Schnabel, W., 1970. Zur Geologie des Kalkalpennordrandes in der Umgebung von Waidhofen/Ybbs, NÖ. Mitt. Ges. Geol. Bergbaustud. 19 131-188.
- Schnabel, W., 1979. Geologie der Flyschzone einschließlich der Klippenzonen. In Arbeitstagung der GBA in Lunz a. S., Blatt 71, Ybbsitz 17-42.
- Schnabel, W. (Bearb.), 1997. Geologische Karte der Republik Österreich. Blatt 58 Baden. Geol. Bundesanst.
- Schnabel, W., 2002. Penninikum und Äquivalente. In: Schnabel, W. (Red.): Geologische Karte von Niederösterreich 1:200.000. Legende und kurze Erläuterung. 33-36 (Geol. Bundesanst. Wien).
- Sissingh, W., 1977. Biostratigraphy of Cretaceous calcareous nannoplankton. Geologie en Mijnbouw, 56, 37–56.
- Stur, D., 1894. Geologische Specialkarte der Umgebung von Wien, Blatt IV, Baden und Neulengbach, 1:75.000. (Verlag d. k. k. geol. R.A.) Wien.
- Stur, D., 1894. Erläuterungen zur Geologischen Specialkarte der Umgebung von Wien, S. 40 ff. (Verlag d. k. fc. geol. R.-A.) Wien.
- Taylor, S.R., McLennan, S.M., 1985. The Continental Crust: Its Composition and Evolution. Blackwell, Oxford. 312 pp.
- Tollmann, A., 1977. Geologie von Österreich. Band I: Die Zentralalpen. 766 p., Wien (Franz Deuticke).
- Tollmann, A., 1985. Geologie von Österreich. Band II: Außerzentralalpiner Anteil. 710 p., Wien (Franz Deuticke).

Trauth, F., 1907. Ein neuer Aufschluß im Klippengebiete von Ober-St.-Veit (Wien). Verfc. d. k. k. geol. R.-A., 1907, S. 241 (Wien).

Trauth, F., 1909. Die Grestener Schichten der österreichischen Voralpen und ihre Fauna. Eine stratigraphisch-paläontoologische Studie. Beiträge zur Paläontologie und Geologie Österreich-Ungarns und des Orients, 22: 1-142.

Trauth, F., 1921. Über die Stellung der „pieninischen Klippenzone“ und die Entwicklung des Jura in den niederösterreichischen Voralpen. Mitteilungen der Geologischen Gesellschaft in Wien, 14: 105-265.

Trauth, F., 1923. Über eine Doggerfauna aus dem Lainzer Tiergarten bei Wien. Ann. Naturhist. Mus Wien, 36: 183.

Trauth, F., 1930. Geologie der Klippenregion von Ober-St.Veit und des Lainzer Tiergartens. Mitteilungen der Geologischen Gesellschaft in Wien, 21 (1928), 35-132.

Trauth, F., 1950. Die fazielle Ausbildung und Gliederung des Oberjura in den nördlichen Ostalpen. Verhandlungen der Geologischen Bundesanstalt, 1948, 145-218.

Trauth, F., 1954. Zur Geologie des Voralpengebietes zwischen Waidhofen a. d. Ybbs und Steinmühl. Verhandlungen der Geologischen Bundesanstalt, 1954, 89-140, Wien.

Trautwein, B., Dunkel, J., Kuhlemann, J. & Frisch, W., 2001. Geodynamic evolution of the Rhenodanubian Flysch Zone – evidence from apatite and circon fissiontrack geochronology and morphology studies on circon. In Piller & Rasser [Eds.] Paleogene of the Eastern Alps, Österr. Akad. Wissen., Schriftenr. Erdwiss. Komm., 14, 111-128, Wien.

Uhlig, V., 1890. Ergebnisse geologischer Aufnahmen in den westgalizischen Karpathen. II. Teil: Der pieninische Klippenzug. Jb. k. k. geol. R.-A., 40, p. 814.

Wagreich, M., 2007. Rosental: Kleingärten in der Tiefsee. In: Hofmann, T. (ed.): Wien, Niederösterreich, Burgenland. Wanderungen in die Erdgeschichte, 22, 38-39 (Verlag Dr. Friedrich Pfeil, München).

Wagreich, M., 2008. Lithostratigraphic definition and depositional model of the Hüttdorf Formation (Upper Albian - Turonian, Rhenodanubian Flysch Zone, Austria). Austrian Journal of Earth Sciences, 101, 70-80.

Wessely, G., 1967. Ein Fossilpunkt im Lias von Groisbach(NÖ) und seine Geologische Stellung. Verh. Geol. B. A. 1967, 1/2, 37-50, Wien.

Wessely, G., 1974. Rand und Untergrund des Wiener Beckens – Verbindungen und Vergleiche. Mitteilungen der Geologischen Gesellschaft in Wien, 66-67, 265-287.

Wessely, G., 1982. Bericht 1981 über geologische Aufnahmen auf Blatt 58 Baden. In Verh. Geol. B.-A., 1982, Heft 1, 38-40.

Wessely, G., 2006. Geologie der österreichischen Bundesländer: Niederösterreich. 1-416, (Geol. B.-A.) Wien.

Wessely, G., 2008. Kalkalpine Schichtfolgen und Strukturen im Wienerwald. Journal of Alpine Geology, 49, pp.201-214.

Widder, R.W., 1988. Zur Stratigraphie, Fazies und Tektonik der Grestener Klippenzone zwischen Maria Neustift und Pechgraben/O.Ö. Mitt. Ges Geol. Bergbaustud. Österr., 34/35 79-133.

Woletz, G., 1967a. Schwermineralvergesellschaftungen aus ostalpinen Sedimentationsbecken der Kreidezeit. Geol. Rundsch., Stuttgart, 56, pp.308-320.

Woletz, G., 1967b. Schwermineralanalysen von Kreidesandsteinen aus den westlichen Karpaten (Bericht 1966). Verh. Geol. B.-A., 1967, 65.

Yan, D., Chen, D., Wang, Q. and Wang, J., 2010. Large-scale climatic fluctuations in the latest Ordovician on the Yangtze block, south China. Geology, 38, 599-602.

## List of Figures

Fig. 1 Geological site map of the Lainz Tunnel (section LT33+LT31) (sketch based on geological map sheet 58 Baden, Schnabel, 1997).....	10
Fig. 2 Topographic map showing the different sample sites in Austria and Slovakia. The location numbers are explained in the table below (adapted from Google maps).....	11
Fig. 3 Table with the sample sites and GPS data. ....	11
Fig. 4 LT33:2522.1m The author (on the left side) investigating rocks of the St.Veit Klippenzone. ....	14
Fig. 5 LT33/2505.20m The author taking samples of the St.Veit Klippenzone. ....	15
Fig. 6 LT33/2558.50m Tunnel face (SVK) beeing secured and covered with concrete .....	15
Fig. 7 Picture of workmen and engineers at LT31/1385.00 (last station of LT31). ....	15
Fig. 8 Composite stratigraphic succession of St. Veit Klippenzone and related klippen successions in the Wienerwald area according to Janoschek et al. (1956), Prey (1975, 1979, 1991), Tollmann (1985) and Schnabel (2002).....	20
Fig.9 Bedding planes in Schmidt' net segmented for tunnel section intervals (LT33/station 1000 to 2780m and LT31/station 799 to1385m ). ....	27
Fig. 10 Tunnel section with indications of mean dip of strata observed.....	27
Fig. 11 Simplified and adapted „Tunnelband” from the Lainz Tunnel (LT33 + LT31), showing a vertical and a horizontal profile with formations assigned. Between station 1300 to 1200m (LT31) (Keuper sandstone) the center of the anticlinal structure can be found. The original „Tunnelband” was generated and provided by office Bechthold. Different colour impressions comparing LT33 and LT31 are caused by different mapping styles of the geologists.....	28
Fig. 12 Sketch of the tunnel face at LT31/1197.5m showing an example of „block in matrix” structure. In this case the blocks can be expected to be of Jurassic age and the matrix is most probably of Flysch material ( sketch provided by office Bechthold).....	29
Fig. 13 Composite stratigraphic log from the Lainz tunnel (no scale).....	31
Fig. 14 Legend of lithologies for Fig. 13, Fig. 15.....	31
Fig. 15 Strongly simplified section from the Lainz tunnel (lithologies see Fig. 14). .....	32
Fig. 16 Results of nannofossil analysis LT33, from 1000 - 2593m, (only samples with nannofossil markers included), zonal marker species indicated grey (Preservation: vp - very poor; p – poor; m – medium; abundance in nannofossils per field(s) of view). Nannofossil standard zonation by Perch-Nielsen (1985: CC zones).....	34

Fig. 17 Results of nannofossil analysis LT31, from 841.5 - 1039m (only samples with nannofossil markers included). For legend and abbreviations see Fig. 16.....	35
Fig. 18 Tunnel face at LT33/2576m, lithologies from the Hütteldorf Formation (red shales) are tectonically mixed with rocks from the St.Veit Klippenzone (brownish radiolarite and grey limestones).....	36
Fig. 19 Sketch from the tunnel face at LT33/2576m showing fault zones. The different lithologies are classified according to their rheology (provided by office Bechthold).....	37
Fig. 20 Red marlstone from LT33/2576m. ....	37
Fig. 21 Thin-section from LT33/2576m, red marlstone with foraminifera <i>Marginotruncana</i> spp. Lower/ Upper Cretaceous.....	37
Fig. 22 Tunnel face at LT33/1873.40m, the block of dolomite breccia is visible at the right bottom.....	38
Fig. 23 Partial view of the right bottom tunnel face at LT33/1873.40m showing a block of dolomite breccia. Bottomline of the picture measures approx. 60cm.....	39
Fig. 24 Thin-section of the dolomite breccia at LT33/1874m texture: non-planar crystals in a xenotopic mosaic (XPL). .....	39
Fig. 25 Dolomite breccia at LT33/1874m. ....	39
Fig. 26 Tunnel face at LT33/1861.4m, general view with the embedded block of strongly altered basalt in red shales of the Hütteldorf Formation.....	40
Fig. 27 Partial view of the left tunnel face at LT33/1861.4m showing a block of strongly altered basalt. The picture depicts approximately 3m of tunnel face.....	40
Fig. 28 Strongly altered basalt: LT33/1861.4m. ....	40
Fig. 29 Strongly altered basalt: LT33/1861.4m (LPL), pseudomorphosis of strongly altered feldspar-, pyroxene-, amphibole- and olivine phenocrysts in a chloritized matrix. Voids are filled partly with calcite. ....	41
Fig. 30 Tunnel face at LT33/1850.4m, several small (max.40cm diameter) dark red blocks of strongly altered volcanicite were found in a red brown shale matrix at the left bottom.....	41
Fig. 31 Strongly altered volcanic rock: LT33/1850m.....	42
Fig. 32 Thin section strongly altered volcanic rock: LT33/1850m (LPL), calcite filled voids together with some relicts of strongly altered feldspar.....	42
Fig. 33 LT31/1215.50m, light grey, hard sandstone (Keuper) together with red shale (Keuper). ....	44
Fig. 34 31/1277.20m, sandstone (Keuper). ....	45
Fig. 35 Sandstone/arkose (Keuper) LT31/1277.2 m. ....	45

Fig. 36 Thin section of arkose sandstone (Keuper), LT31/1277m, containing quartz, feldspar, kaolinite, lithic rock fragments (consisting of quartzite) (XPL).....	45
Fig. 37 Sandstone from the SVK (LT33/1893.4m) although a different colour (pale green), mineralogy and heavy mineral assemblage indicate Keuper sandstone. ....	45
Fig. 38 Sandstone from the SVK (LT33/1900m) the colour (pale green), mineralogy and heavy mineral assemblage indicate also Keuper sandstone.....	45
Fig. 39 Green/red shale/mud from LT31/1277.2m found in direct contact with the Keuper sandstones. .....	46
Fig. 40 Grey /red shale/ mud from LT31/1381.2m found next to the Keuper sandstones.....	46
Fig. 41 Red shale/ mud from LT31/1200m found in direct contact with the Keuper sandstones. ....	46
Fig. 42 Dolomite (Keuper)LT31/1277.2m. ....	47
Fig. 43 Thin section of dolomite (Keuper): LT31/1277.2m (XPL) totally recrystallized, with a nonplanar, equigranular sutured mosaic crystallisation texture. The calcite vein in the left bottom shows several generations (colored with Alicarin S; calcite = red, calcite + Fe = magenta, dolomite = colourless, Fe-rich ankerite =light blue, pores = intense blue). ....	47
Fig. 44 Results of nannofossil analysis of presumably Jurassic samples of LT31 and LT33. For legend and abbreviations see Fig. 16.....	49
Fig. 45 Sandstone/siltstones (Lower/Middle Jurassic) at LT33/2666m.....	49
Fig. 46 Sandstone/siltstone of Lower/Middle Jurassic age LT33/2666m which yielded a probably Early/Middle Jurassic age, according to nannofossils.....	50
Fig. 47 Thin-section of sandstone/siltstone, Lower/Middle Jurassic LT33/2666m which yielded a probably Early/Middle Jurassic age, according to nannofossils, consisting of quartz, mica, biotite, feldspar and some coal in a bioturbated grey shale/silt matrix.(XPL). ....	50
Fig. 48 Marlstones of probably Early/Middle Jurassic age at LT31/1366.9m according to nannofossils.....	50
Fig. 49 Sketch from LT31/1366.9m showing a typical „Block-in-matrix” structure, according to nannofossils probably Early/Middle Jurassic age (provided by office Bechthold). ....	50
Fig. 50 Sample from LT31/1366.9m which yielded a probably Early/Middle Jurassic age, according to nannofossils.....	50
Fig. 51 (calcareous) marlstones of probably Early/Middle Jurassic age at LT33/2730m according to nannofossils.....	50

Fig. 52 Sketch from LT33/2730m showing the tectonic mixing of different Jurassic rocks (provided by office Bechthold).....	51
Fig. 53 Sample from LT33/2730m which yielded of probably Early/Middle Jurassic age, according to nannofossils.....	51
Fig. 54 Fragments of ammonites were found at LT31/1200m in a „Block-in-matrix” situation. Because of stability problems the tunnel face was only opened in small sections.....	51
Fig. 55 Fragments of ammonites (Arnioceras: Sinemurian) were found at LT31/1160m in a „Block-in-matrix”situation, together with calcareous mudstones. ....	51
Fig. 56 Sketch from LT31/1201.5m typical „Block-in-matrix” situation, fragments of ammonites indicate probably Sinemurian age (provided by office Bechthold).....	51
Fig. 57 Sample LT31/1200m: sandy calcareous marlstone with endocast of an ammonite....	51
Fig. 58 Sample LT31/1160m: sandy calcareous marlstone with ammonite (Arnioceras: Sinemurian).....	52
Fig. 59 Thin-section of sample LT31/1200m (Sinemurian) biomicritic packstone / calcareous marlstone (66% CaCO <sub>3</sub> ) containing radiolaria, spiculae, filaments (planktonic bivalvae), crinoids and some coal particles in a micritic matrix (LPL).....	52
Fig. 60 Tunnel face at 1188/LT31m where a nautiloid (probably Sinemurian) was found. ....	52
Fig. 61 Sketch from LT31/1188.5m with typical „Block-in-matrix” situation, were the nautiloid (probably Sinemurian) was found (sketch provided by office Bechthold).....	52
Fig. 62 Nautiloid from LT31/1188.5m (probably Sinemurian age), cut and polished. Partly pyritized in the center.....	52
Fig. 63 Tunnel face at LT33/2401m klippen rocks of probably Early/Middle Jurassic age....	52
Fig. 64 Samples from LT33/2401m klippen rocks of probably Lower/Middle Jurassic age... Fig. 65 Thin-section 33/2401m: pelletal grainstone / argillaceous limestone (CaCO <sub>3</sub> =85%), the foraminifera in the red circle is a shallow water species (maybe <i>Gypsina moussavian</i> ) (LPL).....	53
Fig. 66 Calcareous mudstone (lower - middle Bajocian) Rescue pit Veitingergasse 0-2m....	53
Fig. 67 Rescue pit Veitingergasse calcareous mudstone with an aptychus (lower - middle Bajocian) sample no. RSVG1m.....	54
Fig. 68 Thin-section from rescue pit Veitingergasse: calcareous/biomicritic packstone (lower - middle Bajocian) with filaments and crinoidal debris. Sample RSVG 0/1m containing aptychi (XPL).....	54
Fig. 69 Rescue shaft Veitingergasse: outcrop of red cherts and shales station 1-2m (picture bottom aprox. 2m).....	55

Fig. 70 Chert (early - middle Bajocian) Rescue pit Veitingergassegasse 1m.....	55
Fig. 71 Rescue pit Veitingergasse:thin-section of a chert (early - middle Bajocian) sample RSVG 1m with some radiolaria. The calcite veins show different generations (XPL) .....	55
Fig. 72 Tunnel face at 2165.5m/LT33 with a chert/radiolarite block in the uppermost right part of the picture.....	56
Fig. 73 Chert (Valanginian) found at LT33/2165m.....	56
Fig. 74 Chert from LT31/898m.....	57
Fig. 75 LT31/1364.3m: Chert nodule in siliceous limestone (Lower Cretaceous, Middle and Upper Berriasian).....	57
Fig. 76 Tunnel face with marlstone to argillaceous limestone (Tithonian-Berriasian/Valanginian) LT33/2333m.....	58
Fig. 77 Tunnel face with marlstone to argillaceous limestone (Tithonian-Berriasian/Valanginian) LT33/2552m.....	59
Fig. 78 Argillaceous limestone with Tithonian-Berriasian/Valanginian ammonite ( <i>Protancyloceras</i> sp) LT33/2333m.....	59
Fig. 79 Marlstone to argillaceous limestone showing bioturbation (Tithonian-Berriasian/Valanginian) LT33/2552m.....	59
Fig. 80 Thin-section LT33/2333: marlstone to argillaceous limestone/bioclastic packstone showing filaments (Tithonian-Berriasian/ Valanginian) (LPL).....	59
Fig. 81 Thin-section LT33/2552m: marlstone to argillaceous limestone (Tithonian-Berriasian/ Valanginian): bioclastic packstone showing bioclasts (filaments) and a big crinoid stem (XPL). .....	59
Fig. 82 Original/mould close up of the Tithonian-Berriasian/Valanginian ammonite ( <i>Protancyloceras</i> sp.) LT33/2333m.....	60
Fig. 83 Argillaceous limestone with unidentified ammonite fragment LT33/2320.6m.....	61
Fig. 84 Rescue pit Angermayergasse 241m=LT33/2280m; marlstone with belemnite.....	61
Fig. 85 Rescue pit Angermayergasse 241m=LT33/2280m, marlstone with pectinid.....	61
Fig. 86 Tunnel face at LT33 2165.5m: the sample discussed in this chapter below derived from the marlbody in the upper right area.....	61
Fig. 87: Different samples archived from LT33/2165.5m, at the bottom of the picture lies a argillaceous limestone. The sample is still partly covered with some sheared mudstones.....	61

Fig. 88 Thin section LT33/2165m: argillaceous limestone with <i>Trocholina</i> spp. (~Upper Triassic - Upper Cretaceous) right in the middle of the picture (LPL) (colored with Alicarin S).....	62
Fig. 89 Thin section LT33/2165m: argillaceous limestone with <i>Textularia</i> spp right in the middle of the picture (LPL) (colored with Alicarin S). ....	62
Fig. 90 Tunnel face at LT31/975.5m below red and grey mudstone a bigger block of marlstone was encountered. ....	62
Fig. 91 marlstone from LT31/975.5m - reflections are caused by calcite crystals on the surface.....	62
Fig. 92 Thin section LT31/975m: sandy marlstone with Upper Jurassic- Lower Cretaceous - small sized planktonic foraminifera species (LPL)(colored with Alicarin S). ....	62
Fig. 93 Tunnel face at LT33/2552.0m, blocks of siliceous limestone were embedded in the grey shale/marl matrix on the right side.....	63
Fig. 94 Light grey blocks of siliceous limestone (Middle and Upper Berriasian) at LT31/869m. ....	63
Fig. 95 Siliceous limestone (Middle and Upper Berriasian) LT33/2552m.....	64
Fig. 96 Thin-section: Siliceous biomicritic limestone (Middle and Upper Berriasian) LT31/860m containing calpionellids (XPL). ....	64
Fig. 97 Thin section photographs of calpionellids (see text above for identification). 1-2. <i>Colomisphaera carpathica</i> (Borza) 3. <i>Calpionellopsis oblonga</i> (Cadisch) 4-5. <i>Tintinnopsella carpathica</i> (Murgeanu et Filipescu) 6. <i>Remaniella filipescui</i> Pop All pictures thin section of sample LT31/869.5 (plate 1 was made by A. Lukeneder and D. Rehakova). ....	65
Fig. 98 Thin section photographs of calpionellids: <i>Calpionella elliptica</i> Cadisch, <i>Remaniella cadischiana</i> (Colom) <i>Tintinnopsella carpathica</i> (Murgeanu et Filipescu) 1 - 3 thin section sample LT31/869.5 (plate 2 was made by A. Lukeneder and D. Rehakova). ....	66
Fig. 99 Thin section photograph of calpionellids: Slightly bioturbated and silicified biomicrite limestone (mudstone to wackestone). It contains predominantly sponges, less radiolarians and rarely calpionellid loricas. Thin section LT31/869.5m. (picture was made by A. Lukeneder and D. Rehakova). ....	66
Fig. 100 Heavy mineral analysis of the samples of the Lainz Tunnel, table on the right side shows calculated heavy mineral contents without baryte. Samples arranged according to tunnel section meter (LT33/LT31).....	67

Fig. 101 Kahlenberg Formation sandstones: counts of heavy minerals found in the samples and total numbers of heavy minerals counted per sample.....	68
Fig. 102 Kahlenberg Formation sandstones: mean percentage of heavy minerals, without baryte.....	68
Fig. 103 Hütteldorf Formation sandstones: counts of heavy minerals found in the samples and total numbers of heavy minerals counted per sample.....	69
Fig. 104 Hütteldorf Formation sandstones: mean percentage of heavy minerals, without baryte.....	69
Fig. 105 Jurassic sandstones: counts of heavy minerals found in the samples and total numbers of heavy minerals counted per sample.....	70
Fig. 106 Jurassic sandstones: mean percentage of heavy minerals, without baryte.....	70
Fig. 107 Keuper sandstones: counts of heavy minerals found in the samples and total numbers of heavy minerals counted per sample.....	71
Fig. 108 Keuper sandstones: mean percentage of heavy minerals, without baryte.....	71
Fig. 109 Keuper sandstones: counts of heavy minerals found in the samples and total numbers of heavy minerals counted per sample.....	72
Fig. 110 Keuper sandstones: mean percentage and total numbers of heavy minerals,without baryte.....	72
Fig. 111 Carbonate contents of different lithologies found in the St.Veit Klippenzone.....	74
Fig. 112 Maximum carbonate contents in the Lainz Tunnel plotted along section.....	74
Fig. 113 Lists of samples used for XRD analysis and results.....	76
Fig. 114 LT33/2552 The figure shows the result (XRD) of one sample considered to be a typical Jurassic sandstone from the St.Veit Klippenzone with significant amounts of calcite, quartz, dolomite, feldspar, chlorite and mica. ....	76
Fig. 115 LT31/1277m XRD analysis (+ 2 $\mu$ fraction) of one sample considered to be a typical Keuper sandstone containing quartz, feldspar, chlorite, kaolinite mica and a regular interstratified (illit/smectite) mixed layer mineral (top diagram: green graph = tempered at +550C°, red graph = treated with ethylenglycol, blue graph = no treatment; bottom diagram: red graph = treated with K + ethylenglycol, green graph = treated with K, blue graph = treated with Mg + glycerine, purple graph = treated with Mg). ....	77
Fig. 116 Different geochemical approaches to classify clastic provenance and tectonic setting. ....	79
Fig. 117 Samples of Keuper sandstones and Gresten quartzites.....	81
Fig. 118 Screeplot Keuper sandstones and Gresten quartzites: Importance of the factors. ....	82

Fig. 119 Factor vs. factor plots of the Keuper and Gresten sandstones.....	82
Fig. 120 Cr vs TiO <sub>2</sub> plot of the Keuper and Gresten sandstones.....	84
Fig. 121 TiO <sub>2</sub> vs V plot of the Keuper and Gresten sandstones.....	84
Fig. 122 Th/U vs Th plot of the Keuper and Gresten sandstones (adapted after Mc Lennan et al., 1993). .....	84
Fig. 123 100xFe <sub>2</sub> O <sub>3</sub> /SiO <sub>2</sub> vs 100xAl <sub>2</sub> O <sub>3</sub> /SiO <sub>2</sub> plot of the Keuper and Gresten sandstones (adapted after Bhatia, 1983).....	84
Fig. 124 Al <sub>2</sub> O <sub>3</sub> /SiO <sub>2</sub> vs Fe <sub>2</sub> O <sub>3</sub> +MgO plot of the Keuper and Gresten sandstones (adapted after Bhatia, 1983).....	85
Fig. 125 K <sub>2</sub> O/Na <sub>2</sub> O vs SiO <sub>2</sub> plot of the Keuper and Gresten sandstones (adapted after Bhatia, 1983). .....	85
Fig. 126 SiO <sub>2</sub> vs (Al <sub>2</sub> O <sub>3</sub> +K <sub>2</sub> O+Na <sub>2</sub> O) plot of the Keuper and Gresten sandstones (adapted after Bhatia, 1983). .....	85
Fig. 127 TiO <sub>2</sub> vs (Fe <sub>2</sub> O <sub>3</sub> +MgO) plot of the Keuper and Gresten sandstones (adapted after Bhatia, 1983). .....	85
Fig. 128 Th, Ce, La and Sc vs (SiO <sub>2</sub> +Al <sub>2</sub> O <sub>3</sub> +Fe <sub>2</sub> O <sub>3</sub> +MgO+Na <sub>2</sub> O+TiO <sub>2</sub> ) plots of the Keuper and Gresten sandstones (adapted after Madhavavaju, 2010).....	86
Fig. 129 V/Zr vs Zr/Ni, Zr/Al <sub>2</sub> O <sub>3</sub> , Ti/Zr plots of the Keuper and Gresten sandstones (adapted after Schnabel and Adamova, 1999).....	87
Fig. 130 REE plot from St.Veit Klippenzone and Groisbach Keuper sandstones.....	88
Fig. 131 REE plot from Gresten Klippenzone sandstones.....	88
Fig. 132 REE plot from Drietoma Unit Keuper sandstones.....	89
Fig. 133 CIA vs CPA plot from Keuper and Gresten sandstones.....	89
Fig. 134 CIA plot from Keuper and Gresten sandstones. ....	89
Fig. 135 Jurassic sandstones from different sample sites.....	90
Fig. 136 Screeplot of Jurassic sandstones and Keuper sandstones: Importance of the factors.	91
Fig. 137 Factor vs factor plots of the Keuper and Jurassic sandstones.....	92
Fig. 138 100xFe <sub>2</sub> O <sub>3</sub> /SiO <sub>2</sub> vs 100xAl <sub>2</sub> O <sub>3</sub> /SiO <sub>2</sub> plot of Jurassic and Keuper sandstones (adapted after Bhatia, 1983). .....	93
Fig. 139 Al <sub>2</sub> O <sub>3</sub> /SiO <sub>2</sub> vs Fe <sub>2</sub> O <sub>3</sub> /MgO plot of Jurassic and Keuper sandstones (adapted after Bhatia, 1983).....	93
Fig. 140 TiO <sub>2</sub> vs (Fe <sub>2</sub> O <sub>3</sub> +MgO) plot of Jurassic and Keuper sandstones (adapted after Bhatia, 1983). .....	93
Fig. 141 Th vs La plot of Jurassic and Keuper sandstones. ....	93

Fig. 142 Th vs Sc plot of Jurassic and Keuper sandstones. ....	94
Fig. 143 Th/U vs Th plot of Jurassic and Keuper sandstones (adapted after Mc Lennan et al., 1993). ....	94
Fig. 144 REE plot of Jurassic sandstones from the St.Veit Klippenzone, Groisbach, Drietoma Unit and Manín Unit. ....	94
Fig. 145 CIA vs CPA plot from Keuper and Jurassic sandstones. ....	95
Fig. 146 CIA plot from Keuper and Jurassic sandstones. ....	95
Fig. 147 Samples of Keuper shales. ....	97
Fig. 148 Jurassic shales from the Lainz Tunnel and Drietoma Unit. ....	98
Fig. 149 Screeplot Keuper shales and Jurassic shales: Importance of the factors. ....	98
Fig. 150 Factor vs factor plots of the Keuper and Jurassic shales. ....	99
Fig. 151 K <sub>2</sub> O/Na <sub>2</sub> O vs SiO <sub>2</sub> plot of Keuper and Jurassic shales (adapted after Bhatia, 1983). ....	100
Fig. 152 SiO <sub>2</sub> /Al <sub>2</sub> O <sub>3</sub> vs K <sub>2</sub> O/Na <sub>2</sub> O plot of Keuper and Jurassic shales (adapted after Bhatia, 1983). ....	100
Fig. 153 Th/U vs Th plot of Keuper and Jurassic shales (adapted after Mc Lennan et al., 1993). ....	100
Fig. 154 REE plot of Keuper shales from the St.Veit Klippenzone and Drietoma Unit.....	101
Fig. 155 REE plot of Jurassic shales from the St.Veit Klippenzone and Drietoma Unit.....	101
Fig. 156 CIA vs CPA plot from Keuper shales and Jurassic shales.....	102
Fig. 157 CIA plot from Keuper shales and Jurassic shales.....	102
Fig. 158 Jurassic carbonates from the Lainz Tunnel and comparison units. ....	105
Fig. 159 Screeplot of Jurassic carbonates: Importance of the factors. ....	106
Fig. 160 Factor vs. factor plots of the Jurassic carbonates.....	107
Fig. 161 Pearson Correlation values „r“ of selected characteristics. ....	108
Fig. 162 Th-Sc-La plot of the Jurassic carbonates (adapted after Taylor and Mc Lennan, 1985). ....	109
Fig. 163 Th/U vs Th plot of the Jurassic carbonates (adapted after Mc Lennan et al., 1993). ....	109
Fig. 164 Ce, La, Sc and Th vs (SiO <sub>2</sub> +Al <sub>2</sub> O <sub>3</sub> +Fe <sub>2</sub> O <sub>3</sub> +MgO+Na <sub>2</sub> O+TiO <sub>2</sub> ) plots of the Jurassic carbonates (adapted after Madhavavaju, 2010). ....	109
Fig. 165 V/Zr vs Zr/Ni,Ti/Zr and Zr/Al <sub>2</sub> O <sub>3</sub> plots of the Jurassic carbonates (adapted after Schnabel and Adamova, 1999). ....	110
Fig. 166 REE plot of Jurassic carbonates from the St.Veit Klippenzone. ....	111

Fig. 167 REE plot of Jurassic carbonates from Groisbach.....	111
Fig. 168 REE plot of Jurassic carbonates from the Drietoma Unit.....	112
Fig. 169 REE plot of Jurassic carbonates from the PKB .....	112
Fig. 170 REE plot of Jurassic carbonates from the Gresten and Ybbsitz Klippenzone.....	112
Fig. 171 CIA vs CPA plot from Jurassic carbonates.....	113
Fig. 172 CIA plot from Jurassic carbonates.....	113
Fig. 173 Jurassic cherts from the Lainz Tunnel and comparison units.....	116
Fig. 174 Screeplot of Jurassic cherts: Importance of the factors.....	116
Fig. 175 Factor vs.factor plots of the Jurassic cherts .....	117
Fig. 176 St Veit Klippenzone: selected correlations of elements used in the plots below.....	118
Fig. 177 Ybbsitz Klippenzone: selected correlations of elements used in the plots below ..	118
Fig. 178 Drietoma Unit: selected correlations of elements used in the plots below .....	118
Fig. 179 Cu vs Ni plot of Jurassic cherts.....	119
Fig. 180 Cu vs Zn plot of Jurassic cherts.....	119
Fig. 181 TiO <sub>2</sub> vs MnO plot of Jurassic cherts.....	119
Fig. 182 TiO <sub>2</sub> vs Fe <sub>2</sub> O <sub>3</sub> plot of Jurassic cherts.....	119
Fig. 183 SiO <sub>2</sub> vs (Al <sub>2</sub> O <sub>3</sub> +K <sub>2</sub> O+Na <sub>2</sub> O) plot of Jurassic cherts (adapted after Bhatia, 1983)..	119
Fig. 184 La, Sc, Ce and Th vs (Al <sub>2</sub> O <sub>3</sub> +K <sub>2</sub> O+Na <sub>2</sub> O) plots of Jurassic cherts (adapted after Madhavavaju, 2010). .....	120
Fig. 185 REE plot from the St.Veit Klippenzone and Gutenbachtal. ....	121
Fig. 186 REE plot from Drietoma Unit and Krížna Nappe.....	121
Fig. 187 REE plot from Ybbsitz Klippenzone and Kysuca Unit (PKB).....	122
Fig. 188 CIA vs CPA plot from Jurassic cherts. ....	122
Fig. 189 CIA plot from Jurassic cherts. ....	122
Fig. 190 Siliceous <i>Calpionella</i> limestones from the Lainz Tunnel and comparison units.....	123
Fig. 191 Screeplot of siliceous <i>Calpionella</i> limestones: Importance of the factors.....	123
Fig. 192 Factor vs.factor plots of the siliceous <i>Calpionella</i> limestones. ....	124
Fig. 193 REE plot from siliceous <i>Calpionella</i> limestonesfrom the St.Veit Klippenzone.....	125
Fig. 194 REE plot from siliceous <i>Calpionella</i> limestonesfrom the Drietoma Unit and Krížna Nappe. ....	125
Fig. 195 REE plot from siliceous limestones from the Kysuca unit (PKB).....	125
Fig. 196 REE plot from Siliceous limestones from the Gresten Klippenzone.....	126
Fig. 197 CIA vs CPA plot from siliceous <i>Calpionella</i> limestones. ....	126
Fig. 198 CIA plot from siliceous <i>Calpionella</i> limestones.....	126

Fig. 199 Table of samples used for $^{87}\text{Sr}/^{86}\text{Sr}$ -isotopes from the Lainz Tunnel and Lainzer Tiergarten.....	128
Fig. 200: $^{87}\text{Sr}/^{86}\text{Sr}$ results of the Lainz Tunnel and the Lainzer Tiergarten plotted into the Sr-curve of McArthur et al. (2001).....	129
Fig. 201 Stable isotope measurements of the Lainz Tunnel.....	130
Fig. 202 Plot of carbon vs. oxygen isotope ratios (red = Hütteldorf Formation, yellow = Kahlenberg Formation/Hütteldorf Formation, green = L/M-Jurassic carbonates LT33, blue = L/M-Jurassic carbonates LT31).....	131
Fig. 203 Plot of carbon isotope values against Jurassic seawater values of Jenkyns et al. (2002) (green bracket indicates range of values measured).....	131
Fig. 204 Schematic N-S section through the Eastern Alps in Late Jurassic time (based on Faupl & Wagreich, 2000) and possible positions of the St. Veit Klippenzone (1-4). ....	135
Fig. 205 Map of the western part of the Western Carpathians indicating the Drietoma unit (light blue) at the southern margin of the Pieniny Klippen Belt (PKB), north of equivalents to the Northern Calcareous Alps (NCA Triassic + Brezova Gosau Group); taken from Hók et al. (2009).....	139
Fig. 206 NW-SE-Section of the western part of the Western Carpathians indicating the Drietoma unit (Dr) at the southern margin of the Pieniny Klippen Belt (PKB: Cz, Ky) and other „Periklippen“ units of Tatic/Fatric attribution (Klape = Kl; Manín = Ma; Krížna = Kr), Choč Nappe = Ch = equivalent to the Northern Calcareous Alps (Go = Brezova Gosau Group); taken from Plašienka & Jurewicz (2006).....	140
Fig. 207 Schematic N-S section through the Eastern Alps in Late Jurassic time (based on Faupl & Wagreich, 2000) and inferred Lower Austroalpine/marginal Austroalpine plate position of the St. Veit Klippenzone at the northern margin of the Austroalpine. ....	140









Method		1DX	1DX
Analyte		TI	Se
Unit		ppm	ppm
MDL		0.1	0.5
LT33 2451 KM	Rock Pulp	0.1	<0.5
LT33 2552 HST	Rock Pulp	0.3	<0.5
LT33 2552 SST	Rock Pulp	<0.1	<0.5
LT33 2576 TST	Rock Pulp	<0.1	<0.5
LT33 2592 TST	Rock Pulp	<0.1	<0.5
LT33 2592 KM	Rock Pulp	<0.1	<0.5
LT33 2713 TST	Rock Pulp	<0.1	1.3
LT33 2748 M	Rock Pulp	<0.1	<0.5
LT33 2775 HST	Rock Pulp	<0.1	<0.5
LT33 2775 KM	Rock Pulp	<0.1	<0.5
LT31 1219.5 SST	Rock Pulp	<0.1	<0.5
LT31 1277 TST	Rock Pulp	0.1	<0.5
LT31 1277 SST	Rock Pulp	<0.1	<0.5
LT31 1308 KM	Rock Pulp	<0.1	<0.5
LT31 1326 TST	Rock Pulp	<0.1	1.1
LT31 1326 HM	Rock Pulp	0.1	0.8
LT31 1364 HST	Rock Pulp	<0.1	<0.5
LT31 1366 TST	Rock Pulp	<0.1	<0.5
LT31 1366 M	Rock Pulp	<0.1	<0.5
LT31 1365 SST	Rock Pulp	<0.1	<0.5

#### Appendix 4 Quality report of the geochemical analysis (LT33/LT31) – comparisons with standards.

Method	4A-4B	4A-4B	4A-4B	4A-4B	4A-4B	4A-4B	4A-4B	4A-4B	4A-4B	4A-4B	4A-4B	4A-4B	4A-4B	4A-4B	4A-4B	4A-4B	4A-4B	4A-4B	4A-4B	4A-4B	4A-4B	4A-4B
Analyte	SiO <sub>2</sub>	Al <sub>2</sub> O <sub>3</sub>	Fe <sub>2</sub> O <sub>3</sub>	MgO	CaO	Na <sub>2</sub> O	K <sub>2</sub> O	TiO <sub>2</sub>	P <sub>2</sub> O <sub>5</sub>	MnO	Cr <sub>2</sub> O <sub>3</sub>	Ni	Sc	LOI	Sum	Ba	Be	Co	Cs	Ga		
Unit	%	%	%	%	%	%	%	%	%	%	%	ppm	ppm	%	ppm							
MDL	0.01	0.01	0.04	0.01	0.01	0.01	0.01	0.01	0.01	0.01	0.002	20	1	-5.1	0.01	1	1	0.2	0.1	0.5		
LT31 1366 M	Rock Pulp	23.00	7.71	2.42	1.61	32.92	0.48	1.63	0.30	0.09	0.52	0.006	26	7	29.2	99.88	91	2	11.0	3.6	9.9	
Pulp Duplicates																						
LT33 2748 M	Rock Pulp	15.11	1.84	1.04	0.98	44.31	0.18	0.40	0.08	0.03	0.05	0.003	<20	2	35.9	99.91	24	<1	2.0	1.2	1.7	
REP LT33 2748 M	QC																					
Reference Materials																						
STD CSC	Standard																					
STD DS7	Standard																					
STD DS7	Standard																					
STD OREAS76A	Standard																					
STD SO-18	Standard	58.10	14.12	7.61	3.33	6.37	3.68	2.15	0.69	0.83	0.39	0.548	43	24	1.9	99.71	505	1	26.9	7.0	17.2	
STD SO-18	Standard	58.10	14.13	7.60	3.33	6.37	3.68	2.15	0.69	0.82	0.39	0.548	42	24	1.9	99.73	499	1	26.8	7.0	17.4	
STD SO-18	Standard	57.97	14.18	7.63	3.35	6.39	3.69	2.16	0.69	0.83	0.39	0.549	45	24	1.9	99.74	500	<1	27.0	7.0	17.1	
STD SO-18	Standard	57.93	14.19	7.65	3.35	6.40	3.70	2.16	0.69	0.83	0.39	0.550	44	24	1.9	99.74	500	<1	27.1	7.0	17.4	
STD CSC Expected																						
STD OREAS76A Expected																						
STD DS7 Expected																						
STD SO-18 Expected		58.47	14.23	7.67	3.35	6.42	3.71	2.17	0.69	0.83	0.39	0.55	44	25			514		26.2	7.1	17.6	
BLK	Blank																					
BLK	Blank																					
BLK	Blank	<0.01	<0.01	<0.04	<0.01	<0.01	<0.01	<0.01	<0.01	<0.01	<0.01	<0.002	<20	<1	0.0	<0.01	<1	<1	<0.2	<0.1	<0.5	
BLK	Blank	<0.01	<0.01	<0.04	<0.01	<0.01	<0.01	<0.01	<0.01	<0.01	<0.01	<0.002	<20	<1	0.0	<0.01	<1	<1	<0.2	<0.1	<0.5	

Method	4A-4B	4A-4B	4A-4B	4A-4B	4A-4B	4A-4B	4A-4B	4A-4B	4A-4B	4A-4B	4A-4B	4A-4B	4A-4B	4A-4B	4A-4B	4A-4B	4A-4B	4A-4B	4A-4B	4A-4B	4A-4B	4A-4B
Analyte	Hf	Nb	Rb	Sn	Sr	Ta	Th	U	V	W	Zr	Y	La	Ce	Pr	Nd	Sm	Eu	Gd	Tb		
Unit	ppm	ppm	ppm	ppm	ppm	ppm	ppm	ppm	ppm	ppm	ppm	ppm	ppm	ppm	ppm	ppm	ppm	ppm	ppm	ppm	ppm	ppm
MDL	0.1	0.1	0.1	1	0.5	0.1	0.2	0.1	8	0.5	0.1	0.1	0.1	0.1	0.02	0.3	0.05	0.02	0.05	0.01		
LT31 1366 M	Rock Pulp	1.8	6.5	63.7	2	405.5	0.4	5.9	1.2	46	1.2	55.5	17.5	19.6	36.4	4.62	17.6	3.42	0.71	3.21	0.50	
Pulp Duplicates																						
LT33 2748 M	Rock Pulp	0.4	2.1	16.8	<1	530.3	<0.1	1.4	0.8	14	<0.5	12.7	9.2	9.5	14.2	1.62	8.0	1.31	0.25	1.23	0.19	
REP LT33 2748 M	QC																					
Reference Materials																						
STD CSC	Standard																					
STD DS7	Standard																					
STD DS7	Standard																					
STD OREAS76A	Standard																					
STD SO-18	Standard	9.7	21.2	28.4	15	407.1	7.2	9.9	16.2	203	14.7	284.3	31.5	12.0	27.0	3.40	13.8	2.86	0.85	2.67	0.50	
STD SO-18	Standard	9.7	21.2	28.4	15	408.8	7.2	10.0	16.2	203	14.7	285.2	31.5	12.0	27.2	3.40	13.8	2.85	0.85	2.67	0.47	
STD SO-18	Standard	9.5	20.7	28.3	15	402.4	7.0	10.1	16.3	203	14.7	282.6	31.3	12.0	26.8	3.40	13.8	2.83	0.85	2.69	0.50	
STD SO-18	Standard	9.7	20.1	28.4	15	404.2	7.0	10.0	16.4	205	14.8	281.9	31.3	11.9	27.2	3.42	13.9	2.89	0.86	2.69	0.50	
STD CSC Expected																						
STD OREAS76A Expected																						
STD DS7 Expected																						
STD SO-18 Expected		9.8	20.9	28.7	15	407.4	7.4	9.9	16.4	200	15.1	280	33	12.3	27.1	3.45	14	3	0.89	2.93	0.53	
BLK	Blank																					
BLK	Blank																					
BLK	Blank	<0.1	<0.1	<0.1	<1	<0.5	<0.1	<0.2	<0.1	<8	<0.5	2.2	<0.1	<0.1	<0.1	<0.1	<0.2	<0.3	<0.05	<0.02	<0.05	<0.01
BLK	Blank	<0.1	<0.1	<0.1	<1	<0.5	<0.1	<0.2	<0.1	<8	<0.5	2.2	<0.1	<0.1	<0.1	<0.1	<0.2	<0.3	<0.05	<0.02	<0.05	<0.01



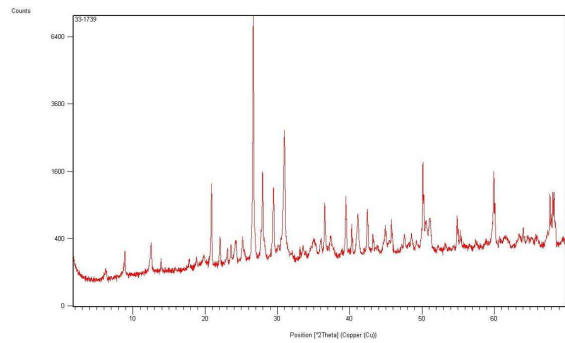




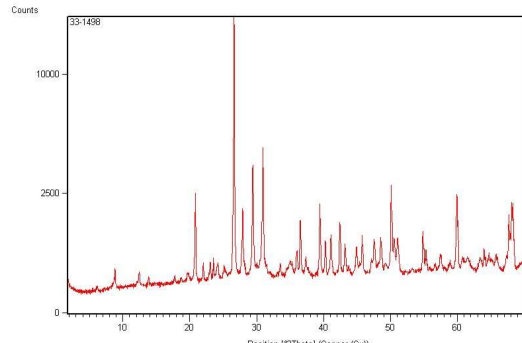


	2A B	4A-4B	4A-4B	4A-4B	4A-4B	4A-4B	4A-4B	4A-4B	4A-4B	4A-4B	4A-4B	4A-4B	4A-4B	4A-4B	4A-4B	4A-4B								
	B	SiO2	Al2O3	Fe2O3	MgO	CaO	Na2O	K2O	TiO2	P2O5	MnO	Cr2O3	Ni	Sc	LOI	Sum	Ba	Be	Co	Cs				
	ppm	%	%	%	%	%	%	%	%	%	%	%	ppm	ppm	%	%	ppm	ppm	ppm	ppm				
	3	0.01	0.01	0.04	0.01	0.01	0.01	0.01	0.01	0.01	0.01	0.002	20	1	-5.1	0.01	1	1	0.2	0.1				
STD C3 Expected		42																						
BLK	Blank																							
BLK	Blank	<0.01	<0.01	<0.04	<0.01	<0.01	<0.01	<0.01	<0.01	<0.01	<0.01	<0.002	<20	<1	0.0	<0.01	<1	<1	<0.2	<0.1				
BLK	Blank																							
BLK	Blank	<0.01	<0.01	<0.04	<0.01	<0.01	<0.01	<0.01	<0.01	<0.01	<0.01	<0.002	<20	<1	0.0	<0.01	<1	<1	<0.2	<0.1				
BLK	Blank																							
BLK	Blank	<3																						
	4A-4B	4A-4B	4A-4B	4A-4B	4A-4B	4A-4B	4A-4B	4A-4B	4A-4B	4A-4B	4A-4B	4A-4B	4A-4B	4A-4B	4A-4B									
	Ga	Hf	Nb	Rb	Sn	Sr	Ta	Th	U	V	W	Zr	Y	La	Ce	Pr	Nd	Sm	Eu	Gd				
	ppm	ppm	ppm	ppm	ppm	ppm	ppm	ppm	ppm	ppm	ppm	ppm	ppm	ppm	ppm	ppm								
	0.5	0.1	0.1	0.1	1	0.5	0.1	0.2	0.1	8	0.5	0.1	0.1	0.1	0.1	0.1	0.1	0.02	0.3	<0.05	<0.02	<0.05		
STD C3 Expected																								
BLK	Blank																							
BLK	Blank	<0.5	<0.1	<0.1	<0.1	<1	<0.5	<0.1	<0.2	<0.1	<8	<0.5	<0.1	<0.1	<0.1	<0.1	<0.1	<0.2	<0.3	<0.05	<0.02	<0.05		
BLK	Blank																							
BLK	Blank	<0.5	<0.1	<0.1	<0.1	<1	<0.5	<0.1	<0.2	<0.1	<8	<0.5	<0.1	<0.1	<0.1	<0.1	<0.1	<0.2	<0.3	<0.05	<0.02	<0.05		
BLK	Blank																							
BLK	Blank																							
	4A-4B	2A Leco	2A Leco	IDX	IDX	IDX	IDX	IDX	IDX	IDX	IDX	IDX	IDX	IDX	IDX	IDX								
	Tb	Dy	Ho	Er	Tm	Yb	Lu	TOT/C	TOT/S	Mo	Cu	Pb	Zn	Ni	As	Cd	Sb	Bi	Ag	Au				
	ppm	%	%	ppm	ppm	ppm	ppm	ppm	ppm	ppm	ppm	ppm	ppm	ppm	ppm	ppm	ppb							
	0.01	0.05	0.02	<0.03	<0.01	<0.05	<0.01			0.1	0.1	0.1	1	0.1	0.5	0.1	0.1	0.5	<0.1	<0.1	<0.1	<0.1	<0.5	
STD C3 Expected																								
BLK	Blank									<0.1	<0.1	<0.1	<1	<0.1	<0.5	<0.1	<0.1	<0.1	<0.1	<0.1	<0.1	<0.1	<0.5	
BLK	Blank																							
BLK	Blank	<0.01	<0.05	<0.02	<0.03	<0.01	<0.05	<0.01																
BLK	Blank																							
BLK	Blank																							
	1DX	1DX	1DX																					
	Hg	Tl	Se																					
	ppm	ppm	ppm																					
	0.01	0.1	0.5																					
STD C3 Expected																								
BLK	Blank	<0.01	<0.1	<0.5																				
BLK	Blank																							
BLK	Blank																							
BLK	Blank																							
BLK	Blank																							
BLK	Blank																							

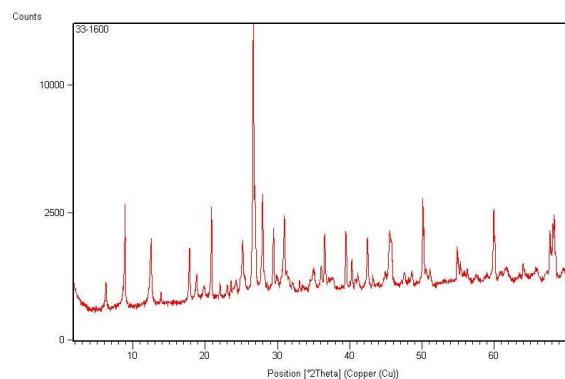
## APPENDIX 2 XRD RESULTS



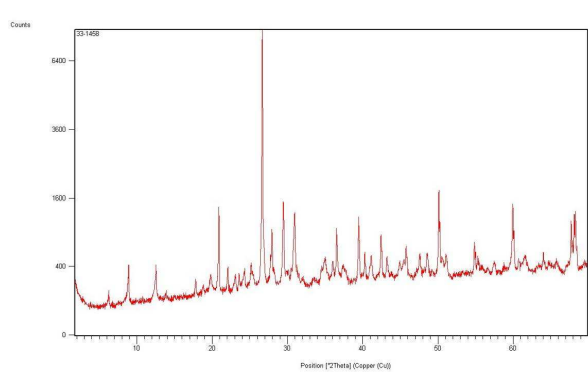
Appendix 7 LT33/1739



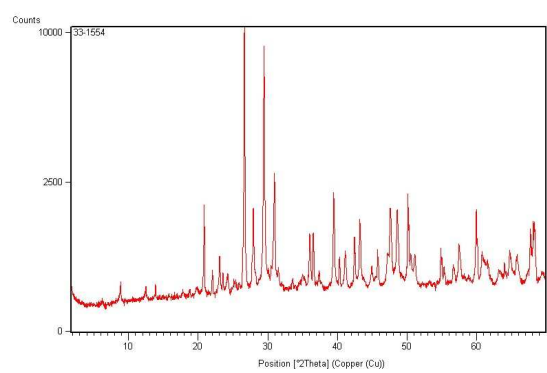
Appendix 10 LT33/1498



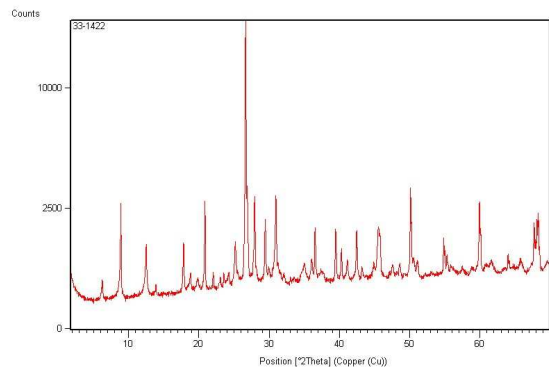
Appendix 8 LT33/1600



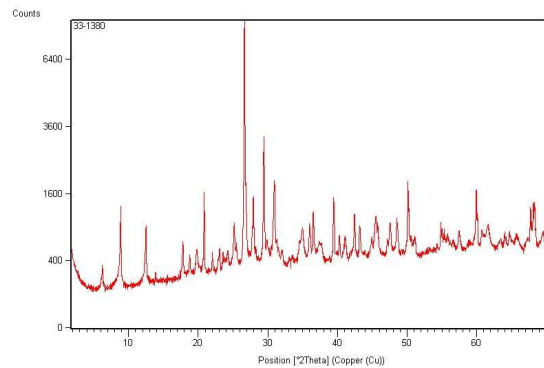
Appendix 11 LT33/1458



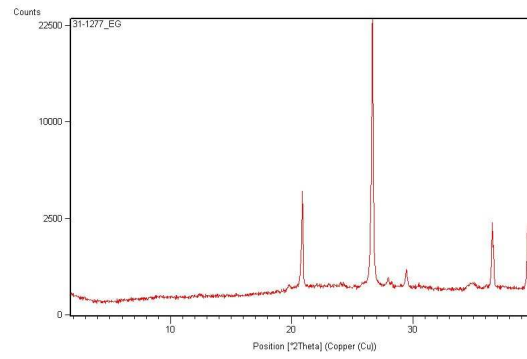
Appendix 9 LT33/1554



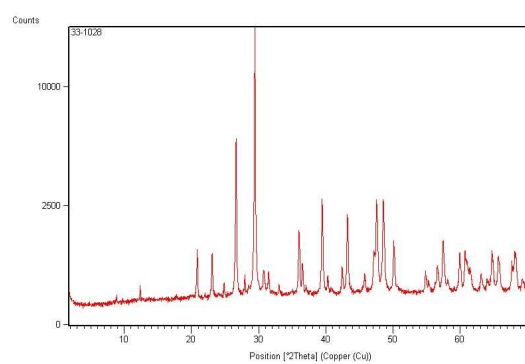
Appendix 12 LT33/1422



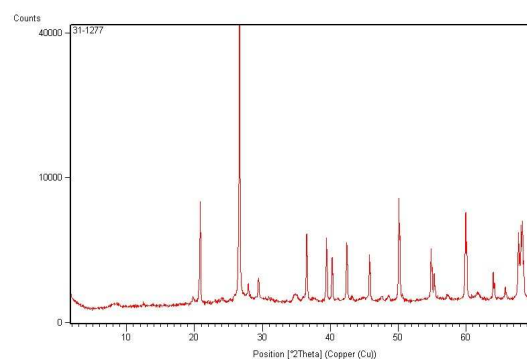
**Appendix 13 LT33/1380**



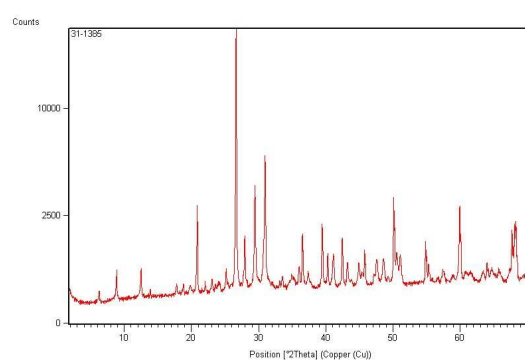
**Appendix 16 LT31/1277+EG**



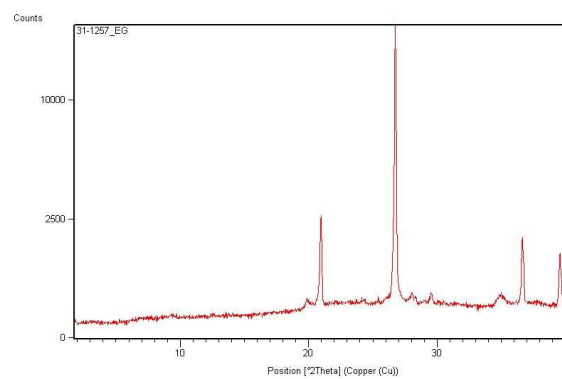
**Appendix 14 LT33/1028**



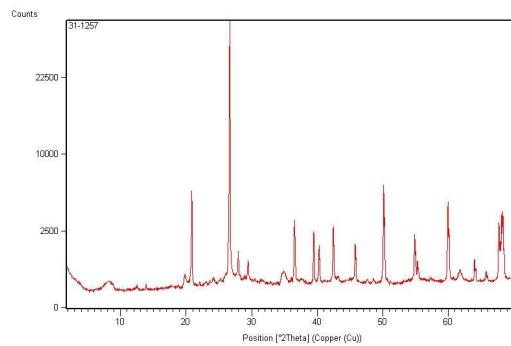
**Appendix 17 LT31/1277**



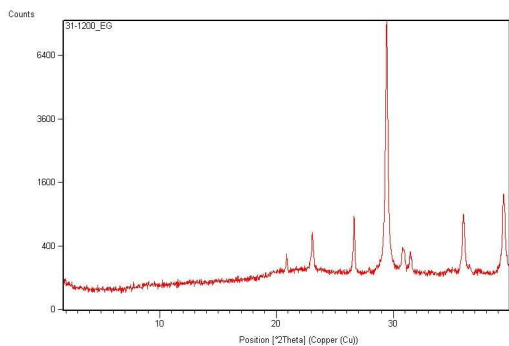
**Appendix 15 LT31/1385**



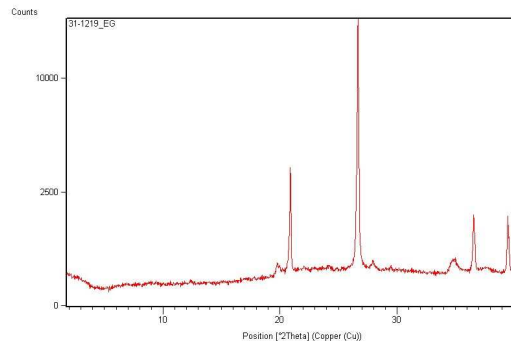
**Appendix 18 LT31/1257+EG**



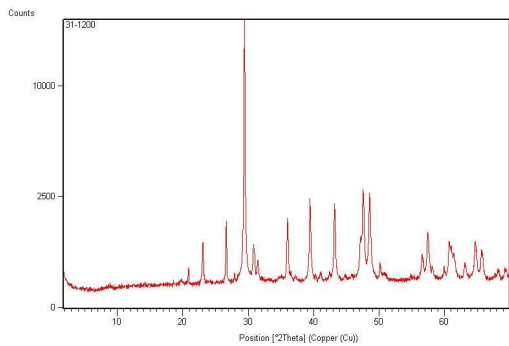
**Appendix 19 LT31/1257**



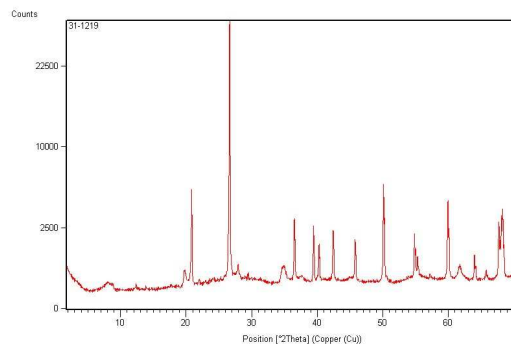
**Appendix 23 LT31/1200+EG**



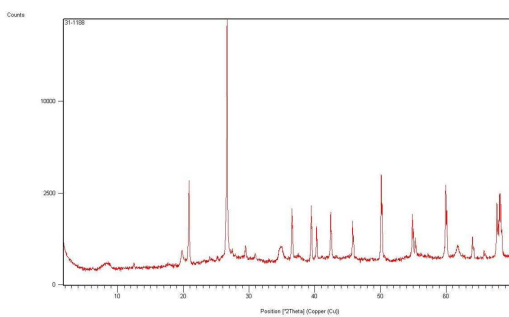
**Appendix 20LT31/1219+EG**



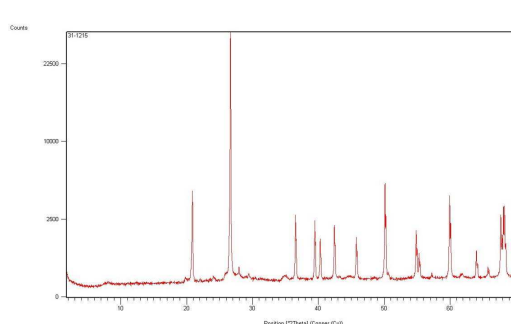
**Appendix 24 LT31/1200**



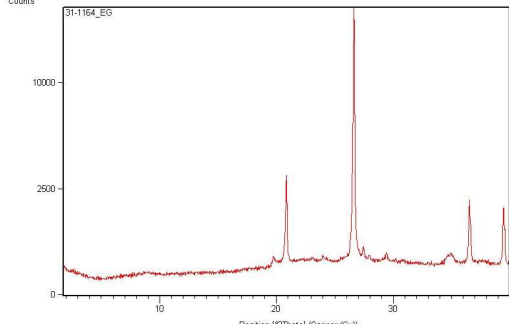
**Appendix 21 LT31/1219**



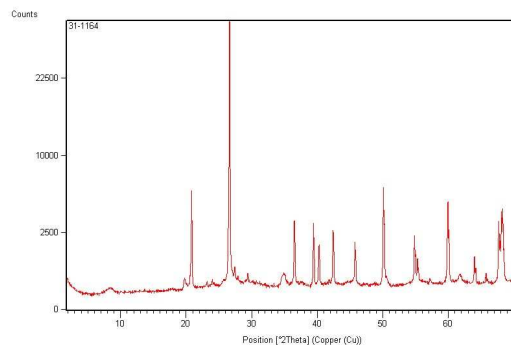
**Appendix 25 LT31/1188**



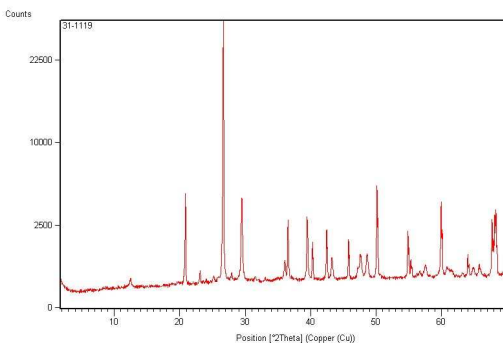
**Appendix 22 LT31/1215**



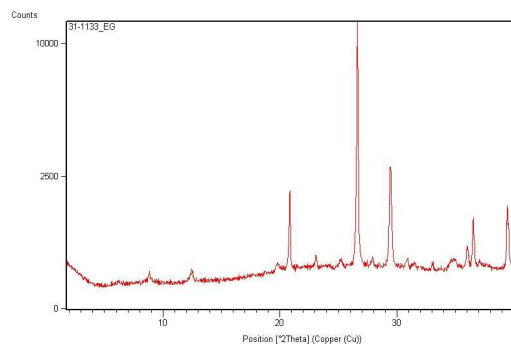
**Appendix 26 LT31/1164+EG**



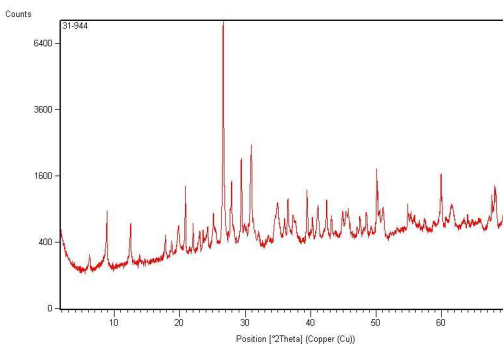
**Appendix 27 LT31/1164**



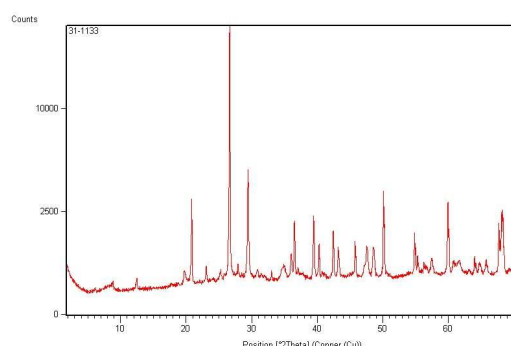
**Appendix 31 LT31/1119**



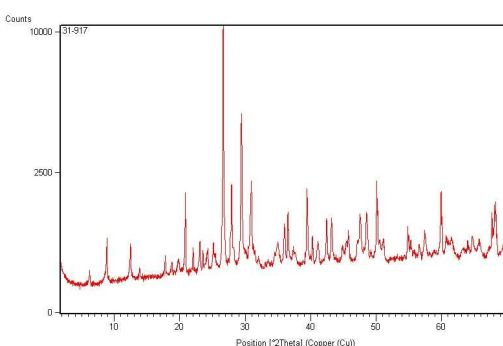
**Appendix 28 LT31/1133+EG**



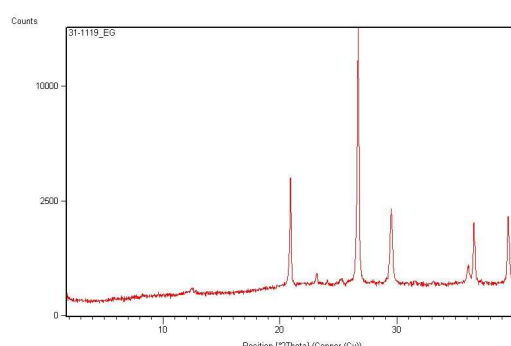
**Appendix 32 LT31/944**



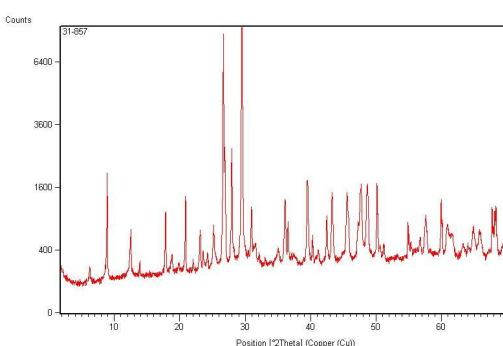
**Appendix 29 LT31/1133**



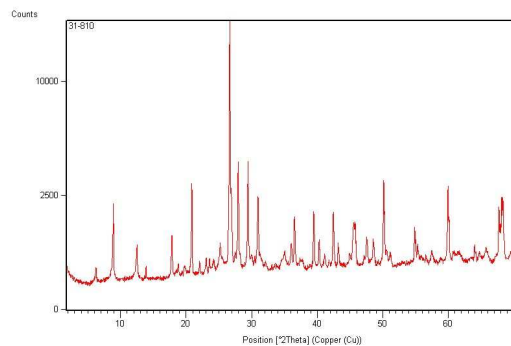
**Appendix 33 LT31/917**



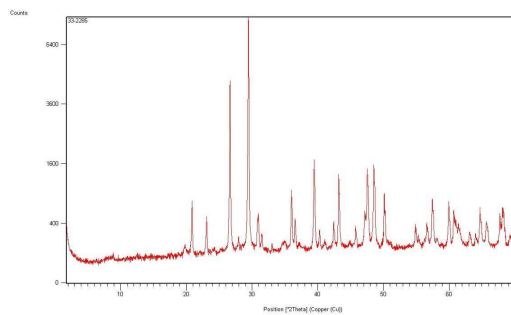
**Appendix 30 LT31/1119+EG**



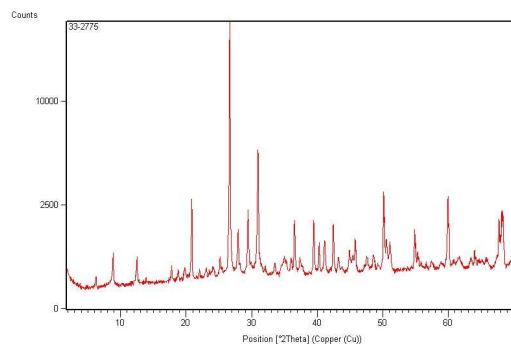
**Appendix 34 LT31/857**



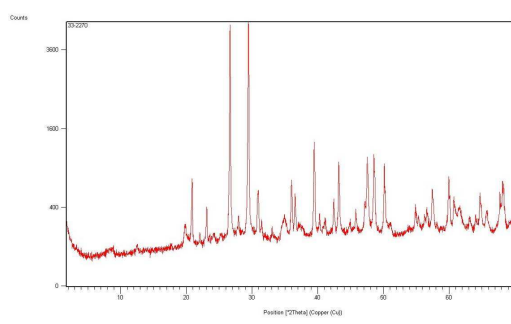
**Appendix 35 LT31/810**



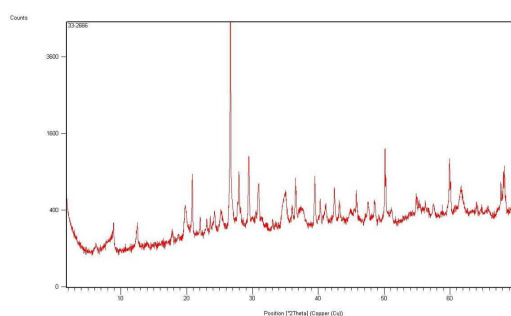
**Appendix 39 LT33/2285**



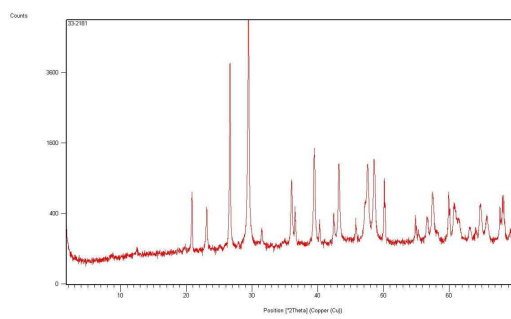
**Appendix 36 LT33/2775**



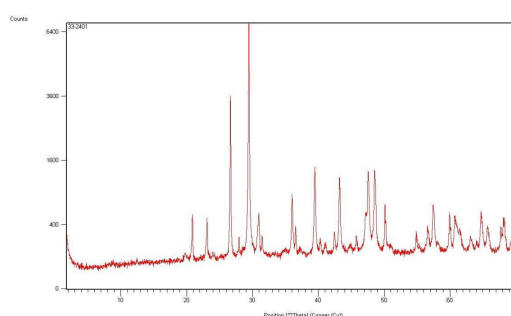
**Appendix 40 LT33/2270**



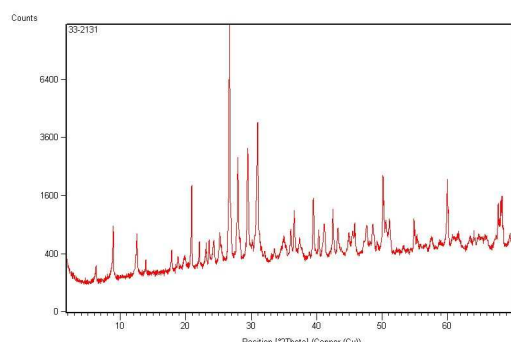
**Appendix 37 LT33/2666**



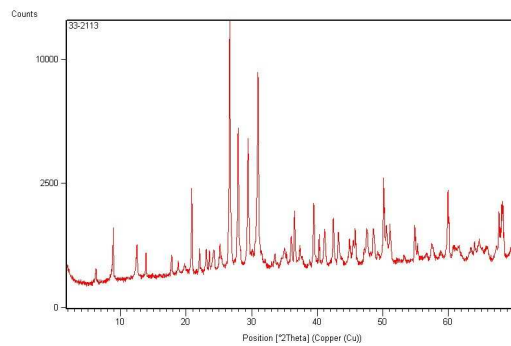
**Appendix 41 LT33/2181**



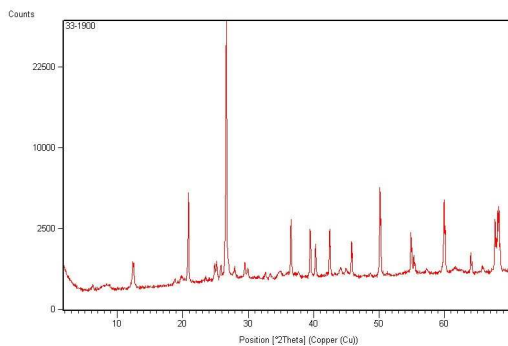
**Appendix 38 LT33/2401**



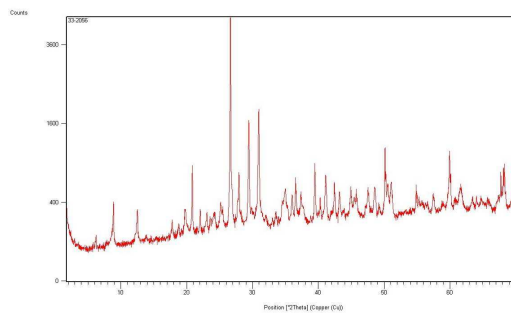
**Appendix 42 LT33/2131**



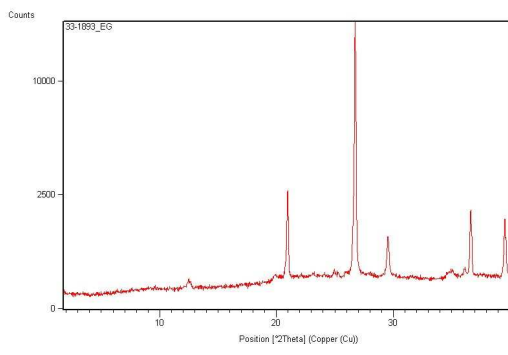
**Appendix 43 LT33/2113**



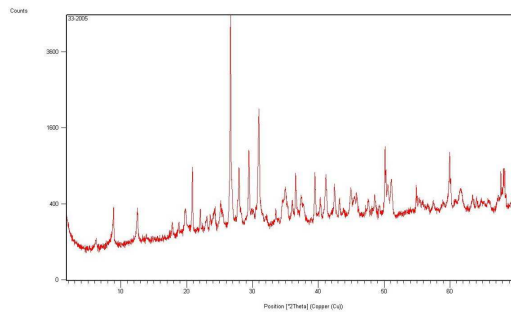
**Appendix 47 LT33/1900**



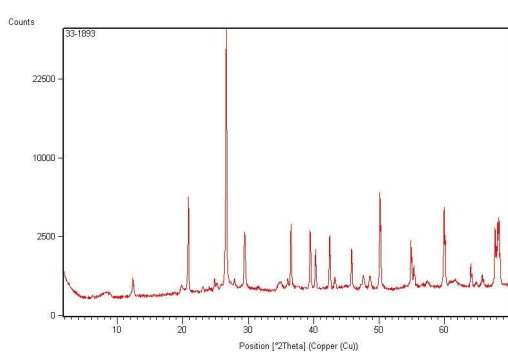
**Appendix 44 LT33/2056**



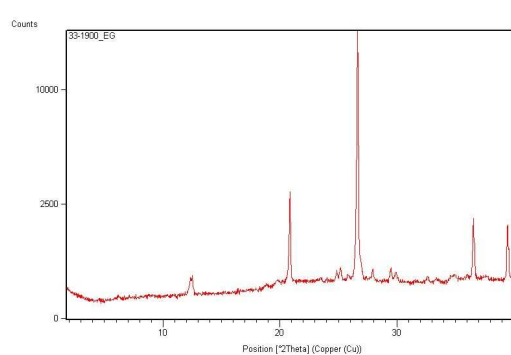
**Appendix 48 LT33/1893+EG**



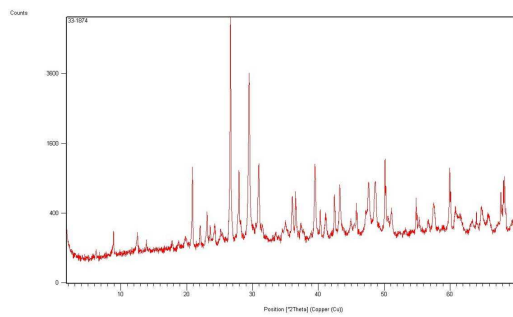
**Appendix 45 LT33/2005**



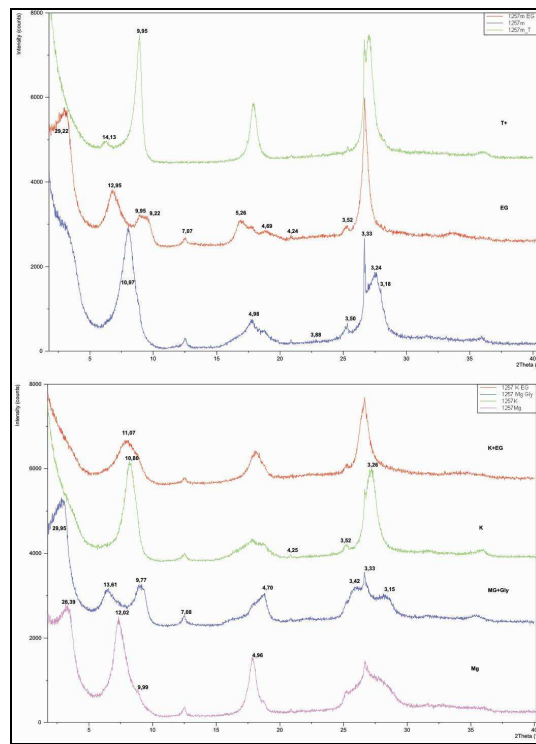
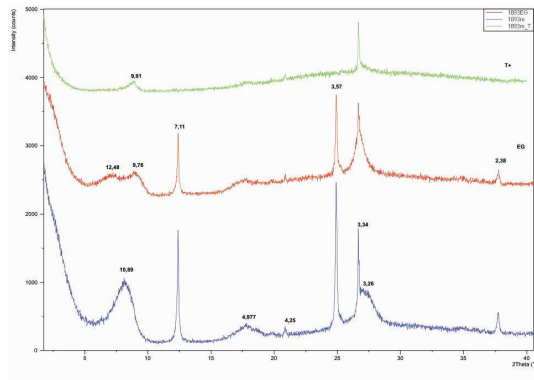
**Appendix 49 LT33/1893**



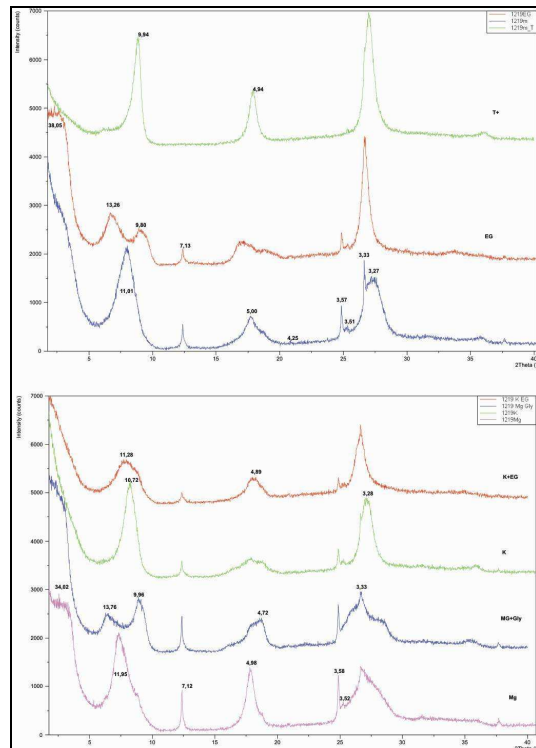
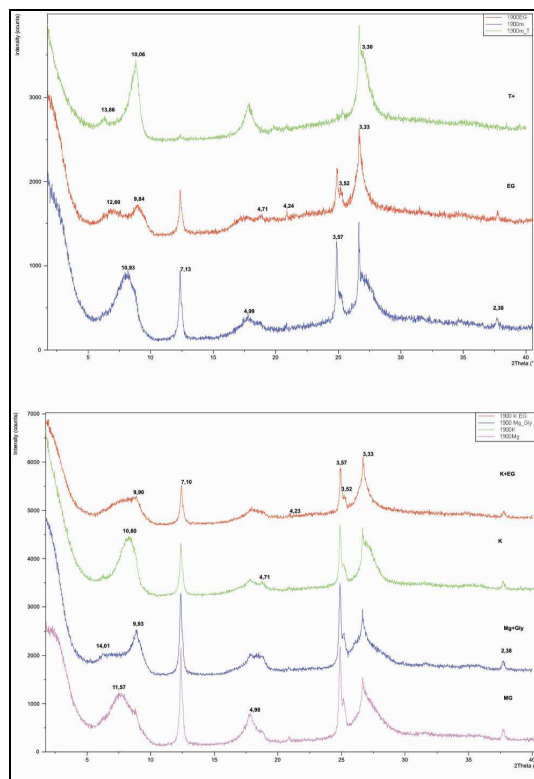
**Appendix 46 LT33/1900+EG**



**Appendix 50 LT33/1874m**

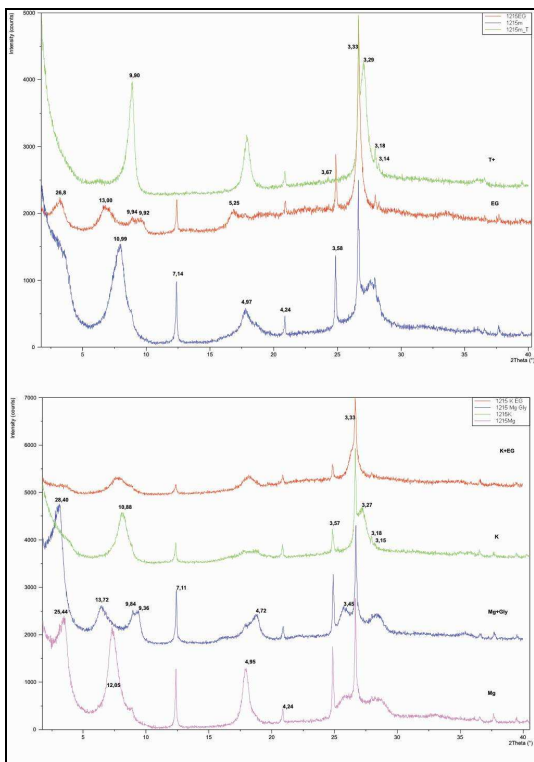


**Appendix 53 LT/1257m**

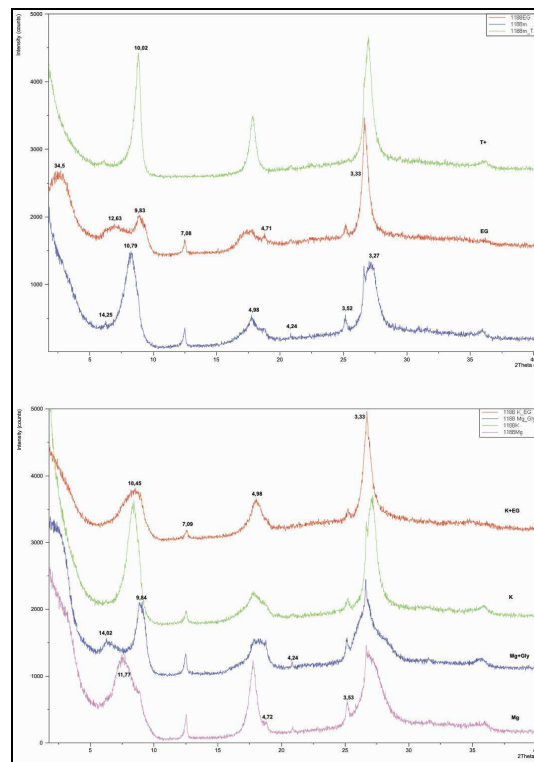


**Appendix 54 LT31/1219m**

**Appendix 52 LT33/1900m**



**Appendix 55 LT31/1215m**



**Appendix 56 LT31/1188m**

## APPENDIX 3 CARBONATE ANALYSIS RESULTS

	Station(m)	max.		Station(m)	max		Station(m)	max	CaCO3%
		CaCO3%			CaCO3%				CaCO3%
LT33	5	37	LT33	1028	67	LT31		1381	82
LT33	15	55	LT33	1076	62	LT31		1367	61
LT33	18	67	LT33	1104	75	LT31		1348	36
LT33	21	57	LT33	1173	61	LT31		1326	46
LT33	31	70	LT33	1232	63	LT31		1308	51
LT33	74	37	LT33	1292	14	LT31		1258	0
LT33	49	70	LT33	1338	16	LT31		1202	60
LT33	90	66	LT33	1381	24	LT31		1200	75
LT33	113	62	LT33	1427	13	LT31		1189	80
LT33	135	71	LT33	1459	16	LT31		1165	61
LT33	155	71	LT33	1499	30	LT31		1134	36
LT33	169	56	LT33	1535	38	LT31		1120	20
LT33	187	61	LT33	1554	24	LT31		1102	54
LT33	200	65	LT33	1600	14	LT31		1088	46
LT33	220	58	LT33	1693	14	LT31		1074	46
LT33	235	72	LT33	1739	21	LT31		1055	53
LT33	243	57	LT33	1780	26	LT31		1040	59
LT33	260	55	LT33	1831	18	LT31		1023	80
LT33	280	50	LT33	1874	30	LT31		1009	74
LT33	302	67	LT33	1923	20	LT31		994	58
LT33	326	60	LT33	1939	19	LT31		981	23
LT33	337	69	LT33	1962	14	LT31		976	27
LT33	357	57	LT33	1981	13	LT31		963	35
LT33	380	73	LT33	2005	28	LT31		945	16
LT33	394	64	LT33	2034	16	LT31		933	29
LT33	413	6	LT33	2056	24	LT31		918	28
LT33	429	64	LT33	2074	10	LT31		898	53
LT33	452	13	LT33	2113	38	LT31		886	52
LT33	470	14	LT33	2132	27	LT31		875	0
LT33	490	11	LT33	2182	82	LT31		870	79
LT33	506	59	LT33	2212	83	LT31		857	64
LT33	515	38	LT33	2230	40	LT31		842	66
LT33	528	29	LT33	2245	85	LT31		811	10
LT33	542	11	LT33	2271	42				
LT33	563	0	LT33	2286	53				
LT33	578	0	LT33	2300	77				
LT33	596	6	LT33	2313	69				
LT33	611	11	LT33	2331	74				
LT33	630	0	LT33	2375	34				
LT33	641	0	LT33	2401	85				
LT33	663	8	LT33	2418	22				
LT33	675	0	LT33	2418	80				

LT33	688	17	LT33	2452	77			
LT33	703	60	LT33	2475	48			
LT33	712	57	LT33	2505	43			
LT33	724	43	LT33	2535	64			
LT33	734	65	LT33	2552	48			
LT33	750	31	LT33	2552	85			
LT33	765	61	LT33	2552	56			
LT33	780	63	LT33	2577	49			
LT33	802	4	LT33	2592	21			
LT33	835	74	LT33	2592	65			
LT33	880	70	LT33	2609	30			
LT33	926	97	LT33	2645	57			
LT33	986	67	LT33	2666	18			
LT33	1006	62	LT33	2695	67			
			LT33	2731	46			
			LT33	2748	39			
			LT33	2776	81			

#### Appendix 57

## APPENDIX 4 GEOCHEMISTRY RESULTS

### Erklärte Gesamtvarianz

Komponente	Anfängliche Eigenwerte			Summen von quadrierten Faktorladungen für Extraktion			Rotierte Ladungen		
	Gesamt	% der Varianz	Kumulierte %	Gesamt	% der Varianz	Kumulierte %	Gesamt	% Varianz	Kumulierte %
1	19,065	50,171	50,171	19,065	50,171	50,171	13,901	36,582	36,582
2	5,599	14,735	64,905	5,599	14,735	64,905	8,194	21,563	58,144
3	3,786	9,963	74,868	3,786	9,963	74,868	6,355	16,724	74,868
4	2,949	7,762	82,630						
5	2,779	7,312	89,942						
6	1,368	3,600	93,543						
7	,992	2,612	96,154						
8	,835	2,199	98,353						
9	,281	,740	99,093						
10	,141	,371	99,464						
11	,103	,270	99,734						
12	,063	,166	99,900						
13	,038	,100	100,000						
14	8,917E-16	2,347E-15	100,000						
15	8,125E-16	2,138E-15	100,000						
16	6,022E-16	1,585E-15	100,000						
17	5,515E-16	1,451E-15	100,000						
18	4,912E-16	1,293E-15	100,000						
19	4,035E-16	1,062E-15	100,000						
20	3,485E-16	9,170E-16	100,000						
21	2,842E-16	7,479E-16	100,000						
22	2,666E-16	7,017E-16	100,000						
23	1,523E-16	4,009E-16	100,000						
24	9,136E-17	2,404E-16	100,000						
25	8,297E-18	2,183E-17	100,000						
26	-5,726E-17	-1,507E-16	100,000						
27	-7,809E-17	-2,055E-16	100,000						
28	-1,424E-16	-3,747E-16	100,000						
29	-2,725E-16	-7,170E-16	100,000						
30	-3,176E-16	-8,357E-16	100,000						
31	-4,259E-16	-1,121E-15	100,000						
32	-5,015E-16	-1,320E-15	100,000						
33	-5,456E-16	-1,436E-15	100,000						
34	-5,921E-16	-1,558E-15	100,000						
35	-6,468E-16	-1,702E-15	100,000						
36	-6,847E-16	-1,802E-15	100,000						
37	-8,308E-16	-2,186E-15	100,000						
38	-9,891E-16	-2,603E-15	100,000						

Extraktionsmethode: Hauptkomponentenanalyse.

Appendix 58 Factor analysis Keuper sandstones + Gresten sandstones.

**Komponentenmatrix<sup>a</sup>**

	Komponente		
	1	2	3
Yb	,954		-,181
Lu	,954		-,185
U	,945	-,189	-,146
Tm	,937	,151	-,214
Nb	,915	-,312	
Th	,894	-,326	-,189
Y	,892	,265	-,231
Ta	,888	-,262	
Sc	,875	,261	,105
Hf	,860	-,384	-,230
TiO2	,853	-,236	,205
Ce	,852	-,217	-,437
Zr	,849	-,365	-,271
Rb	,832	-,298	,274
La	,830	-,128	-,489
K2O	,816	-,384	,175
Al2O3	,777		,446
MgO	,775		,114
Cs	,763	-,104	,422
Eu	,742	,451	-,388
V	,731	,135	-,110
Ga	,728		,470
SiO2	-,720	-,603	
Sr	,691		-,264
Fe2O3	,612	,357	,517
Cr	,421		,144
Mo	-,361	,248	
W	,323		
MnO	,252	,905	-,253
As	,100	,895	
Cu		,846	-,192
CaO	,397	,823	-,171
Na2O	,124	,653	,243
Pb	,315	,323	
Co	,599	,164	,656
Ni	,320		,636
Zn	,575	,177	,626
Ba	,444	-,281	-,516

Extraktionsmethode: Hauptkomponentenanalyse.

a. 3 Komponenten extrahiert

**Appendix 59 Factor analysis Keuper sandstones + Gresten sandstones.**

**Erklärte Gesamtvarianz**

Komponente	Anfängliche Eigenwerte			Summen von quadrierten Faktorladungen für Extraktion			Rotierte Summe der quadrierten Ladungen		
	Gesamt	% der Varianz	Kumulierte %	Gesamt	% der Varianz	Kumulierte %	Gesamt	% der Varianz	Kumulierte %
1	24,181	54,958	54,958	24,181	54,958	54,958	15,422	35,049	35,049
2	6,788	15,427	70,385	6,788	15,427	70,385	13,619	30,953	66,003
3	3,491	7,934	78,319	3,491	7,934	78,319	5,419	12,316	78,319
4	2,700	6,135	84,454						
5	2,162	4,914	89,368						
6	1,124	2,554	91,922						
7	,986	2,242	94,164						
8	,687	1,561	95,725						
9	,527	1,198	96,923						
10	,317	,720	97,642						
11	,236	,537	98,179						
12	,212	,482	98,661						
13	,185	,420	99,080						
14	,149	,338	99,419						
15	,095	,215	99,634						
16	,077	,174	99,809						
17	,048	,109	99,917						
18	,036	,083	100,000						
19	,000	,000	100,000						
20	,000	,000	100,000						
21	,000	,000	100,000						
22	,000	,000	100,000						
23	,000	,000	100,000						
24	,000	,000	100,000						
25	,000	,000	100,000						
26	,000	,000	100,000						
27	,000	,000	100,000						
28	,000	,000	100,000						
29	,000	,000	100,000						
30	,000	,000	100,000						
31	,000	,000	100,000						
32	,000	,000	100,000						
33	,000	,000	100,000						
34	,000	,000	100,000						
35	,000	,000	100,000						
36	,000	,000	100,000						
37	,000	,000	100,000						
38	,000	,000	100,000						
39	,000	,000	100,000						
40	,000	,000	100,000						
41	,000	,000	100,000						
42	,000	,000	100,000						
43	,000	,000	100,000						
44	,000	,000	100,000						

**Appendix 60 Factor analysis Keuper shales and Jurassic shales.**

**Komponentenmatrixa**

	Komponente		
	1	2	3
TiO2	,961	-,128	
Ga	,960	-,212	
Sc	,954	-,107	
Ce	,937	,190	,219
Th	,931	-,273	
Al2O3	,929	-,289	
La	,927	,267	,198
Yb	,919	,275	,194
Ta	,912		,232
Lu	,906	,276	,178
Zr	,906	-,220	,223
Tm	,884	,299	,225
LOI	-,881	,257	,254
Hf	,878	-,315	,115
Cs	,872	-,261	
CaO	-,870	,379	,234
TOC	-,870	,353	,205
Sn	,865	-,302	-,192
Nb	,849		,267
W	,833		-,378
Rb	,820	-,494	
U	,810	,260	-,132
SiO2	,786	-,277	-,308
Co	,773	,578	
V	,734	,398	-,138
Fe2O3	,726	-,381	
K2O	,709	-,546	
Pb	,700	,335	,331
Eu	,696	,493	,375
Y	,682	,565	,313
Cr	,645	,460	-,331
P2O5	,642	,604	,185
Be	,597	-,401	-,155
Sr	-,501	,767	
Cu	,314	,655	-,624
Ba	,441	,596	,286
MnO	-,236	,563	,131
Mo	-,138	,317	,250
MgO		-,245	
Ni	,250	,529	-,662
Na2O	,441	,576	-,642
Zn	,300	,549	-,578
As	,356		,458
TOTS	-,207	,230	-,316

**Appendix 61 Factor analysis Keuper shales and Jurassic shales.**

**Erklärte Gesamtvarianz**

Komponente	Anfängliche Eigenwerte			Summen von quadrierten Faktorladungen für Extraktion			Rotierte Summe der quadrierten Ladungen		
	Gesamt	% der Varianz	Kumulierte %	Gesamt	% der Varianz	Kumulierte %	Gesamt	% der Varianz	Kumulierte %
1	22,081	50,183	50,183	22,081	50,183	50,183	13,212	30,027	30,027
2	5,870	13,341	63,524	5,870	13,341	63,524	13,102	29,776	59,803
3	4,033	9,166	72,689	4,033	9,166	72,689	5,670	12,886	72,689
4	3,307	7,516	80,206						
5	2,295	5,215	85,421						
6	1,750	3,976	89,397						
7	1,548	3,518	92,915						
8	,914	2,077	94,991						
9	,719	1,633	96,625						
10	,538	1,223	97,848						
11	,349	,793	98,641						
12	,252	,573	99,214						
13	,162	,368	99,582						
14	,064	,146	99,728						
15	,058	,132	99,860						
16	,041	,094	99,953						
17	,020	,047	100,000						
18	,000	,000	100,000						
19	,000	,000	100,000						
20	,000	,000	100,000						
21	,000	,000	100,000						
22	,000	,000	100,000						
23	,000	,000	100,000						
24	,000	,000	100,000						
25	,000	,000	100,000						
26	,000	,000	100,000						
27	,000	,000	100,000						
28	,000	,000	100,000						
29	,000	,000	100,000						
30	,000	,000	100,000						
31	,000	,000	100,000						
32	,000	,000	100,000						
33	,000	,000	100,000						
34	,000	,000	100,000						
35	,000	,000	100,000						
36	,000	,000	100,000						
37	,000	,000	100,000						
38	,000	,000	100,000						
39	,000	,000	100,000						
40	,000	,000	100,000						
41	,000	,000	100,000						
42	,000	,000	100,000						
43	,000	,000	100,000						
44	,000	,000	100,000						

#### Appendix 62 Factor analysis Jurassic sandstones and Keuper sandstones.

##### Komponentenmatrixa

	Komponente		
	1	2	3
Nb	,953	-,195	
Ta	,939	-,188	
TiO2	,938		-,157
Sc	,930	,163	-,246
Sn	,925	-,120	-,165
Co	,914	,139	-,134
Lu	,907	-,181	,305
Al2O3	,907		-,342
Tm	,903	-,112	,327
Yb	,903	-,173	,317
Ga	,894		-,383
Rb	,894		-,220
Cs	,868		-,367
Ce	,865	-,326	,275
V	,849	,197	-,331
Fe2O3	,818	,205	-,476
La	,818	-,347	,317
Eu	,813	,183	,340
Y	,805		,449
K2O	,796	-,191	
Th	,792	-,479	,177
U	,777	-,367	,433
P2O5	,751	,435	-,253
Zn	,734	,175	-,574
Cr	,731	,166	-,215
Hf	,716	-,500	,365
Zr	,704	-,492	,375
As	,698	,388	-,322
Pb	,649	,131	
W	,597	,139	,210
MgO	,364	,265	,179
Ni	,135		
TOC	,237	,793	,252
CaO	,214	,785	,255
LOI	,417	,748	,178
SiO2	-,639	-,654	
Cu	,420	,645	
Na2O	,156	,491	,176
MnO		,453	,448
Ba		-,450	-,442
Be	,399	-,410	,195
Mo	-,334	,398	,159
Sr		-,308	-,575
TOTS	,112	-,420	-,467

Appendix 63 Factor analysis Jurassic sandstones and Keuper sandstones.

**Erklärte Gesamtvarianz**

Komponente	Anfängliche Eigenwerte			Summen von quadrierten Faktorladungen für Extraktion			Rotierte Summe der quadrierten Ladungen		
	Gesamt	% der Varianz	Kumulierte %	Gesamt	% der Varianz	Kumulierte %	Gesamt	% der Varianz	Kumulierte %
1	22,975	52,217	52,217	22,975	52,217	52,217	14,822	33,687	33,687
2	5,614	12,759	64,975	5,614	12,759	64,975	10,671	24,253	57,940
3	2,973	6,758	71,733	2,973	6,758	71,733	6,069	13,793	71,733
4	2,420	5,501	77,234						
5	1,406	3,195	80,429						
6	1,354	3,077	83,506						
7	1,199	2,724	86,231						
8	1,070	2,432	88,663						
9	,842	1,914	90,577						
10	,660	1,500	92,077						
11	,623	1,416	93,493						
12	,506	1,149	94,642						
13	,428	,974	95,616						
14	,348	,790	96,406						
15	,289	,656	97,062						
16	,245	,557	97,619						
17	,188	,428	98,047						
18	,146	,333	98,380						
19	,126	,287	98,666						
20	,108	,244	98,911						
21	,094	,214	99,125						
22	,075	,171	99,296						
23	,060	,135	99,431						
24	,045	,103	99,533						
25	,036	,083	99,616						
26	,031	,070	99,687						
27	,026	,060	99,746						
28	,024	,054	99,800						
29	,020	,047	99,847						
30	,019	,042	99,889						
31	,011	,025	99,914						
32	,009	,021	99,934						
33	,007	,015	99,949						
34	,006	,014	99,963						
35	,004	,009	99,972						
36	,003	,007	99,979						
37	,003	,006	99,985						
38	,002	,005	99,990						
39	,002	,004	99,994						
40	,002	,003	99,997						
41	,001	,002	99,999						
42	,000	,001	100,000						
43	,000	,000	100,000						
44	,000	,000	100,000						

**Appendix 64 Factor analysis Jurassic carbonates.**

**Komponentenmatrixa**

	Komponente		
	1	2	3
Al <sub>2</sub> O <sub>3</sub>	,977		
Ga	,975		,108
TiO <sub>2</sub>	,969		,167
Nb	,965		
Sc	,965		
Th	,963		,200
Rb	,951		
K <sub>2</sub> O	,943		
Cs	,939		
Ta	,936		,104
V	,893		,255
Fe <sub>2</sub> O <sub>3</sub>	,891	-,102	
W	,852		
CaO	-,845	,214	,279
Sn	,833	,186	,289
Ce	,830		
Co	,827		-,412
LOI	-,827	,225	,358
Hf	,815		,382
Zr	,805		,369
Zn	,797	-,461	-,156
La	,795	,228	
Ni	,758	-,394	-,351
Cr	,725	-,365	-,373
SiO <sub>2</sub>	,724	-,248	-,453
Na <sub>2</sub> O	,712	-,177	,362
Be	,681	,330	,322
Y	,679	,190	
TOC	-,552	-,359	,231
Cu	,549	-,369	-,504
U	,513		,490
Pb	,490	-,402	-,387
Ba	,463		
Sr	-,457	-,231	,371
Tm		,963	-,173
Eu	,224	,944	-,164
Mo		,878	-,293
Lu	,437	,876	-,106
Yb	,629	,741	
TOTS	,142	,384	
As	,195	-,317	,247
MnO	,259		-,346
MgO	,236		,336
P <sub>2</sub> O <sub>5</sub>			,105

**Appendix 65 Factor analysis Jurassic carbonates.**

**Erklärte Gesamtvarianz**

Komponente	Anfängliche Eigenwerte			Summen von quadrierten Faktorladungen für Extraktion			Rotierte Summe der quadrierten Ladungen		
	Gesamt	% der Varianz	Kumulierte %	Gesamt	% der Varianz	Kumulierte %	Gesamt	% der Varianz	Kumulierte %
1	23,579	53,588	53,588	23,579	53,588	53,588	23,449	53,292	53,292
2	6,442	14,641	68,228	6,442	14,641	68,228	6,422	14,597	67,889
3	5,138	11,677	79,905	5,138	11,677	79,905	5,287	12,016	79,905
4	1,755	3,988	83,893						
5	1,523	3,462	87,355						
6	1,248	2,837	90,192						
7	,840	1,909	92,102						
8	,648	1,473	93,575						
9	,532	1,209	94,784						
10	,504	1,145	95,929						
11	,352	,800	96,729						
12	,337	,767	97,496						
13	,285	,647	98,143						
14	,193	,439	98,582						
15	,154	,350	98,931						
16	,129	,293	99,225						
17	,097	,220	99,445						
18	,066	,150	99,595						
19	,054	,123	99,718						
20	,036	,081	99,799						
21	,031	,070	99,870						
22	,018	,041	99,910						
23	,014	,032	99,942						
24	,010	,022	99,964						
25	,007	,016	99,980						
26	,004	,010	99,990						
27	,003	,007	99,997						
28	,001	,003	100,000						
29	,000	,000	100,000						
30	,000	,000	100,000						
31	,000	,000	100,000						
32	,000	,000	100,000						
33	,000	,000	100,000						
34	,000	,000	100,000						
35	,000	,000	100,000						
36	,000	,000	100,000						
37	,000	,000	100,000						
38	,000	,000	100,000						
39	,000	,000	100,000						
40	,000	,000	100,000						
41	,000	,000	100,000						
42	,000	,000	100,000						
43	,000	,000	100,000						
44	,000	,000	100,000						

Appendix 66 Factor analysis Jurassic cherts.

**Komponentenmatrix**

	Komponente		
	1	2	3
TiO <sub>2</sub>	,988		
Zr	,987		
K <sub>2</sub> O	,980		,122
Al <sub>2</sub> O <sub>3</sub>	,979		,139
Ga	,977		,113
Sc	,977		,161
Th	,975		,116
MgO	,974		,185
Hf	,974		
Rb	,971		,160
Nb	,969	-,136	
Cs	,964		,156
Yb	,928	,165	-,270
Ta	,923	-,211	
Fe <sub>2</sub> O <sub>3</sub>	,921	-,101	,164
Ce	,917		,293
La	,913	,329	
Lu	,902	,135	-,344
Eu	,878		-,407
P <sub>2</sub> O <sub>5</sub>	,868	,176	
V	,862	-,112	-,166
Tm	,827		-,490
Y	,792	,469	
U	,757	,224	
Be	,744	-,194	-,418
Sn	,744	-,194	-,418
Na <sub>2</sub> O	,728	,168	
TOTS	,697		-,531
Co	,621	-,325	,415
LOI		,959	
CaO	-,151	,955	
SiO <sub>2</sub>	-,194	-,945	
TOC	,167	,933	-,136
Sr	-,166	,860	
W		-,680	-,386
MnO		,549	,275
Zn	,185		,867
Cr	,203	-,300	,799
Cu	,340		,735
Ni	,173	-,413	,698
Pb		,181	,579
Mo	,231	-,363	-,485
Ba		-,287	-,305
As	-,143	,205	,251

Appendix 67 Factor analysis Jurassic cherts.

**Erklärte Gesamtvarianz**

Komponente	Anfängliche Eigenwerte			Summen von quadrierten Faktorladungen für Extraktion			Rotierte Summe der quadrierten Ladungen		
	Gesamt	% der Varianz	Kumulierte %	Gesamt	% der Varianz	Kumulierte %	Gesamt	% der Varianz	Kumulierte %
1	24,814	56,395	56,395	24,814	56,395	56,395	22,322	50,732	50,732
2	8,350	18,977	75,371	8,350	18,977	75,371	7,992	18,163	68,895
3	5,111	11,616	86,987	5,111	11,616	86,987	7,961	18,092	86,987
4	2,215	5,033	92,021						
5	1,512	3,435	95,456						
6	1,143	2,598	98,054						
7	,623	1,416	99,470						
8	,233	,530	100,000						
9	1,219E-15	2,770E-15	100,000						
10	8,652E-16	1,966E-15	100,000						
11	6,698E-16	1,522E-15	100,000						
12	6,143E-16	1,396E-15	100,000						
13	5,354E-16	1,217E-15	100,000						
14	4,975E-16	1,131E-15	100,000						
15	4,586E-16	1,042E-15	100,000						
16	4,067E-16	9,243E-16	100,000						
17	3,736E-16	8,490E-16	100,000						
18	3,463E-16	7,870E-16	100,000						
19	2,500E-16	5,681E-16	100,000						
20	2,085E-16	4,738E-16	100,000						
21	1,764E-16	4,009E-16	100,000						
22	1,660E-16	3,772E-16	100,000						
23	1,290E-16	2,931E-16	100,000						
24	6,729E-17	1,529E-16	100,000						
25	4,458E-17	1,013E-16	100,000						
26	5,029E-18	1,143E-17	100,000						

27	-1,781E-17	-4,047E-17	100,000						
28	-3,365E-17	-7,647E-17	100,000						
29	-7,253E-17	-1,648E-16	100,000						
30	-1,033E-16	-2,348E-16	100,000						
31	-1,176E-16	-2,672E-16	100,000						
32	-2,040E-16	-4,637E-16	100,000						
33	-2,909E-16	-6,611E-16	100,000						
34	-3,162E-16	-7,187E-16	100,000						
35	-3,515E-16	-7,988E-16	100,000						
36	-3,939E-16	-8,951E-16	100,000						
37	-4,210E-16	-9,568E-16	100,000						
38	-5,406E-16	-1,229E-15	100,000						
39	-5,796E-16	-1,317E-15	100,000						
40	-6,111E-16	-1,389E-15	100,000						
41	-6,981E-16	-1,587E-15	100,000						
42	-7,848E-16	-1,784E-15	100,000						
43	-1,135E-15	-2,579E-15	100,000						
44	-1,312E-15	-2,981E-15	100,000						

Extraktionsmethode: Hauptkomponentenanalyse.

**Appendix 68 Factor analysis *Calpionella* limestones.**

**Komponentenmatrix<sup>a</sup>**

	Komponente		
	1	2	3
Th	,996		
Nb	,996		
Rb	,995		
Ga	,994		
K2O	,993		,101
Ce	,988		
Hf	,973		,219
Al2O3	,971		,210
Sc	,969		,125
Zr	,967		,223
Cu	,962	-,145	-,220
Cs	,955		-,218
TiO2	,953		,283
Zn	,934	-,301	
Ni	,934		,121
Fe2O3	,933	-,155	,319
V	,915		,169
Pb	,913	-,259	,190
Co	,910	-,125	
CaO	-,908	-,117	,378
LOI	-,884		,405
Cr	,855	-,120	,224
MgO	,794	-,208	,400
La	,775	,267	-,562
SiO2	,775	,173	-,572
Na2O	,769	-,176	,409
P2O5	,705	,260	-,597
Y	,666	,196	-,636
Ta	,638	,589	-,376
Eu		,987	,123
TOC		-,986	-,117
Mo	-,269	,948	
Lu	,272	,941	,114
Tm	-,287	,903	,312
TOTS	-,277	,842	,390
Yb	,613	,661	-,257
As	-,212	-,570	,170
W	-,107	,345	-,255
Ba		-,270	
Sn	,358	,639	,659
Be	,358	,639	,659
U	,347	-,340	,613
MnO		-,196	-,589
Sr	-,189	-,497	,525

Extraktionsmethode: Hauptkomponentenanalyse.

**Komponentenmatrix<sup>a</sup>**

	Komponente		
	1	2	3
Th	,996		
Nb	,996		
Rb	,995		
Ga	,994		
K2O	,993		,101
Ce	,988		
Hf	,973		,219
Al2O3	,971		,210
Sc	,969		,125
Zr	,967		,223
Cu	,962	-,145	-,220
Cs	,955		-,218
TiO2	,953		,283
Zn	,934	-,301	
Ni	,934		,121
Fe2O3	,933	-,155	,319
V	,915		,169
Pb	,913	-,259	,190
Co	,910	-,125	
CaO	-,908	-,117	,378
LOI	-,884		,405
Cr	,855	-,120	,224
MgO	,794	-,208	,400
La	,775	,267	-,562
SiO2	,775	,173	-,572
Na2O	,769	-,176	,409
P2O5	,705	,260	-,597
Y	,666	,196	-,636
Ta	,638	,589	-,376
Eu		,987	,123
TOC		-,986	-,117
Mo	-,269	,948	
Lu	,272	,941	,114
Tm	-,287	,903	,312
TOTS	-,277	,842	,390
Yb	,613	,661	-,257
As	-,212	-,570	,170
W	-,107	,345	-,255
Ba		-,270	
Sn	,358	,639	,659
Be	,358	,639	,659
U	,347	-,340	,613
MnO		-,196	-,589
Sr	-,189	-,497	,525

Extraktionsmethode: Hauptkomponentenanalyse.

a. 3 Komponenten extrahiert

### Appendix 69 Factor analysis *Calpionella* limestones.

	SiO <sub>2</sub>	Al <sub>2</sub> O <sub>3</sub>	Fe <sub>2</sub> O <sub>3</sub>	MgO	CaO	Na <sub>2</sub> O	K <sub>2</sub> O	TiO <sub>2</sub>	MnO	Sc	LOI	Ga	Hf	U	V	W	Y	La	Ce	Eu	Tm	Yb	Lu	Cu
Fe <sub>2</sub> O <sub>3</sub>	<b>-.959</b>	.480																						
CaO	<b>-.983</b>	.449	<b>.962</b>	.727																				
TiO <sub>2</sub>	-.560	.607	.672	.655	.476	<b>.901</b>	-.017																	
MnO	<b>-.976</b>	.425	<b>.965</b>	.717	<b>.998</b>	.456	-.047	.494																
Sc	<b>-.981</b>	.527	<b>.974</b>	.778	<b>.979</b>	.601	-.051	.610	<b>.985</b>															
LOI	<b>-.989</b>	.488	<b>.959</b>	.754	<b>.998</b>	.455	.026	.482	<b>.994</b>	<b>.977</b>														
Ga	-.790	<b>.945</b>	.717	.838	.668	.826	.375	.729	.649	.739	.693													
Nb	-.272	.384	.433	.475	.207	.848	-.317	<b>.913</b>	.242	.378	.203	.471	.721											
Rb	-.330	.609	.211	.186	.226	.186	<b>.953</b>	.201	.178	.192	.251	.605	-.290											
U	<b>-.928</b>	.478	<b>.973</b>	.710	<b>.923</b>	.580	.055	.722	<b>.929</b>	<b>.939</b>	<b>.923</b>	.707	.148											
V	<b>-.904</b>	.736	<b>.922</b>	.855	.843	.804	.080	.811	.839	<b>.906</b>	.849	<b>.906</b>	.050	.888										
Zr	.017	.023	.188	.156	-.046	.466	-.270	.714	-.008	.068	-.045	.083	<b>.983</b>	.307	.220	.576								
Y	<b>-.975</b>	.433	<b>.977</b>	.692	<b>.993</b>	.460	.022	.529	<b>.992</b>	<b>.979</b>	<b>.988</b>	.673	-.142	<b>.948</b>	.863	-.012								
Ce	-.816	.302	<b>.922</b>	.529	.837	.430	-.078	.665	.837	.830	.824	.582	.183	<b>.935</b>	.820	.032	<b>.889</b>	<b>.967</b>						
Eu	<b>-.964</b>	.403	<b>.978</b>	.687	<b>.986</b>	.455	-.002	.552	<b>.989</b>	<b>.972</b>	<b>.982</b>	.643	-.060	<b>.968</b>	.844	.022	<b>.993</b>	.852	.899					
Tm	<b>-.966</b>	.418	<b>.982</b>	.693	<b>.988</b>	.471	-.024	.539	<b>.988</b>	<b>.978</b>	<b>.980</b>	.666	-.134	<b>.939</b>	.873	.029	<b>.997</b>	.882	.895	<b>.986</b>				
Yb	<b>-.972</b>	.440	<b>.988</b>	.706	<b>.987</b>	.480	.017	.567	<b>.986</b>	<b>.976</b>	<b>.982</b>	.683	-.094	<b>.960</b>	.880	.001	<b>.998</b>	.890	.912	<b>.993</b>	<b>.997</b>			
Lu	<b>-.975</b>	.447	<b>.989</b>	.724	<b>.990</b>	.487	-.006	.564	<b>.989</b>	<b>.980</b>	<b>.986</b>	.685	-.098	<b>.956</b>	.882	.014	<b>.997</b>	.878	<b>.901</b>	<b>.993</b>	<b>.997</b>	<b>.999</b>		
TOC	<b>-.982</b>	.447	<b>.962</b>	.728	<b>.1000</b>	.440	-.010	.474	<b>.998</b>	<b>.979</b>	<b>.998</b>	.665	-.205	<b>.921</b>	.842	-.025	<b>.992</b>	.817	.834	<b>.985</b>	<b>.988</b>	<b>.986</b>	<b>.990</b>	
Mo	.247	-.442	-.040	-.151	-.179	.186	-.828	.267	-.117	-.063	-.212	-.360	.650	-.048	-.096	<b>.977</b>	-.145	-.177	-.029	-.103	-.106	-.129	-.122	
Cu	-.836	.554	.862	.733	.810	.811	-.181	.770	.836	<b>.911</b>	.805	.736	.110	.843	.882	.375	.825	.619	.699	.822	.831	.824	.830	
Zn	-.883	.521	<b>.936</b>	.881	.870	.680	-.275	.710	.877	<b>.912</b>	.871	.703	.116	.870	<b>.910</b>	.277	.867	.740	.786	.868	.885	.884	.896	.858
As	<b>-.917</b>	.646	.883	.862	.880	.750	-.117	.677	.894	<b>.945</b>	.889	.781	-.014	.862	.880	.204	.864	.585	.661	.867	.857	.859	.870	<b>.948</b>
	7	7	7	7	7	7	7	7	7	7	7	7	7	7	7	7	7	7	7	7	7	7	7	

### Appendix 70 Korrelations after Pearson (r) for the Keuper sandstones.

Korrelationen																													
SiO <sub>2</sub>	A <sub>2</sub> O <sub>3</sub>	Fe <sub>2</sub> O <sub>3</sub>	MgO	CaO	Na <sub>2</sub> O	P <sub>2</sub> O <sub>5</sub>	MnO	Cr	Sc	LOI	Ba	Co	Cs	Hf	Nb	Sn	Sr	Th	U	V	W	Y	La	Ce	Tm	Yb	TOTS	Mo	
MgO	-.833	.433	<b>.978</b>																										
CaO	<b>-.995</b>	.860	.839	.828																									
MnO	<b>-.936</b>	.634	<b>.981</b>	<b>.962</b>	<b>.928</b>	.605	-.354																						
Cr	-.249	.002	.577	.426	-.202	<b>.922</b>	.130	.471																					
LOI	<b>-.987</b>	<b>.924</b>	.764	.736	<b>.988</b>	.200	-.566	.870	.170	.338																			
Co	-.817	.459	<b>.988</b>	<b>.941</b>	.796	.796	-.231	<b>.961</b>	.681	.378	.725	-.244																	
Cs	-.783	<b>.959</b>	.354	.356	.794	-.291	-.821	.528	-.232	.739	.851	-.264	.315																
Ga	-.649	<b>.940</b>	.167	.136	.656	-.398	.791	.350	-.249	.859	.749	-.414	<b>.146</b>	<b>.966</b>															
Nb	-.365	.134	.621	.465	.328	.864	.280	.533	<b>.918</b>	.477	.316	-.669	.686	-.143	.154														
Rb	<b>.523</b>	<b>.644</b>	.180	.268	.540	-.420	<b>.903</b>	.331	-.446	.589	.546	.242	.138	.822	-.158	-.536													
Sr	-.723	.813	.324	.401	.753	-.400	-.620	.485	-.484	.659	.778	.059	.226	<b>.907</b>	-.712	-.324	.362												
U	-.858	.788	.591	.669	.882	-.111	.596	.715	-.263	.403	.865	.107	.499	.852	-.667	-.140	.586	<b>.947</b>	<b>.978</b>										
V	.890	<b>.980</b>	-.526	-.503	-.899	.092	.615	-.674	.065	.606	<b>.950</b>	.400	-.477	<b>.942</b>	.767	-.121	-.135	<b>.874</b>	<b>.806</b>	.860									
Zr	.591	-.574	-.356	-.380	-.620	.128	-.063	-.437	.246	.357	-.650	.182	-.242	-.513	<b>.995</b>	-.125	-.167	<b>.694</b>	<b>.498</b>	.656	.715	.145							
Y	-.178	-.276	.505	.636	.185	.428	.039	.420	.094	.658	.033	.725	.462	-.192	.211	<b>.151</b>	<b>.935</b>	.014	.380	.268	.198	-.558							
La	.267	-.404	-.196	.003	-.235	-.340	-.050	-.207	.601	.156	-.329	<b>.985</b>	-.269	-.154	.299	-.752	.646	.132	.204	.158	.338	<b>.914</b>	.682						
Ce	.422	-.557	-.293	-.107	-.395	-.307	.066	-.330	-.548	.247	<b>.989</b>	<b>.960</b>	-.351	-.318	.425	.723	.557	-.045	.029	.023	.502	.835	.653	<b>.983</b>					
Eu	.392	.540	-.272	-.077	-.360	-.322	.122	-.307	-.589	.240	<b>.955</b>	<b>.933</b>	-.345	-.306	.322	.719	.587	.006	.025	.025	.463	.868	.657	<b>.984</b>	<b>.992</b>				
Tm	-.214	-.205	.470	.625	.230	.293	-.017	.410	-.058	.538	.084	.786	.406	-.090	.113	<b>.173</b>	<b>.968</b>	.155	.471	.379	.112	<b>.681</b>	<b>.985</b>	.752	.702				
Yb	-.119	-.249	.343	.511	.137	.171	-.069	.294	-.164	.470	-.004	.857	.282	-.096	.201	<b>.314</b>	<b>.933</b>	.149	.438	.342	.438	.342	.438	.169	-.752	<b>.963</b>	.840	.797	<b>.987</b>
Lu	.261	-.632	.111	.252	-.252	.256	.234	-.003	.036	.705	-.395	.852	.086	-.507	.496	-.239	.726	-.284	.009	-.099	.574	<b>.564</b>	<b>.903</b>	.803	.841	.875	<b>.901</b>		
TOC	-.869	<b>.954</b>	.533	.482	.874	-.014	-.481	.665	.034	-.559	<b>.935</b>	-.530	.490	.867	-.823	.266	.030	.787	.698	.771	<b>.980</b>	.123	-.292	-.490	-.639	-.222	-.299		
TOTS	<b>-.920</b>	<b>.596</b>	<b>.988</b>	<b>.974</b>	<b>.911</b>	<b>.827</b>	<b>-.309</b>	<b>.998</b>	<b>.477</b>	<b>.208</b>	<b>.848</b>	<b>.171</b>	<b>.985</b>	<b>.488</b>	<b>.454</b>	<b>.542</b>	<b>.611</b>	<b>.462</b>	<b>.754</b>	<b>.701</b>	<b>.844</b>	<b>.033</b>	<b>.452</b>	<b>.188</b>	<b>-.307</b>	<b>.441</b>	<b>.321</b>		
Mo	-.876	<b>.540</b>	<b>.992</b>	<b>.961</b>	<b>.859</b>	<b>.712</b>	<b>-.317</b>	<b>.987</b>	<b>.586</b>	<b>.284</b>	<b>.792</b>	<b>-.204</b>	<b>.991</b>	<b>.420</b>	<b>.322</b>														

Korrelationen																																				
	SiO <sub>2</sub>	Al <sub>2</sub> O <sub>3</sub>	MgO	CaO	K <sub>2</sub> O	TiO <sub>2</sub>	Cr	Sc	LOI	Co	Cs	Ga	Hf	Nb	Rb	Sn	U	V	W	Zr	Y	Ce	Tm	TOC	Zn											
MgO	-.981	-.779																																		
CaO	-.792	-.977	.719																																	
TiO <sub>2</sub>	.856	.998	-.769	.976	.734																															
Sc	.892	.996	-.811	.969	.720	.994	.548																													
LOI	-.991	-.896	.974	.840	-.446	.889	-.667	-.915																												
Co	.777	.649	-.720	-.496	-.004	.666	.972	.665	-.761																											
Ga	.848	.980	-.769	.978	.752	.986	.462	.985	-.876	.612	.195																									
Hf	.834	.814	-.755	-.718	.290	.838	.817	.833	-.829	.924	.533	.830																								
Rb	.833	.973	-.761	-.966	.829	.966	.359	.976	-.862	.491	.090	.976	.711	-.513																						
Sn	.952	.798	-.929	-.742	.423	.785	.538	.844	-.917	.635	.028	.810	.740	-.639	.825																					
Th	.868	.881	-.801	-.835	.659	.853	.470	.897	-.859	.521	.151	.831	.625	-.401	.902	.896																				
W	.935	.889	-.880	-.815	.391	.902	.758	.910	-.937	.876	.377	.899	.970	-.776	.819	.851	.757	.841																		
Zr	.795	.747	-.708	-.612	.166	.766	.919	.762	-.781	.977	.680	.727	.974	-.614	.610	.682	.929	.700	.922																	
Y	.701	.416	-.706	-.276	-.275	.439	.870	.454	-.665	.915	.455	.426	.818	-.772	.285	.586	.677	.492	.777	.849																
La	.915	.741	-.875	-.610	.117	.749	.901	.772	-.889	.957	.485	.721	.932	-.744	.638	.829	.812	.683	.942	.948	.897															
Ce	.959	.869	-.949	-.830	.415	.876	.631	.892	-.972	.765	.148	.889	.875	-.877	.836	.881	.557	.861	.963	.795	.721															
Eu	.624	.429	-.690	-.407	-.067	.459	.516	.448	-.650	.647	.059	.489	.672	-.959	.357	.468	.268	.682	.705	.594	.794	.776														
Trn	.573	.353	-.584	-.231	.306	.386	.828	.373	-.566	.878	.505	.364	.776	-.778	.193	.397	.610	.542	.710	.803	.960	.652														
Yb	.750	.656	-.725	-.568	.068	.688	.807	.670	-.762	.913	.478	.679	.932	-.838	.527	.590	.704	.779	.900	.906	.903	.847	.927													
Lu	.686	.374	-.702	-.243	.302	.398	.816	.418	-.644	.872	.369	.401	.788	-.778	.260	.593	.622	.444	.753	.807	.994	.711	.945													
TOC	-.963	-.946	.933	.920	-.593	.941	-.561	-.960	.983	-.680	-.135	-.940	-.810	.759	-.934	-.902	-.538	-.875	-.925	-.733	-.555	-.965	-.466													
TOTS	.132	.240	-.196	-.407	.417	.266	-.382	.239	-.201	-.175	-.574	.376	.106	-.468	.342	.116	-.366	.427	.199	-.106	-.056	.362	.042	-.310												
Mo	.923	-.952	.884	.940	-.616	.957	-.539	-.962	.952	-.684	-.153	-.968	-.851	.772	-.934	-.851	-.553	-.912	-.943	-.754	-.564	-.970	-.507	.984												
Ni	.116	.429	-.077	-.586	.889	.412	-.521	.413	-.166	-.402	-.483	.471	-.085	.114	.593	.229	-.249	.261	.050	-.242	-.562	.149	-.602	-.328	.894											
As	.264	.024	-.257	.154	-.607	.047	.835	.034	-.233	.766	.718	-.028	.510	-.399	-.180	.091	.602	.179	.383	.645	.816	.254	.854	-.088	.998											
n	6	6	6	6	6	6	6	6	6	6	6	6	6	6	6	6	6	6	6	6	6	6	6	6	6	6	6	6	6	6	6	6				

Appendix 72 Korrelations after Pearson (r) for the Keuper shales.

Korrelationen																																	
	SiO <sub>2</sub>	Al <sub>2</sub> O <sub>3</sub>	Fe <sub>2</sub> O <sub>3</sub>	CaO	Na <sub>2</sub> O	K <sub>2</sub> O	TiO <sub>2</sub>	P <sub>2</sub> O <sub>5</sub>	Sc	LOI	Co	Cs	Ga	Hf	Nb	Rb	Sn	Ta	Th	V	Y	La	Ce	Tm	Yb								
Fe <sub>2</sub> O <sub>3</sub>	.676	.935																															
O <sub>3</sub>	-.963	-.922	-.824																														
TiO <sub>2</sub>	.753	.960	.864	-.864	.514	.838																											
Sc	.790	.994	.830	-.914	.596	.880	.972	.564																									
LOI	-.973	-.902	-.797	.993	-.698	-.866	-.852	-.474	-.896																								
Cs	.782	.896	.817	-.877	.754	.906	.851	.633	.916	-.882	.799																						
Ga	.795	.981	.884	-.911	.681	.907	.961	.613	.982	-.904	.810	.918																					
Hf	.768	.934	.808	-.869	.506	.842	.962	.587	.939	-.846	.726	.785	.926																				
Nb	.620	.790	.649	-.706	.587	.788	.905	.900	.827	-.722	.906	.792	.863	.839																			
Rb	.774	.908	.814	-.886	.792	.984	.882	.669	.924	-.889	.813	.944	.944	.857	.828																		
Sn	.771	.927	.810	-.880	.724	.880	.859	.436	.908	-.866	.621	.833	.940	.887	.717	.891																	
Ta	.649	.817	.685	-.741	.603	.813	.919	.885	.856	-.751	.915	.817	.878	.875	.991	.851	.742																
Th	.742	.965	.874	-.871	.647	.898	.978	.675	.975	-.862	.862	.882	.985	.950	.903	.937	.912	.923															
U	.787	.804	.612	-.839	.618	.863	.866	.748	.822	-.828	.694	.766	.848	.906	.872	.836	.810	.894	.870														
V	.764	.959	.924	-.871	.430	.787	.954	.541	.963	-.654	.812	.864	.926	.900	.806	.840	.806	.835	.925														
Zr	.717	.923	.799	-.822	.457	.805	.981	.651	.933	-.806	.788	.774	.926	.984	.894	.836	.843	.914	.957	.915													
La	.593	.815	.705	-.707	.596	.819	.918	.870	.856	-.719	.937	.813	.873	.842	.980	.862	.731	.975	.923	.825	.891												
Ce	.580	.818	.720	-.702	.593	.821	.917	.860	.860	-.713	.946	.816	.873	.839	.971	.868	.723	.967	.925	.825	.893	.997											
Eu	.273	.494	.398	-.373	.461	.595	.661	.966	.556	-.400	.887	.579	.600	.561	.893	.631	.397	.871	.680	.555	.950	.885	.884										
Trn	.478	.795	.749	-.639	.605	.818	.864	.841	.832	-.644	.952	.798	.857	.781	.924	.865	.715	.924	.906	.793	.915	.954	.963										
Yb	.530	.851	.792	-.683	.57																												

	Korrelationen																																				
	SiO <sub>2</sub>	Al <sub>2</sub> O <sub>3</sub>	Fe <sub>2</sub> O <sub>3</sub>	CaO	K <sub>2</sub> O	TiO <sub>2</sub>	MnO	Cr	Sc	LOI	Ba	Co	Cs	Ga	Hf	Nb	Rb	Ta	U	V	Y	La	Ce	Eu	Tm	Yb											
Fe <sub>2</sub> O <sub>3</sub>	-,191	,943																																			
Sc	-,282	,969	,910	-,254	,838	,944	-,255	,806																													
LOI	-,924	-,141	-,163	,952	-,002	-,131	,832	,225	-,082																												
Co	-,600	,871	,803	,098	,745	,790	,125	,835	,904	,302	-,494																										
Cs	-,422	,957	,925	-,127	,760	,731	-,107	,899	,911	,081	-,168	,928																									
Ga	-,252	,999	,942	-,315	,846	,835	-,273	,827	,969	-,119	-,132	,881	,964																								
Nb	-,163	,859	,830	-,301	,711	,990	-,290	,700	,951	-,161	-,432	,805	,760	,850	,853																						
Rb	-,346	,945	,817	-,203	,969	,801	-,198	,718	,916	-,022	-,172	,846	,891	,946	,068	,775																					
Sn	-,444	,908	,863	-,081	,899	,848	-,150	,782	,927	,079	-,246	,865	,876	,908	,196	,831	,936																				
Sr	,601	-,139	-,028	-,528	-,233	-,480	-,454	-,268	-,331	-,575	,999	-,494	-,168	-,142	-,360	-,439	-,190																				
Ta	-,236	,912	,832	-,250	,779	,961	-,243	,720	,979	,096	-,428	,887	,842	,908	,499	,972	,853																				
Th	,136	,885	,932	-,606	,609	,770	,595	,699	,851	-,480	-,139	,621	,791	,874	,464	,816	,731	,799																			
V	-,268	,911	,896	-,237	,719	,941	-,183	,772	,974	-,061	-,382	,900	,868	,909	,498	,970	,820	,978	,748																		
Zr	,297	,248	,344	-,369	,023	,621	-,449	,233	,405	-,403	-,339	,159	,099	,223	,996	,650	,057	,493	,710	,506																	
Y	-,401	,692	,683	,040	,575	,924	-,070	,701	,842	,141	,680	,797	,652	,685	,665	,926	,620	,884	,922	,895																	
La	-,171	,868	,919	-,304	,648	,927	-,351	,816	,923	-,169	-,274	,762	,796	,856	,620	,950	,738	,895	,827	,937	,878																
Ce	-,248	,829	,883	-,208	,815	,933	-,247	,802	,913	-,071	-,383	,793	,775	,820	,638	,958	,705	,902	,849	,951	,929	,989															
Eu	-,632	,735	,710	,245	,645	,842	,041	,830	,844	,357	,659	,891	,767	,735	,406	,837	,700	,845	,878	,861	,942	,826	,875														
Tm	-,258	,659	,684	-,059	,513	,909	-,247	,669	,808	-,003	-,563	,692	,591	,646	,761	,916	,558	,845	,938	,862	,975	,904	,940	,891													
Yb	-,086	,648	,671	-,233	,465	,920	-,306	,593	,794	-,162	-,527	,631	,541	,632	,855	,935	,517	,850	,903	,857	,943	,898	,926	,797	,971												
Lu	-,081	,612	,641	-,210	,451	,904	-,316	,547	,769	-,159	-,512	,603	,502	,596	,857	,918	,493	,829	,886	,841	,939	,881	,914	,791	,978	,992											
TOC	-,829	-,343	-,362	,984	-,148	-,259	,819	-,028	-,262	,972	-,574	,104	-,141	-,324	-,396	-,300	-,204	-,257	,001	-,232	,033	-,319	-,215	,218	-,089	-,245											
Mo	-,419	-,338	-,246	,486	-,363	-,231	,912	-,162	-,257	,608	-,414	,052	-,182	-,314	-,178	-,198	-,327	-,208	-,250	-,111	-,005	-,259	-,144	-,010	-,145	-,144											
Pb	-,267	,790	,722	-,122	,603	,886	,265	,785	,866	-,018	-,556	,789	,742	,781	,595	,892	,679	,895	,910	,853	,879	,850	,852	,848	,864	,866											
As	-,505	,826	,861	,066	,601	,777	-,141	,971	,856	,193	-,381	,855	,872	,823	,353	,799	,713	,803	,826	,847	,829	,887	,890	,917	,816	,735											
n	62	62	62	62	62	62	62	62	62	62	62	62	62	62	62	62	62	62	62	62	62	62	62	62	62	62	62	62	62	62							
	8	8	8	8	8	8	8	8	8	8	8	8	8	8	8	8	8	8	8	8	8	8	8	8	8	8	8	8	8	8	8						

#### Appendix 74 Korrelations after Pearson (r) for the Jurassic sandstones.

	Korrelationen																																						
	SiO <sub>2</sub>	Al <sub>2</sub> O <sub>3</sub>	Fe <sub>2</sub> O <sub>3</sub>	CaO	K <sub>2</sub> O	TiO <sub>2</sub>	Cr	Sc	Be	Co	Cs	Ga	Hf	Nb	Rb	Sn	Ta	Th	V	Y	La	Eu	Tm	Yb	Lu	Zn													
Fe <sub>2</sub> O <sub>3</sub>	,708	,855																																					
CaO	-,963	-,813	-,797																																				
K <sub>2</sub> O	,612	,959	,769	-,751																																			
TiO <sub>2</sub>	,643	,987	,864	-,782	,933																																		
Sc	,679	,977	,846	-,808	,955	,967	-,632																																
LOI	-,982	-,795	-,802	,977	-,731	,758	-,759	-,790																															
Co	,734	,750	,710	-,777	,748	,705	,839	,728	,455																														
Cs	,600	,945	,752	-,736	,977	,924	,663	,928	,617	,750																													
Ga	,659	,996	,848	-,797	,962	,985	,671	,972	,661	,747	,950																												
Hf	,450	,795	,834	-,583	,692	,870	-,402	,775	,669	,507	,709	,800																											
Nb	,677	,973	,847	-,802	,916	,987	,645	,952	,634	,726	,919	,968	,655																										
Rb	,618	,969	,790	-,758	,990	,946	,669	,950	,640	,748	,979	,975	,720	,928																									
Sn	,406	,859	,642	-,579	,852	,849	,509	,850	,495	,553	,839	,859	,691	,811	,843																								
Ta	,648	,933	,800	-,777	,888	,952	,599	,916	,664	,697	,890	,927	,827	,958	,895	,827																							
Th	,611	,963	,883	-,751	,903	,982	,587	,943	,705	,698	,904	,965	,912	,968	,920	,843	,931																						
V	,572	,864	,882	-,698	,802	,907	,504	,856	,759	,631	,813	,865	,923	,882	,822	,780	,871	,821																					
W	,639	,825	,779	-,744	,790	,797	,605	,793	,595	,736	,788	,825	,631	,789	,813	,720	,772	,796	,712																				
Zr	,456	,781	,850	-,584	,																																		

	SiO <sub>2</sub>	A <sub>2</sub> O <sub>3</sub>	Fe <sub>2</sub> O <sub>3</sub>	MgO	CaO	K <sub>2</sub> O	TiO <sub>2</sub>	Sc	LOI	Be	Cs	Ga	Hf	Nb	Rb	Ta	Th	Zr	Y	La	Eu	Tm	Yb
Fe <sub>2</sub> O <sub>3</sub>	-102	<b>.938</b>																					
MgO	-220	<b>.979</b>	<b>.943</b>																				
CaO	<b>-.938</b>	-227	-233	-124																			
K <sub>2</sub> O	-123	<b>.992</b>	<b>.956</b>	<b>.978</b>	-225																		
TiO <sub>2</sub>	-181	<b>.987</b>	<b>.908</b>	<b>.966</b>	-163	<b>.981</b>																	
Sc	-200	<b>.984</b>	<b>.928</b>	<b>.980</b>	-144	<b>.983</b>	<b>.973</b>																
LOI	<b>-.982</b>	-063	-081	.036	<b>.984</b>	-062	.001	.016															
Cs	-111	<b>.987</b>	<b>.959</b>	<b>.968</b>	-237	<b>.993</b>	<b>.966</b>	<b>.973</b>	-.071	.684													
Ga	-116	<b>.993</b>	<b>.920</b>	<b>.967</b>	-229	<b>.984</b>	<b>.982</b>	<b>.976</b>	-.065	.695	<b>.977</b>												
Hf	-197	<b>.966</b>	<b>.874</b>	<b>.943</b>	-141	<b>.959</b>	<b>.984</b>	<b>.953</b>	.023	.683	<b>.948</b>	<b>.962</b>											
Nb	-075	<b>.981</b>	<b>.926</b>	<b>.949</b>	-266	<b>.969</b>	<b>.977</b>	<b>.961</b>	-.105	.678	<b>.962</b>	<b>.975</b>	<b>.958</b>										
Rb	-114	<b>.990</b>	<b>.963</b>	<b>.976</b>	-235	<b>.997</b>	<b>.971</b>	<b>.980</b>	-.071	.676	<b>.997</b>	<b>.981</b>	<b>.953</b>	<b>.967</b>									
Sn	.032	.670	.643	.634	-275	.692	.684	.666	-.146	<b>1.000</b>	.684	.695	.683	.678	.676								
Ta	.003	<b>.920</b>	.851	.871	-324	<b>.914</b>	<b>.920</b>	.895	-.167	.710	<b>.901</b>	<b>.931</b>	<b>.912</b>	<b>.947</b>	<b>.911</b>								
Th	-169	<b>.987</b>	<b>.926</b>	<b>.971</b>	-177	<b>.983</b>	<b>.985</b>	<b>.973</b>	-.011	.651	<b>.978</b>	<b>.976</b>	<b>.975</b>	<b>.969</b>	<b>.982</b>	<b>.907</b>							
Zr	-202	<b>.970</b>	.887	<b>.958</b>	-137	<b>.966</b>	<b>.993</b>	<b>.960</b>	.024	.700	<b>.942</b>	<b>.967</b>	<b>.977</b>	<b>.964</b>	<b>.952</b>	<b>.906</b>	<b>.970</b>						
La	-490	.876	.820	<b>.909</b>	-176	.886	.895	<b>.912</b>	.330	.587	.864	.871	.890	.837	.877	.770	<b>.903</b>	<b>.897</b>	<b>.932</b>				
Ce	-219	<b>.928</b>	<b>.915</b>	<b>.942</b>	-110	<b>.944</b>	<b>.898</b>	<b>.952</b>	.043	.598	<b>.944</b>	<b>.926</b>	.885	.880	<b>.951</b>	.822	<b>.925</b>	.872	.810	<b>.914</b>			
Tm	-169	.734	.641	.724	-088	.733	.799	.724	.039	.802	.693	.746	.779	.750	.697	.732	.729	.839	.635	.700	<b>.991</b>		
Yb	.313	.852	.770	.863	.012	<b>.855</b>	<b>.899</b>	.864	.157	.759	.817	.860	.880	.847	.827	.805	.854	<b>.928</b>	.833	.879	<b>.982</b>	<b>.950</b>	
Lu	.271	.819	.730	.823	-.017	.821	.873	.826	.124	.790	.783	.831	.852	.817	.790	.786	.819	<b>.905</b>	.768	.826	<b>.995</b>	<b>.978</b>	<b>.992</b>
TOC	<b>-.960</b>	.077	.050	.172	<b>.918</b>	.079	.165	.142	<b>.946</b>	-.064	.044	.074	.176	.048	.056	-.027	.124	.203	.550	.430	.268	.236	.335
TOTS	.078	.598	.568	.598	-134	.604	.661	.585	-.033	.717	.569	.599	.642	.625	.571	.619	.589	.700	.457	.540	.878	<b>.908</b>	.815
n	29	29	29	29	29	29	29	29	29	29	29	29	29	29	29	29	29	29	29	29	29	29	29

#### Appendix 76 Korrelations after Pearson (r) for the cherts

	SiO <sub>2</sub>	A <sub>2</sub> O <sub>3</sub>	Fe <sub>2</sub> O <sub>3</sub>	MgO	CaO	Na <sub>2</sub> O	K <sub>2</sub> O	TiO <sub>2</sub>	P <sub>2</sub> O <sub>5</sub>	Cr	Sc	LOI	Be	Co	Cs	Ga	Hf	Nb	Rb	Th	V	Zr	Y	Ce	Eu	Tm	Lu	TOC	Cu	Pb	
Fe <sub>2</sub> O <sub>3</sub>	0.511	<b>.988</b>																													
MgO	0.331	<b>.863</b>	<b>.908</b>																												
CaO	<b>-.967</b>	<b>-.797</b>	<b>-.707</b>	<b>-.531</b>																											
Na <sub>2</sub> O	.288	.831	.867	<b>.955</b>	<b>-.495</b>																										
K <sub>2</sub> O	.709	<b>.989</b>	<b>.961</b>	<b>.822</b>	<b>-.861</b>	<b>.803</b>																									
TiO <sub>2</sub>	.560	<b>.994</b>	<b>.989</b>	.855	<b>-.748</b>	<b>.840</b>	<b>.979</b>																								
P <sub>2</sub> O <sub>5</sub>	<b>.929</b>	.540	.441	.0249	.891	.174	.632	.468																							
Cr	.546	<b>.908</b>	<b>.895</b>	<b>.650</b>	<b>-.689</b>	<b>.577</b>	<b>.888</b>	<b>.911</b>	.527																						
Sc	.688	<b>.974</b>	<b>.958</b>	.888	<b>-.838</b>	<b>.839</b>	<b>.973</b>	<b>.949</b>	.570	.823																					
LOI	<b>-.974</b>	<b>-.769</b>	<b>-.680</b>	<b>-.521</b>	<b>.992</b>	<b>-.469</b>	<b>-.837</b>	<b>-.713</b>	<b>-.887</b>	<b>-.678</b>	<b>-.828</b>																				
Co	.655	.880	.855	.814	<b>-.792</b>	<b>.866</b>	<b>.908</b>	.863	.571	.680	.885	<b>-.771</b>	.261																		
Cs	.883	.871	.805	.640	<b>-.597</b>	<b>.627</b>	<b>.933</b>	<b>.844</b>	.835	.788	.884	<b>-.950</b>	.255	.883																	
Ga	.712	<b>.968</b>	<b>.965</b>	.839	<b>-.864</b>	<b>.800</b>	<b>.959</b>	<b>.973</b>	.652	.877	<b>-.977</b>	<b>-.838</b>	.393	.998	<b>.924</b>																
Hf	.618	<b>.992</b>	<b>.979</b>	.857	.795	<b>.850</b>	<b>.990</b>	<b>.993</b>	.549	.881	<b>.982</b>	<b>-.761</b>	.493	<b>.903</b>	<b>.883</b>	<b>.988</b>															
Nb	.759	.774	<b>.934</b>	.767	<b>-.896</b>	<b>.751</b>	<b>.995</b>	<b>.961</b>	.694	.888	<b>.954</b>	<b>-.870</b>	.373	<b>.900</b>	<b>.958</b>	<b>.990</b>	<b>.976</b>														
Rb	.743	<b>.974</b>	<b>.939</b>	.802	<b>-.884</b>	<b>.795</b>	<b>.996</b>	<b>.962</b>	.670	.862	<b>.927</b>	<b>-.861</b>	.390	<b>.927</b>	<b>.954</b>	<b>.990</b>	<b>.981</b>	<b>.996</b>													
Sn	.002	.0425	.0437	.0378	<b>-.147</b>	<b>.444</b>	.0407	.0489	.0000	.0376	.0359	-.090	<b>.1000</b>																		
Th	.749	<b>.978</b>	<b>.946</b>	.808	<b>-.889</b>	.767	<b>.994</b>	<b>.962</b>	.689	.878	<b>.973</b>	<b>-.867</b>	.401	.084	<b>.943</b>	<b>.997</b>	<b>.978</b>	<b>.992</b>	<b>.982</b>												
U	-.101	.502	.545	.385	<b>-.065</b>	.042	.445	.563	<b>-.234</b>	.264	.321	.390	<b>-.052</b>	.0375	.274	<b>.224</b>	<b>.385</b>	.477	.408	.400	.371										
V	.609	<b>.926</b>	<b>.913</b>	.718	<b>-.761</b>	<b>.647</b>	<b>.930</b>	<b>.933</b>	.645	<b>.946</b>	.864	<b>-.732</b>	.451	.746	<b>.859</b>	<b>.934</b>	<b>.925</b>	<b>.932</b>	<b>.917</b>	<b>.937</b>											
W	.153	<b>-.198</b>	<b>-.235</b>	<b>-.0374</b>	<b>-.005</b>	<b>-.443</b>	<b>-.112</b>	<b>-.184</b>	.308	<b>.051</b>	<b>-.200</b>	<b>-.088</b>	<b>-.010</b>	<b>-.275</b>	<b>-.098</b>	<b>-.135</b>	<b>-.185</b>	<b>-.073</b>	<b>-.090</b>	<b>-.073</b>	<b>-.110</b>										
Zr	.603	<b>.995</b>	<b>.984</b>	.839	<b>-.783</b>	<b>.816</b>	<b>.984</b>	<b>.996</b>	<b>.947</b>	<b>.913</b>	<b>.951</b>	<b>-.745</b>	.463	.870	<b>.865</b>	<b>.984</b>	<b>.994</b>	<b>.973</b>	<b>.970</b>	<b>.973</b>	<b>.944</b>										
Y	<b>.915</b>	.501	.593	.209	<b>-.875</b>	.149	.581	.444	<b>.914</b>	.423	.551	<b>-.853</b>	.071	.492	.740	.607	.495	.643	.609	.636	.541	.505									
La	<b>.968</b>	.612	.503	.306	<b>.948</b>	.280	.704	.565	<b>.964</b>	.535	.649	<b>-.931</b>	.078	.646	.876	.714	.626	.762	.741	.749	.652	.616	<b>.956</b>								
Ce	.811	<b>.949</b>	<b>.903</b>	.0771	<b>-.926</b>	.753	<b>.978</b>	<b>.921</b>	.705	.825	<b>.965</b>	<b>-.918</b>	.256	<b>.917</b>	<b>.962</b>	<b>.972</b>	<b>.943</b>	<b>.983</b>	<b>.984</b>	<b>.977</b>	.077	.866	<b>.932</b>	.677							
Tm	-.240	<b>-.294</b>	<b>-.304</b>	<b>-.270</b>	<b>-.</b>																										

## APPENDIX 5 SAMPLE LIST

LT33	1028,3m	marlstone	
LT33	1028,3m	sandstone	
LT33	1075,9m	marlstone	
LT33	1103,6m	marlstone	
LT33	1103,6m	siltstone	
LT33	1172,8m	marlstone	
LT33	1232,3m	shale	
LT33	1232,3m	siltstone	
LT33	1291,5m	shale	
LT33	1338,0m	marlstone	
LT33	1338,0m	shale	
LT33	1380,5m	sandstone	
LT33	1422,1m	sandstone	
LT33	1458,5m	sandstone	
LT33	1498,5m	sandstone	
LT33	1498,5m	siltstone	
LT33	1498,5m	shale	
LT33	1535,0m	sandstone	
LT33	1535,0m	shale	
LT33	1554,4m	siltstone	
LT33	1554,4m	shale/marlstone	
LT33	1693,0m	siltstone	
LT33	1600,4m	sandstone	
LT33	1600,4m	shale	
LT33	1739,0m	marlstone	
LT33	1739,0m	shale/marlstone	
LT33	1739,0m	siltstone	
LT33	1780,0m	marlstone	
LT33	1831,0m	shale	
LT33	1831,0m	shale	
LT33	1850,0m	picrite	
LT33	1862,4m	picrite	
LT33	1874,0m	shale	
LT33	1874,0m	marlstone	
LT33	1874,0m	sandstone	
LT33	1893,4m	sandstone	
LT33	1893,4m	shale	
LT33	1893,4m	shale	
LT33	1900,0m	sandstone	
LT33	1900,0m	picrite	
LT33	1923,4m	siltstone	
LT33	1923,4m	shale	
LT33	1939,4m	shale	

LT33	1939,4m	shale
LT33	1962,4m	shale
LT33	1962,4m	shale
LT33	1981,4m	shale
LT33	1981,4m	shale
LT33	2005,4m	siltstone
LT33	2023,7m	shale
LT33	2056,2m	siltstone
LT33	2056,2m	shale
LT33	2074,4m	siltstone
LT33	2074,4m	shale
LT33	2113,4m	sandstone
LT33	2113,4m	siltstone
LT33	2131,7m	sandstone
LT33	2131,7m	shale
LT33	2131,7m	siltstone
LT33	2165,0m	shale
LT33	2165,0m	shale
LT33	2165,0m	chert nodule
LT33	2181,5m	sandstone
LT33	2181,5m	shale
LT33	2181,5m	shale
LT33	2211,5m	calcareous marlstone/marlstone
LT33	2211,5m	siltstone
LT33	2211,5m	shale
LT33	2229,0m	marlstone
LT33	2244,5m	sandstone
LT33	2270,5m	sandstone
LT33	2285,5m	sandstone
LT33	2299,5m	calcareous marlstone/marlstone
LT33	2313,0m	calcareous marlstone/marlstone
LT33	2331,0m	calcareous marlstone/marlstone
LT33	2375,0m	sandstone
LT33	2401,0m	sandstone
LT33	2418,1m	calcareous marlstone/marlstone
LT33	2451,6m	calcareous marlstone/marlstone
LT33	2475,3m	argillaceous limestone
LT33	2505,2m	calcareous marlstone/marlstone
LT33	2535,1m	calcareous marlstone/marlstone
LT33	2552,0m	shale
LT33	2552,0m	chert nodule
LT33	2552,0m	sandstone
LT33	2552,0m	marlstone
LT33	2576,5m	shale/marlstone
LT33	2576,5m	shale
LT33	2576,5m	shale/marlstone

LT33	2592,2m	marlstone
LT33	2592,2m	marlstone/limestone
LT33	2592,2m	calcareous marlstone/marlstone
LT33	2609,2m	calcareous marlstone/marlstone
LT33	2645,0m	calcareous marlstone/marlstone
LT33	2666,3m	calcareous marlstone/marlstone
LT33	2694,9m	shale
LT33	2694,9m	sandstone
LT33	2713,1m	shale
LT33	2713,1m	calcareous marlstone/marlstone
LT33	2731,3m	calcareous marlstone/marlstone
LT33	2748,2m	calcareous marlstone/marlstone
LT33	2748,2m	shale
LT33	2748,2m	shale
LT33	2775,5m	shale/marlstone
LT33	2775,5m	chert nodule
LT33	2775,5m	marlstone
Rs-Angermayerg.	256,39	calcareous marlstone/marlstone
Rs-Angermayerg.	255,39	calcareous marlstone/marlstone
Rs-Angermayerg.	254,39	calcareous marlstone/marlstone
Rs-Angermayerg.	253,39	calcareous marlstone/marlstone
Rs-Angermayerg.	251,93	calcareous marlstone/marlstone
Rs-Angermayerg.	250,43	calcareous marlstone/marlstone
Rs-Angermayerg.	247,43	calcareous marlstone/marlstone
Rs-Angermayerg.	245,93	calcareous marlstone/marlstone
Rs-Angermayerg.	242,93	calcareous marlstone/marlstone
Rs-Angermayerg.	239,93	calcareous marlstone/marlstone
Rs-Angermayerg.	235,43	calcareous marlstone/marlstone
Rs-Angermayerg.	330,09	calcareous marlstone/marlstone
Rs-Angermayerg.	227,93	calcareous marlstone/marlstone
Rs-Angermayerg.	224,93	calcareous marlstone/marlstone
Rs-Angermayerg.	220,47	calcareous marlstone/marlstone
Rs-Angermayerg.	217,43	calcareous marlstone/marlstone
Rs-Angermayerg.	209,93	calcareous marlstone/marlstone
Rs-Angermayerg.	206,92	calcareous marlstone/marlstone
Rs-Angermayerg.	200,93	calcareous marlstone/marlstone
Rs-Angermayerg.	198,85	calcareous marlstone/marlstone
LT31	810,5m	shale
LT31	810,5m	shale
LT31	841,5m	limestone
LT31	841,5m	shale
LT31	841,5m	marlstone
LT31	857,0m	siltstone
LT31	857,0m	shale
LT31	857,0m	shale
LT31	869,5m	shale

LT31	869,5m	shale
LT31	869,5m	limestone
LT31	886,0m	siltstone
LT31	886,0m	shale
LT31	886,0m	shale
LT31	898,0m	marlstone
LT31	898,0m	shale
LT31	898,0m	shale
LT31	898,0m	chert nodule
LT31	917,5m	sandstone
LT31	917,5m	siltstone
LT31	932,5m	siltstone
LT31	932,5m	shale
LT31	932,5m	shale
LT31	944,5m	sandstone
LT31	944,5m	shale
LT31	962,5m	shale
LT31	962,5m	shale
LT31	975,5m	siltstone
LT31	980,5m	siltstone
LT31	980,5m	shale
LT31	993,5m	marlstone
LT31	993,5m	shale
LT31	993,5m	limestone
LT31	1008,5m	marlstone
LT31	1008,5m	shale
LT31	1021,5m	shale
LT31	1021,5m	shale
LT31	1025,5m	marlstone
LT31	1039,5m	marlstone
LT31	1039,5m	shale
LT31	1054,5m	marlstone
LT31	1054,5m	shale
LT31	1073,5m	calcareous marlstone/marlstone
LT31	1073,5m	marlstone
LT31	1087,5m	shale
LT31	1087,5m	marlstone
LT31	1101,5m	marlstone
LT31	1101,5m	shale
LT31	1101,5m	shale
LT31	1119,5m	shale
LT31	1119,5m	shale
LT31	1119,5m	shale
LT31	1133,5m	shale
LT31	1133,5m	shale
LT31	1133,5m	siliceouslimestone

LT31	1133,5m	sandstone
LT31	1133,5m	calcareous marlstone/marlstone
LT31	1149,5m	shale
LT31	1149,5m	marlstone
LT31	1164,5m	shale
LT31	1164,5m	shale
LT31	1164,5m	sandstone
LT31	1177,5m	shale
LT31	1188,5m	sandstone
LT31	1188,5m	marlstone
LT31	1188,5m	shale
LT31	1200,0m	sandstone
LT31	1201,5m	marlstone
LT31	1201,5m	shale
LT31	1215,5m	sandstone
LT31	1215,5m	shale
LT31	1218,5m	coal
LT31	1219,5m	sandstone
LT31	1219,5m	shale
LT31	1257,7m	sandstone
LT31	1257,7m	shale
LT31	1277,2m	shale
LT31	1277,2m	sandstone
LT31	1294m	calcareous marlstone/marlstone
LT31	1308,0m	calcareous marlstone/marlstone
LT31	1317m	shale
LT31	1326,4m	shale
LT31	1326,4m	calcareous marlstone/marlstone
LT31	1326,4m	marlstone
LT31	1348m	marlstone
LT31	1364,3m	chert nodule
LT31	1366,9m	shale
LT31	1366,9m	shale
LT31	1366,9m	calcareous marlstone/marlstone
LT31	1381,2m	marlstone
LT31	1385m	sandstone
Rs-Veitingergasse	0m	limestone
Rs-Veitingergasse	1m	limestone
Rs-Veitingergasse	4m	siliceouslimestone
Rs-Veitingergasse	9m	siliceouslimestone
Rs-Veitingergasse	12m	limestone
Rs-Veitingergasse	14m	limestone
Rs-Veitingergasse	14m	shale
Rs-Veitingergasse	14m	chert nodule
Rs-Veitingergasse	23m	limestone
Rs-Veitingergasse	23m	limestone

Rs-Veitingergasse	23m	marlstone	
Rs-Veitingergasse	34,6m	limestone	
Rs-Veitingergasse	34,6m	marlstone	
Rs-Veitingergasse	34,6m	siltstone	
Rs-Veitingergasse	34,6m	limestone	
Rs-Veitingergasse	35,6m	siliceouslimestone	
Rs-Veitingergasse	39,6m	limestone	
Rs-Veitingergasse	40,6m	limestone	
Rs-Veitingergasse	40,6m	siliceouslimestone	
Rs-Veitingergasse	42,2m	shale	
Rs-Veitingergasse	42,2m	shale	
Rs-Veitingergasse	42,2m	marlstone	
Rs-Veitingergasse	42,2m	chert nodule	
Rs-Veitingergasse	45,2m	limestone	
Rs-Veitingergasse	45,2m	shale	
Rs-Veitingergasse	45,2m	shale	
Lainz Tiergarten	08/14	Doppelklippe west Hohenauer Wiese	limestone
Lainz Tiergarten	08/20	Hohenauer Wiese	sandy limestone
Lainz Tiergarten	08/21	Hohenauer Wiese	sandy limestone
Lainz Tiergarten	08/22	Hohenauer Wiese	sandy limestone
Lainz Tiergarten	08/23	Doppelkl. west Hohenauer W.	limestone
Maurer Wald	08/24	north Schießstätte	sandy limestone
St. Veit	08/25	Glasauer Steinbruch	sandy marlstonelimestone
Maurer Wald	08/26	Antonshöhe	siliceous limestone
Maurer Wald	08/27	Antonshöhe	siliceous limestone
Maurer Wald	08/28	Antonshöhe	siliceous limestone
St. Veit	08/29	Roter Berg	sandy limestone
Lainz Tiergarten	08/30	Stockwiese	limestone
Lainz Tiergarten	08/31	Stockwiese	marlstone/limestone
Lainz Tiergarten	08/32	Stockwiese	limestone
Lainz Tiergarten	08/33	Stockwiese	limestone
Lainz Tiergarten	08/34	Stockwiese	limestone
Lainz Tiergarten	08/35	Stockwiese	limestone
Lainz Tiergarten	08/36	Stockwiese	limestone
Lainz Tiergarten	08/37	Stockwiese	limestone
Lainz Tiergarten	08/38	Stockwiese	limestone
Lainz Tiergarten	08/39	Stockwiese	limestone
Lainz Tiergarten	08/40	bei Kleefrische Wiese	sandstone
Lainz Tiergarten	08/41	bei Kleefrische Wiese	limestone
Lainz Tiergarten	08/42	bei Kleefrische Wiese	limestone
Lainz Tiergarten	08/43	bei Kleefrische Wiese	limestone
Lainz Tiergarten	08/44	bei Kleefrische Wiese	limestone
Lainz Tiergarten	08/50	Inzersdorfer Wald	sandy limestone
Lainz Tiergarten	08/51	Inzersdorfer Wald	limestone
Lainz Tiergarten	08/52	Inzersdorfer Wald	marlstone/limestone
Lainz Tiergarten	08/53	Inzersdorfer Wald	limestone

Lainz Tiergarten	08/54	Inzersdorfer Wald	limestone
Lainz Tiergarten	08/60	westlich Teichhaus	limestone
Lainz Tiergarten	08/61	westlich Teichhaus	limestone
Lainz Tiergarten	08/65	Saulackenmais	limestone
Lainz Tiergarten	08/68	Widpretwiese	limestone + chert
Lainz Tiergarten	08/70	Widpretwiese	limestone+ chert
ExOmV2010	H1	Hinterbrühl	Keuper
ExOmV2010	H2	Hinterbrühl	limestone
ExOmV2010	GU2	Gutenbachtal	sandstone
ExOmV2010	GU3	Gutenbachtal (bei Blaschke)	chert
ExOmV2010	GU1	Gutenbachtal	limestone
ExOmV2010	GR1	Groisbach	Keuper
ExOmV2010	GR2	Groisbach	marlstone
ExOmV2010	GR4	Groisbach	Gryphaea
ExOmV2010	G4	Gemeindeberggasse 36	marlstone
ExOmV2010	G3	Gemeindeberggasse 36	Keuper
ExOmV2010	G2	Gemeindeberggasse 105	siliceous limestone
ExOmV2010	G1	Gemeindeberggasse 105	siliceous limestone
Karp 09	Kp1	Pechgraben/Konradsheimfm.	
Karp Ex 09	Kp2	Pechgraben/Scheibsbachfm.	
Karp Ex 09	Kp3	Pechgraben/Blassensteinsch.	
Karp Ex 09	Kp4	Steinbruch Reidl 1	chert Base
Karp Ex 09	Kp5	Steinbruch Reidl 2	chert Base
Karp Ex 09	Kp6	Steinbruch Reidl 3	chert Med.
Karp Ex 09	Kp7	Steinbruch Reidl 4	siliceous limestone hellgrau
Karp Ex 09	Kp8	Lampelsbergsch.1	siliceous limestone grau
Karp Ex 09	Kp9	Lampelsbergsch.2	chert
Karp Ex 09	Kp10	Lampelsbergsch.3	chert
Karp Ex 09	Kp11	Posidonienmarlstone Klauskogel	
Karp Ex 09	Kp12	Haselbachgraben	
Karp Ex 09	Kp13	Arzberggraben Blassensteinsch.	
Karp Ex 09	Kp14	Myjava1	limestone
Karp Ex 09	Kp15	Myjava2	chert
Karp Ex 09	Kp16	Brinze pod Javorinov 1	limestone
Karp Ex 09	Kp17	Brinze pod Javorinov 2	siltstone
Karp Ex 09	Kp18	Brinze pod Javorinov 3	siltstone
Karp Ex 09	Kp19	Brinze pod Javorinov 4	limestone
Karp Ex 09	Kp20	Brinze pod Javorinov 5	limestone
Karp Ex 09	Kp21	Turá Lúka 1	chert
Karp Ex 09	Kp22	Turá Lúka 2	chert
Karp Ex 09	Kp23	Turá Lúka 3	chert
Karp Ex 09	Kp24	Podbranc 1	limestone/marlstone
Karp Ex 09	Kp25	Podbranc 2	siltstone
Karp Ex 09	Kp26	Podbranc 3	siliceous limestone
Karp Ex 09	Kp27	Dolny Mlyn 1	shale/marlstone
Karp Ex 09	Kp28	Dolny Mlyn 2	marlstone

Karp Ex 09	Kp29	Dolny Mlyn 3	limestone
Karp Ex 09	Kp30	Krasnik	dolomite
Karp Ex 09	Kp31	Antonhöhe	weißAptychenschichten
Karp Ex 09	KP32	Antonshöhe	rote Aptychenschichten
Zazriva 11	Z1	Keuper sandstone	
Zazriva 11	Z2	Kössen limestone	
Zazriva 11	Z3	Liassic sandstone	
Zazriva 11	Z4	spotted marl	
Zazriva 11	Z5	spotted limestone	
Zazriva 11	Z6	silic. limestone	
Zazriva 11	Z7	chert	
Zazriva 11	Z8	chert	
Zazriva 11	Z9	chert	
Zazriva 11	Z10	calpionel. limestone	
Zazriva 11	Z11	neoc. limestone	
Sk 11	Drietoma 1	shale	
Sk 11	Drietoma 2	sandstone	
Sk 11	Drietoma 3	sandstone	
Sk 11	Drietoma 4	breccia	
Sk 11	Drietoma 5	liassic sandstone	
Sk 11	Drietoma 6	liassic sandstone	
Sk 11	Drietoma 6a	liassic shale	
Sk 11	Drietoma 7	marlstone	
Sk 11	Drietoma 8	Crinoidenlimestone	
Sk 11	Drietoma 9	limestone	
Sk 11	P10	sandstone	
Sk 11	P11	Keuper	
Sk 11	P11a	Keuper shale red	
Sk 11	P12	limestone	
Sk 11	P13	sandstone	
Sk 11	P14	chert	
Sk 11	P15	limestone	
Sk 11	P16	limestone	
Sk 11	P17	chert	
Sk 11	P18	sandstone	
Sk 11	P19	marlstone	
Sk 11	P20	chert	
Sk 11	P21	marlstone	
Sk 11	P22	chert	
Sk 11	P23	limestone	
Sk 11	P24	chert	
Sk 11	P25	limestone	
Geochemistry calculation no.	Sample site	Label	
1	LT/St.Veit	1133,5 m LT33 Radiol,	

2	LT/St.Veit	1900 m LT33 Sandst gr fein	
3	LT/St.Veit	2074,4 m LT33 marlstone	
4	LT/St.Veit	2165 m LT33 Radiol,	
5	LT/St.Veit	33/2165marlstone	
6	LT/St.Veit	33/2181calcareous marlstone/marlstone	
7	LT/St.Veit	33/2211,5calcareous marlstone/marlstone	
8	LT/St.Veit	33/2211,5schw tst	
9	LT/St.Veit	33/2270calcareous marlstone/marlstone	
10	LT/St.Veit	33/2299,5calcareous marlstone/marlstone	
11	LT/St.Veit	2313 m LT33 AmmnFm	
12	LT/St.Veit	33/2331calcareous marlstone/marlstone	
13	LT/St.Veit	2401,2 m LT33 Crinsplimestone	
14	LT/St.Veit	LT33 2451 KM	
15	LT/St.Veit	33/2525calcareous marlstone/marlstone	
16	LT/St.Veit	LT33 2552 HAST	
17	LT/St.Veit	LT33 2552 limestone sandy	
18	LT/St.Veit	LT33 2576 TST	
19	LT/St.Veit	LT33 2592 TST	
20	LT/St.Veit	LT33 2592 KM	
21	LT/St.Veit	33/2592gr Tm	
22	LT/St.Veit	33/2666,3calcareous marlstone/marlstone	
23	LT/St.Veit	33/2694,9calcareous marlstone/marlstone	
24	LT/St.Veit	LT33 2713 TST	
26	LT/St.Veit	LT33 2748 M	
27	LT/St.Veit	LT33 2775 HST	
28	LT/St.Veit	LT33 2775 KM	
29	LT/St.Veit	33/ 2775,5Km	
30	LT/St.Veit	33/ 2775,3tst grau	
31	LT/St.Veit	LT31 1385 sandstone	
32	LT/St.Veit	31/1381,2calcareous marlstone/marlstone	
33	LT/St.Veit	LT31 1366 M	
34	LT/St.Veit	LT31 1366 TST	
35	LT/St.Veit	31/1364,3marlstone	
36	LT/St.Veit	LT31 1364 HST	
37	LT/St.Veit	31/1257tst rot	
38	LT/St.Veit	LT31 1326 KM	
39	LT/St.Veit	LT31 1326 TST	
40	LT/St.Veit	LT31 1308 KM	
41	LT/St.Veit	LT31 1277 sandstoneKeuper	
42	LT/St.Veit	LT31 1277 TSTKeuper	
43	LT/St.Veit	LT31 1219,5 sandstoneKeuper fein	
44	LT/St.Veit	31/1219tst rot	
45	LT/St.Veit	31/1201,5marlstone	
46	LT/St.Veit	1188,5 m LT31 calcareous marlstone/marlstone	
47	LT/St.Veit	1188,5 m LT31 SandstKeuper fein	
48	LT/St.Veit	31/1188,5schw tst	

49	LT/St.Veit	1164,5 m LT31 AKST	
50	LT/St.Veit	31/1133,5calcareous marlstone/marlstone	
51	LT/St.Veit	31/1133,5tst rot	
52	LT/St.Veit	31/1133,5tst schw	
53	LT/St.Veit	1119,5 m LT31 ch	
54	LT/St.Veit	31/1101,5gr marlstone	
57	LT/St.Veit	31/1073,5calcareous marlstone/marlstone	
59	LT/St.Veit	993,5 m LT31 w limestone	
60	LT/St.Veit	980,5 m LT31 marlstone 2	
61	LT/St.Veit	31/898chert bunt	
62	LT/St.Veit	31/869,5gr tst	
63	LT/St.Veit	810,5 m LT31 Sandst	
64	LT/St.Veit	0m RS VG rot Aptychenschichten	
65	LT/St.Veit	14 m RS VG weißerJuraKal	
66	LT/St.Veit	35,6 m RS VG Radiol,	
67	LT/St.Veit	40, 6 m RS VG Radiol,	
68	LT/St.Veit	45,2 m RS VG Crinsplimestone	
69	Antonshöhe	Antonhöhe weißAptychenschichten	
70	Antonshöhe	Antonshöhe rote Aptychenschichten	
71	Groisbach	Lias marlstone,sandig	
72	Groisbach	Lias marlstone	
73	Groisbach	kl Waldwiese,gryph,	
74	Groisbach	Keuper	
75	Groisbach	Blaschke,limestone	
76	Gutenbachtal	chert,Oxford	
77	Gutenbachtal	Lias,Sandst	
78	Typloc.Driet	roter Ton	
79	Typloc.Driet	sandstone	
81	Typloc.Driet	Breccia	
82	Typloc.Driet	liassic sandstone	
83	Typloc.Driet	liassic sandstone	
84	Typloc.Driet	liassic shale	
85	Typloc.Driet	marlstone	
86	Typloc.Driet	limestone	
87	Typloc.Driet	limestone	
88	Drietoma	limestone	
89	Drietoma	sandstone	
90	Drietoma	chert	
91	Drietoma	calpion.limestone	
93	Drietoma	chert	
94	Drietoma	marlstone	
95	Drietoma	chert	
96	Drietoma	marlstone	
97	Drietoma	chert	
98	Drietoma	limestone	
99	Drietoma	chert	

100	Drietoma	limestone	
101	Zazriva	Keuper,sandstone	
102	Zazriva	Keuper, shale	
105	Zazriva	sandst,P3	
106	Zazriva	marlstone	
107	Zazriva	siliceous limestone, P5	
108	Zazriva	siliceous limestone P5	
109	Zazriva	chert,P6	
110	Zazriva	chert, P6	
111	Zazriva	limestone	
112	Zazriva	marlstone	
113	Gresten	Pechgraben/Konradsheimfm,heller K	
114	Gresten	Pechgraben/Scheibsbachfm,dunkler	
115	Gresten	Pechgraben/Blassensteinsch,grauer	
116	Gresten	Lampelsbergsch,Iroter M	
117	Gresten	Lampelsbergsch,2dunkler TM	
118	Gresten	Lampelsbergsch,3dunkler TM	
119	Gresten	Posidonienmarlstone Klauskogelsandig	
120	YbbsitzKZ	Haselbachgrabendunkler marlstone	
121	Gresten	ArzberggrabenBlassensteinsch,hell	
122	YbbsitzKZ	Steinbruch Reidl 1Hst	
123	YbbsitzKZ	Steinbruch Reidl 2Hst	
124	YbbsitzKZ	Steinbruch Reidl 3Hst	
125	YbbsitzKZ	Steinbruch Reidl 4Hst	
126	Manín Unit	Grestener sandstone	
127	Kopieniz Fm	sandstone	
128	Krížna nappe	Keuper	
129	Krížna nappe	Keuper shale red	
130	PKB Kysuca U	Myjava1	
130	Gresten	GRE1	
131	PKB Kysuca U	Myjava2	
131	Gresten	GRE2	
132	PKB Nedzov N	Brinze pod Javorinov 1	
132	Gresten	GRE3	
133	PKB Nedzov N	Brinze pod Javorinov 2	
133	Gresten	GRE4	
134	PKB Nedzov N	Brinze pod Javorinov 3	
134	Gresten	GRE5	
135	PKB Nedzov N	Brinze pod Javorinov 4	
136	PKB Nedzov N	Brinze pod Javorinov 5	
137	PKB Kysuca U	Turá Lúka 1	
138	PKB Kysuca U	Turá Lúka 2	
139	PKB Kysuca U	Turá Lúka 3	
140	PKB Kysuca U	Podbranc 1	
141	PKB Kysuca U	Podbranc 2	
142	PKB Kysuca U	Podbranc 3	

143	PKB Czorszty	Dolny Mlyn 1	
144	PKB Czorszty	Dolny Mlyn 2	
145	PKB Czorszty	Dolny Mlyn 3	

# **CURRICULUM VITAE**

## **Mag. Clemens Pfersmann**

Date of birth: 21. 11. 1980  
Place of birth: Vienna

### **EDUCATION**

01.03.2009: Start of PhD study (Geology), Department of Geodynamics and Sedimentology, University of Vienna.

Stratigraphy and Lithofacies inventory of the St. Veit Klippenzone and the Flysch units from the Lainzer Tunnel (OMV F&E Project FA536006).

29.01.2009: Mag. rer. nat., Geology; Department of Geodynamics and Sedimentology, University of Vienna.

„Stratigraphie und Sedimentpetrographie der Gesteine der Flyschzone im Lainzer Tunnel“ passed with distinction.

01/2006-01/2009: University of Vienna: Geology.

19.01.2006: University of Vienna: Earth sciences: first diploma.

02/2002-10/2002: Military service.

01.10.2001: University of Vienna: Earth sciences

### **ADDITIONAL ACTIVITIES**

23.-27.02.2009: Participation at Flügel course (carbonate facies and carbonate sedimentation-systems), University of Nürnberg-Erlangen, Germany.

30.8.-2.9.2011: Participation at “Sedimentary Provenance Analysis” short course, University of Göttingen, Germany.

### **PUBLICATIONS AND ABSTRACTS**

Wagreich, M., Pfersmann, C., Aubrecht, R. & Plašienka, D., 2012. The westernmost end of the Pieniny Klippen Belt in Austria - the St. Veit Klippenzone and its correlation into the Carpathians. In: Józsa, Š., Rehákovaá, D. & Vojtko, R. (Eds.). Environmental, Structural and Stratigraphical Evolution of the Western Carpathians. 8th Conference 2012, December, 6-7, 2012, Bratislava, Abstract Book, p. 53.

Pfersmann, C., Wagreich, M. & Arzmüller, G., 2011. Flysch and Klippenzone rocks from the Lainz Tunnel as analogues of drilled strata below the Neogene rocks of the Vienna Basin. Proceedings 73rd EAGE Conference and Exhibition, Extended abstract, May 23 – 26, 2011 Vienna, Austria.

Pfersmann, C., Wagreich, M. & Arzmüller, G., 2010. The westernmost end of the Pieniny Klippen Belt? The St. Veit Klippenzone in Austria. Journal of Alpine Geology 52:79.

Pfersmann, C., Wagreich, M. & Arzmüller, G., 2010. Die Geologie des Lainzer Tunnels. Journal of Alpine Geology 52:79.

Pfersmann, C., Wagreich, M., 2009. The geology of the western part of the Lainz Tunnel of the Rhenodanubian Flysch Zone in the Wienerwald (Austria): Kahlenberg Formation and Hütteldorf Formation (Cretaceous). Journal of Alpine Geology 51:59-71.

Pfersmann, C., Wagreich, M., Koch, G., 2008. Stratigraphie und Sedimentpetrographie der Gesteine der Flyschzone im Lainzer Tunnel. Journal of Alpine Geology 49:79.